PhD-FSTM-2023-022
The Faculty of Science, Technology and Medicine

DISSERTATION

Presented on 02/03/2023 in Luxembourg
to obtain the degree of

DOCTEUR DE L'UNIVERSITÉ DU LUXEMBOURG EN BIOLOGIE

By
Mudiwa Nathasia MUWANIGWA
Born on 14 September in Harare (Zimbabwe)

SENESCENCE AS A CONVERGING MECHANISM IN PARKINSON'S DISEASE

Dissertation defense committee
Dr Jens C. Schwamborn, Dissertation Supervisor
Professor, Université du Luxembourg

Dr Rejko Krüger, Chairman
Professor, Université du Luxembourg

Dr Hilal Lashuel
Professor, École Polytechnique Fédérale de Lausanne

Dr Tiago Outeiro
Professor, University of Göttingen

UNIVERSITY OF LUXEMBOURG

DOCTORAL THESIS

SENESCENCE AS A CONVERGING MECHANISM IN PARKINSON'S DISEASE

By

Mudiwa Nathasia Muwanigwa

Developmental and Cellular Biology Group

Luxembourg Centre for Systems Biomedicine

Dissertation defense committee

Prof. Dr. Jens C. Schwamborn, Dissertation Supervisor

Prof. Dr. Rejko Kruger, Chairman

Prof. Dr. Hilal Lashuel

Prof. Dr. Tiago Outeiro

Dr Silvia Bolognin (CET Committee Member)

Prof. Dr. Jeroen Pasterkamp (CET Committee Member)

March 2, 2023

Affidavit

I hereby declare that this PhD Thesis entitled "Senescence as a converging mechanism in Parkinson's disease" has been written independently and without any other sources than cited.

Mudiwa Nathasia MUWANIGWA

Luxembourg, 02/03/2023

"I didn't want to just know the names of things. I remember really wanting to know how it all worked."

Elizabeth Blackburn,

Nobel laureate known for her work on the discovery of telomeres.

Acknowledgements

The past four years have represented a profoundly important period of my life. During the course of this PhD, I feel that I have not only grown as a scientist, but overall, as a person in immeasurable ways, and I am so grateful for all that this experience has taught me. Being able to successfully complete this journey was certainly not due to my own efforts alone, but greatly impacted by several individuals for who I am deeply grateful.

Firstly, I would like to express my sincere gratitude to my PhD supervisor, Professor Jens Schwamborn. The opportunity to work in his group has been one of the greatest joys of my life, and his guidance throughout the years was incredibly impactful for my growth and development as a young scientist. I am also extremely grateful for the patience and understanding he showed me during some very difficult periods that I faced in these past four years, for that I am forever appreciative. I would like to also give an enormous thank you to Dr Silvia Bolognin, who co-supervised me during the PhD, was part of my CET committee and was someone I came to see as a mentor. Silvia's inputs into my project throughout the years helped guide and shape my research, and I could not have achieved what I did without her. I also always felt I could confide in her when I was experiencing challenges, and she was always supportive.

I would like to thank Professor Jeroen Pasterkamp for serving on my CET committee since the start of my PhD. Jeroen has been watching my growth as a scientist since before I even began the PhD as I spent my 2nd Master's internship in his lab. I am grateful for the feedback he provided during the CET, and for also being a part of evaluating this thesis. I would also like to thank the members of my jury, Professor Rejko Krüger, Professor Tiago Outeiro and Professor Hilal Lashuel, for agreeing to evaluate my thesis and taking time out of their busy schedules to be a part of this important part of my PhD journey.

Thank you to the funding bodies that supported my research, specifically the FNR and the US Department of Defense.

One of the things I am most grateful for is my wonderful DVB colleagues, those currently present and those who left during the time I was a part of the group. The DVB team is truly a group of kind,

friendly and warm-spirited people. I am thankful for everyone's willingness to always help and share their knowledge, which made the working environment very positive and enjoyable. I enjoyed our interactions – the lunches, the "Well done" beers, the retreats, random conversations in the coffee lounge and in the office. I'd like to give a special shout out to "*the girls*" with whom I developed deeper friendships with, and I will truly miss our weekend brunches. I especially would like to thank Raquel, who showed up towards the last year of my PhD. We quickly became two peas in a pod, and her motivating me to go to the gym kept my mental health in check during some of the stressful times of the PhD. I would also like to thank my colleagues from the PARK-QC doctoral training unit, some of whom also became very good friends – a special mention to Alessia.

My family and friends have been my biggest cheerleaders throughout this journey. Prudence, Alexia, Kuzivakwashe, Hazel, Chenai, you all have literally been there from way back and have seen the highs, the lows and everything in between. Super grateful for your support, always. To my Visibility STEM Africa team, Nata, Adama, Anne and Elaine, thank you for being a significant part of my PhD journey and for the bond we created that will always connect us. To my parents, thank you for always believing in me and making me feel like the brightest star in the galaxy. You always supported me since I was an overachieving kid who wanted to do absolutely *everything*. To my mom, I am so grateful that you are here to witness me accomplish this milestone. Almost losing you during my PhD was one of the hardest experiences of my life, but watching you bounce back and be your strong, wonderful self is such an inspiration for me. Your resilience is absolutely astounding and motivates me to keep going no matter how tough things may seem. To my dad, *'the father of the daughter'*, thank you for always being a rock that we could all count on and for always making me believe I am capable of achieving any and everything I set my mind to. Thank you to my big brother who has always reminded me how proud he is of me at every step of the journey. Not getting to go home to Zimbabwe since I started the PhD was really difficult, but there is never a moment where I felt a lack of support from my family, and I am so, so grateful for that.

Last but certainly far from least, I am so deeply grateful for my partner, Dr Luke Davis, for being the most incredible support system. You inspire me and motivate me to keep pushing beyond what I can see, and for that, I am eternally thankful.

Abstract

Neurodegenerative diseases are one of the leading causes of disability and mortality, affecting millions of people worldwide. Parkinson's disease (PD) is the second most common neurodegenerative disease globally, and while it was first described over 200 years ago, curative treatments remain elusive. One of the main challenges in developing effective therapeutic strategies for PD is the complex molecular pathophysiology of the disease has not been well recapitulated in classically used animal models systems, and studies using post-mortem tissue from patients only represents the end point of disease. Human derived brain organoid models have revolutionized the field of neurological disease modeling, as they are able to recapitulate key cellular and physiological features reminiscent of the human brain.

This thesis describes the use of human midbrain organoids (hMO) to model and gain a deeper understanding of genetic forms of PD. In the first manuscript, patient-specific hMO harboring a triplication in the *SNCA* gene (3xSNCA hMO) were able to recapitulate the key neuropathological hallmarks of PD. We observed the progressive loss and dysfunction of midbrain dopaminergic neurons in 3xSNCA hMO, and the accumulation of pathological α-synuclein including elevated levels of pS129 α-synuclein and the presence of α-synuclein aggregates. We also identified a phenotype indicative of senescence in the 3xSNCA hMO, which represents a mechanism that has recently gained more attention as a driving factor in PD pathogenesis and progression. The second manuscript of this thesis investigated the pathogenic role of LRRK2-G2019S in astrocytes using a combination of post-mortem brain tissue, induced pluripotent stem cell derived astrocytes and hMO. The iPSC derived astrocytes and organoids recapitulated the phenotypes seen in the post-mortem tissue, emphasizing the validity of these models in reflecting the *in vivo* situation. Interestingly, single-cell RNA sequencing of the hMO revealed that astrocytes from the LRRK2-G2019S organoids showed a senescent-like phenotype. Thus, this thesis highlights the relevance of senescence as a converging mechanism in PD.

Finally, this thesis explores the future development of organoid models as they are combined with technologies such as microfluidic devices as in Manuscript III to improve their complexity and

reproducibility. Ultimately, this will lead to the development of more representative models that can better recapitulate and model PD as well as other neurodegenerative disorders.

Table of Contents

Abbreviations

2D	two-dimensional
3D	three-dimensional
AD	Alzheimer's disease
ATP13A2	ATPase cation transporting 13A2
BCL2	B-cell lymphoma 2
BSA	bovine serum albumin
cDNA	complementary DNA
CFD	computational fluid dynamic
CNS	central nervous system
CRC	core regulatory circuit
D + Q	Dasatinib and Quercetin
DA	dopaminergic
DAT	dopamine transporter
DEG	differentially expressed genes
DMEM	Dulbecco's Modified Eagle Medium
DMSO	dimethyl sulfoxide
DNA	deoxyribonucleic acid
Drop-Seq	droplet sequencing
EAAT2	Excitatory amino acid transporter 2
EDTA	Ethylenediaminetetraacetic acid
ELISA	enzyme linked immunosorbent assay
EN1	engrained homeobox 1

FGF	fibroblast growth factor
FOXA2	forkhead box protein A2
GBA	glucocerebrosidase
GFAP	glial fibrillary protein
hBDNF	human brain derived neurotrophic factor
HCL	hydrochloric acid
hESC	human embryonic stem cell
hGDNF	human glial derived neurotrophic factor
hMO	human midbrain organoid
IL	interleukin
IPSC	induced pluripotent stem cell
LB	Lewy Body
LN	Lewy Neurite
LRRK2	leucine rich repeat kinase 2
MAP2	microtubule associated protein 2
MMP3	matrix metallopeptidase 3
MPP+	1-methyl-4-phenylpyridinium
MPTP	1-methyl-4-phenyl-1,2,3,6-tetrahydropyridine
NAC	non Aß component of Alzheimer's
NACP	precursor of the non Aß component of Alzheimer's
NESC	neuroepithelial stem cell
NURR1	nuclear receptor-related factor 1
OCT4	octamer binding transcription factor 4
O-GlcNAcylation	O-linked-N-acetylglucosaminylation
(q)PCR	(quantitative) polymerase chain reaction

PAX6	paired box protein 6
PD	Parkinson's Disease
PBS	phosphate buffer saline
PFA	paraformaldehye
PFF	pre-formed fibril
PINK1	PTEN-induced kinase 1
pRb	retinoblastoma protein
PRKN	parkin RBR E3 ubiquitin protein ligase
PTM	post translational modification
RIPA	radioimmunoprecipitation assay
RNA	ribonucleic acid
ROS	reactive oxygen species
S100ß	S100 calcium-binding protein B
SASP	senescence associated secretory phenotype
scRNA-seq	single cell RNA sequencing
SHH	sonic hedgehog
SNAP25	synaptosomal-associated protein 25
SNARE	soluble N-ethylmaleimide-sensitive factor attachment protein receptor
SNpc	substantia nigra pars compacta
SOX2	Sex determining region Y box 2
TCCD	2,3,7,8-tetrachlorodibenzodioxin
TGFß	Transforming growth factor ß
TH	tyrosine hydroxylase
TNF	tumor necrosis factor
UMAP	Uniform Manifold Approximation and Projection

VAMP2   vesicle associated membrane protein 2

VMAT2   vesicular monoamine transporter 2

VTA   ventral tegmental area

WNT   Wingless-related integration site

List of Figures

List of Tables

1. *Introduction*

1.1 Parkinson's Disease

Due to an increasing global aging population, age-associated disorders have significantly risen in prevalence over the past few decades. Neurodegenerative disorders such as Parkinson's disease (PD), Alzheimer's disease (AD), multiple system atrophy, progressive supranuclear palsy and Huntington's disease comprise a large subset of such disorders and are a leading cause of morbidity and mortality in the elderly. Given that many neurodegenerative diseases have no cures, and most treatments only serve to slow disease progression, these disorders pose a significant socio-economic burden, making them issues of great public health concern. As the most common movement disorder and the second most common neurodegenerative disease, PD is a major healthcare and societal challenge. Over two centuries following James Parkinson's 1817 seminal essay 'On the Shaking Palsy' (Parkinson, 2002), the description of the cardinal features of the disease he described have stood the test of time. However, until now there is still no curative treatment for the disease. Despite this, significant research efforts have been made towards better understanding the disease so that effective therapies can be developed.

1.1.1 Epidemiology

Globally, the incidence of PD ranges from 5 to >35 new cases per 100,000 individuals yearly (Twelves *et al.*, 2003). The onset of PD is rare before 50 years of age, however the incidence of the disease increases between 5 to 10-fold between the ages of 60 and 90 years old (Twelves *et al.*, 2003). In most populations, PD is more prevalent in men than in women, potentially due to the protective effect of estrogen on nigrostriatal dopaminergic neurons (Cerri *et al.*, 2019; Lee *et al.*, 2019). The incidence of PD has been steadily increasing in recent decades and it is the fastest growing neurological disease with regards to prevalence, disability, and mortality (Dorsey *et al.*, 2018).

Between 1990 and 2015, the global prevalence of PD doubled from an estimated 2.5 million to 6.1 million (Dorsey *et al.*, 2018). According to the World Health Organization, it was estimated that there were over 8.5 million individuals with PD globally in 2019 (World Health Organization, 2022). By 2040, it is anticipated that this number will increase to over 12 million, potentially surpassing AD as the most prevalent neurodegenerative disorder globally (Dorsey & Bloem, 2018).

1.1.2   Clinical Manifestation

Clinically, PD is defined by several cardinal motor symptoms, most common of which are bradykinesia, resting tremor, rigidity, and postural instability (Kalia & Lang, 2015). The presence of these symptoms is often used to distinguish PD from other related parkinsonian disorders (Jankovic, 2008). Individuals with PD may also show other motor symptoms such as shuffling gait, loss of facial expressions (hypomimia), dysphagia and dystonia (Jankovic, 2008). Besides motor symptoms, PD also presents with diverse non motor symptoms. These can include psychotic symptoms like hallucinations as well as mood disturbances such as depression, anxiety, and apathy. Sleep disturbances including restless leg syndrome, rapid eye movement behavior disorder and sleep apnea have also been described in a significant proportion of PD patients. Gastrointestinal disturbances, especially constipation, are often experienced. (Jankovic, 2008; Kalia & Lang, 2015; Váradi, 2020). Many of the non-motor systems appear decades prior to the onset of motor symptoms, suggesting that the progression of the disease likely occurs for many years before patients are diagnosed (Kalia & Lang, 2015). Indeed, it is now well established that PD is characterized by a prodromal or premotor phase that precedes the onset of motor symptoms and the diagnosis of the disease (Figure 1.1). Interestingly, there appears to be sex specific differences with regards to clinical phenotypes, potentially indicating distinct pathogenic mechanisms in men and women (Cerri *et al.*, 2019).
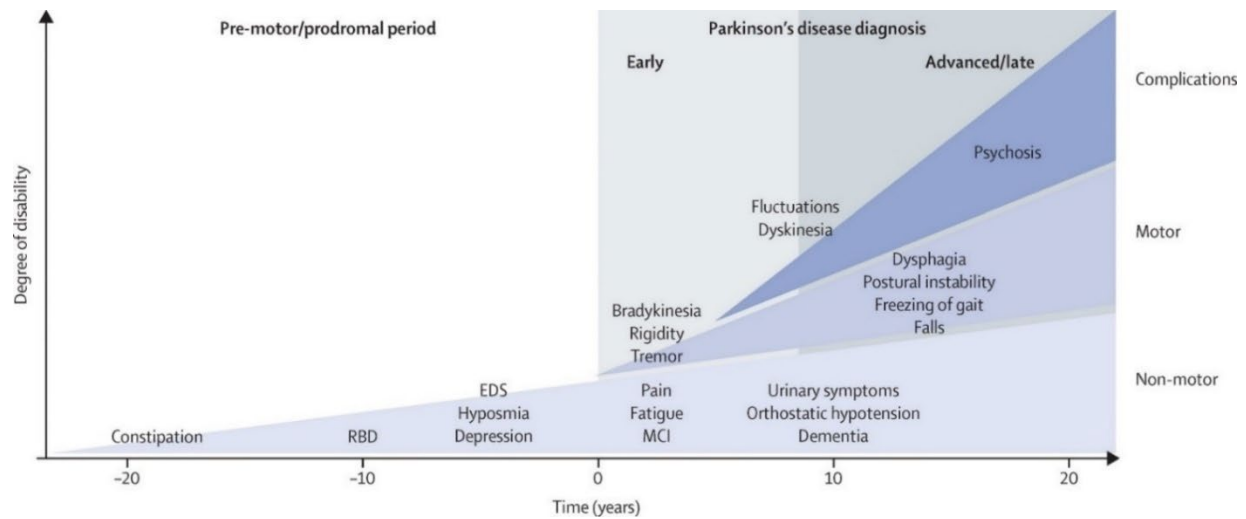
Figure 1.1 Clinical symptoms and time course of Parkinson's disease (Kalia & Lang, 2015). Decades before a diagnosis, PD is characterized by a prodromal period which typically presents with non-motor symptoms like gastrointestinal issues and sleep disturbances. At diagnosis, PD presents with the cardinal motor symptoms, i.e., bradykinesia, rigidity, and tremor. Over time, symptoms worsen, and complications arise that greatly reduce quality of life. EDS = excessive daytime sleepiness. MCI = mild cognitive impairment. RBD = REM sleep behavior disorder

1.1.3 Neuropathology

Neuronal Loss in PD

While gross macroscopic atrophy is not usually observed in PD, the brains of some patients show mild atrophy of the frontal cortex and in some cases, ventricular dilation (Burton *et al.*, 2004; Camicioli *et al.*, 2011). The main distinctive morphological change in the PD brain is observed in the brainstem, where almost all cases present with loss of the darkly pigmented area in the substantia nigra pars compacta (SNpc) and locus coeruleus. This loss of pigmentation is due to the death of neuromelanin containing dopaminergic (DA) neurons in the SNpc and noradrenergic neurons in the locus coeruleus (Dickson, 2012). Neuronal loss has also been documented at late stages of disease in other brain regions including the pedunculopontine nucleus, basal forebrain, intralaminar thalamus, and the dorsal motor nucleus of the vagus (Sulzer & Surmeier, 2013). Due

to constraints of working with post-mortem human tissue the magnitude and timing of neuronal loss, especially in regions outside of the SNpc is poorly defined (Giguère *et al.*, 2018).

Selective vulnerability of SNpc DA neurons

The loss of dopaminergic neurons in the SNpc is one of the main neuropathological hallmarks of PD. Cell death in the SNpc is mostly restricted to a specific group of neuromelanin-containing dopaminergic neurons, namely the A9 neurons, while other neuronal and glial cell types are largely spared (Fu *et al.*, 2016). Most projections that originate from these DA neurons innervate the dorsal striatum. Interestingly, even within the SNpc, the majority of dopaminergic neurons lost are in the ventral tier, whereas there is far less dopaminergic neuron death in the dorsal tier (Damier *et al.*, 1999; Fearnley & Lees, 1991). Several hypotheses have been proposed to explain the selective vulnerability of SNpc dopaminergic neurons in PD.

Dopamine toxicity

The oxidation of dopamine can lead to the generation of reactive quinones, that can be cytotoxic (Jana *et al.*, 2011). Dopamine quinones have been shown to induce mitochondrial dysfunction, perturb protein degradation, as well as induce the formation of neurotoxic α-synuclein protofibrils and oxidative stress (Segura-Aguilar *et al.*, 2014). Dopamine oxidation has been implicated in the production of neuromelanin in SNpc, which will be addressed in the next section. While dopamine toxicity is likely an important contributing factor in dopaminergic vulnerability, this phenomenon alone does not explain why other dopaminergic subgroups, for example those in the ventral tegmentum area (VTA), are less vulnerable to cell death.

Autonomous pacemaking activity

A distinctive feature of mature SNpc DA neurons is their autonomous pacemaking activity, meaning they have the ability to spike on their own without excitatory synaptic input (Guzman *et al.*, 2009). Their autonomous pacemaking activity is driven by calcium channels, whereas in the less vulnerable VTA DA neurons and juvenile SNpc DA neurons pacemaking activity is driven by voltage gated sodium channels (Chan *et al.*, 2007). The reliance of SNpc DA neurons on calcium for their pacemaking activity leads to increased levels of calcium in the cytosol and elevated levels of oxidative stress, which may be a contributing factor to increased vulnerability (Guzman *et al.*, 2010).

Axonal arborization, high energetic demands and oxidative stress

DA neurons in the SNpc show a massive degree of axonal arborization, with an estimate of over a million neurotransmitter release sites per dopaminergic neuron in humans (Bolam & Pissadaki, 2012). Additionally, the DA neurons of the SNpc are unmyelinated. It has been proposed that this particular neuronal architecture would lead to high energy requirements, not only to maintain the cell's normal biological functions, but also in the maintenance of the membrane potential, propagation of action potentials, and in synaptic transmission - all energetically expensive processes (Bolam & Pissadaki, 2012; Surmeier *et al.*, 2017). The heavy bioenergetic burden on these cells leaves little room for additional energetic stress and thus any negative effect on energy supply such as mitochondrial dysfunction or increased oxidative stress could have a detrimental impact.

Iron content

The accumulation of iron in the SNpc with increased age has been observed in several studies (Daugherty & Raz, 2013; Haacke *et al.*, 2010). SNpc DA neurons may display elevated iron content due to their high bioenergetic demands and the fact that the mitochondrial electron transport chain depends on iron sulfur clusters for its proper functioning. Iron is a well-established player in ROS production through the Fenton reaction, which can induce cellular oxidative stress (Zhao, 2019). Additionally, iron is chelated by neuromelanin which is mostly found within SNpc DA neurons, further described in the next section.

While it is likely that all these factors contribute to variable extents to the selective vulnerability of the A9 SNpc DA neurons, the molecular underpinnings of this phenomenon are vague. However, a recent single nuclei RNA sequencing (scRNA-seq) study identified a transcriptionally distinct subtype of SOX6+ AGTR1 expressing DA neurons in the ventral tier of the SNpc. (Kamath *et al.*, 2022). This vulnerable subset showed upregulation of *TP53* and *NR2F2*, transcription factors associated with neurodegeneration, and an enrichment for the expression of PD associated loci. The specific identification of this subset of cells may allow for the study of cell-intrinsic processes that determine the vulnerability of specific DA neurons to degeneration in PD.

Loss of neuromelanin

Neuromelanin, a dark pigment structurally related to melanin, accumulates in the human SNpc and the locus coeruleus in an age dependent manner. PD patients often present with loss of 50-60% of neuromelanin in comparison to age matched healthy individuals due to the preferential loss of neuromelanin-containing dopaminergic neurons during the course of disease progression (Zecca *et al.*, 2002). While the function of neuromelanin is still not well understood, it is thought to play either a neuroprotective or neurotoxic role depending on the context. Neuromelanin has been shown to be protective against dopamine toxicity by converting toxic dopamine quinones to a more stable and inactive polymer, thus preventing the damaging effects of the reactive quinones on the neurons (Segura-Aguilar *et al.*, 2014). Neuromelanin may also exert a protective effect due to its ability to sequester metals such as iron, zinc, copper, lead, aluminum, cobalt, manganese, mercury, and selenium (Zecca *et al.*, 2008; Zecca *et al.*, 1994; Zecca *et al.*, 2001). Neuromelanin binds other toxic molecules known to induce PD-like symptoms, for example paraquat and 1-methyl-4-phenylpyridinium (MPP+) (D'Amato *et al.*, 1987; Lindquist *et al.*, 1988) as another protective mechanism. However, under different circumstances, neuromelanin can be toxic. One mechanism by which this occurs is through iron overload where neuromelanin can bind iron in its reactive form and promote noxious redox reactions (Double *et al.*, 2002). This is supported by the increased presence of redox active iron in the neuromelanin present in the SNpc of PD patients (Faucheux *et al.*, 2003). There is also evidence that neuromelanin accumulation leads to the inhibition of the ubiquitin-26S proteasome system, leading to dysfunctional protein degradation (Shamoto-Nagai *et al.*, 2004). Furthermore, neuromelanin has been proposed to exacerbate neuroinflammation. The release of neuromelanin from dying neurons leads to sustained microglial activation, which can further induce neurodegeneration (Viceconte *et al.*, 2015; Zhang *et al.*, 2011). Given the apparent dual nature of neuromelanin's role, it is challenging to say whether increased or decreased levels of neuromelanin are helpful or harmful in the context of PD. What is likely is that neuromelanin plays a different role depending on the stage of disease.

Lewy pathology

In 1912, Fritz Jacob Heinrich Lewy published his seminal study in which histopathological analysis revealed the presence of eosinophilic inclusions within neurons of particular brain nuclei

in patients with *Paralysis agitans* – the former name for PD (Lewy, 1912). Konstantin Nikolaevich Trétiakoff subsequently found these same inclusions within the SNpc of Parkinson's patients and named them "Lewy bodies" (LB) (if present in neuronal cell bodies) and "Lewy neurites" (LN) (if present in neuronal processes) after Fritz Jacob (Trétiakoff, 1919). The presence of these inclusions became one of the two main pathological hallmarks associated with the shaking palsy, however, it was only in 1997 when the main constituent of the inclusions was revealed to be α-synuclein (Spillantini *et al.*, 1997). The exact process by which Lewy bodies form is still not well understood. Currently, the leading hypothesis proposes that intraneuronal α-synuclein forms abnormal oligomers due to the uptake of pathogenic aggregated α-synuclein species. These oligomers can then be further transformed into β-sheet rich amyloid fibrils which form the basis of Lewy bodies (Goedert, 2015). Genomic mutations and multiplications of *SNCA*, the gene that encodes α-synuclein, have been associated with Lewy body and Lewy neurite formation. Several post-translational modifications such as phosphorylation, nitration, ubiquitination, and truncation have been associated with α-synuclein misfolding and aggregation and the formation of Lewy pathology (further discussed in section 1.2.2) (Manzanza *et al.*, 2021; Pajarillo *et al.*, 2019). Besides α-synuclein, LBs and LNs are rich in ubiquitin, neurofilament protein, lipids, cytoskeletal proteins, organelles, and membranous fragments (Galloway *et al.*, 1992; Mahul-Mellier *et al.*, 2020). LBs show a high degree of diverse structural, morphological, and molecular compositions in different patients and across different brain regions. It is still unclear whether this diversity reflects distinct pathologies or a continuum of conformations reflecting different stages of LB formation and maturation.

LB pathology has been observed within and beyond the basal ganglia, reaching regions such as the cortex and hippocampus. Braak's hypothesis, which is based on the post-mortem analysis of hundreds of brains from PD patients at different disease stages, proposed that LB pathology could be classified based on a specific pattern of α-synuclein spreading across the different brain regions (Braak *et al.*, 2003). LB pathology was proposed to ascend caudo-rostrally, beginning at the lower brainstem, through susceptible regions of the midbrain and forebrain and finally into the cerebral cortex (Braak *et al.*, 2003; Visanji *et al.*, 2013). Braak and colleagues postulated that the initiator of LB pathology is a neurotropic pathogen that enters the body nasally or via the gut, which then spreads to the central nervous system (CNS) via the olfactory bulb or the vagus nerve respectively (Hawkes *et al.*, 2007, 2009).

Altogether, Lewy pathology is a defining hallmark of PD, routinely used by neuropathologists to confirm PD diagnoses in post-mortem tissue. Surprisingly, some genetic forms of PD do not present LB pathology in some instances. For example, there have been several reports of the lack of LB pathology in Parkin-associated PD (Doherty *et al.*, 2013; Gouider-Khouja *et al.*, 2003; Hayashi *et al.*, 2000; Johansen *et al.*, 2018). However, for most other genetic forms and idiopathic PD, Lewy pathology is observed.

1.1.4 Risk Factors

Aging and Senescence

Aging is the biggest risk factor for developing PD. Therefore, understanding the process of aging has become pertinent in understanding the onset and progression of the disorder. Aging is defined as the time related accumulation of biological changes that contributes to an organism's physiological and functional decline. Despite significant advancements in the field of mammalian aging, the understanding of its underlying mechanisms remains limited.

During aging, tissues of the body are characterized by low level, chronic inflammation, a phenomenon coined 'inflammaging', which is thought to contribute to the majority of aging associated pathologies (Chinta *et al.*, 2015). In the brain, aging is associated with mitochondrial dysfunction, increased free radical production, genomic instability, decline in the proteosome, impaired cellular clearance pathways (e.g., autophagy), activation of microglia, and impaired response to neurotrophic factors which impairs the brain's ability to recover from damage (Dahlmann, 2007; Hindle, 2010; Lodato *et al.*, 2018; Lopez-Otin *et al.*, 2013; Migliore & Coppedè, 2009). Due to the postmitotic nature of neurons, they may be particularly susceptible to the cumulative effects of these declining processes. Moreover, the distinct nature of dopaminergic neurons in the SNpc is thought to increase their vulnerability during aging for the reasons highlighted in the previous section (*see: 1.1.3 selective vulnerability of SNpc DA neurons*).
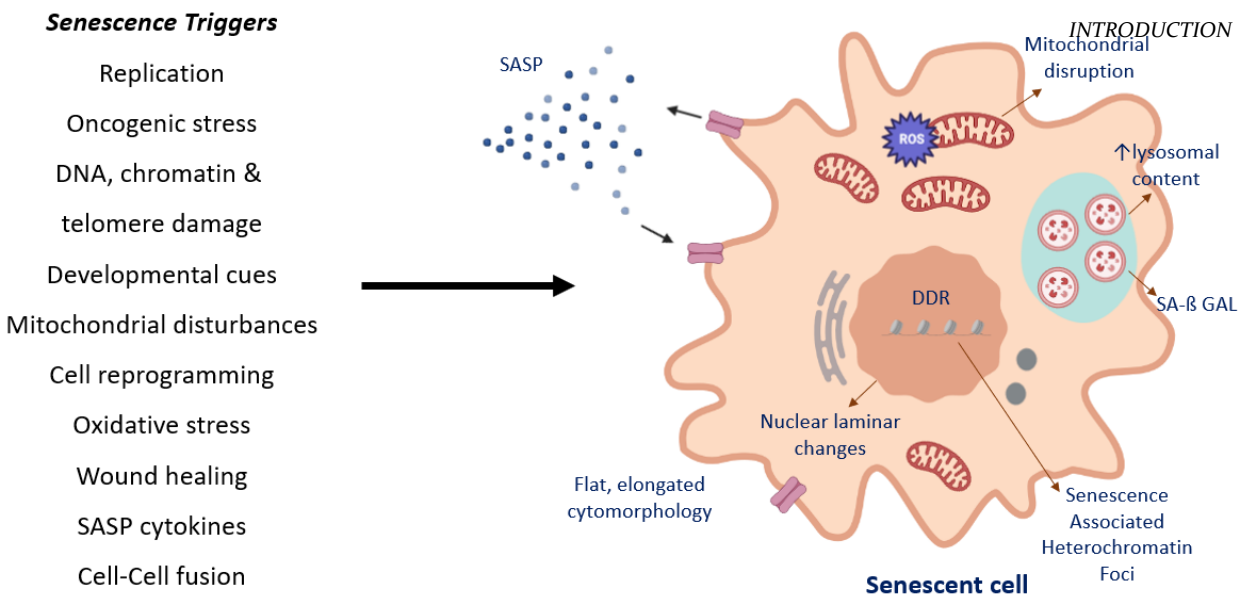
Figure 1.2 Hallmarks of Senescence. Several molecular and physiological triggers can induce cellular senescence. Senescent cells are characterized by specific hallmarks including the emergence of the senescence associated secretory phenotype, altered cytomorphology, nuclear lamina deficits and the upregulation of senescence associated ß-galactosidase. Adapted from (Martínez-Zamudio *et al.*, 2017). Created in BioRender. DDR = DNA damage response. SA-ß GAL = senescence associated ß-galactosidase. SASP = senescence associated secretory phenotype.

The accumulation of senescent cells is thought to be an important contributor to age associated inflammation in the brain. Senescence is an important homeostatic process which arrests the proliferation of dysfunctional cells and prevents neoplastic transformation. It also plays an important role in embryogenesis and wound healing (Muñoz-Espín & Serrano, 2014). Several lines of evidence have indicated that the accumulation of senescent cells contributes to loss of function observed during aging and age-associated pathologies.

Senescence was first described in the context of fibroblasts that had reached their limit of cell division – the so called "Hayflick's limit" after the scientist who first made this observation (Hayflick & Moorhead, 1961). Since this discovery, the understanding of senescence has expanded vastly, and includes developmentally programmed senescence and damage-induced senescence. Damaged induced senescence has further been characterized into subtypes such as 'replicative senescence', 'DNA-damage-induced senescence', 'stress-induced senescence', 'mitochondrial dysfunction-associated senescence' and 'oncogene-induced senescence' (Hernandez-Segura *et al.*, 2018; Muñoz-Espín & Serrano, 2014). Senescent cells can be distinguished from other cellular states

(e.g., quiescence and terminal differentiation) through several distinct markers and morphological changes. Most notably, some features of senescence are cell cycle arrest, resistance to apoptosis, increased expression of senescence associated ß-galactosidase, expression of cell cycle inhibitors and tumor suppressors, the presence of DNA damage foci, and the secretion of inflammatory cytokines, chemokines and other signaling molecules, collectively known as the senescence associated secretory phenotype (SASP) (Figure 1.2).

Several studies have indicated the association between PD and senescence. The genes that encode senescent marker p16[INK4a] and several SASP factors including proinflammatory cytokines interleukin 6 (IL6), interleukin 1α (IL1α), interleukin 8 (IL8) and the proteinase matrix metallopeptidase 3 (MMP3) were shown to be elevated in postmortem tissue of PD patients in comparison to healthy age matched controls (Chinta *et al.*, 2018). Multiple other studies have also reported elevated levels of the same and other SASP factors, including interleukin 1ß (IL1ß), interleukin 2 (IL2), tumor necrosis factor α (TNFα) and interferon gamma (IFNγ) (Brodacki *et al.*, 2008; Hofmann *et al.*, 2009; Lindqvist *et al.*, 2012; Mogi, Harada, Kondo*, et al.*, 1994; Mogi, Harada, Riederer*, et al.*, 1994; Scalzo *et al.*, 2010). Interestingly, the SASP factor MMP3 has been shown to co-localize with Lewy bodies in postmortem brains of PD patients (Choi *et al.*, 2011). It is important to note that many SASP factors are also commonly factors released by immune cells such as microglia in the brain, therefore it can be challenging to distinguish whether the upregulation of many of the proinflammatory factors is directly related to senescence, or the occurrence of neuroinflammation. Reduced levels of the nuclear lamina protein lamin B1, another hallmark of cellular senescence, has also been observed in PD astrocytes (Chinta *et al.*, 2018). Another study demonstrated abundant retinoblastoma protein (pRb) cytoplasmic staining in neurons of the SNpc, mid-frontal cortex, and hippocampus in autopsy tissue from PD patients (Jordan-Sciutto *et al.*, 2003). In its active hypophosphorylated form, pRb is a central mediator of senescence as it suppresses genes related to DNA replication and thereby leads to cell cycle arrest (Therese & Sebastian, 2013). The herbicide paraquat, which has been strongly associated with inducing the development of idiopathic PD, has been shown to induce astrocyte senescence in mouse astrocytes, further indicating a link between PD pathogenesis and senescence (Chinta *et al.*, 2018). Altogether, these studies provide compelling evidence for the association between senescence and PD.

Genetic Risk Factors

Several genetic risk variants and monogenic risk factors have been identified to contribute to, or be causative for, PD. Risk variants tend to be relatively common, individually having a small effect size, but collectively significantly increasing disease risk. On the other hand, causative monogenic variants are relatively rare with a large effect size and considered to be directly causative for disease (Jia *et al.*, 2022). However, there is a complex interplay between monogenic causative variants and risk variants which may affect disease penetrance. In addition, some of the autosomal dominant monogenic forms of PD show age-dependent incomplete penetrance affected by many other factors, like the influence of the patient genetic background (Guadagnolo *et al.*, 2021). While most cases of PD are apparently idiopathic, about 10-15% are familial with a clearly defined autosomal pattern of inheritance (Table 1.1). The first PD associated gene was identified in 1997 (*SNCA)*, and since then over 20 genes have been associated with the development of PD.

SNCA

Mutations in *SNCA*, the gene encoding α-synuclein, were the first to be linked to familial PD (Polymeropoulos *et al.*, 1997). Following this, the identification of α-synuclein as a major constituent of LBs further cemented the relevance of α-synuclein in PD pathogenesis (Spillantini *et al.*, 1997). With regards to PD risk, *SNCA* is pleiomorphic as both common variants and rare mutations alter the risk of developing the disease. Deleterious point mutations and multiplications of the *SNCA* gene have been found to cause early-onset PD, with an autosomal dominant inheritance pattern. So far, eight missense variants have been identified to cause autosomal dominant PD (Table 1.1) (Appel-Cresswell *et al.*, 2013; Fujioka *et al.*, 2014; Hoffman-Zacharska *et al.*, 2013; Kiely *et al.*, 2013; Krüger *et al.*, 1998; Pasanen *et al.*, 2014; Polymeropoulos *et al.*, 1997; Zarranz *et al.*, 2004). The A53T mutation has been associated with increased aggregation while *SNCA* duplications have been shown to cause a phenotype resembling idiopathic PD and are more common that missense mutations or triplications. Interestingly, some *SNCA* duplication carriers remain asymptomatic after 70 years of age, indicating reduced penetrance (Nishioka *et al.*, 2009). On the other hand, *SNCA* triplication causes a rapidly progressing, early-onset form of PD (Olgiati *et al.*, 2015; Singleton *et al.*, 2003). Variability in non-coding regions within this locus have also been shown to confer an increased risk of developing PD (Maraganore *et al.*, 2006).

LRRK2

Leucine-rich repeat kinase 2 (LRRK2) has been largely implicated in PD as mutations in this gene are the most common cause of familial PD. Mutations in *LRRK2* have also been shown to contribute to a significant proportion of apparently idiopathic cases. Clinically, LRRK2-PD is indistinguishable from idiopathic PD on an individual level, however collectively, it is thought to have a milder phenotype with less non-motor symptoms (Kestenbaum & Alcalay, 2017). The G2019S mutation is the most common LRRK2 mutation accounting for 1% of all PD cases, however several other LRRK2 mutations have been found to be causative for PD (Li *et al.*, 2014). LRRK2 is a large, multifunctional protein with various protein–protein interaction domains and an enzymatic core that generates serine–threonine kinase and GTPase activities. Extensive studies have shown that most PD-linked pathogenic *LRRK2* mutations cause a toxic gain-of-function increase in LRRK2 kinase activity (Alessi & Sammler, 2018; Rui *et al.*, 2018). This has promoted the development of therapeutic approaches making use of LRRK2 kinase inhibitors (Christensen *et al.*, 2017).

PRKN and PINK1

Mutations in *PRKN* are the most common cause of early-onset PD (Lesage *et al.*, 2020). *PRKN* encodes Parkin RBR E3 ubiquitin protein ligase, a protein that facilitates the ubiquitination of lysine residues. A variety of mutations in *PRKN* have been described including exonic deletions or multiplications, missense mutations, nonsense mutations, small insertions or deletions and splice-site alterations. Phenotypically, Parkin-PD is characterized by early disease onset, absence of cognitive impairment, lower limb dystonia, dyskinesias and sustained response to levodopa (Lesage *et al.*, 2020; Lücking *et al.*, 2000). *PINK1* is the second most common cause of autosomal recessive PD and phenotypically presents with typical PD features like bradykinesia, rigidity, and tremor (Albanese *et al.*, 2005). PTEN-induced kinase 1 (PINK1) is a mitochondrial serine/threonine kinase. Similar to *PRKN*, several mutations in *PINK1* have been identified to be causative for PD including missense mutations, nonsense mutations, exon rearrangements including deletions or duplications. Mutations in *PRKN* and *PINK1* have been proposed to affect PINK1/parkin mediated mitophagy, an important mitochondrial degradation pathway for selective removal of impaired mitochondria (Ge *et al.*, 2020). PINK1 and parkin function as initiators of a signaling pathway that activates mitochondrial quality control pathways in response to mitochondrial damage. Thus, mutations in these two genes are likely to contribute to mitochondrial dysfunction, one of the most well described pathological mechanisms in PD.

Table 1.1 Monogenic forms of Parkinson's disease. Adapted from (Jia *et al.*, 2022; Kalia & Lang, 2015)

Gene	Protein	Pathogenic mutation(s)
Autosomal dominant		
SNCA	α-synuclein	Missense mutations - A18T, A29S, A30P, A53E, A53T, E46K, H50Q, G51D; Multiplications – duplications and triplications.
LRRK2	Leucine rich repeat kinase 2	Missense mutations - N1437H, R1441C, R1441G, R1441H, Y1699C, G2019S, I2020T
VPS35	Vacuolar sorting protein 35	Missense mutation - D620N
DNAJ13C	Receptor-mediated endocytosis 8 (REM-8)	Missense mutation - N855S
EIF4G1	Eukaryotic translation initiation factor 4-γ 1	Missense mutations - A502V, R1205H
CHCHD2	Coiled-coil-helix-coil-helix domain containing 2	Missense mutation – T61I, R145Q; splice-site alteration - c.300 + 5G > A
Autosomal recessive		
PRKN	Parkin	Exon rearrangements including deletions or multiplications, missense mutations, nonsense mutations, small insertions or deletions, splice-site alterations
PINK1	PTEN-induced putative kinase 1	Missense mutations, nonsense mutations, exon rearrangements including deletions or duplications
PARK7 (DJ1)	DJ1	Missense mutations, exon rearrangements, splice-site alterations

GBA

Mutations in *GBA1*, the gene encoding the enzyme glucocerebrosidase, are the most common genetic risk factor for PD. Glucocerebrosidase breaks down glucosylceramide to ceramide and glucose. Variants in GBA are found in about 8.5% of PD patients (Skrahina *et al.*, 2021) however the prevalence differs based on the population with particular high occurrence in the Ashkenazi Jewish PD population (Schapira, 2015). Homozygous pathogenic mutations in GBA are causative for Gaucher's disease, an inherited metabolic disorder in which glucocerebrosidase deficiency leads to lipid accumulation throughout the body, causing multiorgan dysfunction (Riboldi & Di Fonzo,

2019). Interestingly, Gaucher's disease may or may not present with neurological involvement. Clinically, GBA-PD is almost identical to idiopathic PD, however, often presents with earlier onset, higher prevalence of cognitive deterioration and faster progression of motor symptoms (Cilia *et al.*, 2016; Jesús *et al.*, 2016; Sidransky *et al.*, 2009). Over 300 mutations in *GBA1,* including insertions, deletions and point mutations have been identified (Oeda *et al.*, 2015; Smith *et al.*, 2017). The N370S and L444p mutations are the most common *GBA1* mutations worldwide and increase the risk of developing PD by 4 times and 12 times respectively, however the heterogeneity of penetrance of individual *GBA1* variants limits the utility of these estimates (Day & Mullin, 2021).

Environmental Risk Factors

Exposure to certain environmental factors has been associated with PD etiology for decades (Calne & William Langston, 1983; Koller, 1991). Epidemiological studies have revealed that pesticide exposure, heavy metal exposure, illicit drug use, prior traumatic brain injury, rural living, β-blocker usage, agriculture occupation and well-water drinking may increase the risk of PD (Ball *et al.*, 2019; Priyadarshi *et al.*, 2001). Knowledge of environmental toxins that are associated to PD pathogenesis has formed the basis of neurotoxin models used to study PD (Bové & Perier, 2012; Sherer *et al.*, 2003). Given the heterogeneity of PD, it is speculated that individual susceptibility to environmental factors plays a significant role in the development of PD (Ball *et al.*, 2019).

Altogether, PD etiology is due to a complex interplay between the risk factors discussed in this section and others. This complexity highlights why understanding this disease has been a pertinent challenge since it was first described over 200 years ago.

1.2 α-synuclein

While significant progress has been made in understanding the physiological role of α-synuclein and its pathological role in PD, there are still many areas of contention within the field regarding this protein. α-synuclein is predominantly expressed in the brain, particularly in the neocortex, hippocampus, midbrain, thalamus and the cerebellum (Emamzadeh, 2016).

Interestingly, erythrocytes contain high levels of α-synuclein, and peripheral α-synuclein is most abundant in this cell type (Barbour *et al.*, 2008). Given its prominence in PD, there are significant research efforts towards better understanding this protein.

1.2.1   α-synuclein: Structure

The first synuclein was identified in the electric ray fish *Torpedo californica (*Maroteaux *et al., 1988)* where it was shown to be a neuronal protein that localized at the nucleus and at presynaptic terminals – hence its name. Subsequently, a 140 amino acid protein was identified in a rat brain cDNA library which showed high homology with the synuclein identified in the electric ray fish. The study of amyloid plaques of AD patients identified a protein named NAC for non-Aß component of AD amyloid. Its precursor protein, NACP, was found to be homologous to rat synuclein (Ueda *et al.*, 1993) and is now known to be α-synuclein. Since then, three families of synuclein have been described – α-synuclein, ß-synuclein and γ-synuclein (George, 2002). The synucleins are highly evolutionarily conserved and abundant in the nervous systems of vertebrates (Clayton & George, 1998). During development, α-synuclein redistributes from neuronal cell bodies to synaptic terminals during neuronal differentiation (Baltic *et al.*, 2004; Clayton & George, 1999), and its expression is increased during periods of synaptic plasticity (George *et al.*, 1995).

α-synuclein is encoded by the *SNCA* gene, present on the long arm of chromosome 4 (Chr 4q22.1). It is a small 140 amino acid (14kDa) protein that contains three domains: an N-terminal lipid binding α-helix, an amyloid binding central domain, known as the NAC, and an acidic C-terminal tail (Emamzadeh, 2016)(Figure 1.3). The N-terminal domain is positively charged and includes a series of seven 11-amino acid repeats which contain a highly conserved hexameric KTKEGV motif, also found in the α-helical domain of apolipoproteins. These repeats are important for α-synuclein's interaction with lipids. Interestingly, all the currently known PD associated *SNCA* mutations cluster within the N-terminal region (Figure 1.3A). Another note of interest is that rodent α-synuclein normally contains a threonine at position 53, which is a pathogenic mutation in humans (Bendor *et al.*, 2013). The NAC domain of α-synuclein is involved with the formation of fibrils and aggregates as it has the ability to form cross β-structures. The acidic C-terminal tail is present in a random coil due to its low hydrophobicity and high net negative charge.
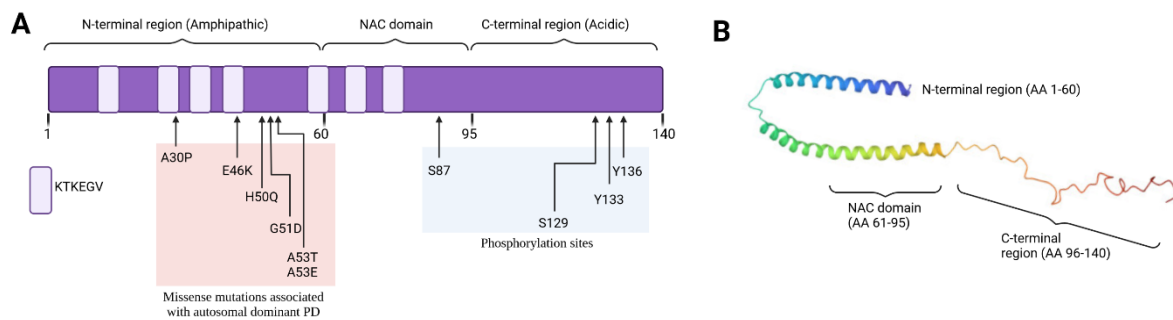
Figure 1.3 α-synuclein structure. A Schematic representation of α-synuclein structure. The N-terminal region and NAC domain contain seven highly conserved hexameric KTKEGV motif repeats which contribute to membrane binding. Missense mutations associated with autosomal PD are found in the N-terminal region. The C-terminal region contains most known phosphorylation sites. Adapted from (Fan *et al.*, 2021) and (Mori *et al.*, 2020). Created in BioRender. **B** Structural model of human α-synuclein. Image from RCSB Protein Data Bank. PDB DOI: 10.2210/pdb1XQ8/pdb.

α-synuclein has a dynamic structure (Fig 1.4). Monomeric α-synuclein is a soluble, intrinsically disordered protein found in the cytosol (Burré *et al.*, 2013; Chandra *et al.*, 2003; Fauvet *et al.*, 2012; Weinreb *et al.*, 1996) which folds into an α-helical state when bound to phospholipid membranes (Chandra *et al.*, 2003; Cole *et al.*, 2002; Davidson *et al.*, 1998; Jo *et al.*, 2000; Nuscher *et al.*, 2004). There is strong evidence supporting the idea that physiological α-synuclein exists as helically folded tetramers (Bartels *et al.*, 2011; Wang *et al.*, 2011; Xu *et al.*, 2019). The different conformations of α-synuclein are thought to exist in equilibrium, and the imbalance of this equilibrium can promote aggregation of the protein (Dettmer *et al.*, 2015; Fanning *et al.*, 2020). Monomeric α-synuclein can aggregate to give rise to oligomers which can take on various morphologies including spherical, chain-like, pore-like annular and tubular (Lashuel *et al.*, 2002b). Pathological α-synuclein has been shown to adopt a ß-sheet amyloid conformation, which is associated with α-synuclein aggregation, fibril formation and the formation of Lewy bodies (Fig 1.4) (Conway *et al.*, 1998; El-Agnaf *et al.*, 1998; Greenbaum *et al.*, 2005; Uversky, 2007; Yonetani *et al.*, 2009). This ß-sheet conformation has been proposed to be neurotoxic, however, this is still not well characterized.
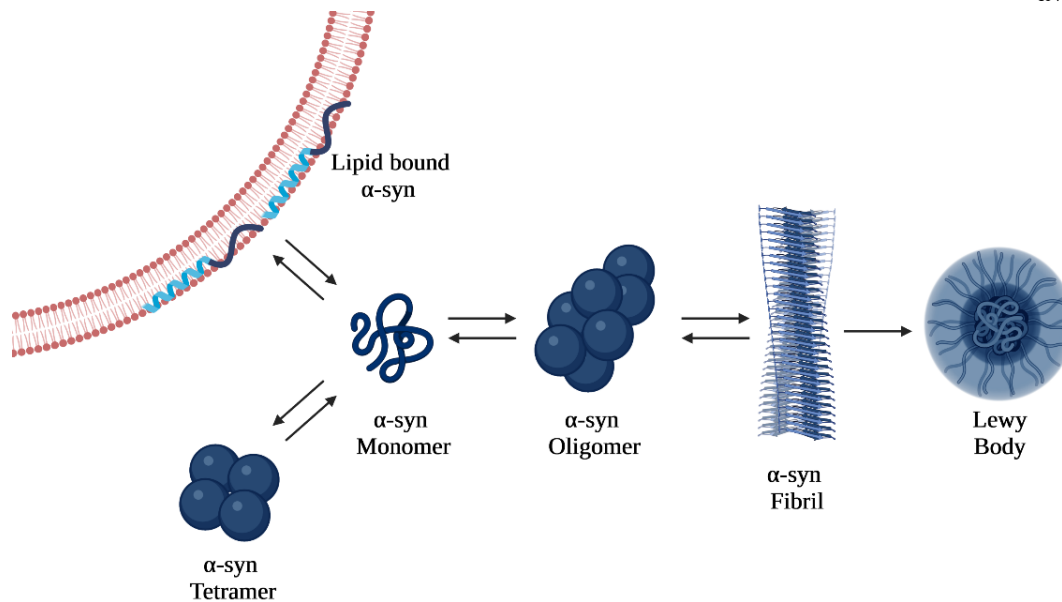
Figure 1.4 α-synuclein aggregation. Monomeric α-synuclein exists as a soluble monomer which can bind lipid membranes to form an α-helical structure and there is evidence that it also exists in equilibrium with stable tetramers. Monomeric α-synuclein can aggregate to form soluble prefibrillar oligomeric nuclei. These nuclei can elongate into mature amyloid fibrils. Fibrillar aggregates may then be sequestered into Lewy bodies or Lewy neurites. Adapted from (Cox *et al.*, 2014) and (Du *et al.*, 2020). Created in BioRender.

1.2.2 α-synuclein: Post-translational Modifications

Several post-translational modifications (PTMs) in α-synuclein have been described. These PTMs lead to alteration in the protein's structure and charge, thus affecting its interactions with other proteins, lipids and with itself. Furthermore, several PTMs have been shown to contribute to α-synuclein pathogenicity.

Phosphorylation

The phosphorylation of α-synuclein is a reversible PTM that has been proposed to regulate its structure, its membrane binding abilities, and impact its aggregation (Fujiwara *et al.*, 2002). Under physiological conditions, the levels of α-synuclein phosphorylation are low (Fujiwara *et al.*, 2002; Okochi *et al.*, 2000). However, under pathological conditions, phosphorylation of serine (S87, S129) and tyrosine (Y125, Y133, Y136) have been detected in aggregated α-synuclein (Figure 1.3A) (Xu *et al.*, 2015). Over 90% of α-synuclein deposition in LBs is phosphorylated at S129, in contrast to just

4% in healthy tissue, suggesting an important role of this PTM in α-synuclein pathology (Anderson *et al.*, 2006; Fujiwara *et al.*, 2002; Takahashi *et al.*, 2003). The exact kinases mediating α-synuclein phosphorylation are still not well defined, however casein kinases (Ishii *et al.*, 2007; Okochi *et al.*, 2000), polo like kinase 2 (Inglis *et al.*, 2009) and G-protein coupled receptor kinases (Pronin *et al.*, 2000; Sakamoto *et al.*, 2009) were able to phosphorylate α-synuclein in *in vitro* and animal models. Despite the fact that pS129 is found abundantly in LBs and α-synuclein aggregates, there is conflicting data on its role as it has been found to be neuroprotective in some animal studies (Gorbatyuk *et al.*, 2008) and cell models (Tenreiro *et al.*, 2014). Other studies have reported neutral findings regarding the pS129 modification enhancing or diminishing α-synuclein aggregation and neurotoxicity (Azeredo da Silveira *et al.*, 2009; McFarland *et al.*, 2009).

Ubiquitination and SUMOylation

Ubiquitination is a PTM in which ubiquitin is covalently attached to lysine (or sometimes cysteine, serine, or threonine) residues of target proteins. Ubiquitination of proteins targets them for degradation by the ubiquitin-proteasome system (UPS) or sometimes by macroautophagy. Mono-ubiquitination of α-synuclein promotes its degradation by the UPS (Abeywardana *et al.*, 2013; Rott *et al.*, 2011) whereas poly-ubiquitination leads to its degradation by the endosomal-lysosomal pathway (Tofaris *et al.*, 2011). It is well established that α-synuclein colocalizes with ubiquitin in Lewy bodies and Lewy neurites (Gómez-Tortosa *et al.*, 2000; Mezey *et al.*, 1998) and multiple studies have reported that mono-ubiquitinated α-synuclein is a predominant species within Lewy pathology (Hasegawa *et al.*, 2002; Lowe *et al.*, 1990; Tofaris *et al.*, 2003).

α-synuclein has also been found to be conjugated to small ubiquitin-like modifiers (SUMO) at lysine residues. SUMOylation by PIAS2, a SUMO E3 ligase, was shown to directly promote the aggregation of α-synuclein (Rott *et al.*, 2017). Moreover, SUMOylation impaired α-synuclein ubiquitination, preventing its degradation. Interestingly, SUMOylation by PIAS2 also increased the release of α-synuclein into the extracellular medium. Thus the authors of the study suggested the use of SUMOylation blockers to inhibit α-synuclein aggregation (Rott *et al.*, 2017). Conversely, another study found that SUMOylation of α-synuclein inhibited α-synuclein aggregation and neurotoxicity (Krumova *et al.*, 2011). Further studies would be required to resolve these seemingly contradictory findings.

Nitration

Nitration has been implicated in synucleinopathies as nitrated α-synuclein has been identified in LB inclusions as well as in the insoluble fractions of affected brain regions in patients with various synucleinopathies (Giasson *et al.*, 2000). The four tyrosine residues of α-synuclein (Y39, Y125, Y133 and Y136) are susceptible to nitration. Several studies have shown that nitration of α-synuclein accelerates oligomerization (Danielson *et al.*, 2009) and fibrillization of the protein (Hodara *et al.*, 2004). On the other hand, a different study found that nitration of α-synuclein inhibited fibril formation due to the formation of stable soluble oligomers (Yamin *et al.*, 2003). It is still unclear whether nitration of α-synuclein is a primary contributor to aggregation or whether nitration occurs upon reaction of aggregated α-synuclein with ROS. There is conflicting evidence whether nitration promotes or inhibits α-synuclein fibrillization. The impact of nitration may be dependent on which tyrosine residue is actually nitrated. Indeed, this is supported by Burai *et al* who showed distinct aggregation properties based on the nitration of different tyrosine residues of α-synuclein (Burai *et al.*, 2015).

Glycosylation

O-linked-N-acetylglucosaminylation (*O*-GlcNAcylation) is a type of glycosylation where the monosaccharide *O*-GlcNac is conjugated to serine or threonine residues of nucleocytoplasmic proteins (Hart *et al.*, 2007). *O*-GlcNAcylation has been detected on threonine residues of α-synuclein isolated from post-mortem tissue of patients with Dementia with Lewy Bodies (DLB) and from mouse models of synucleinopathy (Alfaro *et al.*, 2012; Wang *et al.*, 2010). Levine *et al* showed that *O*-GlcNAcylation of specific residues inhibited the toxicity of extracellular α-synuclein fibrils in primary cell culture experiments. Furthermore, they showed that *O*-GlcNAcylation can inhibit the aggregation of A53T α-synuclein, which is known to have a higher tendency to aggregate (Levine *et al.*, 2019). Other studies support the finding that *O*-GlcNAcylation reduces α-synuclein aggregation (Marotta *et al.*, 2012; Zhang *et al.*, 2017). Research into this PTM is still limited, thus the physiological and pathological roles of glycosylation of α-synuclein remain poorly understood and further research is required.

<u>Truncation</u>

C- and N- terminally truncated forms of α-synuclein have been found in both healthy individuals and PD patients (Baba *et al.*, 1998; Crowther *et al.*, 1998; Liu *et al.*, 2005; Muntané *et al.*, 2012), suggesting that some degree of truncation occurs under physiological conditions. Truncated α-synuclein, particularly C-terminally truncated, has been estimated to represent about 15% of all α-synuclein in LBs and LNs. These truncated α-synuclein species have been proposed to act as seeds that promote aggregation and prion-like spreading of α-synuclein (Terada *et al.*, 2018; van der Wateren *et al.*, 2018). Mouse and *Drosophila* models overexpressing α-synuclein showed the association of truncated α-synuclein with increased aggregation and neurotoxicity (Periquet *et al.*, 2007; Tofaris *et al.*, 2006). It is still unclear which cleaving proteases are responsible for the generation of the truncated α-synuclein species, although neurosin and calpain have been proposed as candidates due to their presence in Lewy bodies (Dufty *et al.*, 2007; Iwata *et al.*, 2003; Mishizen-Eberz *et al.*, 2003; Ogawa *et al.*, 2000). Cathepsin D (Sevlever *et al.*, 2008), matrix metalloproteases (Sung *et al.*, 2005) and ubiquitin-independent degradation of α-synuclein by the proteosome (Tofaris *et al.*, 2001) have also been implicated in C-terminal proteolytic cleavage of α-synuclein .

1.2.3 α-synuclein: Function

The physiological role of α-synuclein remains unclear. The structural flexibility of α-synuclein allows it to adopt a wide range of conformations depending on its environment and binding partners, thus suggesting it may have multifunctional properties. Although it is still quite unclear what α-synuclein's primary physiological role(s) is (are), various studies have implicated the protein in a variety of cellular processes.

<u>Synaptic vesicle trafficking and neurotransmitter release</u>

The fact that α-synuclein localizes to presynaptic terminals and associates with membranes strongly suggests that it plays a role in neurotransmitter release. There is conflicting evidence regarding whether it helps promote vesicle release, or whether it plays an inhibitory role. The

association of α-synuclein with vesicles is modulated by synaptic activity, as it has been observed that it dissociates from synaptic vesicles after electrical stimulation, after which it slowly reassociates (Fortin *et al.*, 2005). Transgenic expression of α-synuclein could rescue neurodegeneration and synaptic dysfunction in mice lacking the synaptic co-chaperone cysteine-string protein α. In addition, α-synuclein could reverse the soluble N-ethylmaleimide-sensitive factor attachment protein receptor (SNARE)-complex assembly impairment that was seen in cysteine-string protein α knockout mice (Chandra *et al.*, 2005). There is also evidence showing that α-synuclein directly interacts with the SNARE-complex through its binding to synaptobrevin 2/vesicle associated membrane protein 2 (VAMP2) (Burré *et al.*, 2010). The SNARE-complex plays a critical role in vesicle docking, priming, fusion and synchronization of neurotransmitter release. Triple knockout mice lacking the three synucleins (α, ß and γ) also displayed decreased SNARE-complex assembly and neurological impairments, suggesting the role of synucleins in sustaining normal SNARE-complex assembly (Burré *et al.*, 2010). α-synuclein has also been shown to regulate dopamine transporter (DAT) and vesicle monoamine transporter 2 (VMAT2), which are both proteins that regulate the amounts of free dopamine in dopaminergic neurons (Sidhu *et al.*, 2004).

Synucleins are only present in vertebrates and no homologues have been identified in worms, flies, and yeast, suggesting that synucleins are not required for synaptic transmission or more generally for membrane trafficking. Moreover, α-synuclein knockout mice often only show subtle abnormalities in neurotransmission, indicating that α-synuclein may play a non-essential role at the synapse.

Anti-apoptotic activity

α-synuclein has been shown to play a neuroprotective role by being anti-apoptotic. Jin *et al.*, found that α-synuclein can suppress apoptosis in dopaminergic neurons through the negative regulation of protein kinase Cδ (Jin *et al.*, 2011). Another study demonstrated that wild type α-synuclein as well as the A30P mutant lead to the protection of neuronal cell lines from apoptosis through the attenuation of caspase-3 activity (Li & Lee, 2005). This was further supported by Costa *et al* who also showed that α-synuclein lowered the p53-dependent caspase-3 activation in response to apoptotic stimuli (Alves da Costa *et al.*, 2002).

Regulation of dopamine biosynthesis

In 2002, Perez *et al* proposed a role for α-synuclein in dopamine biosynthesis. The rationale of the study was that α-synuclein has homology with the chaperone molecule 14-3-3, which binds to and activates tyrosine hydroxylase (TH), the rate limiting enzyme in dopamine production. They confirmed that α-synuclein indeed bound TH in brain homogenates and in MN9D dopaminergic cells using immunoprecipitation and immunoelectron microscopy. Interestingly, they found a dose-dependent inhibition of TH by α-synuclein. Given this, they suggested that loss of soluble α-synuclein, for example by aggregation, could increase dopamine biosynthesis which could simultaneously increase the presence of reactive dopamine metabolites (Perez *et al.*, 2002).

Nuclear function

Despite the fact that α-synuclein was reported to be present in the nucleus upon its discovery (Maroteaux *et al.*, 1988), there has been some debate over its nuclear localization as some studies were unable to reproduce this observation (George *et al.*, 1995; Iwai *et al.*, 1995). The cause of this discrepancy has been attributed to the cross-reactivity of antibodies used against α-synuclein during immunohistochemistry with other non-α-synuclein proteins in the nucleus (Huang *et al.*, 2011). However, more recent studies have confirmed the localization of α-synuclein in the nucleus using other methods including chromatin immunoprecipitation (Siddiqui *et al.*, 2012) and subcellular fractionation (Pinho *et al.*, 2018; Zhou *et al.*, 2013). Koss *et al* used multiple approaches including immunohistochemistry along with immunoblot and mass spectrometry to confirm the presence of α-synuclein within the nuclei of post-mortem brain tissue from both DLB patients and control individuals (Koss *et al.*, 2022). Interestingly, they observed higher levels of pS129 α-synuclein and aggregated α-synuclein in the DLB nuclei, which may have implications on disease pathogenesis or progression.

It is still quite unclear what the physiological role of α-synuclein is in the nucleus. Some studies have reported that α-synuclein's interaction with DNA may influence transcription and is thus important for normal cellular functioning (Kim *et al.*, 2014; Pinho *et al.*, 2019; Siddiqui *et al.*, 2012). Supporting this, it has been shown that α-synuclein normally binds retinoic acid and translocates to the nucleus to selectively enhance gene transcription (Davidi *et al.*, 2020). A 2019 study from Schaser and colleagues have reported a novel role of α-synuclein as a player in the DNA damage response. They found colocalization of α-synuclein with DNA damage foci under

physiological conditions in human and mouse cells. Removal of α-synuclein and knockout models showed an increase in double strand breaks. They proposed that under pathological conditions, α-synuclein is diverted from the nucleus into cytoplasmic LBs, and thus cannot perform one of its functional roles in promoting DNA repair (Schaser *et al.*, 2019). This hypothesis would indeed have interesting implications for PD pathogenesis.

1.2.4 α-synuclein: Dysfunction

The presence and accumulation of α-synuclein has been associated with not only PD, but other neurodegenerative diseases such as DLB and multiple system atrophy. Collectively, these diseases are known as synucleinopathies. Under pathological conditions, the NAC domain of α-synuclein becomes destabilized and can adopt an insoluble ß-sheet amyloid conformation to form pathological species of α-synuclein (Emamzadeh, 2016). PD associated mutations in *SNCA* A30P and A53T have been shown to promote the formation of protofibrillar aggregates of α-synuclein (Lashuel *et al.*, 2002a). Other factors also increase the propensity of α-synuclein to form fibrils, including environmental toxins, oxidative stress, PTMs, and high metal concentrations (Manzanza *et al.*, 2021). Fibrillar and oligomeric forms of α-synuclein have been posited to play various dysfunctional roles.

Synaptic dysfunction

Given the physiological role of α-synuclein at the synapse, it is likely that pathological α-synuclein induces synaptic dysfunction. Oligomeric α-synuclein has been shown to inhibit SNARE-complex formation, thus impeding the fusion of synaptic vesicles with the plasma membrane and reducing neurotransmitter release (Choi *et al.*, 2013; Garcia-Reitböck *et al.*, 2010). Sequestration of the synaptic proteins VAMP2 and synaptosomal associated protein 25 (SNAP25) by α-synuclein aggregates has been reported to contribute to neurotoxicity (Choi *et al.*, 2018). Furthermore, exogenous treatment of primary neurons with α-synuclein pre-formed fibrils (PFFs) led to the

formation of inclusions resembling Lewy bodies and Lewy neurites, and these were associated with the selective reduction of synaptic proteins, including VAMP2 and SNAP25, and the disruption of network activity (Volpicelli-Daley *et al.*, 2011). Another study also supported these findings in an α-synuclein overexpression mouse model where accumulation of α-synuclein was found to decrease the levels of synapsins and complexins, important mediators of neurotransmitter release (Nemani *et al.*, 2010). The same study showed that the accumulation of α-synuclein inhibited synaptic vesicle exocytosis and disrupted synaptic vesicle clustering (Nemani *et al.*, 2010). Altogether, these studies highlight the contribution of pathological α-synuclein to synaptic dysfunction, which has significant implications on PD and other related synucleinopathies.

Mitochondrial dysfunction

Physiochemical properties of the N-terminal region of α-synuclein gives the protein a high affinity for mitochondrial membranes (Nakamura *et al.*, 2008). Some studies have provided evidence that α-synuclein may play a direct physiological role in mitochondrial size maintenance through influencing mitochondrial fusion and fission (Nakamura *et al.*, 2011; Pozo Devoto *et al.*, 2017). PD associated mutations in *SNCA*, which are all located in the N-terminal region affect the membrane binding affinity of the protein, cause different effects on mitochondrial fragmentation (Pozo Devoto *et al.*, 2017). Mice α-synuclein are more susceptible to the toxic effects of 1-methyl-4-phenyl-1,2,3,6-tetrahydropyridine (MPTP) in contrast to *SNCA* knockout mice which do not show this same susceptibility, indicating that mitochondria are involved in toxicity related to α-synuclein (Dauer & Przedborski, 2003; Klivenyi *et al.*, 2006). Post-translationally modified α-synuclein binds to translocase of outer membrane (TOM20) and this has been demonstrated to inhibit the import of proteins into the mitochondria both *in vitro* and *in vivo*. Moreover, an abnormal association between α-synuclein and TOM20 was seen in nigrostriatal dopaminergic neurons in postmortem tissue of PD patients, and this correlated with a loss in imported mitochondrial proteins (Di Maio *et al.*, 2016). Accumulation of α-synuclein in the mitochondria of human dopaminergic neurons has been reported to reduce mitochondrial complex I activity and increase the production of ROS (Devi *et al.*, 2008). This is consistent with previous studies showing complex I deficiency in PD patient brains (Parker *et al.*, 2008; Schapira *et al.*, 1990). The interaction of α-synuclein oligomers with mitochondrial membranes leads to mitochondrial fragmentation which is followed by a decline in respiration and neuronal death (Nakamura *et al.*, 2011). Collectively, these observations highlight a

role for α-synuclein in regulating mitochondrial function and thus accumulation of the protein or mutations can contribute to bioenergetic defects observed in PD.

<u>Nuclear dysfunction</u>

Overexpression of α-synuclein in hippocampal nuclei has been shown to lead to memory and motor impairments in mice (Pan *et al.*, 2022). The authors speculated that this nuclear overexpression of α-synuclein induced DNA damage in hippocampal neurons, leading to aberrant blocking of the cell cycle, apoptosis induction, and an inflammatory reaction. They further suggested that nuclear translocation of α-synuclein may contribute to cognitive decline in mice due to hippocampal neuron decline. (Pan *et al.*, 2022). They did not however relate how this could be translated in or relevant to the human context. Chronic nuclear accumulation of endogenous α-synuclein has also been shown to elicit toxic phenotypes such as motor impairment and cortical dysfunction in mice, independent of aggregation (Geertsma *et al.*, 2022). Kontopoulos *et al* showed that α-synuclein promotes neurotoxicity by inhibition of histone acetylation in the nucleus. Furthermore, A30P and A53T α-synuclein mutants were found to be increasingly targeted to the nucleus compared to the wild type version (Kontopoulos *et al.*, 2006). Oxidized and oligomeric α-synuclein were shown to induce DNA damage in *in vitro* models. It was proposed that DNA nicking activity was mediated by the chemical nuclease activity of an oxidized peptide segment in misfolded synuclein (Vasquez *et al.*, 2017). As the nuclear role of α-synuclein gains more attention, it is likely that novel pathogenic mechanisms associated with its nuclear expression will be revealed.

1.3 PD Modeling

Disease modeling has played a crucial role in understanding the pathogenesis and progression of PD. While the use of post-mortem brain tissue from patients has provided immense insights into the disease, this only reflects the end point of disease and thus only offers a snapshot of the complex disease etiology. Furthermore, studying post-mortem tissues does not allow for the temporal study of disease progression and offers limited opportunities for experimental intervention. Historically, animal models, most notably rodent models, have been used to study PD

in a laboratory setting. Recently, cell models have emerged as a relevant and useful tool in the study of the disease.

1.3.1   Animal Models

The evolutionary conservation of basic biological principles has allowed for the use of animal models to provide insights into the mechanisms underlying human development and disease. Establishing relevant models has been an important aspect in better recapitulating PD specific pathology. Three major animal groups have been commonly used in PD modeling, namely rodents, non-human primates, and non-mammalian species. Rodents have often been used due to their ease of care in a laboratory setting, as well as the widespread availability of transgenic
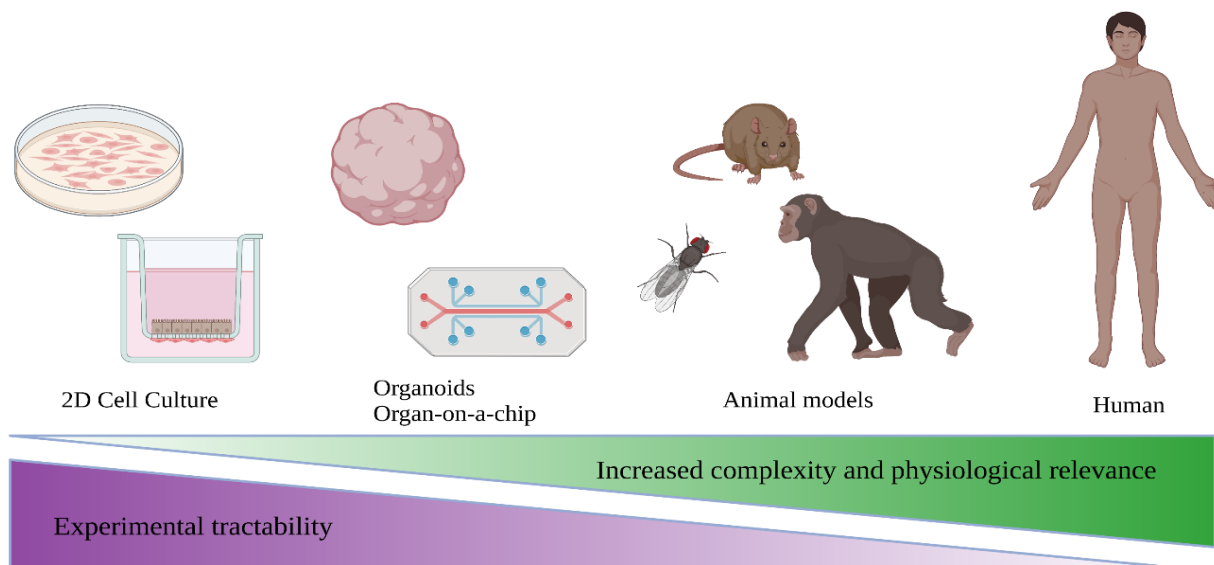

Figure 1.5 PD Model Systems. Various model systems have been used for studying PD ranging from 2D cell culture models to human material. The model systems lie on a spectrum of complexity and physiological relevance, as well as ease of experimental manipulation. Adapted from (Aguilar *et al.*, 2021; Jackson & Lu, 2016). Created in BioRender.

models and well-established protocols for studying physiology and behavior. Nigrostriatal deficiencies in mice have been shown to directly correlate to motor deficits which can be measured

and assessed within a laboratory setting. The use of rodent models however presents several limitations. The human brain far exceeds the complexity of mouse and rat counterparts. Some cell types, such as outer radial glia which are found in the human cortex are absent, or only present in very small numbers, in rodents (Lui *et al.*, 2011). Moreover, most PD rodent models are based on the use of neurotoxins such as 6-hydroxydopamine and MPTP, which selectively accumulate in the SNpc leading to dysfunction and cytotoxicity (Javier *et al.*, 2016). While these models can replicate some of the cellular dysfunction seen in PD, the extent to which they effectively reproduce the human situation is highly contentious. Genetic mouse models, where PD related mutations are introduced into mice, offer a promising alternative to neurotoxic models, however, many studies have been unable to observe significant DA neuron loss (Goldberg *et al.*, 2003; Hinkle *et al.*, 2012; Sanchez *et al.*, 2014).

Non-human primates are very closely genetically and physiologically related to humans and thus can provide critical insights that may not be recapitulated in rodent or other animal models. Parkinson's related pathology is usually induced using neurotoxins or delivery of abnormal proteins by viral delivery. However, working with non-human primates is expensive, labor intensive and has significant ethical considerations. Non-human primate studies are thus often limited to preclinical evaluation of promising therapeutic interventions.

Non-mammalian species, such as *Caenorhabditis (C.) elegans* and *Drosophila* have also been used as models of PD in the past few decades. Due to the ease of generating genetic manipulations, their rapid reproductive cycles, low maintenance costs and well-established neuropathology and behavior, they offer strong advantages in comparison to other animal models. However, the limited neurological complexity that they present in comparison to the human brain limits their utility and translatability.

1.3.2 2D iPSC Derived Cultures

In 2006, Shinya Yamanaka and his team revolutionized the field of stem cell technology with their study demonstrating the reprogramming of somatic cells to a stem cell-like state by the forced expression of four transcription factors, Oct4, cMyc, Klf4 and Sox2 (Takahashi & Yamanaka,

2006). These cells, so called induced pluripotent stem cells (iPSC), had the ability to be differentiated into cell types from mesoderm, ectoderm, and endoderm lineages, if exposed to the right conditions and factors. Since then, the derivation of specific cell types has become a powerful research tool across the fields of regenerative medicine, disease modeling and drug discovery.

The development of iPSC derived midbrain dopaminergic neuron cultures has been instrumental in probing the underlying molecular mechanisms of PD. Several protocols have been developed to generate midbrain DA neurons based on what is known of midbrain development during embryogenesis (Arenas *et al.*, 2015; Marton & Ioannidis, 2019). To generate DA neurons, iPSC are initially directed towards a neuroectodermal fate through dual SMAD inhibition, which is the inhibition of TGFβ/activin/nodal and BMP pathways (Chambers *et al.*, 2009). Midbrain floor plate identity is then specified by modulation of sonic hedgehog (SHH), wingless-related integration site (WNT) and fibroblast growth factor (FGF) 8 signaling, and from this, midbrain DA progenitors are generated. Neurotrophic factors such as brain-derived neurotrophic factors (BDNF), glial-derived neurotrophic factors (GDNF), and ascorbic acid are used to differentiate and mature the DA neurons (Galet *et al.*, 2020).

Since the development of robust DA neuron differentiation protocols, numerous studies have investigated PD relevant phenotypes in midbrain DA neurons derived from PD patient iPSC harboring monogenic PD mutations (e.g., *SNCA, LRRK2, PINK1* and *PRKN*) as well as those with sporadic disease (Li *et al.*, 2018). Several converging pathological mechanisms that contribute to PD pathogenesis have been reported *in vitro,* including increased α-synuclein expression, mitochondrial dysfunction, reduction in neuronal arborization, impaired autophagy, and altered cellular stress response (Delenclos *et al.*, 2019; Sison *et al.*, 2018).

While iPSC derived midbrain DA cultures have provided novel insights into cellular and molecular dysfunction in PD, these models do have some limitations. Typically, these cultures may lack the neuronal maturity due to the limited time frame of differentiation (usually up to 3 months). In addition, these cultures lack the establishment of synaptic connections to other relevant cell types (Falkenburger & Schulz, 2006). This has been partially addressed by the establishment of co-culture systems as well as the use of microfluidic devices that can recreate direct contact between DA neurons and other cell types. However, these systems do not allow for the concomitant development of midbrain DA neurons with other cell types as it occurs *in vivo*, and thus limiting the maturity and complexity of the cells.

1.3.3   Brain Organoid Models

Advances in human stem cell research and the subsequent emergence of organoid technology has expanded model systems that can be used for studying human development and disease modeling. Organoids are three-dimensional (3D) cell cultures derived from pluripotent stem cells that mimic the structure, function, and cellular complexity of human organs. To date organoids have been generated for several organ systems including intestinal, liver, thyroid, kidney, endometrium, and prostate (Corsini & Knoblich, 2022; Kim *et al.*, 2020). The use of human 3D organoids, as well as other technological advancements like single-cell transcriptomic techniques, has revealed unprecedented insights into human biology and disease mechanisms, especially those that distinguish humans from other species.

In 2013, Lancaster and colleagues published a landmark study describing the generation of cerebral organoids and their use for disease modeling of microcephaly (Lancaster *et al.*, 2013). Since then, various protocols have been developed allowing for the development of regionally specific brain organoids including dorsal (Kadoshima *et al.*, 2013; Qian *et al.*, 2016; Yoon *et al.*, 2019) or ventral (Bagley *et al.*, 2017; Birey *et al.*, 2017) forebrain, cerebellum (Muguruma *et al.*, 2015; Nayler *et al.*, 2021), thalamus (Xiang *et al.*, 2019), hypothalamus (Qian *et al.*, 2016), hindbrain (Eura *et al.*, 2020) and midbrain (Jo *et al.*, 2016; Monzel *et al.*, 2017; Nickels *et al.*, 2020; Tieng *et al.*, 2014).

In the context of PD modeling, human midbrain organoids (hMO) have been developed and used to understand cellular and molecular mechanisms underlying the disease. To generate hMO, signaling cues experienced at the center of the rostral-caudal axis in the developing brain are mimicked. SHH and WNT3A agonists are administered to the developing neural epithelium to attain a midbrain floor plate-like identity and the cells are further maintained in BDNF and GDNF under 3D conditions. Once mature, the resulting hMO contain functional post-mitotic midbrain DA neurons, in addition to glial cells like astrocytes and oligodendrocytes (Jo *et al.*, 2016; Monzel *et al.*, 2017; Nickels *et al.*, 2020). Importantly, a combination of single cell RNA-seq analysis, imaging and electrophysiological analysis revealed that in addition to midbrain DA neurons, hMO also contain other neuronal subtypes including serotoninergic, GABAergic and glutamatergic neurons (Smits *et al.*, 2020), highlighting the complexity of the cellular model.

hMO have emerged as a relevant tool to complement and address limitations of existing PD models. In comparison to *in vitro* midbrain DA neuron cultures, hMO show a transcriptomic profile that is more representative of the prenatal midbrain (Galet *et al.*, 2020). Indeed, single cell RNA-seq analysis confirmed the similarity between hMO and the developing fetal midbrain (Zagare *et al.*, 2022). The concomitant development of glial cells such as astrocytes and oligodendrocytes with neurons in hMO further serves as an improvement from 2D cultures, as this mimics the cues and temporal dynamics that occur during brain development. Moreover, there is mounting evidence for a significant role of astrocyte dysfunction in PD (Booth *et al.*, 2017; Wang *et al.*, 2021), therefore hMO also provide an opportunity to study this aspect of PD etiology. Given the hypothesis that PD may have a neurodevelopmental component (Schwamborn, 2018), the ability to model human midbrain development *in vitro* allows for a unique opportunity to explore this hypothesis.

PD appears to be a human specific disease, as parkinsonism has not been observed in any species outside of *homo sapiens* (Diederich *et al.*, 2019), highlighting the need for human specific models to better understand this complex disorder. Up until recently, most human based studies were limited to postmortem tissue, which only provide an snapshot of the end point of disease, and do not allow the distinction of whether the changes observed are a cause or consequence of disease (McComish *et al.*, 2022). hMO studies can complement postmortem tissue studies as they allow the study of disease progression over time, although it is important to note the limitation that the hMO are more reflective of embryonic stages of development. Nonetheless, they are able to address questions which may not be possible with postmortem tissue, while having the benefit of being human derived cells as opposed to animal-based models.

hMO have been used to model various genetic forms of PD. Patient derived hMO harboring the LRRK2-G2019S mutation showed PD relevant phenotypes such as reduced number and complexity of the DA neurons, which has been observed in PD patient brains (Smits *et al.*, 2019). Consistent with these findings, Kim *et al* reported LRRK2-G2019S hMO had decreased midbrain DA neuron neurite length and reduced expression of midbrain DA neuron identity markers such as TH, DAT, NURR1, PITX2 and EN1 by 60 days of organoid maturation (Kim *et al.*, 2019). Additionally, they found higher levels of pS129 α-synuclein in endosomal compartments. Human MO harboring *PINK1* mutations show reduced differentiation efficiency to dopaminergic neurons compared to controls. This was rescued by treatment with 2-hydroxypropyl-β-cyclodextrin which increased the autophagy and mitophagy capacity of neurons in the PINK1-MO concomitant with an improved

dopaminergic differentiation of patient-specific neurons in hMO (Jarazo *et al.*, 2022). Thus, this study revealed the utility of hMO for drug screening. Another extensive study used hMO to investigate the role of *PRKN*, *PARK7* (DJ1) and *ATP13A2* by knocking out the genes in independent healthy isogenic iPSC lines. Proteomic analysis showed dysregulation of lysosomal and mitochondrial function in hMO derived from all the lines (Ahfeldt *et al.*, 2020) Interestingly, they only observed increased DA neuron death in the MO in the *PRKN* knockout. The *PRKN*-/- MO also showed an upregulation of pathways associated with oxidative phosphorylation, mitochondrial dysfunction, and Sirtuin signaling, as well as a significant depletion of mitochondrial proteins. Therefore, hMO are able to reveal mutation specific pathogenic mechanisms. Importantly, these studies show that hMO can faithfully reproduce PD related hallmarks, which are not consistently observed in genetic animal models. For example, transgenic mice expressing mutant forms of LRRK2 often exhibit limited or no neurodegeneration (Dawson *et al.*, 2010). Several transgenic mouse models expressing different α-synuclein species related to PD pathology have also been developed, however these have also yielded mixed results ranging from a lack of Lewy pathology, to limited dopaminergic degeneration and minimal motor deficits (Thiruchelvam *et al.*, 2004; Wakamatsu *et al.*, 2008).

Taken together, there is a growing body of research highlighting the usefulness and relevance of hMO for modeling PD. This model is well suited to complement some of the limitations of other PD models and therefore its use in the field is rapidly growing.

2. *Motivation and Aims*

PD currently affects millions of people globally, and due to an ever-growing aging population, this number is set to continue growing. Despite extensive research efforts, the pathophysiology of PD is still not fully understood. To date there are no curative treatments for the disease, and current therapeutic interventions only serve to ameliorate specific symptoms. Until recently, there was a significant dependence on animal models for the study of PD, however, these models have not been able to recapitulate some of the pathological hallmarks observed in patients. Interestingly, while some neurological disorders have been observed in non-human mammals, PD appears to be human specific as no spontaneous akinetic-rigid syndrome has been observed in wild mammals including non-human primates. This highlights the importance of a human context in the study of PD.

The advent of hMO has presented an opportunity to generate a human specific model that shows physiological and functional resemblance to the midbrain, which is the most affected brain region in PD. In this thesis, I explore the use of patient-specific hMO for the modeling of two genetic forms of PD with the goal of identifying mechanisms that underlie PD pathogenesis and progression (Manuscript I and II). Additionally, I highlight the need for further advancements in the hMO models and explore the use of microfluidic chips to achieve better long-term culturing of the organoids (Manuscript III).

Thus, the specific aims of this thesis were as follows:

1. Generation and characterization of patient-specific midbrain organoids for PD *in vitro* modeling with a focus on mutations in *SNCA* and *LRRK2*.
2. Validation of the occurrence of PD related pathology in the patient-specific organoids to show their ability to mimic relevant PD hallmarks.
3. Identification of converging pathological mechanisms in patient-specific organoids with different PD related mutations, namely *SNCA* triplication and LRRK2-G2019S.
4. Explore the utility of microfluidic devices to improve midbrain organoid cultures.

3. *Materials and Methods*

All comprehensive information concerning the material and methods that were used in this thesis can be found in the original articles listed in Chapter 4. The following section lists the experimental procedures I conducted myself or took part in.

Methods

hiPSC Culture

see Manuscript I (Muwanigwa *et al., 2023)*

Derivation and Culture of Neuroepithelial Stem Cells

see Manuscript I (Muwanigwa *et al., 2023)*

Generation of Human Midbrain Organoids

see Manuscript I (Muwanigwa *et al., 2023)*

Immunofluorescence Staining

see Manuscript I (Muwanigwa *et al., 2023)*

see Manuscript II (Bolognin *et al., 2023)*

see Manuscript III (Spitz *et al., 2019)*

Western Blot Assay and Analysis

see Manuscript I (Muwanigwa *et al., 2023)*

Dopamine ELISA

see Manuscript I (Muwanigwa *et al., 2023)*

Confocal Microscopy

see Manuscript I (Muwanigwa *et al., 2023*)

High-Content Imaging

see Manuscript I (Muwanigwa *et al., 2023*)

see Manuscript II (Bolognin *et al., 2023*)

High-Content Image Analysis in MATLAB

see Manuscript I (Muwanigwa *et al., 2023*)

High-Content Imaging Data Analysis in R software

see Manuscript I (Muwanigwa *et al., 2023*)

Statistical Analysis in GraphPad

see Manuscript I (Muwanigwa *et al., 2023*)

4. *Results*

Manuscript I: Alpha-synuclein pathology is associated with astrocyte senescence in patient-specific midbrain organoids (**Muwanigwa *et al.*, 2023** – Submitted)

Manuscript II: The Parkinson's disease-associated mutation LRRK2-G2019S alters astrocyte differentiation dynamics and induces senescence in midbrain organoids (Bolognin *et al., 2022* – Submitted)

Manuscript III: Cultivation and characterization of human midbrain organoids in sensor integrated microfluidic chips (Spitz *et al., 2019 – in submission*)

4.1 Manuscript I

Alpha-synuclein pathology is associated with astrocyte senescence in patient-specific midbrain organoids

Mudiwa N. Muwanigwa[1], Jennifer Modamio-Chamarro[1], Paul M.A. Antony[2], Gemma Gomez-Giro[1], Rejko Krüger[3], Silvia Bolognin[1,4] and Jens C. Schwamborn[1,4]

Author affiliations:

1. Developmental and Cellular Biology, Luxembourg Centre for Systems Biomedicine, University of Luxembourg, L-4367, Belvaux, Luxembourg

2. Bioimaging Platform, Luxembourg Centre for Systems Biomedicine, University of Luxembourg, L-4367, Belvaux, Luxembourg

3. Translational Neuroscience, Luxembourg Centre for Systems Biomedicine, University of Luxembourg, L-4367, Belvaux, Luxembourg

4. Co-last authors

Preface

Point mutations and multiplications of the *SNCA* gene, which encodes α-synuclein, are associated with autosomal dominant forms of PD. Furthermore, the accumulation of pathological aggregates of α-synuclein is observed across most genetic and idiopathic forms of the disease. Despite significant research efforts, α-synuclein mediated toxicity is not fully understood, which has impeded the ability to fully understand PD etiology and develop effective therapies. In this article, we showed that patient-specific midbrain organoids harboring the *SNCA* triplication (3xSNCA hMO) recapitulate the key neuropathological hallmarks of PD, including the accumulation of aggregate-like structures reminiscent of Lewy pathology and dopaminergic decline. Consistent with other recent studies (Verma *et al.*, 2021; Yoon *et al.*, 2022), we found an association between the accumulation of pathological α-synuclein and the acquisition of a senescent-like phenotype in the 3xSNCA hMO. Therefore, this study highlights the utility of midbrain organoids in modeling PD specific phenotypes and their ability to reveal relevant pathogenic mechanisms.

This manuscript is the result of my main PhD project. I designed and conducted the experiments, performed the data analysis, conceptualized all the figures, and wrote the original draft of the manuscript. J. Modamio-Chamarro and G. Gomez-Giro contributed to optimization of several α-synuclein characterization assays. I performed high content image analysis using Matlab with the help of P. Anthony. J. Schwamborn and S. Bolognin supervised the project and contributed to writing and editing the manuscript.

Alpha-synuclein pathology is associated with astrocyte senescence in patient-specific midbrain organoids

Mudiwa N. Muwanigwa[1], Jennifer Modamio-Chamarro[1], Paul M.A. Antony[2], Gemma Gomez-Giro[1], Rejko Krüger[3], Silvia Bolognin[1,4] and Jens C. Schwamborn[1,4]

Abstract

Parkinson's disease (PD) is a complex, progressive neurodegenerative disease characterized by the loss of dopaminergic neurons in the substantia nigra pars compacta in the midbrain. Despite extensive research efforts, the molecular and cellular changes that precede neurodegeneration in PD are poorly understood. To address this, here we describe the use of patient specific human midbrain organoids harboring the *SNCA* triplication to investigate mechanisms underlying dopaminergic degeneration. Our midbrain organoid model recapitulates key pathological hallmarks of PD, including the aggregation of α-synuclein and the progressive loss of dopaminergic neurons. We found that these pathological hallmarks are associated with an increase in senescence associated cellular phenotypes in astrocytes including nuclear lamina defects, the presence of senescence associated heterochromatin foci, and the upregulation of cell cycle arrest genes. These results suggest a role of pathological α-synuclein in inducing astrosenescence which may, in turn, increase the vulnerability of dopaminergic neurons to degeneration

Author affiliations:

1. Developmental and Cellular Biology, Luxembourg Centre for Systems Biomedicine, University of Luxembourg, L-4367, Belvaux, Luxembourg

2. Bioimaging Platform, Luxembourg Centre for Systems Biomedicine, University of Luxembourg, L-4367, Belvaux, Luxembourg

3. Translational Neuroscience, Luxembourg Centre for Systems Biomedicine, University of Luxembourg, L-4367, Belvaux, Luxembourg

4.   Co-last authors

Correspondence to: Jens Christian Schwamborn

Full address: Luxembourg Center for Systems Biomedicine (LCSB)

Campus Belval – House of Biomedicine 2

6, Avenue du Swing

L-4367 Belvaux, Luxembourg

E-mail: jens.schwamborn@uni.lu

Running title: α-synuclein pathology induces senescence

Keywords: α-synuclein; astrosenescence; midbrain organoids

Introduction

As the most common movement disorder and second most common neurodegenerative disease, Parkinson's disease (PD) poses a significant healthcare and societal challenge. Pathologically, PD is characterized by the selective loss of dopaminergic neurons in the substantia nigra pars compacta of the midbrain. Moreover, PD is also characterized by the widespread presence of cytoplasmic and neuritic protein inclusions abundant in α-synuclein, known as Lewy bodies and Lewy neurites respectively.[1] α-synuclein is a small 14kDa protein encoded by the *SNCA* gene. While its structure is still debated, the general consensus at present is that it exists in a dynamic equilibrium between a cytosolic soluble, intrinsically disordered monomeric form and a lipid-bound α-helical state.[2-5] Functionally, α-synuclein has been implicated in playing a role in synaptic function and neurotransmitter release due to its presence in presynaptic terminals and due to the observation that α-synuclein directly interacts with the SNARE-complex through binding with synaptobrevin 2.[6,7] Other functions have also been proposed including antiapoptotic activity[8,9] and stabilization of the electron transport chain in mitochondria.[10] Furthermore, there is an emerging interest in α-synuclein's role in the nucleus.[11] For example, Schaser *et al* recently showed that α-synuclein can bind to DNA and modulate the repair of double strand breaks.[12] α-synuclein has also been implicated in interacting with Ras-related

nuclear protein, which transports RNA and proteins through the nuclear pore complex, thus suggesting that α-synuclein may play some role in nucleocytoplasmic transport.[13] Despite there being some evidence towards these proposed functions, α-synuclein's physiological role remains unclear.

Point mutations, duplications and triplications of the *SNCA* gene have been shown to cause early onset forms of PD, with an autosomal dominant pattern of inheritance.[14-22] Moreover, these mutations lead to the abnormal aggregation of α-synuclein and the increased presence of Lewy pathology.[23,24] Pathological α-synuclein has been associated with synaptic dysfunction, mitochondrial dysfunction, increased oxidative stress, perturbation of protein degradation systems, and nuclear dysfunction.[25-28] However, how pathological forms of α-synuclein mediate this dysfunction is not well understood.

Due to limitations in currently used model systems, understanding the temporal mechanisms that underlie α-synuclein pathology in PD remains a pertinent challenge. Rodent models that have predominantly been used in the study of PD often do not capture some of the key characteristic hallmarks observed in PD.[29] The development of stem cell derived human midbrain organoids (hMO) is a profound milestone in PD research as they recapitulate key physiological and functional aspects of the human midbrain.[30,31] These self-organizing three-dimensional tissues contain an abundance of dopaminergic neurons. In addition, they contain glial cells, show electrochemical functionality, and dopamine release.[32,33] We, and others, have described robust protocols for the development of midbrain specific organoids from induced pluripotent stem cells (iPSC).[32-34] Importantly, these organoids have been used in the modeling of various genetic forms of PD, including forms associated with LRRK2, PINK1 and DJ1.[35-38]

Here, we generate hMO from patient specific iPSC lines harboring the *SNCA* triplication, along with healthy age-sex matched controls and compare them until 90 days of organoid maturation. Our model recapitulates key hallmarks of PD, including the aggregation of α-synuclein and the progressive decline of dopaminergic neurons. Interestingly, we found that these pathological hallmarks were associated with an increase in senescence associated phenotypes specifically in astrocytes including nuclear lamina defects, the presence of senescence associated

heterochromatin foci and the upregulation of cell cycle arrest pathways. Our results suggest that pathological α-synuclein contributes to inducing senescence at early stages of PD, increasing the vulnerability of dopaminergic neurons to degeneration.

Materials and methods

iPSC, NESC and Organoid Culture

The sources of the five induced pluripotent stem cell lines (iPSC) used in this study are detailed in Supplementary Table 1. IPSC were cultured in Essential 8 medium (ThermoFisher, cat no. A1517001) with 1% Penicillin/Streptomycin (Invitrogen, cat no. 15140122) in Matrigel-coated plates (Corning, cat no. 354277). Passaging was performed with Accutase (Sigma, cat no. A6964) every 3-4 days. Following passaging, cells were cultured in Essential 8 medium supplemented with 10μM ROCK inhibitor Y-27632 (Merck Millipore, cat no. 688000) for 6-24 h after seeding. The iPSC were characterized for pluripotency markers (Supplementary Fig 1).

Neuroepithelial stem cells (NESC) were derived from iPSC as previously described.[39] NESC were maintained in Geltrex-coated plates and cultured in freshly supplemented N2B27 as described previously.[32] To obtain a homogeneous population of NESC, the cells were passaged at least five times before performing an immunofluorescence staining to confirm neural stem cell identity (Supplementary Fig 2).

Following quality assessment of the NESC by immunostaining, midbrain organoids (hMO) were generated as previously detailed[32], with slight modifications. 9000 NESC were plated in each well of an ultra-low attachment 96 well round bottomed plate (Corning, cat no. 7007) and cultured in maintenance medium for 8 days. After the 8 days, the colonies were embedded in 25μl Geltrex (Invitrogen, cat no. A1413302) and transferred to 24 well ultra-low attachment plates kept at 37°C, 5% CO_2 under dynamic conditions (80 rpm) for up to 90 days or were left unembedded in 96-well ultralow adhesion plates (round bottom, Corning, cat no. 7007).[40]

Western Blot

For Western blotting, six non-embedded organoids were lysed using RIPA buffer (Abcam, cat no. ab156034) with cOmplete™ Protease Inhibitor Cocktail (Roche, cat no. 11697498001) for 20 minutes on ice. In order to disrupt DNA, lysates were sonicated for 10 cycles (30 seconds on / 30 seconds off) using the Bioruptor Pico (Diagenode). Samples were then centrifuged at 4°C for 20 minutes at 14,000g. The protein concentration for each sample was determined using the Pierce™ BCA Protein Assay Kit (ThermoFisher, cat no. 23225). Samples were adjusted to the same concentration by appropriate dilution with RIPA buffer and boiled at 95°C for 5 minutes in denaturing loading buffer. 20μg of protein was loaded per sample for every Western blot. Protein separation was achieved using SDS polyacrylamide gel electrophoresis (Bolt™ 4-12% Bis-Tris Plus Gel, ThermoFisher) and transferred onto a PVDF membrane using iBlot™ 2 Gel Transfer Device (ThermoFisher). For α-synuclein and pS129 α-synuclein Western blots, membranes were then fixed in 0.4% paraformaldehyde (PFA) in PBS for 30 minutes at room temperature (RT), and then washed twice with PBS for 5 minutes each wash. Following PVDF transfer or fixation, membranes were blocked for 1 hour at RT in 5% skimmed milk powder and 0.2% Tween in PBS before incubating overnight at 4°C with the primary antibodies prepared in 5% BSA and 0.02% Tween (see Supplementary Table 2 for list of antibodies used). Membranes were then washed three times for 5 minutes with 0.02% Tween in PBS and incubated with DyLight™ secondary antibodies at a dilution of 1:10,000 (anti-rabbit IgG (H+L) 800, Cell Signaling, cat no. 5151P or anti-mouse IgG (H+L) 680, Cell Signaling, cat no. 5470P). Membranes were scanned in the Odyssey® Fc 2800 Imaging System and exposure time was 2 minutes for all the acquisitions. All conditions were consistently kept the same for all the Western blots at every time point. Western blots were analyzed using ImageJ software. Figures showing Western blots are cropped to display only the cell lines relevant to this study and the original uncropped Western blots can be found in Supplementary Original Blots.

Time Course Western Blot

For the time course of α-synuclein (Fig. 2B), pS129-α-synuclein (Fig. 3B) and TH (Fig 4D), Western blot analysis was performed as described in detail in the previous section. To ensure

robust comparison, the exact same conditions were maintained for each Western blot - Six pooled organoids per line for each batch; 20µg of protein loaded for SDS gel electrophoresis; same order of sample loading, same period of blocking, primary and secondary incubation; same antibody concentration; and same exposition time of 2 minutes for membrane reveal using the same instrument (Odyssey Imaging System). Following protein quantification in ImageJ, relative levels of the proteins were determined by dividing the intensity of the marker of interest with the intensity of ß-actin. These values were then used to generate the time course graph. Mean data from three independently derived organoid batches was plotted at each time point (15, 30, 50, 70 and 90 days). Data was pooled for the two wild type lines, and for the two 3xSNCA lines. To plot the time course, a smooth line of best fit was fitted over the mean value at each time point for WT and 3xSNCA using the geom_smooth function from the ggplot2 library in R (R Studio version 1.3.1073). The geom_sooth function is a non-parametric regression method used to fit a smooth curve to sparse data points. Statistical significance was calculated at each time point using Mann-Whitney U test in R. Statistically significant results were indicated when *p* values were *<0.05, **<0.01 and ***<0.001.

Fractionation of Soluble and Insoluble α-Synuclein

12 non-embedded organoids per cell line were collected and incubated in 250µl of lysis buffer (1% Triton-X 100 with protease inhibitor and phosphatase inhibitor) for 25 minutes on ice. Samples were then lysed by pipetting and sonicated for 10 cycles (30 seconds on, 30 seconds off). Lysates were transferred to ultracentrifuge tubes (Beckman Coulter Polycarbonate Centrifuge Tubes, cat no. 343776) and spun down at 100,000g for 45 minutes at 4°C. The supernatant (i.e., the soluble fraction) was collected and stored at -80°C or used immediately in Western Blot. The remaining pellet was resuspended in 120µl of 8M urea + 8% SDS and allowed to incubate for 15 minutes, after which the samples were sonicated for 10 cycles (30 seconds on, 30 seconds off). The resulting lysate represented the insoluble protein fraction, which was subsequently stored at -80°C or used in a Western Blot as already described above.

Dot Blot for α-synuclein

200µl of media was collected from three individual non-embedded organoids per line, then snap frozen or directly used. Media was thawed on ice and spun down at 300g at 4°C for 5 minutes to sediment any cell debris remaining in media. A Dot Blot Minifold I (Whatman; 10447900) was used according to manufacturer guidelines. A nitrocellulose membrane (Sigma-Aldrich, cat no. GE10600001) was re-hydrated twice with 300ul of PBS per well before sample loading. After sample run (vacuum ON), the membrane was washed with 300µl of PBS per well. Membrane was retrieved and fixed in 0.04% PFA in PBS for 30 minutes at RT, followed by 1 minute wash in PBS to remove the PFA. Blocking and antibody incubation were done exactly as previously described in the Western blotting section. Images were acquired with the Odyssey® Fc 2800 Imaging System. Images were analyzed with ImageJ. Relative α-synuclein amount was normalized to the individual organoid diameter.

Immunofluorescence Stainings for iPSC and NESC Characterization

Immunofluorescent stainings for iPSCs and NESC were perform as previously described in Gomez-Giro *et al* [41] and Monzel *et al* [32] respectively.

Immunofluorescence Staining of Organoid Sections

Immunofluorescence staining of organoids was carried out using a published protocol with slight modifications.[34] Organoids were fixed with 4% PFA overnight at 4°C, and then washed with PBS three times for 15 minutes. Individual organoids (at least three organoids per line for each time point) were embedded in 3% low-melting point agarose. Using a vibrating blade microtome (Leica VT1000s), the organoids were then sliced into 70 µm sections. The sections were permeabilized and blocked with blocking buffer (5% normal goat serum, 2.5 % BSA, and 0.1 % sodium azide) containing 0.5 % Triton X-100. Sections were incubated for 48 hours at 4 °C on an orbital shaker with primary antibodies (see Supplementary Table 2) in blocking

buffer containing 0.1% Triton X-100. Secondary antibody incubation and mounting of sections was performed as previously described.[34]

Image Acquisition

For high-content image analysis, at least three sections from three organoids of each line in three independent organoid batches were acquired using the Yokogawa CV8000 high content screening microscope with a 20x objective. For quantitative analysis of laminB1 at 40x, a confocal laser scanning microscope (Zeiss LSM710) was used. Three randomly selected fields per organoid section were acquired in at least three organoids per line for three independent organoid batches, keeping the same acquisition settings.

Qualitative images were acquired using a confocal laser scanning microscope (Zeiss LSM 710) with either a 20x, 40x or 60x objective.

Dopamine Extracellular Release

Dopamine ELISA (Immusmol BA-E-5300, cat no. BA-E-5300R) was performed for the quantitative determination of dopamine secreted by midbrain organoids at 30 days and 70 days from 3 independent organoid batches. 180 µl of media was collected per organoid (three organoids per line) and 20µl HCl buffer (0.01 M HCl, 4 mM $Na_2O_5S_2$, and 1 mM EDTA) was added to each sample. Samples were then frozen in liquid nitrogen and stored at -80°C until the day of the analysis. The ELISA was performed according to the manufacturer's instructions.

Quantitative PCR

For total RNA extraction, RNeasy Mini Kit (Qiagen, cat no. 74106) was used following the manufacturer's instructions. For cDNA synthesis High-Capacity RNA-to-cDNA™ Kit (Thermo Fisher Scientific, cat no. 4387406) was used following manufacturer's instructions.

Maxima SYBR Green qPCR Master Mix (Thermo Fisher Scientific, cat no. K0221) was used together with the following primers for *CDNK2A*: Forward primer ATCATCAGTCACCGAAGGTC and Reverse primer CTCAAGAGAAGCCAGTAACC. Quantitative PCR was performed in the Aria Mx Real-Time PCR system (Aligent) and AriaMx PC software was used for data extraction and analysis.

Image processing and analysis

Immunofluorescence 3D images of each organoid section obtained from the Yokogawa or LSM710 were processed and analyzed in Matlab (2020a, Mathworks) using a custom image-analysis algorithm as described previously.[42,43]

Data Processing and Statistical analysis

Data plots were generated in GraphPad except for Fig. 2B, 3B and 4D, which were generated in R Studio. Data are presented as mean ± standard deviation. Data was pooled for the two wild type lines, and for the two 3xSNCA lines, and denoted as WT and 3xSNCA respectively in figures. Statistical significance was calculated using Mann-Whitney U test in GraphPad or R. Statistically significant results were indicated when *p* values were $*<0.05$, $**<0.01$ and $***<0.001$. The number (*N*) of samples, replicates and batches are described in the Figure legends.

Ethics statement

The use of existing iPSC lines obtained from previous studies was approved by the local ethical committee (Comité National d'Ethique de Recherche, CNER No 201901/01). Informed consent was obtained from all individuals donating samples to this study prior to the donation using a written form and protocol. Cell lines used in this study are summarized in Supplementary Table 1.

Data availability

All original and processed data as well as scripts that support the findings of this study are publicly available at: https://doi.org/10.17881/zmmj-8z40

Results

Generation and characterization of human midbrain organoids

To investigate whether we could recapitulate PD relevant pathology *in vitro*, we generated hMO from two independent iPSC clones derived from a PD patient with the *SNCA* triplication (3xSNCA-1 and 3xSNCA-2) and two sex-age matched healthy control iPSC lines (WT-1 and WT-2) (Supplementary Table 1). An *SNCA* knockout line isogenic to WT-2 (SNCA-KO) was also included for validation of the specificity of α-synuclein antibodies in some assays. All iPSCs were positive for pluripotency markers SOX2, OCT4, TRA-1-81, TRA-1-60, NANOG, and SSEA-4 as assessed by immunocytochemistry (Supplementary Fig 1). Neuroepithelial stem cells (NESC) were derived from the iPSC lines as previously described.[39] These neural progenitors are patterned towards a midbrain/hindbrain fate, thus increasing differentiation efficiency towards midbrain cell types. We confirmed the identity of NESCs by immunostaining with SOX2, PAX6 and Nestin (Supplementary Fig 2).

To generate the hMO, we used our previously published protocol.[32] Organoids were either embedded in a Geltrex droplet and maintained under shaking conditions or kept unembedded in 96-well ultra-low attachment plates depending on the downstream assay to be performed (Fig 1A). We performed a characterization of the WT hMO to ensure that they expressed the relevant cell types of the midbrain. At 15 days of maturation, hMO display regional organization, with the presence of stem cell niches enriched in SOX2+ cells and the presence of tyrosine hydroxylase (TH) positive dopaminergic neurons in the periphery. (Fig 1B, upper panels). At 30 days, there is an abundance of MAP2 positive mature neurons, some of which are dopaminergic neurons (Fig 1B, third panel). At later time points (>50 days of
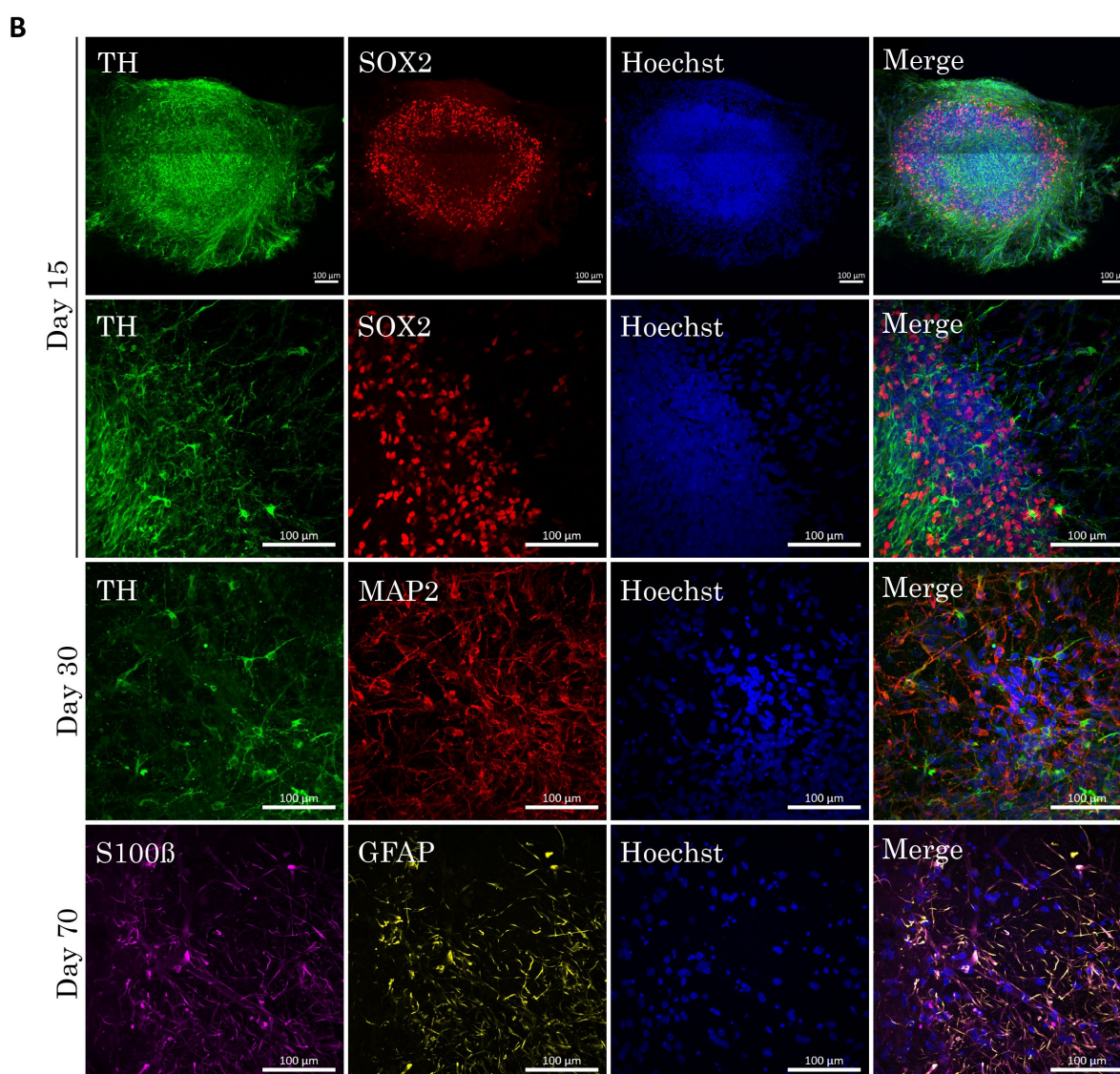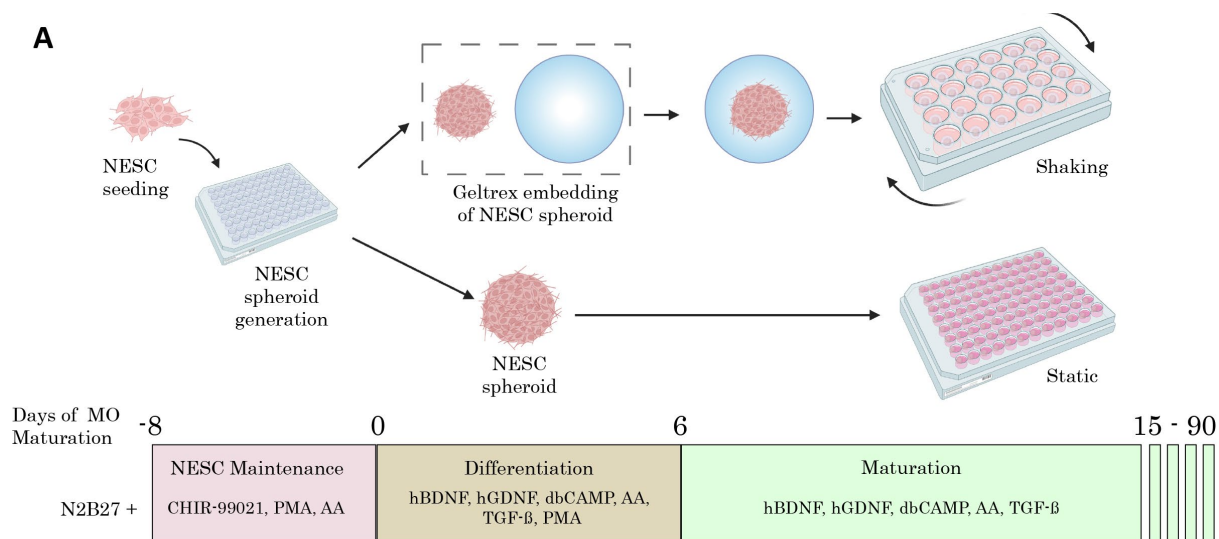
Figure 1. Recapitulation of human midbrain development in hMO. (A) Schematic overview of the hMO generation protocol. NESC – neuroepithelial stem cell. Created in BioRender. **(B)** Representative immunostainings of hMO sections at 15 days of organoid maturation, showing the

presence of TH+ dopaminergic neurons and SOX2+ neural stem cells (upper panels); 30 days of organoid maturation showing TH+ dopaminergic neurons, some of which colocalize with MAP2, a marker for mature neurons (third panel); and 70 days, showing the presence of S100β+ and GFAP+ astrocytes (lower panel). Scale bars = 100μm. TH – tyrosine hydroxylase. SOX2 – SRY-box2. MAP2 – microtubule associated protein 2. S100β – S100 calcium binding protein B. GFAP – glial fibrillary acidic protein.

differentiation) we also observe increased astrogenesis as denoted by increased presence of GFAP+ and S100β+ cells (Fig 1B, lower panel). The hMO show a progressive increase in dopamine release as they mature (Supplementary Fig 3A). Altogether, the hMO show cellular heterogeneity and the presence of functional dopaminergic neurons.

3xSNCA hMO show elevated levels of α-synuclein and α-synuclein related pathological hallmarks

The accumulation and aggregation of α-synuclein is one of the main neuropathological hallmarks of PD. To validate whether this hallmark was recapitulated in our patient specific model, we assessed α-synuclein levels in the organoids. For our analysis, we collectively compared organoids with the *SNCA* triplication (3xSNCA hMO) to the controls (WT hMO) by pooling data from organoids derived from the two 3xSNCA iPSC clones and the two WT lines respectively. Using Western blot, we found significantly higher levels of α-synuclein in the 3xSNCA hMO in comparison to the healthy WT hMO across all assessed time points ranging from 15 to 90 days of organoid culture (Fig 2A, B). Localization of α-synuclein was confirmed to be largely in neurons, as we observed colocalization of α-synuclein and the neuronal marker MAP2 (Fig 2C). Furthermore, the specificity of the α-synuclein antibody was confirmed by the lack of signal in the SNCA KO organoids. 3xSNCA hMO also showed higher extracellular release of α-synuclein in the culture medium at Day 30 (Supplementary Fig 3C, D) and Day 70 (Fig 2D) as assessed by dot blot.
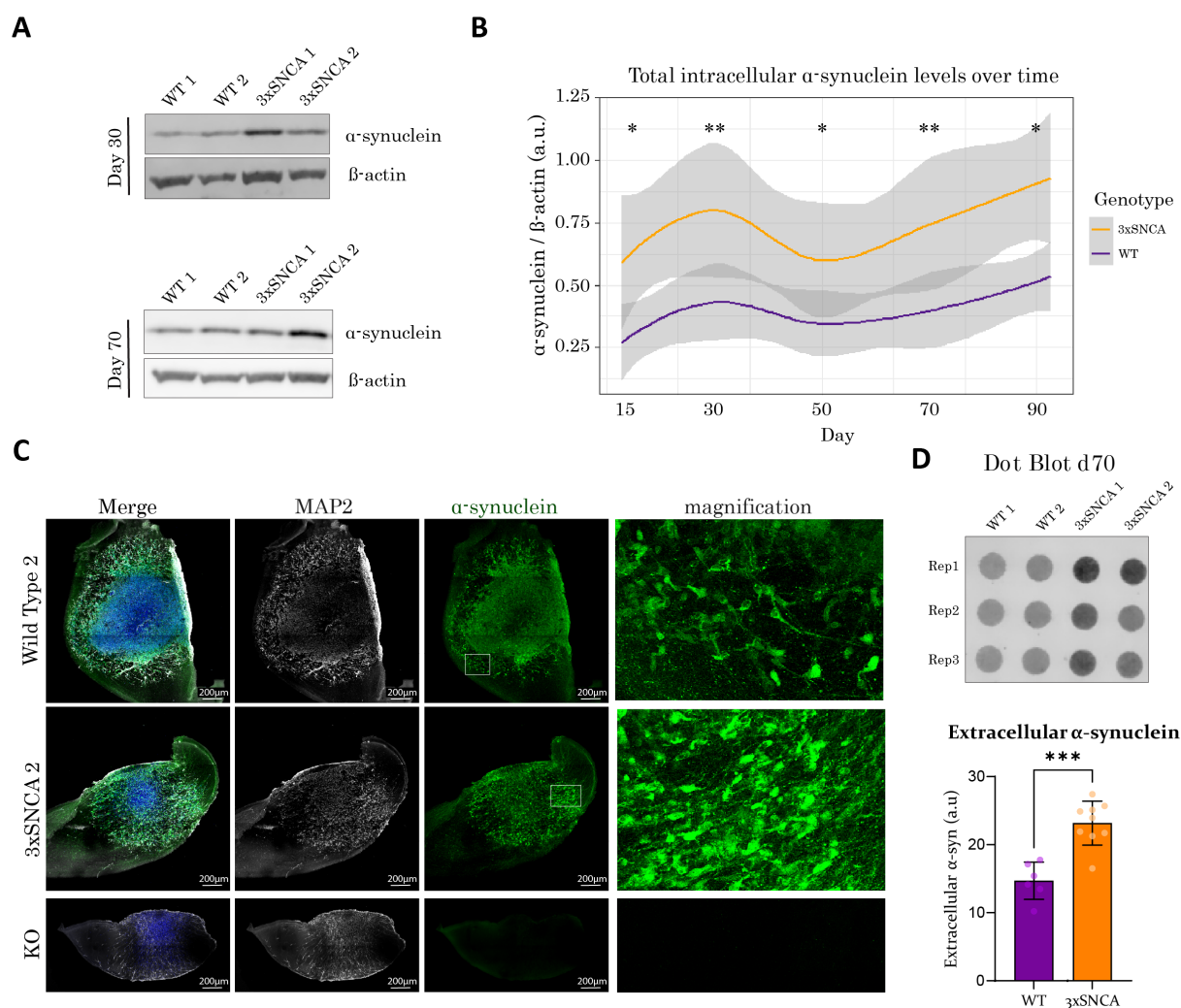
Figure 2. Increased intracellular and extracellular α-synuclein in 3xSNCA hMO. (A) Representative immunoblots of α-synuclein and β-actin at 30 and 70 days of organoid maturation in WT and 3xSNCA hMO. Western blots are cropped from original images found in Supplementary Original Blots. **(B)** Time course of intracellular α-synuclein levels as determined by immunoblots performed at 15, 30, 50, 70 and 90 days of organoid maturation. 3xSNCA hMO show consistently higher levels of α-synuclein across all time points compared to WT hMO. The data represents the summary of three independent hMO batches and is plotted by mutation (WT vs 3xSNCA). Statistical significance by Mann-Whitney U test: *$p < 0.05$ and **$p < 0.01$. Extensive description for how the graph was plotted is in materials and methods. **(C)** Representative images of 30-day old hMO stained with α-synuclein (green) and mature neuron marker MAP2 (white). Specificity of the α-synuclein antibody was confirmed by the absence of staining in the SNCA KO sections. Scale bar = 200μm. **(D)** Representative dot blot (upper panel) showing higher levels of extracellular α-synuclein released by 3xSNCA hMO (lower panel) at 70 days. Data represents points represent individual organoids from three independent hMO batches, N = 2-3 hMO per

line. Statistical significance by Mann-Whitney U test: ***p < 0.001. Rep = replicate. Dot blot is cropped from original image found in Supplementary Original Blots.

The phosphorylation of α-synuclein at serine 129 (pS129) has been associated with aggregation and toxicity of the protein and is an important hallmark of α-synuclein pathology formation.[44] We therefore assessed the levels of pS129 α-synuclein in our hMO model. We found significantly higher levels of pS129 α-synuclein in the 3xSNCA hMO across all assessed time points in Western blots (Fig 3A, B). Immunofluorescence staining also confirmed the higher levels of pS129 α-synuclein in the 3xSNCA organoids, specifically in neurons (Fig 3C). Interestingly, we could also observe the presence of pS129 rich aggregate-like structures in the neuronal cytoplasm and neurites within 3xSNCA hMO which were not observed in WT hMO (Fig 3D, Supplementary Fig 4A). These structures could potentially represent the formation of Lewy-body like pathology in the 3xSNCA hMO. Once again, we validated the specificity of the α-synuclein and pS129 α-synuclein antibodies used in the stainings by confirming the absence of signal in the 3xSNCA KO organoid sections (Fig 3C). Finally, we performed extraction of insoluble α-synuclein, which represents the aggregated form of the protein. Immunoblotting of the insoluble α-synuclein fraction showed significantly higher levels of aggregated α-synuclein in the 3xSNCA hMO at 50 days of organoid maturation (Fig 3E, F). Our findings show that 3xSNCA hMO can model the accumulation and aggregation of α-synuclein and its phosphorylated form as is observed in PD.

3xSNCA hMO show dopaminergic neuron loss

The progressive loss of dopaminergic neurons in the substantia nigra pars compacta is a key neuropathological hallmark of PD. To assess whether we observed this hallmark in our 3xSNCA hMO, we performed an immunofluorescence staining (Fig 4A), which revealed no difference in the levels of dopaminergic neurons at 30 days, as determined by quantifying the levels of TH+ neurons in the hMO (Fig 4B, left panel). However, at 70 days, we found significantly less dopaminergic neurons in the 3xSNCA hMO compared to WT (Fig 4B, right panel), showing a decline in dopaminergic neurons at the later time points in the
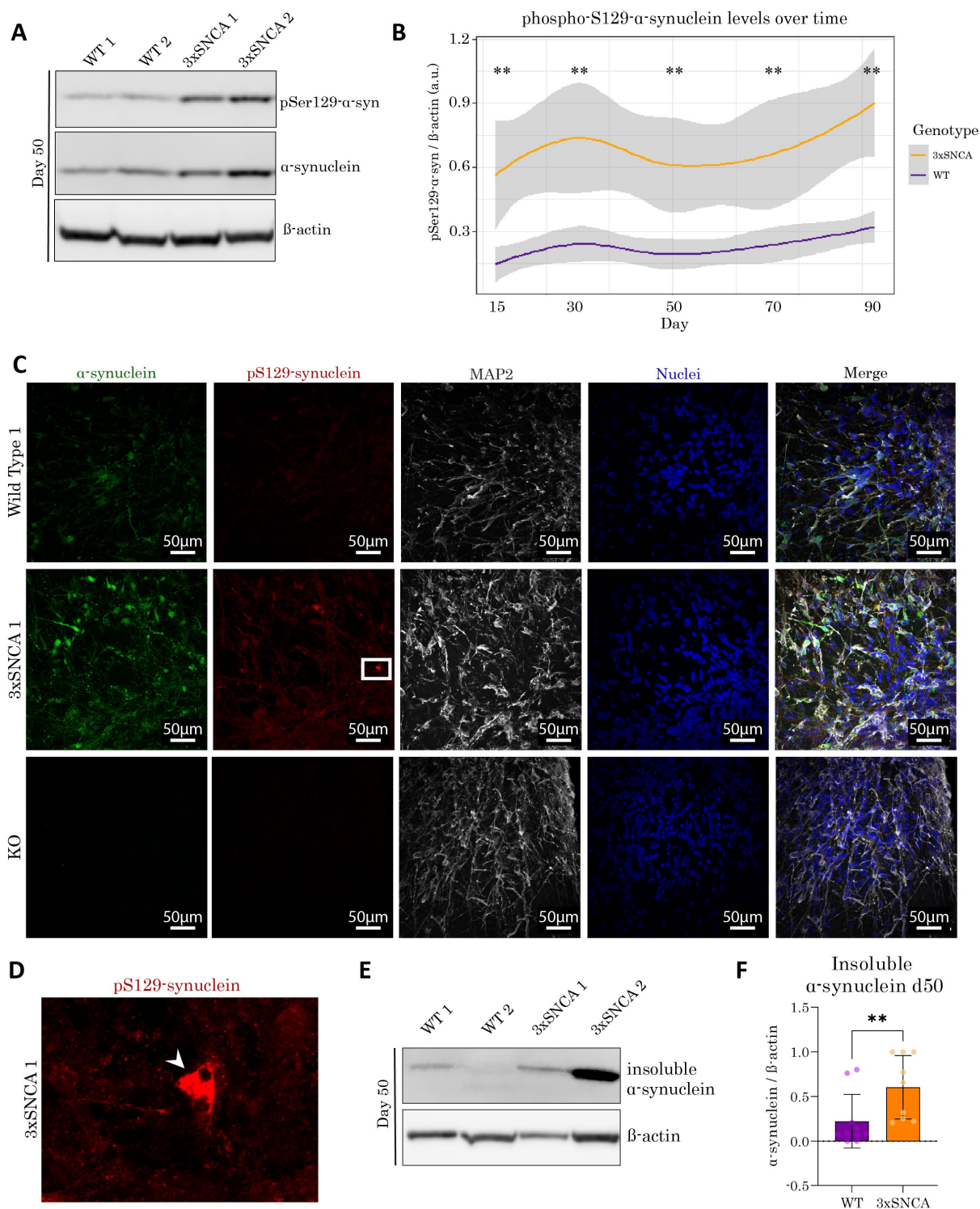
A

B

phospho-S129-α-synuclein levels over time

C

D

pS129-synuclein

E

F

Insoluble α-synuclein d50

Figure 3. Increased pS129 α-synuclein in 3xSNCA hMO. (A) Representative immunoblots of pS129 α-synuclein, total α-synuclein and β-actin at 50 days of organoid maturation in WT and 3xSNCA hMO. Western blot is cropped from original images found in Supplementary Original Blots. **(B)** Time course of intracellular pS129 α-synuclein levels as determined by immunoblots performed at 15, 30, 50, 70 and 90 days of organoid maturation. Levels of pS129 α-synuclein are higher across all time points in 3xSNCA hMO. The data represents the summary of three

independent hMO batches. Data is plotted by mutation (WT vs 3xSNCA). Statistical significance by Mann-Whitney U test: **$p < 0.01$. Extensive description for how this graph was plotted is in materials and methods. **(C)** Representative images of 70-day old hMO stained with total α-synuclein (green), pS129 α-synuclein (red) and mature neuron marker MAP2 (white). 3xhMO show presence of aggregate-like structures rich in pS129 α-synuclein (inset). Scale bar = 50μm. **(D)** Zoom in of inset in **(C)**, showing aggregated pS129 α-synuclein and the presence of structures resembling Lewy neurites (white arrows). **(E)** Representative immunoblot of insoluble α-synuclein, which represents aggregated forms of the protein, at 50 days. Western blot is cropped from original images found in Supplementary Original Blots. **(F)** Quantification of insoluble α-synuclein at 50 days of organoid maturation showing the presence of more α-synuclein aggregates in the 3xSNCA organoids. Data is from 4 independent organoid batches. Each dot represents data from an individual Western blot run, where 12 organoids were pooled per line. Statistical significance by Mann-Whitney U test: **$p < 0.01$.

patient-specific organoids. To further explore this, we assessed the protein levels of the TH enzyme across several time points from 15 to 90 days of organoid maturation using immunoblotting. We observed a tendency towards higher TH levels in the 3xSNCA hMO up until 30 days (Fig 4C, D). The TH levels subsequently dropped at later time points (after 50 days) in the 3xSNCA hMO compared with the WT hMO, and at 90 days this difference was significant. Thus, we observe a progressive loss of dopaminergic neurons in the patient-specific midbrain organoids.

Dopaminergic neurons produce and release the neurotransmitter dopamine. In the context of PD, the decline of dopaminergic neurons reduces the release of dopamine in the striatum, leading to many of the motor deficits observed in the disease. At 30 days, we found no difference in dopamine release levels in the 3xSNCA and WT hMO (Supplementary Fig 3B), whereas at 70 days we observed significantly lower levels of extracellular dopamine released by 3xSNCA hMO (Fig 4E). This observation further reflects the dopaminergic neuron decline observed in the immunostainings and Western blots. Taken together, we see that the 3xSNCA organoids show a progressive loss of dopaminergic neurons.
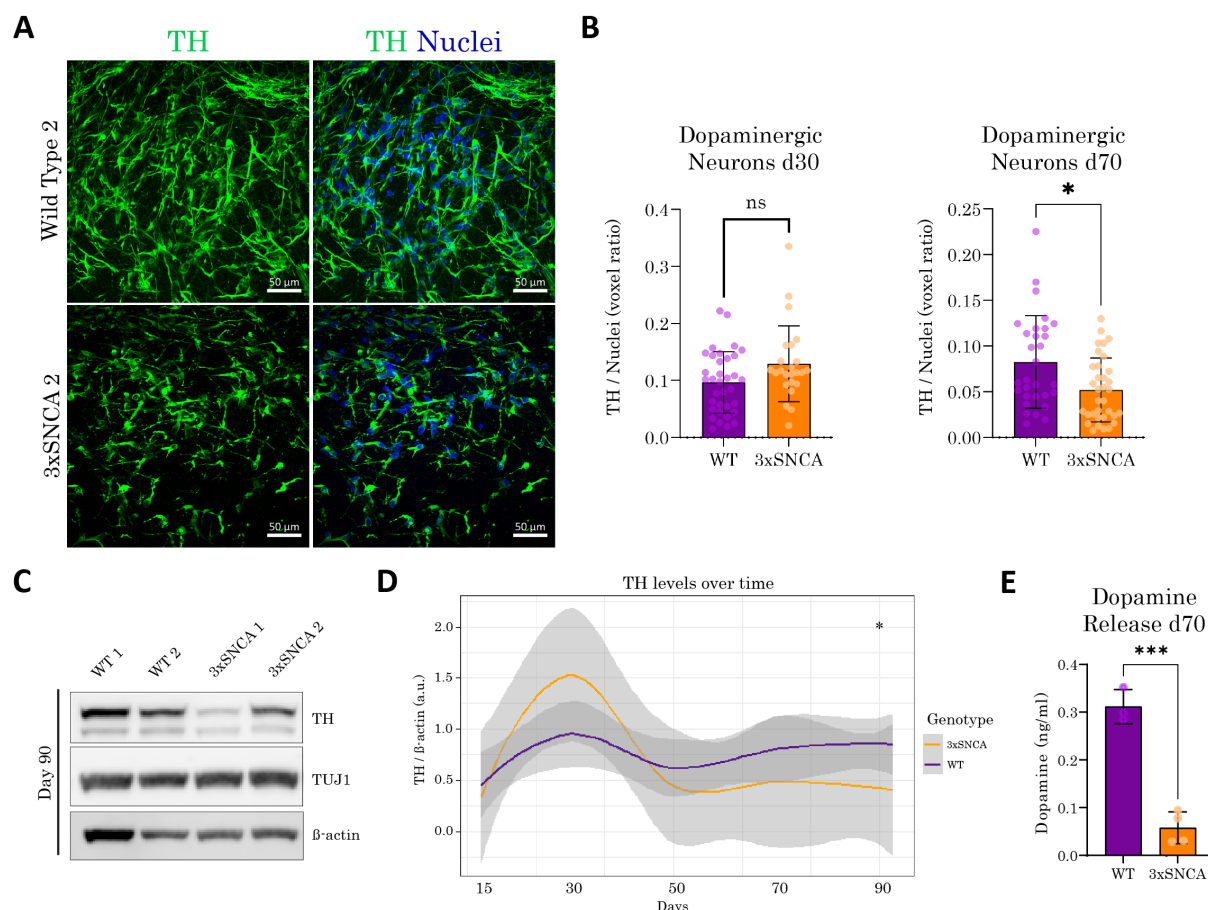
Figure 4. Dopaminergic decline in 3xSNCA hMO. (A) Representative images of 70-day old hMO sections stained with TH (green) and Hoechst (blue) Scale bar = 50μm. **(B)** Quantification of dopaminergic neuron levels at 30 and 70 days of organoid maturation. Data is from three independent organoid batches. Three to four organoids were analyzed per batch and three to six sections were analyzed per organoid. Each data point represents an individual organoid section. For 30 days: N(WT) = 35. N(3xSNCA) = 24. For 70 days: N(WT) = 30. N(3xSNCA) = 34. Statistical significance by Mann-Whitney U test: $*p < 0.05$. **(C)** Representative immunoblot of TH, TUJ1 and β-actin at 90 days of organoid maturation. Western blot is cropped from original images found in Supplementary Original Blots. **(D)** Time course of TH levels as determined by immunoblots performed at 15, 30, 50, 70 and 90 days of organoid maturation. The data represents the summary of three independent hMO batches. Data is plotted by mutation (WT vs 3xSNCA). Statistical significance by Mann-Whitney U test: $*p < 0.05$. Extensive description for how this graph was plotted is in materials and methods. **(E)** 3xSNCA hMO release less dopamine at 70 days of organoid maturation as determined by dopamine ELISA. Each data point represents four independent hMO batches where media was pooled from the wells of three organoids. For this analysis only WT-1 and 3xSNCA-1 were used. N(WT) = 3. N(3xSNCA) = 4. Statistical significance by Mann-Whitney U test: $***p < 0.001$.

Increased 3xSNCA levels are associated with a senescent-like phenotype

Senescence is a cellular state characterized by cell cycle arrest, resistance to apoptosis, nuclear dysfunction and the acquisition of a proinflammatory secretory phenotype.[45] While senescence has important physiological functions in the body, the accumulation of senescent cells has been shown to be damaging to tissues primarily due to the effects of the senescence associated secretory phenotype.[46] Senescence has emerged as a relevant mechanism in neurodegenerative diseases such as Alzheimer's and Parkinson's.[47,48] Recent studies have suggested that pathological α-synuclein may be an inducer of senescence.[49,50] Thus, we sought to investigate whether our 3xSNCA hMO model displayed any of the key senescence related hallmarks.

First, we decided to investigate the presence of senescence associated hallmarks specifically in astrocytes. PD patients have been shown to display elevated levels of astrocytes positive for senescent markers.[51] Moreover, senescence has been better characterized in astrocytes compared to neurons, due to the postmitotic nature of neuronal cells.[52] Initially, we investigated astrocyte levels in the organoids by immunofluorescence staining (Fig 5A) and strikingly we found higher levels in the 3xSNCA hMO than in the WT hMO (Fig 5B) as assessed by quantification of GFAP+ cells. Using an automated Matlab image analysis script that can extract morphometric features from images, we analyzed the complexity of the astrocytes as expressed by the number of branches (links) and points of bifurcation (nodes). This revealed more extensive branching in astrocytes in the 3xSNCA organoids, which may be indicative of increased reactivity (Fig 5C).

Next, we assessed the levels of lamin B1, a nuclear lamina protein that is important in maintaining nuclear integrity.[53,54] Loss of lamin B1 is strongly associated with cellular
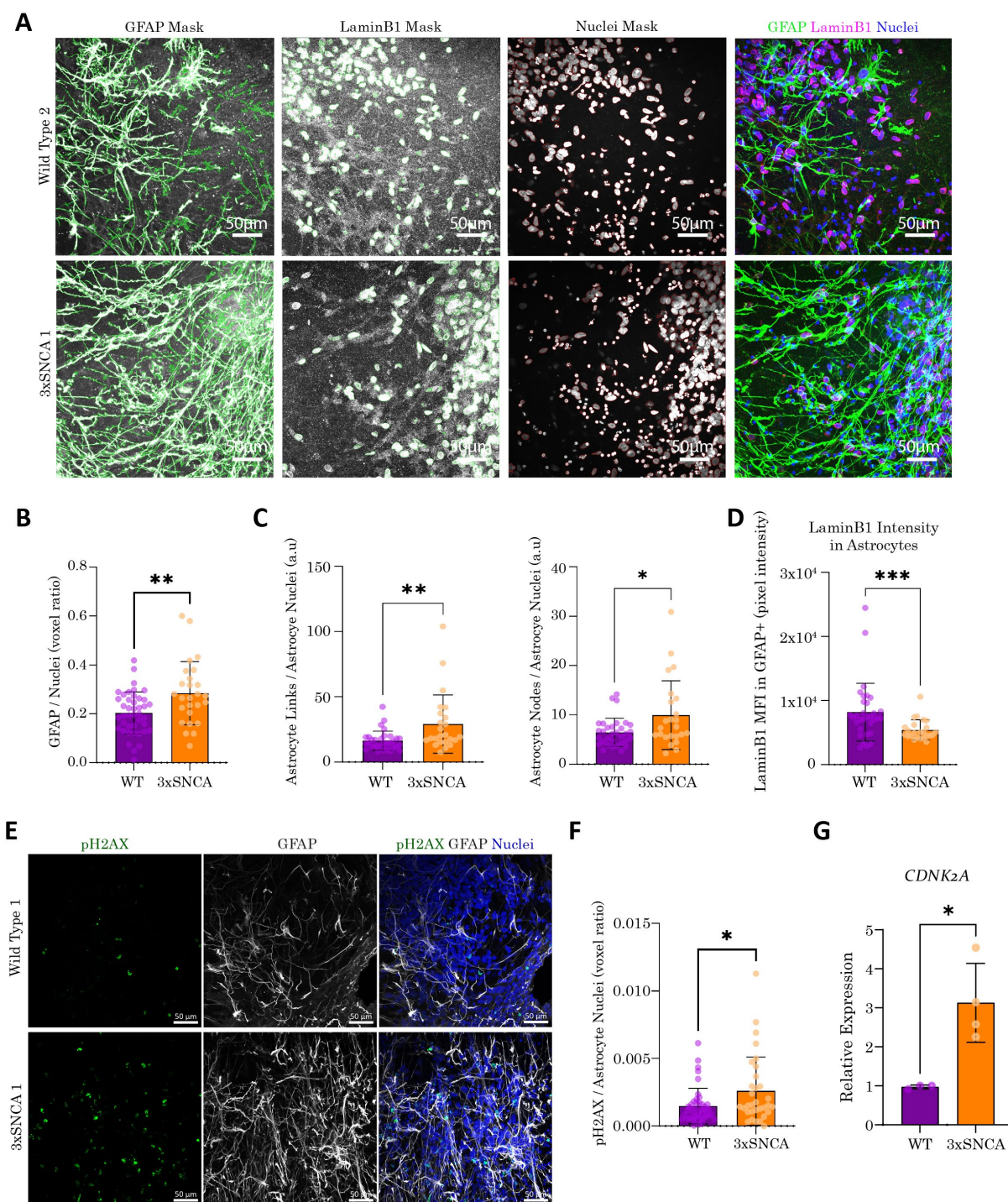
Figure 5. 3xSNCA hMO astrocytes show an increase in senescence associated hallmarks.

(A) Representative images obtained from confocal imaging of 50-day old hMO sections at 40X magnification showing GFAP, lamin B1 and nuclei masks as identified by a Matlab image analysis script. Scale bar = 50μm **(B)** 3xSNCA showed more GFAP+ astrocytes at 50 days. Data is from three independent organoid batches. Three to four organoids were analyzed per batch and three to six sections were analyzed per organoid. Each data point represents an individual organoid section. N(WT) = 32. N(3xSNCA) = 26. Statistical significance by Mann-Whitney U test: **p <

0.01. **(C)** Branching of astrocytes was assessed using a Matlab image analysis script that identifies the number of astrocyte links and nodes, normalized to the number of astrocytes (as determined by the number of nuclei in GFAP+ cells). 3xSNCA hMO astrocytes have significantly more links (left panel) and nodes (right panel), thus are more branched. Data is from three independent organoid batches. Three to four organoids were analyzed per batch and three to six sections were analyzed per organoid. Each data point represents an individual organoid section. N(WT) = 32. N(3xSNCA) = 24. Statistical significance by Mann-Whitney U test: *$p < 0.05$ and **$p < 0.01$. **(D)** The levels of lamin B1 were significantly reduced in 3xSNCA hMO astrocytes at 50 days of organoid maturation. Data is from three independent organoid batches. Three to four organoids were analyzed per batch and three to six sections were analyzed per organoid. Each data point represents an individual organoid section. N(WT) = 33. N(3xSNCA) = 24. Statistical significance by Mann-Whitney U test: ***$p < 0.001$. MFI – mean fluorescence intensity. **(E)** Representative immunostaining of pH2AX foci (green) in nuclei (blue) at 70 days. Scale bar = 10μm. **(F)** There were significantly higher pH2AX foci present in 3xSNCA hMO astrocyte nuclei at 70 days of organoid maturation. Data is from four independent organoid batches. Three to four organoids were analyzed per batch and three to six sections were analyzed per organoid. Each data point represents an individual organoid section. N(WT) = 42. N(3xSNCA) = 32. Statistical significance by Mann-Whitney U test: *$p < 0.05$. **(G)** Real time PCR showed that *CDNK2A* which encodes p14/p16 is upregulated in 3xSNCA hMO at 90 days of organoid maturation. Data is from four independent organoid batches. Six organoids were pooled organoids per batch. Each data point represents qPCR data from one batch. Statistical significance by Mann-Whitney U test: *$p < 0.05$.

senescence in various cell types, including astrocytes.[55,56] We performed immunostaining of lamin B1 in the organoids (Fig 5A) and using the Matlab script, we specifically analyzed the levels of laminB1 in astrocyte nuclei. We found a significant reduction in lamin B1 in astrocytes in the 3xSNCA hMO compared to WT hMO at 50 days of maturation (Fig 5D), which is indicative of senescence. The presence of DNA double strand breaks is also associated with senescence, as it initiates the DNA damage response, which is a potent trigger for senescence.[46] We thus assessed the presence of phosphorylated H2AX (pH2AX), a prominent senescence associated heterochromatin foci (Fig 5E). We found elevated levels of pH2AX foci in astrocyte nuclei in the 3xSNCA hMO (Fig 5F). These findings are indicative of the increased presence of astrocytes in a senescent-like state in the patient specific hMO. Finally, to validate our findings, we performed qPCR for *CDNK2A*, which encodes p14 and p16. Both p14 and

p16 are important tumor suppressors that mediate cell cycle control and inhibit cell proliferation. The upregulation of *CDNK2A* is a characteristic hallmark of senescence.[57,58] In line with our other findings, *CDNK2A* was upregulated in the 3xSNCA hMO (Fig 5G). We also evaluated whether neurons in our model displayed any signs of senescence (Supplementary Fig. 5A). We found no differences in the level of MAP2+ mature neurons at 50 days of organoid maturation (Supplementary Fig. 5B). Interestingly, analysis of lamin B1 in MAP2+ neurons revealed significantly lower levels of the nuclear lamina protein in the 3xSNCA hMO (Supplementary Fig. 5C). However, assessment of pH2AX in non-astrocytic cells did not show any enrichment of heterochromatin foci (Supplementary Fig 5D). As most of the non-astrocytic cells in the hMO are neurons at 50 days, this implies that the neuronal cells do not show accumulation of senescence associated DNA foci. Thus, our findings did not support a senescent-like phenotype in neurons. Altogether, our results suggest that astrocytes in the 3xSNCA hMO acquire a senescent-like phenotype, possibly due to the accumulation of pathological α-synuclein, which may have implications on PD etiology.

Discussion

The progressive degeneration of midbrain dopaminergic neurons and the presence of proteinaceous inclusions mainly comprising α-synuclein are the main neuropathological hallmarks of PD. Here, we describe a robust and reproducible patient-specific *in vitro* model system that is able to endogenously recapitulate these hallmarks, and allows for the study of the temporal molecular and cellular changes that underlie PD pathology and progression. Our 3xSNCA midbrain organoids showed significantly higher levels of intra and extracellular α-synuclein. They also displayed the presence of pS129 rich aggregate-like structures reminiscent of Lewy pathology. Our study supports other recently published work in midbrain organoids with PD related mutations in *SNCA*, showing the recapitulation of PD related phenotypes.[59,60] Moreover, we found an association between the accumulation of pathogenic α-synuclein and the acquisition of a senescent-like phenotype in astrocytes in our patient-specific hMO.

Our study followed a time course of dopaminergic neuron development in the organoids, which allowed us to assess dynamics that may have implications in disease pathogenesis. We found a decline in dopaminergic neurons in the 3xSNCA hMO at 70 days which corresponded with

the progressive decline of TH enzyme levels which began after 50 days and was most significant after 90 days. Moreover, dopamine production was drastically reduced in the 3xSNCA hMO, indicative of reduced functionality of the dopaminergic neurons. Taken together, these findings support the recapitulation of dopaminergic neuron loss in a progressive manner in 3xSNCA organoids.

Astrocytes in the 3xSNCA hMO showed nuclear lamina defects and increased presence of the senescence associated heterochromatin foci pH2AX. We also found an overall upregulation of *CDNK2A,* a gene associated with cell cycle regulation, in the 3xSNCA hMO. These findings suggest that astrocytes from the patient-specific organoids acquire a senescent-like phenotype. On the other hand, while we did observe nuclear lamina deficits in the neurons, this was not accompanied by increased senescence associated heterochromatic foci. Therefore, the acquisition of the senescence-like phenotype appears to be more prominent in astrocytes than in neurons at this time points. The acquisition of the senescence-like phenotype in the astrocytes, which was observed at 50 days, preceded the loss of dopaminergic neurons, which was most significant at 70 days. Therefore, we speculate that the presence of senescent astrocytes may have a detrimental impact on the dopaminergic neurons in the 3xSNCA hMO. Astrosenescence has recently gained attention as the loss of astrocytic function and gain of a proinflammatory phenotype due to senescence is thought to have significant implications for neurodegenerative diseases.[61,62] In addition, several studies have shown that the interaction between healthy neurons and senescent astrocytes impairs neuronal function, synaptic plasticity, synaptic vesicle size and synapse maturation.[63,64] These effects are thought to be mediated through the senescence associated secretory phenotype (SASP)[47], which is the release of proinflammatory mediators, reactive oxygen species and metalloproteinases by senescent cells. Thus, one could speculate that the presence of senescent astrocytes in the 3xSNCA hMO may negatively impact the dopaminergic neurons via the effects of the SASP. We also found an increase in the number of GFAP+ astrocytes in the 3xSNCA hMO at 50 days, which may be indicative of astrogliosis. Mild to moderate astrogliosis is associated with the upregulation of GFAP.[65] While astrosenescence and astrogliosis are two distinct astrocytic states, they are both initiated by cytotoxic injury.[61] Therefore, there is a high likelihood that we have a diverse set of astrocytes in the organoids reflecting different cellular states like reactivity and senescence. Recently, cellular senescence has been identified as a contributor to

neurodegenerative disease as senescent cells accumulate in the context of neurodegenerative diseases like PD, Alzheimer's, multiple sclerosis and amyotrophic lateral sclerosis.[66]

There is mounting evidence that pathological α-synuclein may be a driver of cellular senescence. As the 3xSNCA hMO showed accumulation of α-synuclein and its phosphorylated form, we propose that the pathological α-synuclein may contribute to the observed astrosenescence phenotype. Verma *et al* showed that α-synuclein pre-formed fibrils (PFFs) can induce senescence in cell lines and mouse models.[50] In their study, PFFs triggered senescence in primary astrocytes and microglia, and to a lesser extent in primary cortical neurons. These findings support the idea that glial cells may be particularly vulnerable to pathological α-synuclein induced senescence. This is in line with our findings where we observed a senescent phenotype in the astrocytes but not in the neurons at 50 days. Interestingly, they also found increased GFAP expression in adult mouse midbrains and striatum following injection with PFFs[50], which is also consistent with our results. Recently, another study demonstrated that overexpression of α-synuclein in human neuroblastoma cells has been shown to activate the p53 pathway and DNA damage responses, and induce cellular senescence.[49] Moreover, they found that α-synuclein transgenic mice displayed increased pS129 α-synuclein along with increased presence of DSBs and senescence associated markers at early, presymptomatic stages of disease before dopaminergic neuron loss. This also supports the hypothesis that cellular senescence may be a pathogenic mechanism preceding dopaminergic degeneration. Besides its abundant expression at pre-synaptic terminals, α-synuclein has been shown to be expressed in the nucleus.[11,67] A potential nuclear function of α-synuclein that has been recently proposed is that under physiological conditions, it is a DNA binding protein that modulates DNA repair. It was postulated that the cytoplasmic aggregation of α-synuclein reduces its nuclear levels, thus reducing the DNA repair capacity of cells and increasing the presence of double strand breaks.[12] As DNA damage is a potent inducer of senescence in cells, we speculate that the senescent-like phenotypes we observed in the 3xSNCA hMO may at least in part be explained by this phenomenon. To validate this, it would be important to study the localization of α-synuclein in the nucleus and whether this is altered with aggregation in our model.

As senescence is often associated with aging, it may be surprising that we observed senescence in our organoid model, which is more reflective of the brain during neurodevelopment.

However, while senescence is often associated with aging, there has been a growing body of work describing other mechanisms through which senescence can be induced, independently of aging. For example, DNA-damage-induced senescence and stress-induced senescence are mechanisms that have been implicated in diseases like cancer.[68] Stress-induced senescence can be triggered by reactive oxygen species. Pathological α-synuclein has been implicated in increasing ROS levels[69], and thus this could represent a potential mechanism in which senescence could be induced in our model.

Our findings, which highlight a potential role of senescence in PD pathogenesis, opens opportunities for the use of senolytics as a therapeutic strategy in the disease. Senolytics selectively kill senescent cells by targeting anti-apoptotic pathways that are upregulated during senescence. Recently, several senolytics have shown efficacy in improving cognition and lifespan in mouse models of neurodegeneration.[70-72] Our organoid model could be an ideal system to test the efficacy of different senolytic drugs.

Altogether, our results suggest that elevated α-synuclein is associated to the acquisition of a senescent-like phenotype in astrocytes, preceding dopaminergic degeneration. This may have implications on PD pathogenesis as astrosenescence may promote the vulnerability of dopaminergic neurons. While further research is required to elucidate the underlying mechanisms, our hMO model's ability to recapitulate these phenotypes will allow us to further explore this aspect of PD pathogenesis and test relevant therapeutic strategies.

Acknowledgements

Funding

Competing interests

SB and JCS are cofounders and shareholders of OrganoTherapeutics société à responsabilité limitée simplifiée (SARL-S).

References

1.   Spillantini MG, Schmidt ML, Lee VM, Trojanowski JQ, Jakes R, Goedert M. Alpha-synuclein in Lewy bodies. *Nature*. Aug 28 1997;388(6645):839-40. doi:10.1038/42166
2.   Eliezer D, Kutluay E, Bussell R, Jr., Browne G. Conformational properties of alpha-synuclein in its free and lipid-associated states. *J Mol Biol*. Apr 6 2001;307(4):1061-73. doi:10.1006/jmbi.2001.4538
3.   Ulmer TS, Bax A. Comparison of structure and dynamics of micelle-bound human alpha-synuclein and Parkinson disease variants. *J Biol Chem*. Dec 30 2005;280(52):43179-87. doi:10.1074/jbc.M507624200

4.   Waudby CA, Camilloni C, Fitzpatrick AWP, et al. In-Cell NMR Characterization of the Secondary Structure Populations of a Disordered Conformation of α-Synuclein within E. coli Cells. *PLOS ONE*. 2013;8(8):e72286. doi:10.1371/journal.pone.0072286

5.   Weinreb PH, Zhen W, Poon AW, Conway KA, Lansbury PT, Jr. NACP, a protein implicated in Alzheimer's disease and learning, is natively unfolded. *Biochemistry*. Oct 29 1996;35(43):13709-15. doi:10.1021/bi961799n

6.   Burré J, Sharma M, Tsetsenis T, Buchman V, Etherton MR, Südhof TC. Alpha-synuclein promotes SNARE-complex assembly in vivo and in vitro. *Science*. Sep 24 2010;329(5999):1663-7. doi:10.1126/science.1195227

7.   Fortin DL, Nemani VM, Voglmaier SM, Anthony MD, Ryan TA, Edwards RH. Neural activity controls the synaptic accumulation of alpha-synuclein. *J Neurosci*. Nov 23 2005;25(47):10913-21. doi:10.1523/jneurosci.2922-05.2005

8.   Jin H, Kanthasamy A, Ghosh A, Yang Y, Anantharam V, Kanthasamy AG. α-Synuclein negatively regulates protein kinase Cδ expression to suppress apoptosis in dopaminergic neurons by reducing p300 histone acetyltransferase activity. *J Neurosci*. Feb 9 2011;31(6):2035-51. doi:10.1523/jneurosci.5634-10.2011

9.   Li W, Lee MK. Antiapoptotic property of human alpha-synuclein in neuronal cell lines is associated with the inhibition of caspase-3 but not caspase-9 activity. *J Neurochem*. Jun 2005;93(6):1542-50. doi:10.1111/j.1471-4159.2005.03146.x

10.   Bobela W, Aebischer P, Schneider BL. Alpha-Synuclein as a Mediator in the Interplay between Aging and Parkinson's Disease. *Biomolecules*. 2015;5(4):2675-2700.

11.   Koss DJ, Erskine D, Porter A, et al. Nuclear alpha-synuclein is present in the human brain and is modified in dementia with Lewy bodies. *Acta Neuropathologica Communications*. 2022/07/06 2022;10(1):98. doi:10.1186/s40478-022-01403-x

12.   Schaser AJ, Osterberg VR, Dent SE, et al. Alpha-synuclein is a DNA binding protein that modulates DNA repair with implications for Lewy body disorders. *Scientific Reports*. 2019/07/29 2019;9(1):10919. doi:10.1038/s41598-019-47227-z

13.   Chen V, Moncalvo M, Tringali D, et al. The mechanistic role of alpha-synuclein in the nucleus: impaired nuclear function caused by familial Parkinson's disease SNCA mutations. *Hum Mol Genet*. Nov 4 2020;29(18):3107-3121. doi:10.1093/hmg/ddaa183

14.   Singleton AB, Farrer M, Johnson J, et al. alpha-Synuclein locus triplication causes Parkinson's disease. *Science*. Oct 31 2003;302(5646):841. doi:10.1126/science.1090278

15.   Polymeropoulos MH, Lavedan C, Leroy E, et al. Mutation in the alpha-synuclein gene identified in families with Parkinson's disease. *Science*. Jun 27 1997;276(5321):2045-7. doi:10.1126/science.276.5321.2045

16.   Krüger R, Kuhn W, Müller T, et al. Ala30Pro mutation in the gene encoding alpha-synuclein in Parkinson's disease. *Nat Genet*. Feb 1998;18(2):106-8. doi:10.1038/ng0298-106

17.   Appel-Cresswell S, Vilarino-Guell C, Encarnacion M, et al. Alpha-synuclein p.H50Q, a novel pathogenic mutation for Parkinson's disease. *Mov Disord*. Jun 2013;28(6):811-3. doi:10.1002/mds.25421

18.   Fujioka S, Ogaki K, Tacik PM, Uitti RJ, Ross OA, Wszolek ZK. Update on novel familial forms of Parkinson's disease and multiple system atrophy. *Parkinsonism Relat Disord*. Jan 2014;20 Suppl 1(0 1):S29-34. doi:10.1016/s1353-8020(13)70010-5

19.   Hoffman-Zacharska D, Koziorowski D, Ross OA, et al. Novel A18T and pA29S substitutions in α-synuclein may be associated with sporadic Parkinson's disease. *Parkinsonism Relat Disord*. Nov 2013;19(11):1057-1060. doi:10.1016/j.parkreldis.2013.07.011

20.   Kiely AP, Asi YT, Kara E, et al. α-Synucleinopathy associated with G51D SNCA mutation: a link between Parkinson's disease and multiple system atrophy? *Acta Neuropathol*. May 2013;125(5):753-69. doi:10.1007/s00401-013-1096-7

21.   Pasanen P, Myllykangas L, Siitonen M, et al. Novel α-synuclein mutation A53E associated with atypical multiple system atrophy and Parkinson's disease-type pathology. *Neurobiol Aging*. Sep 2014;35(9):2180.e1-5. doi:10.1016/j.neurobiolaging.2014.03.024

22.   Zarranz JJ, Alegre J, Gómez-Esteban JC, et al. The new mutation, E46K, of alpha-synuclein causes Parkinson and Lewy body dementia. *Ann Neurol*. Feb 2004;55(2):164-73. doi:10.1002/ana.10795

23.   Lashuel HA, Petre BM, Wall J, et al. Alpha-synuclein, especially the Parkinson's disease-associated mutants, forms pore-like annular and tubular protofibrils. *J Mol Biol*. Oct 4 2002;322(5):1089-102. doi:10.1016/s0022-2836(02)00735-0

24.   Miller DW, Hague SM, Clarimon J, et al. Alpha-synuclein in blood and brain from familial Parkinson disease with SNCA locus triplication. *Neurology*. May 25 2004;62(10):1835-8. doi:10.1212/01.wnl.0000127517.33208.f4

25.   Malkus KA, Tsika E, Ischiropoulos H. Oxidative modifications, mitochondrial dysfunction, and impaired protein degradation in Parkinson's disease: how neurons are lost in the Bermuda triangle. *Molecular Neurodegeneration*. 2009/06/05 2009;4(1):24. doi:10.1186/1750-1326-4-24

26.   Choi MG, Kim MJ, Kim DG, Yu R, Jang YN, Oh WJ. Sequestration of synaptic proteins by alpha-synuclein aggregates leading to neurotoxicity is inhibited by small peptide. *PLoS One*. 2018;13(4):e0195339. doi:10.1371/journal.pone.0195339

27.   Volpicelli-Daley LA, Luk KC, Patel TP, et al. Exogenous α-synuclein fibrils induce Lewy body pathology leading to synaptic dysfunction and neuron death. *Neuron*. Oct 6 2011;72(1):57-71. doi:10.1016/j.neuron.2011.08.033

28.   Geertsma HM, Suk TR, Ricke KM, et al. Constitutive nuclear accumulation of endogenous alpha-synuclein in mice causes motor impairment and cortical dysfunction, independent of protein aggregation. *Human Molecular Genetics*. 2022;31(21):3613-3628. doi:10.1093/hmg/ddac035

29.   Potashkin JA, Blume SR, Runkle NK. Limitations of animal models of Parkinson's disease. *Parkinsons Dis*. Dec 20 2010;2011:658083. doi:10.4061/2011/658083

30.   Smits LM, Schwamborn JC. Midbrain Organoids: A New Tool to Investigate Parkinson's Disease. Review. *Frontiers in Cell and Developmental Biology*. 2020-May-19 2020;8doi:10.3389/fcell.2020.00359

31.   Galet B, Cheval H, Ravassard P. Patient-Derived Midbrain Organoids to Explore the Molecular Basis of Parkinson's Disease. Review. *Frontiers in Neurology*. 2020-September-04 2020;11doi:10.3389/fneur.2020.01005

32.   Monzel AS, Smits LM, Hemmer K, et al. Derivation of Human Midbrain-Specific Organoids from Neuroepithelial Stem Cells. *Stem Cell Reports*. May 9 2017;8(5):1144-1154. doi:10.1016/j.stemcr.2017.03.010

33.   Jo J, Xiao Y, Sun AX, et al. Midbrain-like Organoids from Human Pluripotent Stem Cells Contain Functional Dopaminergic and Neuromelanin-Producing Neurons. *Cell Stem Cell*. Aug 4 2016;19(2):248-257. doi:10.1016/j.stem.2016.07.005

34.   Nickels SL, Modamio J, Mendes-Pinheiro B, Monzel AS, Betsou F, Schwamborn JC. Reproducible generation of human midbrain organoids for in vitro modeling of Parkinson's disease. *Stem Cell Research*. 2020/07/01/ 2020;46:101870. doi:https://doi.org/10.1016/j.scr.2020.101870

35.   Smits LM, Reinhardt L, Reinhardt P, et al. Modeling Parkinson's disease in midbrain-like organoids. *npj Parkinson's Disease*. 2019/04/05 2019;5(1):5. doi:10.1038/s41531-019-0078-4

36.   Jarazo J, Barmpa K, Modamio J, et al. Parkinson's Disease Phenotypes in Patient Neuronal Cultures and Brain Organoids Improved by 2-Hydroxypropyl-β-Cyclodextrin Treatment. *Mov Disord*. Jan 2022;37(1):80-94. doi:10.1002/mds.28810

37. Kim H, Park HJ, Choi H, et al. Modeling G2019S-LRRK2 Sporadic Parkinson's Disease in 3D Midbrain Organoids. *Stem Cell Reports*. Mar 5 2019;12(3):518-531. doi:10.1016/j.stemcr.2019.01.020

38. Ahfeldt T, Ordureau A, Bell C, et al. Pathogenic Pathways in Early-Onset Autosomal Recessive Parkinson's Disease Discovered Using Isogenic Human Dopaminergic Neurons. *Stem Cell Reports*. Jan 14 2020;14(1):75-90. doi:10.1016/j.stemcr.2019.12.005

39. Reinhardt P, Glatza M, Hemmer K, et al. Derivation and Expansion Using Only Small Molecules of Human Neural Progenitors for Neurodegenerative Disease Modeling. *PLOS ONE*. 2013;8(3):e59252. doi:10.1371/journal.pone.0059252

40. Zagare A, Gobin M, Monzel AS, Schwamborn JC. A robust protocol for the generation of human midbrain organoids. *STAR Protoc*. Jun 18 2021;2(2):100524. doi:10.1016/j.xpro.2021.100524

41. Gomez-Giro G, Arias-Fuenzalida J, Jarazo J, et al. Synapse alterations precede neuronal damage and storage pathology in a human cerebral organoid model of CLN3-juvenile neuronal ceroid lipofuscinosis. *Acta Neuropathol Commun*. Dec 30 2019;7(1):222. doi:10.1186/s40478-019-0871-7

42. Bolognin S, Fosspré M, Qing X, et al. 3D Cultures of Parkinson's Disease-Specific Dopaminergic Neurons for High Content Phenotyping and Drug Testing. *Adv Sci (Weinh)*. Jan 9 2019;6(1):1800927. doi:10.1002/advs.201800927

43. Monzel AS, Hemmer K, Kaoma T, et al. Machine learning-assisted neurotoxicity prediction in human midbrain organoids. *Parkinsonism Relat Disord*. Jun 2020;75:105-109. doi:10.1016/j.parkreldis.2020.05.011

44. Anderson JP, Walker DE, Goldstein JM, et al. Phosphorylation of Ser-129 is the dominant pathological modification of alpha-synuclein in familial and sporadic Lewy body disease. *J Biol Chem*. Oct 6 2006;281(40):29739-52. doi:10.1074/jbc.M600933200

45. Hernandez-Segura A, Nehme J, Demaria M. Hallmarks of Cellular Senescence. *Trends Cell Biol*. Jun 2018;28(6):436-453. doi:10.1016/j.tcb.2018.02.001

46. Kumari R, Jat P. Mechanisms of Cellular Senescence: Cell Cycle Arrest and Senescence Associated Secretory Phenotype. Review. *Frontiers in Cell and Developmental Biology*. 2021-March-29 2021;9doi:10.3389/fcell.2021.645593

47. Kritsilis M, S VR, Koutsoudaki PN, Evangelou K, Gorgoulis VG, Papadopoulos D. Ageing, Cellular Senescence and Neurodegenerative Disease. *Int J Mol Sci*. Sep 27 2018;19(10)doi:10.3390/ijms19102937

48. Martínez-Cué C, Rueda N. Cellular Senescence in Neurodegenerative Diseases. *Front Cell Neurosci*. 2020;14:16. doi:10.3389/fncel.2020.00016

49. Yoon Y-S, You JS, Kim T-K, et al. Senescence and impaired DNA damage responses in alpha-synucleinopathy models. *Experimental & Molecular Medicine*. 2022/02/01 2022;54(2):115-128. doi:10.1038/s12276-022-00727-x

50. Verma DK, Seo BA, Ghosh A, et al. Alpha-Synuclein Preformed Fibrils Induce Cellular Senescence in Parkinson's Disease Models. *Cells*. Jul 5 2021;10(7)doi:10.3390/cells10071694

51. Chinta SJ, Woods G, Demaria M, et al. Cellular Senescence Is Induced by the Environmental Neurotoxin Paraquat and Contributes to Neuropathology Linked to Parkinson's Disease. *Cell Rep*. Jan 23 2018;22(4):930-940. doi:10.1016/j.celrep.2017.12.092

52. Sikora E, Bielak-Zmijewska A, Dudkowska M, et al. Cellular Senescence in Brain Aging. *Front Aging Neurosci*. 2021;13:646924. doi:10.3389/fnagi.2021.646924

53. Camps J, Erdos MR, Ried T. The role of lamin B1 for the maintenance of nuclear structure and function. *Nucleus*. 2015/01/02 2015;6(1):8-14. doi:10.1080/19491034.2014.1003510

54.   Butin-Israeli V, Adam SA, Jain N, et al. Role of Lamin B1 in Chromatin Instability. *Molecular and Cellular Biology*. 2015;35(5):884-898. doi:doi:10.1128/MCB.01145-14

55.   Freund A, Laberge RM, Demaria M, Campisi J. Lamin B1 loss is a senescence-associated biomarker. *Mol Biol Cell*. Jun 2012;23(11):2066-75. doi:10.1091/mbc.E11-10-0884

56.   Matias I, Diniz LP, Damico IV, et al. Loss of lamin-B1 and defective nuclear morphology are hallmarks of astrocyte senescence in vitro and in the aging human hippocampus. *Aging Cell*. 2022;21(1):e13521. doi:https://doi.org/10.1111/acel.13521

57.   Baker DJ, Jin F, van Deursen JM. The yin and yang of the Cdkn2a locus in senescence and aging. *Cell Cycle*. Sep 15 2008;7(18):2795-802. doi:10.4161/cc.7.18.6687

58.   He S, Sharpless NE. Senescence in Health and Disease. *Cell*. Jun 1 2017;169(6):1000-1011. doi:10.1016/j.cell.2017.05.015

59.   Jo J, Yang L, Tran HD, et al. Lewy Body-like Inclusions in Human Midbrain Organoids Carrying Glucocerebrosidase and α-Synuclein Mutations. *Ann Neurol*. Sep 2021;90(3):490-505. doi:10.1002/ana.26166

60.   Mohamed N-V, Sirois J, Ramamurthy J, et al. Midbrain organoids with an SNCA gene triplication model key features of synucleinopathy. *Brain Communications*. 2021;3(4)doi:10.1093/braincomms/fcab223

61.   Cohen J, Torres C. Astrocyte senescence: Evidence and significance. *Aging Cell*. 2019;18(3):e12937. doi:https://doi.org/10.1111/acel.12937

62.   Lazic A, Balint V, Stanisavljevic Ninkovic D, Peric M, Stevanovic M. Reactive and Senescent Astroglial Phenotypes as Hallmarks of Brain Pathologies. *Int J Mol Sci*. Apr 30 2022;23(9)doi:10.3390/ijms23094995

63.   Limbad C, Oron TR, Alimirah F, et al. Astrocyte senescence promotes glutamate toxicity in cortical neurons. *PLOS ONE*. 2020;15(1):e0227887. doi:10.1371/journal.pone.0227887

64.   Bussian TJ, Aziz A, Meyer CF, Swenson BL, van Deursen JM, Baker DJ. Clearance of senescent glial cells prevents tau-dependent pathology and cognitive decline. *Nature*. Oct 2018;562(7728):578-582. doi:10.1038/s41586-018-0543-y

65.   Sofroniew MV. Astrogliosis. *Cold Spring Harb Perspect Biol*. Nov 7 2014;7(2):a020420. doi:10.1101/cshperspect.a020420

66.   Si Z, Sun L, Wang X. Evidence and perspectives of cell senescence in neurodegenerative diseases. *Biomedicine & Pharmacotherapy*. 2021/05/01/ 2021;137:111327. doi:https://doi.org/10.1016/j.biopha.2021.111327

67.   Goers J, Manning-Bog AB, McCormack AL, et al. Nuclear localization of alpha-synuclein and its interaction with histones. *Biochemistry*. Jul 22 2003;42(28):8465-71. doi:10.1021/bi0341152

68.   Muñoz-Espín D, Serrano M. Cellular senescence: from physiology to pathology. *Nature Reviews Molecular Cell Biology*. 2014/07/01 2014;15(7):482-496. doi:10.1038/nrm3823

69.   Puspita L, Chung SY, Shim JW. Oxidative stress and cellular pathologies in Parkinson's disease. *Mol Brain*. Nov 28 2017;10(1):53. doi:10.1186/s13041-017-0340-9

70.   Zhang P, Kishimoto Y, Grammatikakis I, et al. Senolytic therapy alleviates Aβ-associated oligodendrocyte progenitor cell senescence and cognitive deficits in an Alzheimer's disease model. *Nat Neurosci*. May 2019;22(5):719-728. doi:10.1038/s41593-019-0372-9

71.   Musi N, Valentine JM, Sickora KR, et al. Tau protein aggregation is associated with cellular senescence in the brain. *Aging Cell*. Dec 2018;17(6):e12840. doi:10.1111/acel.12840

72.   Riessland M, Kolisnyk B, Kim TW, et al. Loss of SATB1 Induces p21-Dependent Cellular Senescence in Post-mitotic Dopaminergic Neurons. *Cell Stem Cell*. Oct 3 2019;25(4):514-530.e8. doi:10.1016/j.stem.2019.08.013

Supplementary Information

Supplementary Table 1. IPSC Line Information

Lab identifier	Cell Line Name	Healthy (WT) or Patient (PD) Origin	Sex	Age Of sampling	Age of onset	Source	Ref #	Karyotype
201	WT 1	WT	F	Cord Blood derived	-	GIBCO	A13777	Normal
232	WT 2	WT	F	53	-	Reinhardt *et al.* 2013		Normal
317	3xSNCA 1	PD	F	55	50	Coriell	ND27760	100kb gain in Chr1
336	3xSNCA 2	PD	F	55	50	EBISC - EDi001-A	EDi001-A	Normal
374	SNCA KO	PD	F	55	50	Chen *et al.* 2019	AST23-4KO-5B	Normal

Supplementary Table 2. Antibody List

| Antibody	Species	Concentration	Source	Catalogue Number	RRID	Used In
α-synuclein	rabbit	1:1000	Santa Cruz	sc-7011-R	RRID:AB_2192953	Western Blot
α-synuclein (2A7)	mouse	1:1000	NOVUS Biologicals	NBP1-05194	RRID:AB_1555287	Immunostaining / Western Blot
GFAP	chicken	1:1000	Millipore	AB5541	RRID:AB_177521	Immunostaining
Lamin B1	rabbit	1:1000	Abcam	ab16048	RRID:AB_443298	Immunostaining
MAP2	chicken	1:1000	Abcam	ab92434	RRID:AB_2138147	Immunostaining
MAP2	mouse	1:1000	Millipore	MAB3418	RRID:AB_11212326	Immunostaining
pH2AX	rabbit	1:500	Cell signaling technology	2577S	RRID:AB_2118010	Immunostaining
Phospho-α-Synuclein (Ser129) (D1R1R)	rabbit	1:500	Cell Signaling	23706S	RRID:AB_2798868	Immunostaining / Western Blot

| S100ß	mouse	1:1000	Sigma	S2532	RRID:AB_477499	Immunostaining
ß-actin	mouse	1:50,000	Cell signaling technology	3700	RRID:AB_2242334	Western Blot
ßIII Tubulin	chicken	1:1000	Millipore	AB9354	RRID:AB_570918	Immunostaining
ßIII Tubulin	mouse	1:20,000	BioLegend	801201	RRID:AB_2313773	Western Blot
Tyrosine Hydroxylase	rabbit	1:1000	Abcam	ab112	RRID:AB_297840	Immunostaining / Western Blot
Tyrosine Hydroxylase	mouse	1:400	Sigma/Merck	MAB318	RRID:AB_2201528	Immunostaining
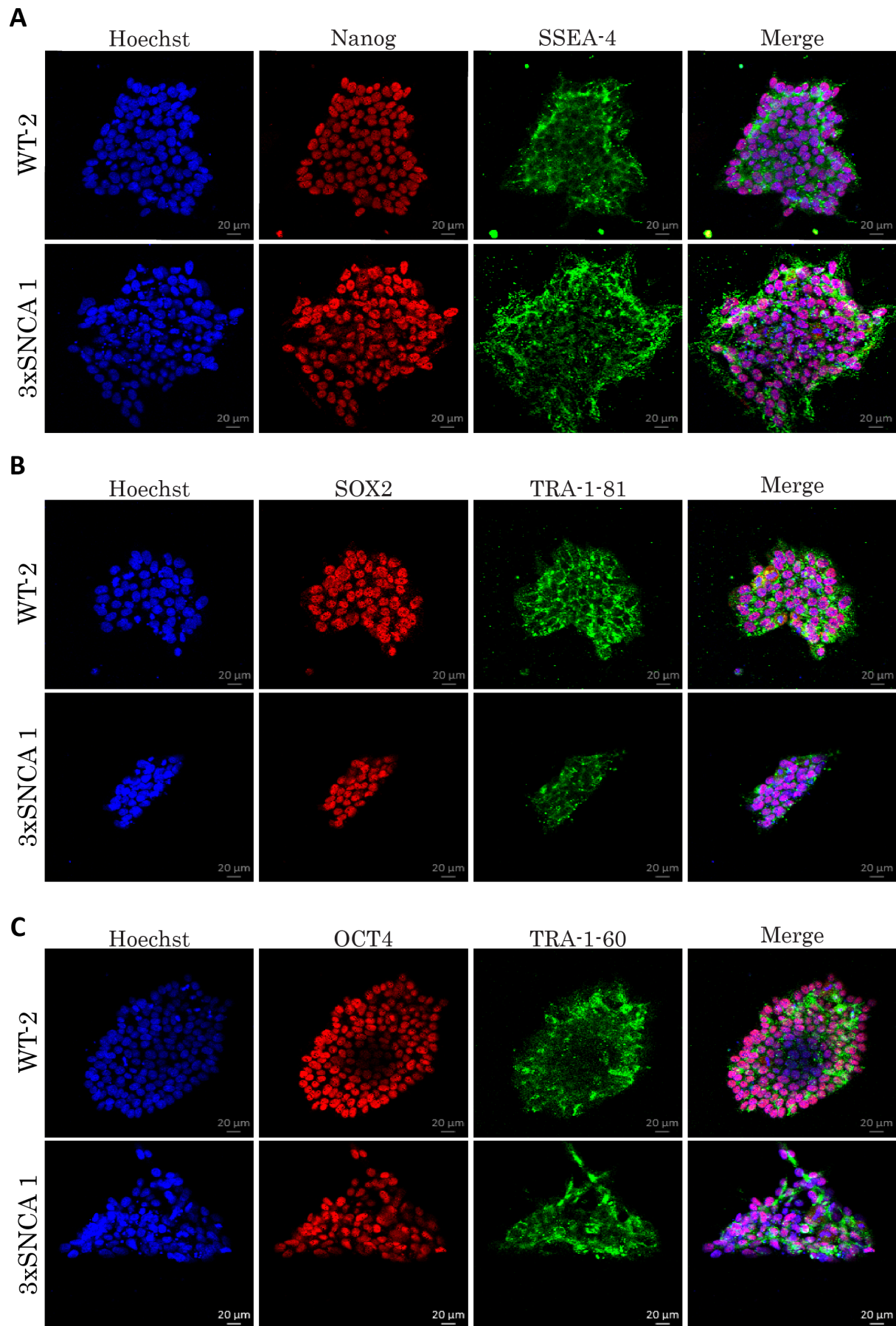
Supplementary Figure 1. Characterization of iPSC. Representative immunofluorescence stainings of WT-1 and SNCA-1 lines showing expression of **(A)** Nanog and SSEA4 **(B)** SOX2 and TRA-1-81**(C)** OCT4 and TRA-1-60. Scale bar = 20μm

A

B
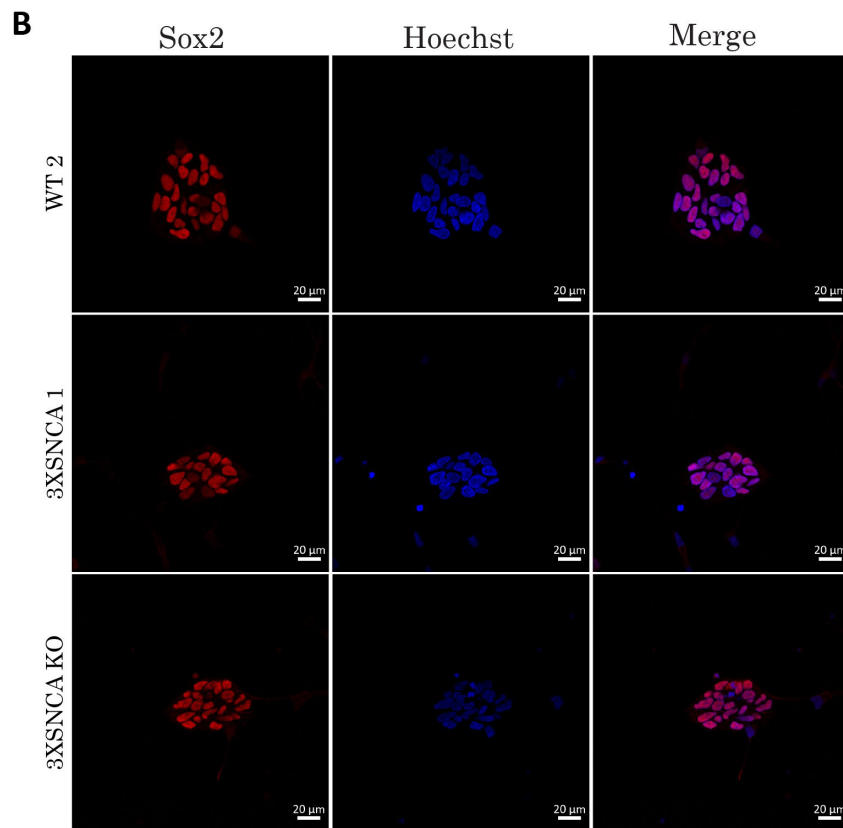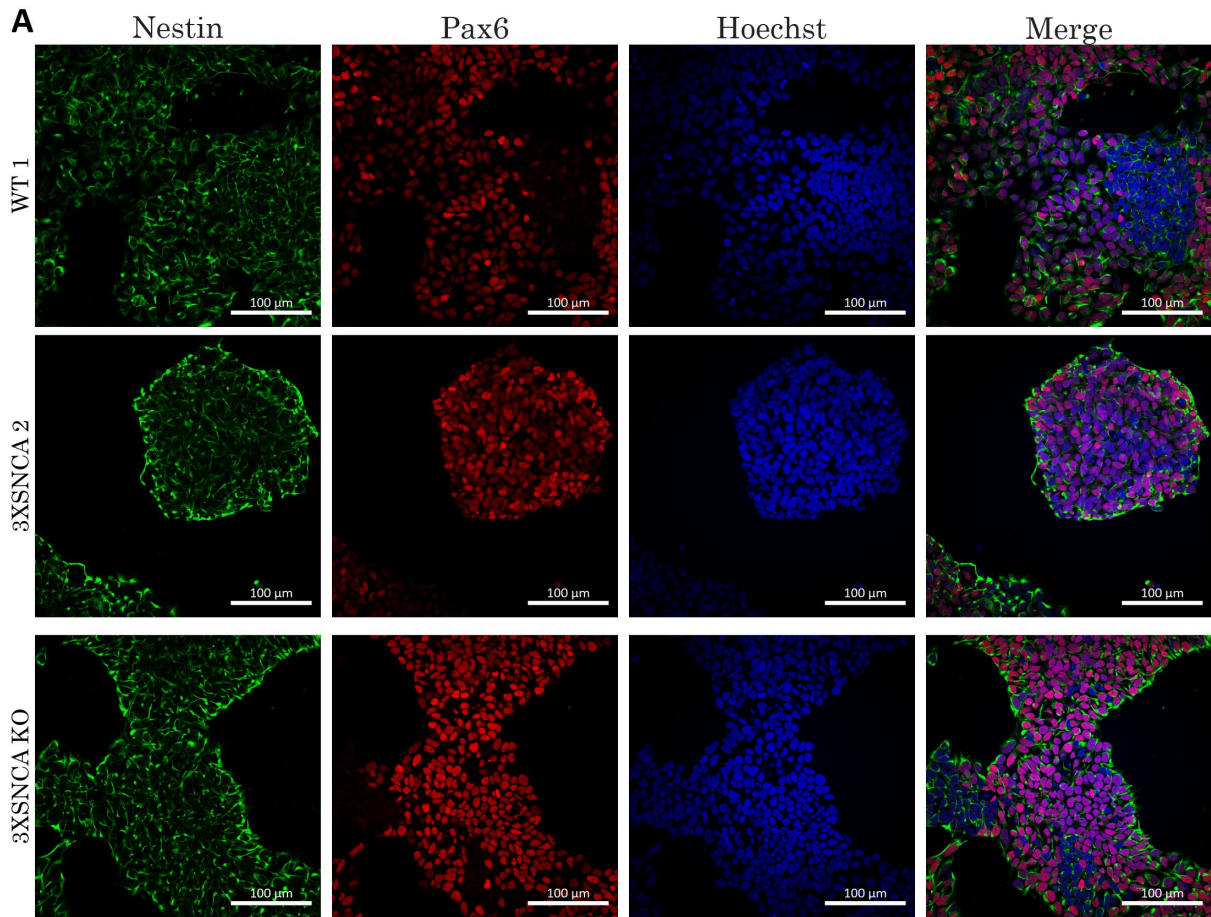
Supplementary Figure 2. Characterization of NESC. Representative immunofluorescence stainings of WT-2, SNCA-2 and SNCA KO lines showing expression of **(A)** Nestin, Pax6 (Scaled bar = 100μm) and **(B)** Sox2 (Scale bar = 20μm).
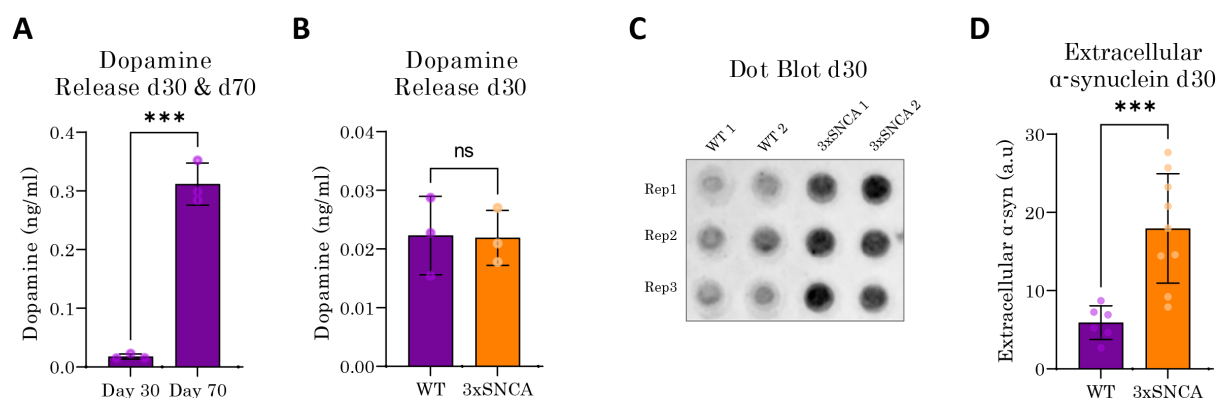
Supplementary Figure 3. Extracellular release of dopamine and α-synuclein. **(A)** WT hMO release increasing amounts of dopamine over time, as quantified at 30 and 70 days of organoid maturation as determined by dopamine ELISA. Data is from three independent organoid batches. Statistical significance by Mann-Whitney U test: ****p* < 0.001. **(B)** There is no difference in dopamine release between 3xSNCA and WT hMO at 30 days of organoid maturation as determined by dopamine ELISA. Data is from three independent organoid batches. Statistical significance by Mann-Whitney U test: not significant **(C)** Representative dot blot of extracellular α-synuclein at 30 days of organoid maturation. Rep = replicate. Dot blot is cropped from original image found in Supplementary Original Blots. **(D)** Quantification of extracellular α-synuclein release at 30 days of organoid maturation. Data represents points represents results from media collected from individual organoids from three independent hMO batches, N = 2-3 hMO per line. Statistical significance by Mann-Whitney U test: ****p* < 0.001.
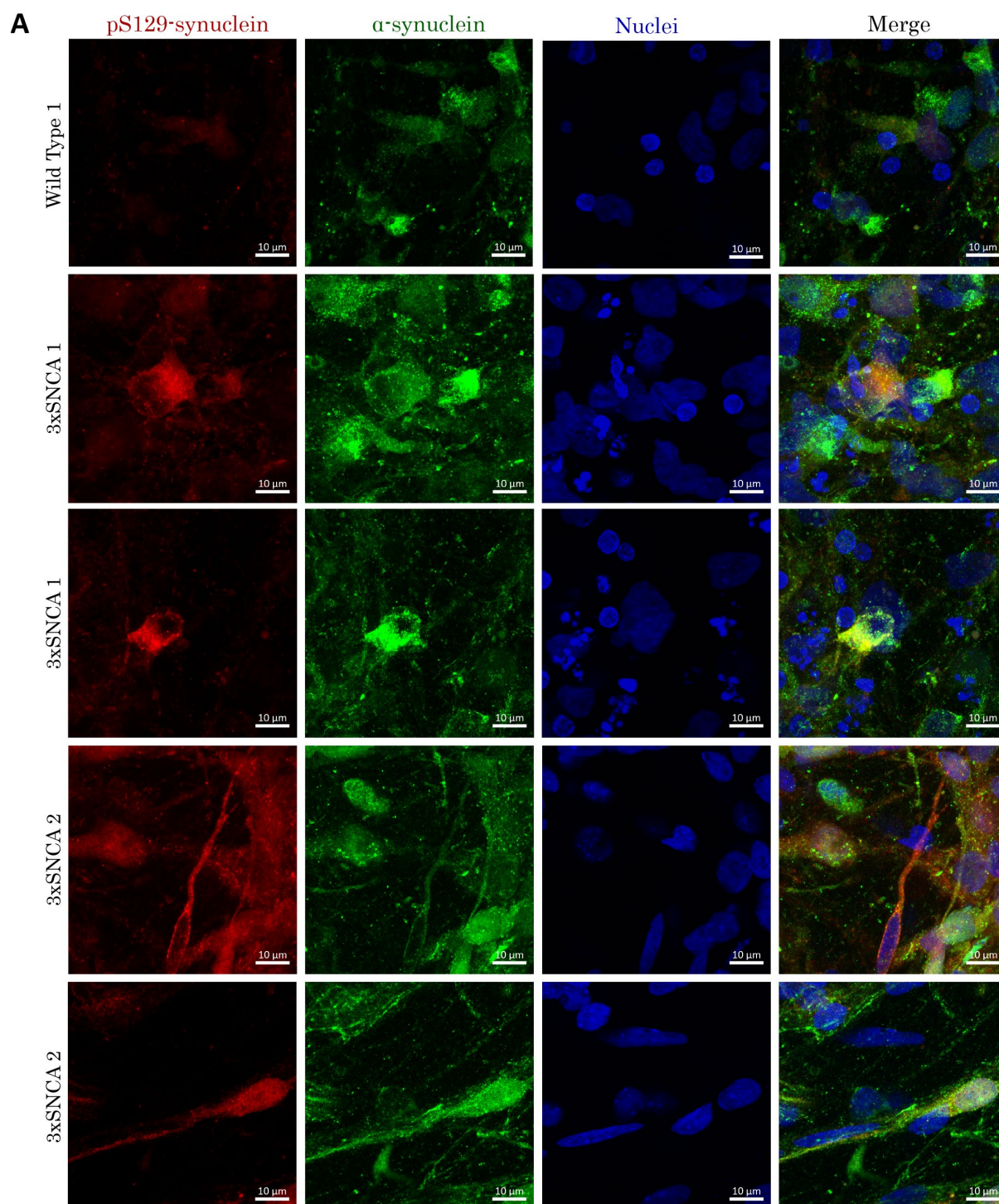
Supplementary Figure 4. 3xSNCA hMO recapitulate α-synuclein aggregation pathology. **(A)**Representative images of 30-day old hMO stained with pS129 α-synuclein (red) and total α-synuclein (green). 3xSNCA hMO show presence of aggregate-like structures rich in pS129 α-synuclein. Scale bar = 10μm.
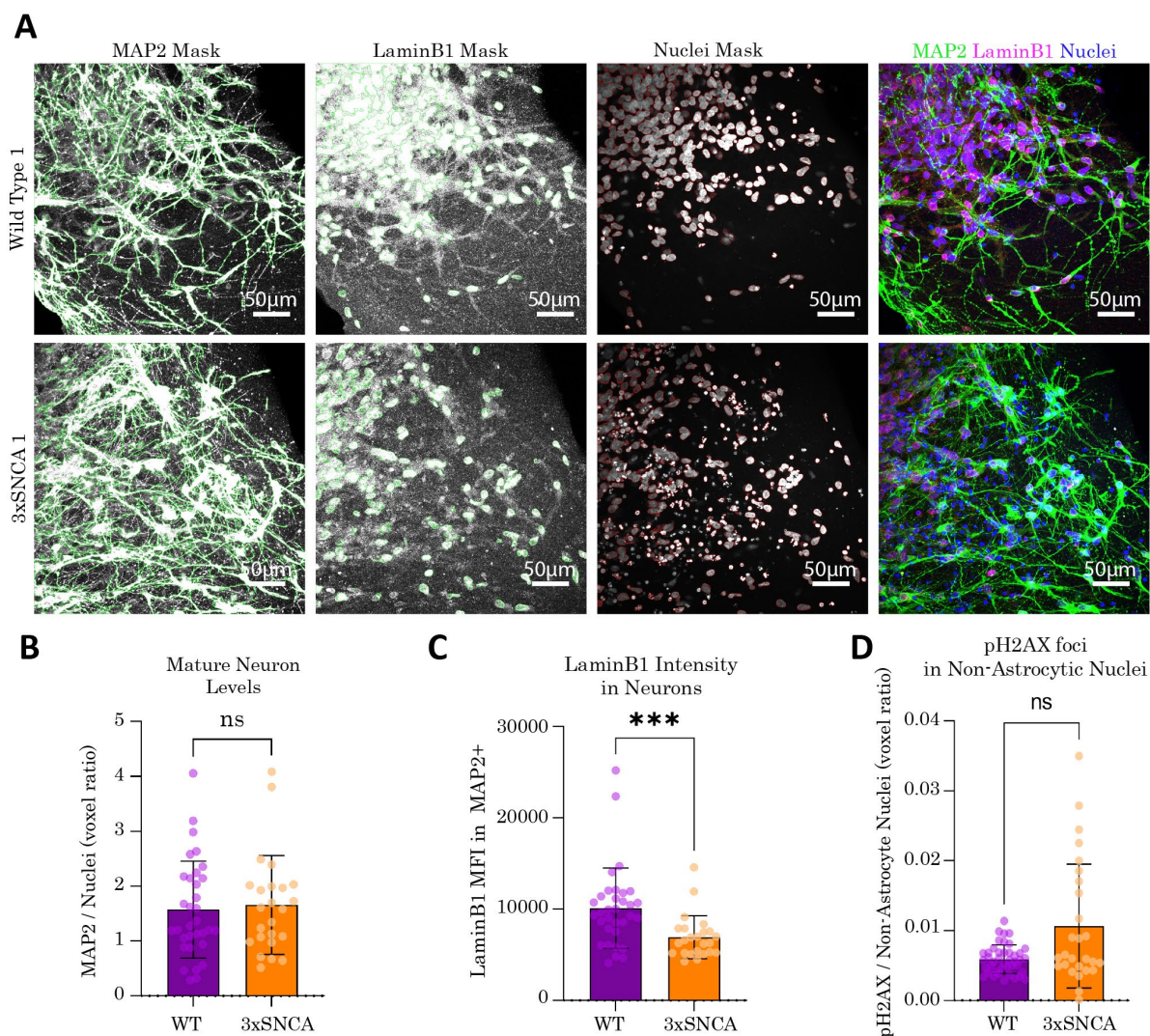
Supplementary Figure 5. Neurons in 3xSNCA hMO show nuclear lamina deficits but not increased senescence associated heterochromatin foci (A) Representative images obtained from confocal imaging of 50-day old hMO sections at 40X magnification showing MAP2, lamin B1 and nuclei masks as identified by a Matlab image analysis script. Scale bar = 50μm. **(B)** Quantification of MAP2+ cells at 50 days revealed no differences in neuronal levels between WT and 3xSNCA hMO. Data is from three independent organoid batches. N = 3-4 organoids per batch. 3-6 sections were analyzed per organoid. *N(*WT) = 33. *N(*3xSNCA) = 24. Statistical significance by Mann-Whitney U test: not significant. **(C)** The levels of lamin B1 were significantly reduced in 3xSNCA hMO neurons at 50 days of organoid maturation. Data is from three independent organoid batches. *N* = 3-4 organoids per batch. 3-6 sections were analyzed per organoid. *N(*WT) = 33. *N(*3xSNCA) = 24. Statistical significance by Mann-Whitney U test: ****p* < 0.001. MFI – mean fluorescence intensity. **(D)** There was no significant difference in pH2AX foci present in non-astrocytic nuclei in 3xSNCA hMO astrocyte nuclei at 70 days of organoid maturation. Data is from three independent organoid batches. *N* = 3-4 organoids per batch. 3-6

sections were analyzed per organoid. N(WT) = 42. N(3xSNCA) = 28. Statistical significance by Mann-Whitney U test: *p < 0.05.

4.2   Manuscript II

The Parkinson's disease-associated mutation LRRK2-G2019S alters astrocyte differentiation dynamics and induces senescence in midbrain organoids

Silvia Bolognin[1*], Lisa Smits[1#], Stefano Magni[1#], Kamil Grzyb[1], Sarah L. Nickels[1], Georgia Woods[2], **Mudiwa N. Muwanigwa[1]**, Paul M.A. Antony[1], Rejko Krüger[1,3,4], Julie K. Andersen[2], Enrico Glaab[1], Alexander Skupin[1,5], and Jens C. Schwamborn[1]

[1] Luxembourg Centre for Systems Biomedicine (LCSB), University of Luxembourg, L-4362 Belvaux, Luxembourg

[2] Buck Institute for Research on Aging, Novato, California 94945.

[3] Transversal Translational Medicine, Luxembourg Institute of Health, Strassen, Luxembourg

[4] Centre Hospitalier de Luxembourg, Luxembourg City, Luxembourg

[5] Center for Research of Biological Systems, University of California San Diego, La Jolla, CA 92093, USA

#These authors contributed equally.

* Correspondence:

Silvia Bolognin, PhD

Luxembourg Centre for Systems Biomedicine (LCSB)

6, Avenue du Swing

L-4367 Belvaux

Luxembourg

003524666445905

This article has been submitted to *Cell Death and Disease*.

Preface

The LRRK2-G2019S mutation is the most common cause of familial PD, thus this particular form of PD has been the focus of extensive research efforts. While LRRK2 is known to be expressed in astrocytes (Miklossy *et al.*, 2006), the impact of the pathogenic G2019S mutation on astrocyte functioning has not been well established. The use of mouse models to study astrocyte dysfunction has significant limitations, most notably since the human astrocyte transcriptome expresses over 600 genes which are not enriched in rodents (Zhang *et al.*, 2016). Therefore, this study harnesses the utility of human derived patient-specific cells, including postmortem tissue and iPSC derived 2D and 3D cultures to characterize the impact of LRRK2-G2019s on astrocyte differentiation. This is the first report of LRRK2-G2019S impairing astrocytic differentiation and predisposing astrocytes to a senescent phenotype. To rescue the impaired astrocyte differentiation, the use of an NR2F1 activator was tested, as NR2F1 has previously been shown to be downregulated in LRRK-2G2019S *in vitro* models (Walter *et al.*, 2021). The NR2F1 activator showed a positive outcome on astrocyte differentiation, highlighting a potential therapeutic intervention.

My contribution to this article was performing immunofluorescence stainings of organoids sections, for the overall quantification of astrocytes (Fig 2B) and the assessment of lamin B1 levels in astrocytes (Fig 5C). I also performed the image acquisition of these stainings using an Operetta high content microscope. Finally, I contributed to reviewing the manuscript.

The Parkinson's disease-associated mutation LRRK2-G2019S alters astrocyte differentiation dynamics and induces senescence in midbrain organoids

Silvia Bolognin[1*], Lisa Smits[1#], Stefano Magni[1#], Kamil Grzyb[1], Sarah L. Nickels[1], Georgia Woods[2], Mudiwa N. Muwanigwa[1], Paul M.A. Antony[1], Rejko Krüger[1,3,4], Julie K. Andersen[2], Enrico Glaab[1], Alexander Skupin[1,5], and Jens C. Schwamborn[1]

[1] Luxembourg Centre for Systems Biomedicine (LCSB), University of Luxembourg, L-4362 Belvaux, Luxembourg
[2] Buck Institute for Research on Aging, Novato, California 94945.
[3] Transversal Translational Medicine, Luxembourg Institute of Health, Strassen, Luxembourg
[4] Centre Hospitalier de Luxembourg, Luxembourg City, Luxembourg
[5] Center for Research of Biological Systems, University of California San Diego, La Jolla, CA 92093, USA

#These authors contributed equally.

* Correspondence:

Silvia Bolognin, PhD
Luxembourg Centre for Systems Biomedicine (LCSB)
6, Avenue du Swing
L-4367 Belvaux
Luxembourg
003524666445905

Keywords: Parkinson's disease; LRRK2-G2019S; astrocytes; senescence; NR2F1.

1

Abstract

Astrocytes have recently emerged as a key player in physiological but also pathological conditions. In particular, their involvement in neurodegenerative processes has been hypothesized. Here, we describe how the Parkinson's disease (PD)-associated mutation LRRK2-G2019S affects astrocytes using autoptic brain samples and PD patient-specific cells, derived from induced pluripotent stem cells. We observed defects in astrocyte differentiation in PD patient-specific midbrain organoids. This is accompanied by an altered transcriptomic profile in astrocytes as shown by single-cell RNA sequencing. The defective astrocyte differentiation is contributing to the acquisition of a immunoreactive and senescent phenotype in organoids carrying the LRRK2-G2019S mutation. In 2D cultures, astrocyte differentiation from LRRK2-G2019S precursor cells is associated with early apoptosis and altered Wnt/βcatenin and TGFβ signaling compared to LRRK2-WT cultures. The treatment with an activator of the transcription factor NR2F1, involved in several phases of brain development, ameliorated the observed astrocyte phenotypes. Together, these data show that the LRRK2-G2019S mutation impairs astrocyte specification and predispose to a senescent phenotype.

Introduction

Glia represent more than 50% of the cells of the human brain and astrocytes are the most abundant members of this family. Astrocytes have been classically ascribed merely supportive functions to neurons, but their role in physiological conditions has gained increasing attention as they can modulate important processes, including synaptic transmission and neuronal metabolism. The concept of tripartite synapse highlights how there is a feedback loop between astrocytic processes and neuronal presynaptic and postsynaptic membranes [1-3]. Astrocytes are also involved in other aspects of synaptic function [4] ranging from the regulation of neurotransmitter uptake [5] to the response to increased synaptic activity [6]. They also produce the glial-derived neurotrophic factor (GDNF), which enhances the survival of midbrain dopaminergic neurons [7]. Considering the importance of these processes for correct brain functioning, their potential role in pathological conditions has been recently evaluated, especially in neurodegenerative disorders like Parkinson's disease (PD) where astrocytes seem to play an active role [8]. However, contradictory are the studies evaluating astrocytes in PD brain samples. Some reported the activation of astrocytes in the *substantia nigra* of PD patients [9-11], while others claimed no difference in either density or morphology of GFAP^{+} cells [12]. A more recent hypothesis proposes that α-synuclein accumulation in PD might suppress astrocyte activation [13]. One of the most common pathogenic mutations causing familial PD is the G2019S mutation in the leucine-rich-repeat-kinase-2 (LRRK2), which is clinically indistinguishable from the idiopathic cases [14]. LRRK2 is expressed both in neurons as well as glia [15, 16]. The majority of the mechanistic insights regarding the potential roles of PD-genes toward the development of disease phenotypes have been obtained in mouse models. However, major differences exist in the expression levels of these genes in astrocytes and neurons when comparing human and murine cells [8]. Human astrocytes are much larger and more complex compared to their rodent counterpart [17, 18]. Moreover, it has been shown that the human astrocyte transcriptome profile has over 600 associated genes which are not enriched in the rodent astrocytes [19]. From this perspective, the use of patient-specific induced pluripotent stem cell (iPSC)-derived cultures to model the human cells seems to be necessary to avoid interspecies differences [20].

To investigate the role of astrocytes in PD neurobiology we used autoptic brain samples and human neuroepithelial stem cells (NESCs) derived from patient-specific iPSCs carrying the LRRK2-G2019S mutation and from healthy individuals, both with their isogenic controls. NESCs were either differentiated into astrocytes in 2D or used for the generation of midbrain organoids. We showed that astrocyte differentiation was impaired both in 3D midbrain organoids and 2D cultures from PD patients carrying the LRRK2-G2019S mutations compared to isogenic lines and healthy individual controls. Using single-cell RNA-sequencing (scRNA-seq), we observed a significantly increased expression of astrocyte-specific genes at 35 days in LRRK2-G2019S organoids compared to LRRK2-WT, which resulted in an abnormal developmental trajectory. This defective astrocyte specification is associated with the acquisition of a senescent phenotype in LRRK2-G2019S organoids. In summary, we propose a novel role of LRRK2-G2019S mutation in impairing astrocytic differentiation and predisposing to senescence.

3

Materials and Methods

Data and Code availability

The scRNA-seq data have been deposited at GEO (GSE128040) and is publicly available. All the data and codes used in this manuscript are available at the following link https://doi.org/10.17881/p1vt-kg48.

Autoptic brain samples

We used sections of midbrain containing *substantia nigra* from three human post-mortem brains. The UK Parkinson's Disease Society Tissue Bank at Imperial College (London, UK) provided us with a PD patient carrying the LRRK2-G2019S mutation (PD235, male, 84-year-old), and two gender and age-matched controls (PDC051, male. 83-year-old; PDC084, male. 83-year-old). The analysis was approved by the local ethical committee (Ethic Review Panel of the University of Luxembourg, ERP-14-019 Astro_PD LB\vg).

Cell culture

All experiments with iPSC and derived cultures were approved by the local ethical committee (Ethic Review Panel of the University of Luxembourg, PDiPS project and CNER No 201305/04). iPSCs were cultured using E8 media (Thermo Scientific, A1517001) on GelTrex (Thermo Scientific, A1413302) coated plates. Accutase (Sigma, A6964) was used for splitting the cells and 5 µM Y-27632 (Merck Millipore, 688000) was added in the E8 media for the following 24h. NESCs were derived from iPSC as previously described[21]. Cells were maintained on GelTrex matrix NUNCLON cell culture ware or Cell carrier-96 plates for imaging. N2B27 maintenance media formulation: Neurobasal (Thermo Scientific, 21103049) and DMEM-F12 (Thermo Scientific, 12634010) 1:1, 1x P/S, 1x GlutaMAX (Thermo Scientific, 35050061), B27 without vitamin A, 1:100 (Thermo Scientific, 12587-010), N2 1:200 (ThermoFisher, 17502048) freshly supplemented with 3 µM CHIR(−99021) (Axon Medchem, AXON1386), 0.75 µM Purmorphamine (PMA) (Enzo Life Science, ALX-420-045-M005) and 150 µM ascorbic acid (AA) (Sigma, A4544). Medium was changed every other day.

Neural stem cells (NSCs) were differentiated from NESCs by adding 1ug/ml FGF in the maintenance medium. On the 4th day, cells were detached with Accutase and re-plated in NSC maintenance medium containing DMEM-F12 medium, 200ng/µl EGF (Peprotech), 200ng/µl FGF, N2 supplement, B27 supplement with vitamin A (ThermoFisher, 17504044), GlutaMAX, Penicillin/Streptomycin and hLIF 1.5ng/ml (Merck, L-5283). NSCs were split (1:2 ratio) at a confluence of 70-80% by using Accutase.

Astrocytic differentiation was induced by switching the NSC Maintenance Medium to the basic astrocytic medium (DMEM-F12 medium, GlutaMAX, Penicillin/Streptomycin) supplemented with 1% FBS (ThermoFisher, 10270106) [22]. Medium was changed every three days. Midbrain organoids were generated and cultured as previously described [23]. Briefly, 3,000 NESCs were seeded per well to a round bottom ultra-low attachment 96-well plate and kept under maintenance conditions for 7 days. LDN and SB were withdrawn to initiate pre-patterning, and after 3 additional days, the concentration of CHIR was reduced to 0.7 µM. On day 9 of differentiation, the medium was changed to neuronal maturation medium containing Neurobasal, DMEM-F12 (1:1) with 10 ng/ml brain-derived neurotrophic factor (BDNF, Peprotech, 450-02), 10 ng/ml glial cell-derived neurotrophic factor (GDNF, Peprotech, 450-44B), 200 µM AA, 500 µM dibutyryl camp (Sigma, D0627), 1 ng/ml TGF-β3 (Peprotech, 100-36E), 2.5 ng/ml ActivinA (ThermoFisher, PHC9561) and 10 µM DAPT (R&D Systems, 2634 /50). The organoids were kept under static culture conditions with media changes every third day for 35, or 70 days.

The pharmacological treatment was conducted with Mli-2 (Tocris, 5756/10) and a NR2F1 activator kindly provided by Prof. Steve Safe, Texas A&M University (DIM-C-Pyr-4[24]) both solved in DMSO. For the 2D experiments, Mli-2 (25nM) and the NR2F1 activator (0.1 and 0.5 µM) were added from the beginning of the astrocyte differentiation and added at each medium change. For the 3D experiments, Mli-2 (25nM) and the NR2F1 activator (0.1 µM) were added at day 3 of differentiation and at each medium change.

Immunohistochemistry

Paraffin-embedded sections were received from the Queen Square Brain Bank for Neurological Disorders (London, UK). Three sections per case were used, and antigen retrieval was performed by inserting the slides in a laboratory pressure cooker in 10 mM citrate buffer (pH 6.0) for 30 minutes, which included also cooling time. The sections were washed for 10 min in phosphate buffer (PBS) and permeabilized for 20 min in a buffer containing 1% normal goat serum (NGS, ThermoFisher, 10000C) and 0.4% Triton X-100 (Carl Roth, 3051.3) in PBS. The sections were then blocked with 5% NGS in PBS 0.05% Triton X-100 for 1h at room temperature. Sections were then incubated over night at 4℃ with GFAP (1:500, Millipore, Cat# AB5541, RRID:AB_177521) in blocking buffer. Followed by three washes of 5 min in PBS+0.025% Tween-20 (Sigma, P7949). The sections were then incubated in the secondary antibody for 2hr in PBS +0.025% Tween-20. After three washes of 5 min in PBS+0.025% Tween-20, the sections were rinsed in bi-distilled water and mounted with FluoroMount-G (VWR, SOUT0100-01). Sections were then acquired on a Yokogawa CV8000. First, the slide was scanned at 4x to identify the area of the tissue. An algorithm, developed in-house in Matlab, was used to randomly sample the tissue with 35 fields taken at 63x.

Immunocytochemistry

For immunofluorescence analysis in 2D, cells were fixed with 4% paraformaldehyde (PFA, Sigma, P6148) in PBS, pH 7.4 for 30 minutes. Cells were rinsed three times for 5 minutes in PBS, then permeabilized with 0.25% Triton X in PBS for ten minutes, washed in PBS for ten minutes, and blocked with 2% NGS, 2% Bovine Serum Albumin (BSA, Sigma, A4503), 0.1% Triton X-100 in PBS for 1h. The primary antibodies were incubated overnight in full blocking buffer, followed by three washed of five minutes in PBS. Secondary antibodies were used at 1:1000 dilution in PBS and 0.02% Tween-20 for two hours. Cells were then washed three times with PBS. The following antibodies at the indicated dilutions were used: anti-Nestin (1:400, Millipore, Cat# MAB5326, RRID:AB_2251134), anti-CC3 (1:500; Cell Signaling, Cat# 9661, RRID:AB_2341188). DNA was stained using Hoechst 33258 (1:10000, Invitrogen, H21492). Plates were then acquired on a Yokogawa CV8000, at 20x.

For immunofluorescence analysis in 3D, midbrain organoids were fixed with 4% PFA in PBS, pH 7.4. Sections were blocked in 5 % NGS, 2 % BSA, 0.5 % Triton X in PBS for 90 min on a shaker. Primary antibodies were incubated in 5 % normal goat serum, 2 % BSA, 0.1 % Triton X in PBS for 48h on a shaker at 4℃. The antibodies used were: Tuj1 (OptimAB Eurogentec, Cat# PRB-435P-050), GFAP (1:1000, Millipore, Cat# AB5541, RRID:AB_177521), S100β (1:1000, Cat# S2532, RRID:AB_477499). Sections were washed three times for 15 minutes and incubated with the secondary antibodies in PBS with 0.05% Tween-20 for two hours on a shaker. Sections were washed three times in 0.05% Tween-20 in PBS for five minutes, and finally washed in H₂O for 5 minutes. Sections were then mounted on glass slides with FluoroMount-G (VWR, SOUT0100-01) and acquired on a Operetta (PerkinElmer), 20x. For the staining of Lamin B1, the following protocol was used: sections were permeabilized with 0.2% Triton X-100 in Tris-buffered saline (TBS) for 30 minutes and blocked for 30 minutes in 5% normal goat serum with 0.2% Triton X-100 in TBS. Sections were incubated at 4℃ for

5

24 h on an orbital shaker with primary antibodies in 5% normal goat serum at the following dilutions: rabbit anti-Lamin B1 (1:200, Abcam, Cat# ab16048, RRID:AB_443298), and GFAP (1:500, Millipore, Cat# AB5541, RRID:AB_177521), **Table S1**.

Live Imaging of 2D cultures

20,000 NSCs were seeded on GelTrek coated imaging plates (cell carrier ultra 96 well plates, PerkinElmer, #6055300) and differentiated for 3, 9, 12 days. Mitochondrial membrane potential ($\Delta\Psi$) was assessed with TMRM (4×10^{-9}M, Thermo Scientific, T668) with MitoTracker Green (1:10 000, Invitrogen, M46750). In addition, cells were costained with Hoechst (1:1000) and Cell Mask (1:5000, Invitrogen, C10046) to visualize nuclei and cell bodies, respectively (Invitrogen). Cells were incubated for 30 min at 37 °C. Fluorescence images were acquired on a Yokogawa CV8000, 63x.

Microarray

mRNA was extracted from NSCs and differentiating astrocytes (24h after the addition of the astrocyte media) using the RNAeasy kit (Quiagen, 74106) following manufacturer's recommendations. mRNA quantity and purity were determined by using a NanoDrop ND-1000 spectrophotometer (NanoDrop Technologies). Additional quality check was performed by the Agilent Bioanalyzer (Agilent). Gene expression profiles were generated using HumanGene 2.0ST arrays according to manufacturer's recommendations (Affymetrix).

Single-cell RNA-sequencing using Droplet-Sequencing (Drop-Seq)

Single-cell RNA-sequencing data (scRNA-Seq) data were generated using the Droplet-Sequencing (Drop-Seq) technique [25] as described previously [26, 27]. The analysis was performed on hMOs derived from the isogenic pair H2/H2-G2019S. For each time point, 35 and 70 day after differentiation, we pooled and analysed 30 midbrain organoids each.

Pre-processing of the digital expression matrices from scRNA-seq

The result of the Drop-Seq scRNA-Seq pipeline and subsequent standard bioinformatics processing is, for every sample (time-point and condition), a digital gene expression matrix (DEM) representing the number of mRNA molecules captured per gene per droplet. Here, we obtained four DEMs, two corresponding to 35 days hMOs (H and H-G2019S) and the other two to 70 days hMOs (H and H-G2019S). After quality cut based on knee plots, we retained for each sample 500 cells with the highest number of total transcripts measured and we performed normalisation of the DEMs separately. Furthermore, the two DEMs corresponding to each time-point were merged for the comparison analysis of H and H-G2019S, resulting respectively in 24336 (at day 35) and 26250 (at day 70) measured genes in common between control and mutant, and a total of 2000 cells retained after quality cuts. Let us underline that these quality cuts are rather stringent, so the results are very conservative. The merged DEMs are further normalised. When also merging the two time-points, 22199 measured genes resulted in common between all days/conditions. The data were analysed by our customized Python analysis pipeline (implemented in Python version 3.6.0, with anaconda version 4.3.1). This pipeline includes the dimensionality reduction and clustering techniques employed to generate **Fig. 3a-f**, **Fig.5a, b** and **Fig.S2a-b**.

Dimensionality reduction and clustering of the scRNA-seq data

The scRNA-seq data so obtained after filtering thus counts 2000 cells, for each of which the expression of more than 22000 genes has been measured. In order to separate the data in groups of cells exhibiting a similar expression profile, we thus performed dimensionality reduction and clustering of these data, shown in **Fig.3a**, **b** and **c**. We first selected the genes corresponding to neuron-, astrocyte- and stem cell-specific lists of genes (**Table S2**). Then, we reduced the dimensionality of this subset of the data by principal component analysis (PCA), keeping only the 12 first principal components, which account for more than 90% of the total variance in the data. We further performed clustering on the dimensionality reduced data, using the k-means clustering method and a fixed number of clusters, chosen to be 9 **(Fig.3b)**. This choice was made to divide the cells in groups sufficiently small to identify and isolate in the data less common cell types of interest (astrocytes). For visualization purposes, we further performed on the 12 principal components (PCs) a non-linear dimensionality reduction method, t-distributed stochastic neighborhood embedding (tSNE) [28]. The data are represented in each subpanel of **Fig.3a**, **b** and **c** using this 2D projection. In **Fig.3a**, cells are coloured according to the sample: H-G2019S and H at day 35 and day 70 (each dot represents a cell). In **Fig.3b**, cells are coloured according to the cluster they belong to. **Fig.3c** colours the cells by the cumulative gene expression of, respectively, neuron-, astrocyte-, and stem cell-specific genes.

Analysis of DEGs from scRNA-Seq data

To determine which and how many genes were differentially expressed between LRRK2-WT and LRRK2-G2019S at each of the two time-points 35 days and 70 days hMOs, we applied one-way ANOVA test, a one-way ANOVA test on ranks (Kruskal-Wallis test), and a Mutual Information based test, on each gene independently. The minimum p-value obtained for each gene across these three tests was retained. Statistical significance for differentially expressed genes (DEGs) was set with $p < 0.05$ after Bonferroni correction for multiple hypotheses testing over the whole genome. The analysis is repeated for each of the two days available. The lists of all DEGs identified across the whole genome, for each day, are reported in **Table S3**.

Cumulative gene expressions from scRNA-Seq data

From literature, we extracted cell-type specific gene lists (**Table S2**) for stem cells, neurons, and astrocytes (respectively [29], [30], and [31]). We further defined lists of genes specific for cellular processes of interest: cell cycle, pro-apoptotic, anti-apoptotic, and caspases which we used in **Fig.S2c**. Note that not all genes listed therein have been measured in our dataset, but the great majority of them has. For each list we defined a score, which we refer to as cumulative gene expression score or simply cumulative gene expression, computed for each cell as the sum of the expressions of the corresponding genes from normalized DEM. Since the expression levels were measured at single cell level, we can consider the cells distributions across the cumulative gene's expression scores (e.g. **Fig.3d** for the astrocytes-specific genes). These histograms report the cumulative gene expression scores normalized to their maxima on the horizontal axis. Thus, on the horizontal axis, a value of 1 corresponds to the maximal cumulative gene expression for one list of genes, while 0 corresponds to no expression of any gene from that list. The vertical axis exhibits the number of cells falling into the corresponding bin of the histogram. In each subpanel the distributions for H and H-G2019S are shown. Statistical

significance of population differences was assessed by Z-test of the means with Bonferroni correction to account for multiple hypothesis testing.

Gene-gene correlations from scRNA-Seq data

From the scRNA-Seq data we also computed gene-gene correlation (by means of Pearson correlation coefficient, which is a measure of linear dependency among two variables, here the expression of two genes across multiple single cells). We did so for astrocytes-specific genes in **Fig.S2e** and for senescence specific genes in **Fig.5b**. The senescence-specific list of genes was extracted from [32], and we add to it few other relevant genes. This list is reported in **Table S2**. Analysis was performed independently for the four samples (35 days H and H-G2019S, 70 days H and H-G2019S) resulting in four correlation matrices for each list of genes. Furthermore, the analysis was repeated for day 70 on only the subset of cells classified as astrocytes according to the clustering procedure detailed above. For each matrix, in the lower triangular matrix all correlation values are shown, whereas in the upper triangular matrix only statistically significant correlations (p-value < 0.05 after Bonferroni correction) are reported. For visual clarity, the elements corresponding to the diagonal (for which correlation is equal to 1 by definition) are masked and those corresponding to genes for which no expression is detected are shown in white as well.

Fold changes of gene expression from scRNA-Seq data

For individual genes, we considered the normalized gene expression across the cell populations. For each selected gene, we compared its expression within the H-G2019S cells with that within the H cells by computing the logarithm 2-fold change (log2FC). This means for each gene to divide the average (over cells) gene expression in G2019S cells by the average gene expression in WT cells, and taking the log2 of the result. We performed this analysis for the genes of the core regulatory circuit of transcription factors led by the gene NR2F1 (**Fig.3f**), for the astrocytes-specific genes mentioned above (Fig.**3e**) and for the senescence-specific genes from Ohashi et al. 2018 (**Fig.5a**). We similarly computed log2FC for the cumulative gene expression scores of other interesting cell types and cellular processes (**Fig.S2c**). In the figures, negative values of log2FC (vertical axes) indicate that a gene is less expressed in H-G2019S than in H cells, positive numbers the opposite. p-values are based on Z-test with Bonferroni correction and significance levels correspond to * = p-value < 0.05, ** = p-value < 0.01, *** = p-value < 0.001, **** = p-value < 0.0001 after Bonferroni correction. For genes/lists where the fold change is not statistically significant, one should consider that no significant difference has been observed. Error bars are based on standard error of the mean (SEM) of the individual cell population average and error propagation in computing log2FC.

Single Cell analysis for astrocyte subtype clustering

Data was pre-processed, integrated and cell types were identified based on [33], without integrating embryonic data. Organoid astrocytes were further subsetted from other cell clusters in Seurat [34]. Reclustering of astrocytes into different subtypes was performed using 10 dimensions and a r=0.9 as resolution. Cluster names were given based on marker expression [35]. Pseudotime analysis was performed using the Monocle package version 3. The subsetted seurat object was uploaded in Monocle workflow and clustering was performed based on 5 principal components and a resolution of r=0.1. UMAP was used for visualization. Since Monocle does not allow a full metadata integration from Seurat

object, cell identities were assigned manually to correspond to the ones previously defined. As a starting point for cell ordering along the pseudotime trajectory, the RGL/activated and transcriptional astrocyte cluster of WT35 was chosen. Differentially expressed genes (DEGs) were detected using the FindMarkers function of the Seurat pipeline with the default thresholds. In all comparisons, we used as ident.1 the MUT midbrain organoids and as ident.2 the WT midbrain organoids. Pathway enrichment analysis was performed with MetaCore™ version 21.1 build 70400 based on DEGs detected with the FindMarkers function from Seurat. DEGs were filtered for p.adj.value < 0.05. Statistical analysis of scRNAseq data is based on RStudio R version 3.6.2 ggplot2 package. Comparison are done using non-parametric Kruskal Wallis. Statistical significance between comparisons are represented with asterisks: $p < 0.05$ *, $p < 0.01$**, $p < 0.001$***, $p < 0.00001$****. Cell cycle analysis was performed by assigning cell-cycle scores in Seurat. G1/G0 phase cells were then subclustered and manually reclassified to either G0 or G1 phase using the G0 marker genes from[36].

Statistical analysis

Data are presented as boxplots and violin plots generated in RStudio. Statistical significance was tested with RStudio with Wilcox test or Mann-Whitney test. Results were denoted statistically significant when p values were *<0.05, **<0.01, ***<0.001, ****<0.0001. The number (n) of samples/repeats are given in the Results and Figure legends. All the statistical analyses of scRNA-Seq data are described in the corresponding sections.

Results

Outline of the study

To study the effect of LRRK2-G2019S in astrocytes, we first analyzed the midbrain region of a PD patient carrying the mutation and two age and gender matched controls. We then used iPSC lines reprogrammed from fibroblasts of PD patients carrying the mutation and from healthy controls (**Fig.S1a**). Isogenic lines where the mutation was either corrected or introduced were also used. Starting from neuroepithelial stem cells (NESCs) we generated midbrain organoids, which contain several neuronal subtypes and astrocytes[23, 27]. These organoids were evaluated after 35 and 70 days of differentiation. To specifically evaluate astrocytes, our experimental setup foresaw also the analysis of differentiating NESCs toward the astrocytic lineage in 2D cultures.

Astrocytes are hypertrophic in human brain tissue from a PD patient with the LRRK2-G2019S mutation

Astrocyte alterations have been previously described in PD brain tissue [37, 38]. To investigate astrocyte morphological alteration in the midbrain region in the presence of the LRRK2-G2019S mutation, we analyzed midbrain samples from one carrier suffering from PD and two age and gender-matched healthy individuals. We performed a staining against the astrocytic marker glial fibrillary acidic protein (GFAP). When astrocytes are subjected to insults, the intermediate filament protein GFAP is upregulated and this is considered a major hallmark of astrocytosis[39]. We used an automated image analysis script developed in Matlab to identify the number of nuclei (identified by the Hoechst staining) and observed this was decreased in the LRRK2-G2019S PD patient compared to the controls (**Fig.1a-b**). The number of GFAP$^+$ astrocytes was also decreased. The algorithm used for the extraction of these features allows also the identification of cell branching expressed as number of branches (links) and point of bifurcation (nodes) [40]. Interestingly, the number of links and nodes of the GFAP$^+$ astrocytes increased in the LRRK2-G2019S PD patient compared to the controls, indicating the astrocytes were more reactive. These findings suggest a potential connection between the LRRK2-G2019S mutation and the GFAP immunoreactivity of ventral astrocytes. To investigate this connection in more details, we made use of patient-specific iPSCs.

PD patient-specific LRRK2-G2019S organoids show reduced number of astrocytes

To verify this finding in a human *in vitro* model of PD, we generated midbrain organoids as previously described [23]. We analyzed the expression of GFAP$^+$ and S100β$^+$ astrocytes in 35 and 70-day-old organoids starting from ventral NESCs (**Fig.2a**). We first grouped all the cell lines (including isogenic controls) based on the absence or presence of the LRRK2-G2019S mutation and observed a decrease of both GFAP$^+$ and s100β$^+$ astrocytes in LRRK2-G2019S compared to LRRK2-WT organoids at 35 days. After 70 days, the levels of both GFAP$^+$ and s100β$^+$ astrocytes were comparable in the two cultures although we observed a tendency toward an increased expression of the markers in the LRRK2-G2019S compared to LRRK2-WT organoids (**Fig.2b-c**). We then grouped the cell lines according to the genetic background of the donors instead to the presence or absence of the LRRK2-G2019S mutation. Strikingly, the PD patient-derived organoids (P-G2019S) showed the most severe phenotype in terms of decreased pixels of both GFAP$^+$ and s100β$^+$ cells at 35 days compared to healthy individual-derived organoids (H). The genetic correction of LRRK2-G2019S mutation to the WT sequence (P-G2019S-GC) ameliorated the phenotype. The insertion of the LRRK2-G2019S mutation in the H lines induced a reduction of GFAP$^+$ cells, although it did not reach statistical significance (**Fig.2d**). At 70 days, P-G2019S organoids still showed decreased amount of positive pixels for GFAP compared to the H

organoids, but not of S100β. However, P-G2019S astrocytes showed increased GFAP and S100β expression compared to their isogenic controls (P-G2019S-GC), suggesting the astrocytes might have acquired a more reactive phenotype (**Fig.2e**). We also investigated whether the neuronal marker Tuj1 was affected in the different cultures (**Fig.S1b-e**). When comparing organoids according to the presence or absence of the LRRK2-G2019S mutation, we observed a significant decrease in the percentage of Tuj1+ neurons in LRRK2-G2019S compared to LRRK2-WT both after 35 and 70 days (**Fig.S1c**). Also in the case of the neurons, P-G2019S organoids showed remarkably less neurons compared both to H and P-G2019S-GC organoids at 35 and 70 days. The introduction of the mutation in the H background induced a decrease Tuj1 expression after 35 days, while the expression levels were unchanged after 70 days (**Fig.S1d-e**). These findings support the observation made in Fig1 regarding an effect of the LRRK2-G2019S mutation on astrocyte differentiation dynamics.

LRRK2-G2019S induces an altered astrocytic transcriptomic profile in midbrain organoids

To evaluate differences in the transcriptomic profile due to the LRRK2-G2019S mutation we performed single cell RNA sequencing (scRNA-Seq) in the organoids after 35 and 70 days of differentiation (**Fig.3**). For this experiment, we analyzed the isogenic pair H2/H2-G2019S derived from a healthy individual. In all the analysis shown here, 500 cells per sample (H and H-G2019S) and per day (for a total of 2000 cells) were selected with stringent quality criteria based on the knee plots. **Fig.3a** shows the dimensionality reduction of these data and the clustering of the cells. We further performed clustering on the dimensionality reduced data, using the k-Means clustering method [62] and a fixed number of clusters, chosen to be 9 (**Fig.3b**). Based on well-known lists of genes identifying different cell types, these clusters were categorized into neuron, astrocyte, and stem cells (**Table S2**; **Fig.3c**).

We then focused on astrocytes and plotted the distributions of cells over the cumulative gene expression score for the astrocyte-specific list of genes (**Fig.3d**). Overall, the number of cells expressing astrocyte-specific genes increased from day 35 to day 70. However, H-G2019S and H transcriptomic profiles differed significantly at day 35, while no significant difference was observed at day 70.

Next, we wanted to establish which individual genes contributed to the differences between the gene expression of cells of H-G2019S and H organoids. For this purpose, we initially performed a search for differentially expressed genes (DEGs) across the whole transcriptome. From the 24336 and 26250 (respectively at day 35 at day 70) distinct genes measured, respectively 308 and 1104 are differentially expressed between H-G2019S and H (p-value < 0.05 after Bonferroni correction), see **Table S3**. These represent approximately 1% and 4% of all expressed genes. When intersecting the lists of DEGs with the astrocytes-specific genes, we found that 5% and 9% of the astrocytes-specific genes are DEGs respectively at day 35 and day 70 (**Table S3**). Similarly, 26% and 36% (corresponding to 7 and 10 genes) of the neuron-specific genes, and 33% and 25% (4 and 3) genes of the stemness-specific genes lists are differentially expressed (**Table S3**).

To investigate further the astrocytes-specific transcriptomic profile, we computed the log2 fold changes in gene expression for these genes at 70 days. We observed the upregulation of *IGFBP2* in the H-G2019S compared to the H astrocytes while *GJA1, VEGFA*, and *DAAM2* were downregulated at day 70 only (**Fig.3e**). *GJA1* is coding for connexin 43, the major gap junction protein of astrocytes [41]. Gap junctions are essential to astrocytes for the transfer of metabolites and ions [42]. The protein has been found downregulated due to inflammation [43], ischemia [44], and in animal models of multiple sclerosis [43]. *VEGFA* promotes proliferation and viability in astrocytes [45] and it was shown to be expressed in reactive astrocytes [46]. When looking at the results of the independent search for DEGs, which we performed over the whole genome on the same single-cell data (**Table S3**), *IGFBP2* was

identified as DEG at both day 35 and day 70, and *VEGFA* at day 70, further supporting the findings for these two genes.

We also analyzed the log2 fold changes (log2FC) in expression between H-G2019S and H for the genes of the core regulatory circuit (CRC) of transcription factors of NESC which we previously identified as being dysregulated by the LRRK2-G2019S mutation in 2D dopaminergic cultures[47]. The CRC maintains the cell identity through a pool of transcription factors, which are controlled by super-enhancers to maintain the cell-type specific gene expression profiles [48]. Five transcription factors were identified in the NESC CRC: *NR2F1, NR2F2, POU3F2, POU3F3*, and SOX2. Among these, *NR2F1* was significantly downregulated in the LRRK2-G2019S compared to LRRK2-WT organoids at both time points (**Fig.3f**). This finding is supported by the fact that *NR2F1* also results as one of the DEGs (both at day 35 and at day 70) in the separate analysis mentioned above which was performed genome-wide. As shown by the log2FC, *POU3F2, POU3F3,* and *SOX2* are significantly upregulated in the H-G2019S compared to H organoids at 35 days, with *SOX2* appearing also in the genome-wide analysis of differentially expressed genes. At day 70, only *POU3F3* is upregulated while *SOX2* and *NR2F1* are downregulated. When restricting the analysis to the cells expressing primarily astrocyte-specific genes, we also observed a downregulation of *NR2F1*, which was statistically significant at day 70, but not at day 35. Interestingly, NR2F1, along with NR2F2, regulates the timing of the switch of neural stem cells from neurogenesis to gliogenesis [49]. Furthermore, also the nuclear factor IA (*NFIA*), implicated in glial fate acquisition, was downregulated in LRRK2-G2019S organoids compared to LRRK2-WT at day 70 (**Fig.S2a**) as well *TGFβ1*(**Fig.S2b**). Overall, these findings indicate a different transcriptomic profile of astrocytes carrying the LRRK2-G2019S mutation compared to LRRK2-WT.

LRRK2-G2019S alters transcriptomic profile of astrocyte subpopulations in midbrain organoids

Recently, the presence of different astrocyte subtypes as well as genes identifying these clusters were described [35]. We next wondered whether the LRRK2-G2019S mutation could impact particular astrocytic subtypes. As starting cell cluster annotation, we used the data object previously published[33] where we subset the glial population (**Fig.S3a-b**). We reclustered the astrocytic population to identify three subpopulations: the homeostatic cluster (*Ntm, Dclk1, Slc1a3*, and *Gria2*), the radial glia (RDG)/activated cluster (Cst3, GFAP, VIM, and CLU), and the subpopulation of genes associated with DNA transcriptional activity (Id1, Id3, and Mat2a) and Cdkn1a. While the H organoids showed an increase in the number of astrocytes of all the three sub clusters from 35 and 70 days in the H-G2019S organoids there was an enrichment of RL/activated astrocytes (**Fig.4a**).

To further appreciate potential developmental differences between healthy and H-G2019S astrocyte subpopulations we performed a reconstruction of the pseudotemporal trajectory and ploted it in the UMAP space (**Fig.4b-d**). As a root (starting point) we chose the healthy homeostatic astrocytes and radial glia cells at day 35 (**Fig.4b**). At 35 days H and H-G2019S mutant radial glia, homeostatic, and transcriptional active astrocytes seemed to cluster in close proximity in the pseudotemporal space, showing similar differentiated states between healthy and mutants (**Fig.4c**). Furthermore, we can observe that healthy astrocytes were situated along the pseudotime trajectory that projects from 35 to 70 days (**Fig.4c**). At 70 days the H astrocytes move from homeostatic, over transcriptional-active, to reactive astrocytes (**Fig.4d**). In contrast to the H at 70 days, the H-G2019S astrocytes were placed on a separate cyclic trajectory, highlighting their limited cellular developmental path (**Fig.4d**). In addition, they seemed to be either strongly reactive and located on a separate developmental path compared to the H or not further differentiating, compared to the 35-day old astrocytes, and remaining in close proximity of the latter (**Fig.4c-d**).

We then quantified the proportion of each subtype present in H and H-G2019S organoids at both time points (**Fig.4e**). We observed that at 35 days of differentiation H and H-G2019S astrocyte subpopulations strongly differ in the proportion of radial glial/ reactive and transcriptional active astrocytes. Although the number of identified astrocytes was law, we could still observe that H astrocytes were mainly transcriptionally active, H-G2019S astrocytes were more radial glial-like. Interestingly, upon healthy development, the proportion of transcriptionally active astrocytes is reduced (54% to 37%) and an increased number of homeostatic astrocytes are specified (23% to 40%). The proportion of radial glial-like astrocytes remains constant over time and represents the smallest of all three populations (25%). On the contrary, in H-G2019S organoids showed similar percentage of both homeostatic and transcriptionally active astrocytes at 35 at 70 days, confirming their limited developmental capacity. The large proportion of radial glial-like/reactive astrocytes remains unchanged between the two time points (45-47%) indicating a less mature differentiation status.

We then looked at the overall trascriptional signature of each of the astrocyte subtypes in H and H-G2019S organoids and performed DEG and downstream pathway analysis. The top 50 DEG between H and H-G2019S astrocytes are visualized within an heatmap showing that homeostatic and transcriptionally active sub clusters shared increased similarities compared to RGL/reactive once (**Fig.4f**). In addition, H-G2019S astrocytes cluster apart from H ones independent of the time point (**Fig.S4a**). Interestingly *NR2F1* showed as one of the DEG significantly downregulated in H-G2019S astrocytes (**Fig.S4a**). Furthermore, a metacore pathway analysis revealed the process networks (**Fig.S4b**) and pathway maps (**Fig.S4c**) deregulated in H-G2019S compared to H astrocytes. Reasonably, we observed that transcriptionally active astrocytes have transcription as the main pathway that is most affected by the mutation. Moreover, the homeostatic astrocytes showed impairments in axonal guidance and neurodevelopment, confirming the observed impaired development due to the LRRK2-G2019S. When looking again at the expression levels of *NR2F1* in the three astrocytic sub clusters we observed a decreased expression of the gene in all the astrocyte types, especially the transcriptionally active ones, in LRRK2-G2019S astrocytes (**Fig.S4d**). Overall, the scRNAseq data indicates that the LRRK2-G2019S mutation delays the astrocyte differentiation trajectory and reduces the acquisition of functional competence by predisposing to the acquisition of a reactive phenotype.

LRRK2-G2019S induces a senescence-like profile in midbrain organoids

Considering the altered astrocytic differentiation shown here and the dopaminergic defects previously described [23], we evaluated whether the presence of LRRK2-G2019S mutation elicited also the activation of a senescent phenotype as observed in human tissue (**Fig.1**). Increasing evidence have highlighted the contribution of cellular senescence to the neurodegenerative process [50], in particular due to the secretion of senescent-associated secretory phenotype (SASP) factors. Astrocytes have also been reported to undergo senescence in PD [50]. We then identified a list of genes encoding for SASP factors based on published literature [32], with the addition of *LMNA* and *CDKN2A* as important genes in the context of senescence (**Table S2**).

The log2 Fold Change in gene expression for each SASP gene showed a different transcriptomic profile between LRRK2-G2019S and LRRK2-WT with three genes significantly differentially expressed at 35 days (not shown), and ten genes showing significant differences at 70 days (**Fig.5a**). In particular, *LAMB1* and *LMNA* are significantly downregulated in LRRK2-G2019S organoids compared to LRRK2-WT at 70 days (also confirmed by the DEGs analysis). *LAMB1* codifies for the nuclear protein lamin B1, which depletion is considered a marker of senescence. At day 70, the genes significantly differentially expressed are: *COL3A1* (#), *MMP14* (#), *CXCR4* (#), *LMNB1* (#), *COL14A1* (#), FN1 (#), *COL11A2*, *COL5A1* (#), *COL1A1,* and *LMNA (#)*, the great majority of which down-regulated. The

13

genes marked with (#) are those which were also identified as DEGs in the separate genome-wide analysis performed above (see Table S3). In addition, the analysis showed as DEGs at day 35 *COL3A1* and *COL1A1*, and at day 70 *IGFBP7*. The gene-gene correlation matrices (Pearson correlation coefficient) between senescence-specific genes, computed for day 70, revealed a striking decreased correlation in the LRRK2-G2019S compared to LRRK2-WT organoids (**Fig.5b**). In the upper triangular matrix of each heatmap, correlations which were not statistically significant where set to zero. Also, the elements on the diagonals, which are equal to 1 by definition, are masked for visual clarity, and we also mask the lines/columns corresponding to genes for which no expression was measured, as this does not allow to compute correlation values. While for LRRK2-G2019S only a few correlation values were significantly different from zero (non-white squares in the upper triangular matrix), in the LRRK2-WT an increased number of correlations was significantly different from zero (and positive, colored in shades of blue). This is in accordance with the acquisition of a senescent profile as previously observed [51]. To validate the finding we performed an immunofluorescence analysis with Lamin B1 in the same lines used for the scRNA-Seq analysis (**Fig.5c-d).** We observed a decrease mean intensity of the Lamin B1 staining in the nuclei of the GFAP$^+$ astrocytes.

In order to further confirm the senescence phenotype from another perspective, we performed a cell cycle analysis on the previously discovered astrocyte subtypes. As senescent astrocytes are not proliferative, we checked for the expression of genes associated to replicative and quiescent phases. In a first step, the proportion of cells in the G1/GO, S, and G2M phases were calculated. We observed that H astrocytes had an increased number of cells in the G2M and S phase compared to H-G2019S astrocytes, whereas H-G2019S astrocytes had more cells in the G0/G1 phase, so in a non-proliferative quiescent state (**Fig.6a**). When looking at subtype-specific differences, H organoids had highly proliferative (S phase) radial glial-like and transcriptional astrocytes, while the homeostatic were quiescent. As senescence is characterized by quiescent cells in cell cycle arrest (G0 phase), we re-clustered the cells that were previously shown to be in the G1/G0 phase based on G0 specific marker expression[36]. Although the number of cells was low, we observed that H astrocytes have an increased number of quiescent cells from 35 to 70 days, whereas the number remained constant in H-G2019S organoids (**Fig.6b**). However, the overall number of quiescent cells in H-G2019S organoids (70-75%) was much higher compared to the H ones (0-30%). The subtype analysis confirms this observation (**Fig.6b**), supporting the overall hypothesis that LRRK-G2019S astrocytes are more inclined to undergo senescence.

LRRK2-G2019S mutation alters the early dynamics of the astrocyte differentiation in 2D

We next used 2D cultures to better evaluate astrocyte early differentiation dynamics. 2D astrocytes were differentiated from NESCs using a previously established protocol [22], **Fig.7a**. The astrocyte differentiation from LRRK2-WT NSCs results in a pure population of astrocytes expressing markers such as GFAP, vimentin, EAAT2, and aquaporin 4 [22]. We particularly focused on the early differentiation time points and assessed the differentiating astrocytes after 3, 9, and 12 days. Considering the data in PD-G2019S organoids showing a decreased abundance of astrocytes after 35 days, we assessed differentiating astrocytes in 2D cultures for apoptosis and mitochondrial morphological alterations. The lines carrying the LRRK2-G2019S mutations showed increased expression of the apoptotic marker cleaved caspase 3. This was increased both in the nucleus and perinuclear zone of P-G2019S lines compared to H. The correction of the mutation in the P-G2019S lines determined a decrease of C-Casp3 (**Fig.7b-c**). Coherently, the introduction of the mutation in the H lines determined an activation of the pathway. The same time points were also analyzed with live imaging in terms of mitochondrial morphology using MitoTracker Green and tetramethylrhodamine,

methyl ester (TMRM) to measure the mitochondrial membrane potential (**Fig.7d-e**). Our Matlab script identified a set of morphological features including mitochondrial skeleton, major axis, branching, and TMRM intensity (**Fig.7f**). The PD-G2019S lines showed increased mitochondrial skeleton but decreased end points. This suggests the PD-G2019S have higher number of mitochondria but their complexity is decreased compared to both PD-G2019S-GC and H. The introduction of the mutation in the healthy background (H-G2019S) determines the same effect.

To evaluate which pathway activity changes were enriched in LRRK2-G2019S lines compared to LRRK2-WT and potentially responsible for the observed phenotype, we performed microarray analysis in the NSCs and NSCs after 24h of exposure to the astrocyte media in the cell line PD1 and PD1-GC (**Fig.2**). This time point was chosen as it did not show any change in cell viability which could have constituted a background noise for the analysis. We also excluded, at this time point, the occurrence of major mitochondrial abnormalities which we evaluated by measuring oxygen consumption using the Seahorse XF Analyzer (data not shown).

Differentially over-expressed (**Fig.S5a**) and under-expressed (**Fig.S5b**) genes were identified in NSCs in maintenance conditions and after 24h exposure to the astrocyte media. The induction of the astrocyte differentiation determined changes in the gene expression profile when comparing the LRRK2-WT and LRRK2-G2019S cultures with 178 genes under-expressed and 162 over-expressed compared to the maintenance (focusing on genes with an absolute fold-change > 1.5). Among 206 genes with a percentage of false predictions (PFP) < 0.05 under astrocyte media exposure, 88 were significant only in this condition and not in hNSCs in maintenance (using the RankProd method for differential expression analysis[52]. The differentially expressed genes were also visualized in the heat map in **Fig. S5c.** Pathway analysis showed that for the comparison PD1 and PD1-GC the most significantly altered pathways were the ones associated to Wnt/β-catenin and TGF-β signaling (**Fig. S5d-f**). Interestingly, the activation of the Wnt/β-catenin signaling pathway was recently shown to disrupt early astrogliogenesis in the developing spinal cord [53]. As main players in the TGF-β signaling, the expression levels of TGF-β1 and TGF-β2 were increased in the LRRK2-G2019S cultures, especially after 24h exposure to the astrocyte media (**Fig. S5f**).

NR2F1 activator rescues certain LRRK2-G2019S dependent phenotypes in astrocytes

Considering the potential role played by NR2F1 in regulating the switch between neurogenesis and astrogenesis [54] and our recent finding showing the downregulation of *NR2F1* in LRRK2-G2019S *in vitro* models [47], we evaluated whether the administration of a NR2F1 activator could rescue some of the observed phenotypes in the astrocytes. We first analyzed the effect of the compound in 2D differentiating astrocytes to verify its effect in this cell type alone at two different concentrations, 0.1 and 0.5 μM (**Fig.8a**). We also included a treatment with the LRRK2-specific kinase inhibitor Mli-2 (25nM). The treatments normalized the increased mitochondrial membrane potential in the P-G2019S lines after 12 days of treatment. The same tendency was observed for the H-G2019S lines although it did not reach statistical significance. Also, the increased mitochondrial skeleton was normalized upon treatments, especially after 3 days. Moreover, the immunoreactivity against the apoptotic marker C-Casp3 decreased in the perinuclear zone after the treatment with broth Mli-2 and NR2F1 activator at 0.5μM after 3 days in the P-G2019S compared to the DMSO-treated lines. The treatment on the H-G2019S lines showed the same trend. After 12 days, the positive effect of the treatment persisted especially in the P-G2019S lines treated with the NR2F1 activator. After verifying that the treatments were effective in 2D, we tested the compounds in the midbrain organoids. We performed the rescue experiments in the PD1/PD1-GC lines and after 35 days of differentiation we stained against GFAP,

15

S100b, and Tuj1. We performed an analysis considering all the extracted features and we visualized them in a heatmap (**Fig.8b**). This clearly showed that the P-G2019S organoids treated with the NR2F1 activator (0.1 µM) clustered with the P-G2019S-GC. In this case, the Mli-2 treated P-G2019S organoids behaved similarly to the P-G2019S organoids treated with vehicle (DMSO). This suggests that a rescue approach based on NR2F1 activation is convincing in the case of the LRRK2-G2019S mutation.

Discussion

It has become increasingly evident that astrocytes are active players in the etiology of PD, but the mechanisms through which they might contribute to neurodegeneration are still largely unknown. The majority of the papers describing functional studies in relation to astrocytes are performed in animal models which do not recapitulate the morphological complexity and the transcriptomic profile of the human astrocytes [19]. The role of astrocytes in the pathogenesis of PD is then under-represented by using animal models. We describe here a previously unknown effect of LRRK2-G2019S mutation in affecting the differentiation of astrocyte from progenitors. This defect was observed in midbrain organoids at 35 days and it was confirmed in 2D differentiating cultures at early time points. Differentiating astrocytes from PD patients carrying the LRRK2-G2019S mutation had increased cell death and mitochondrial morphological alterations compared to isogenic controls and healthy lines. Interestingly, *NR2F1,* an important transcription factor that constitutes the core regulatory circuit of the NESCs [47], was decreased in stem cells, neurons, and astrocytes. A treatment with an activator of NR2F1 partially reversed the observed 2D and 3D phenotypes. The defect in astrocyte specification, certainly along with other factors, renders astrocytes more vulnerable to the acquisition of a senescent-like phenotype.

In brain samples from a PD patient with the LRRK2-G2019 mutation, we identified a decreased count of GFAP$^+$ astrocytes. Although the data on astrocytes in PD are conflicting, this is in line with observations suggesting there might be an inverse correlation between GFAP expression and α-synuclein load [38]. We also recently reported a decrease in the amount of GFAP$^+$ astrocytes in human brains of PD patients with PRKN mutations and midbrain organoids derived from the same subjects. These observations suggest a general astrocyte impairment in both familial and sporadic cases of PD. This would indicate that the different mutations are not the only driving forces but that they might exacerbate the phenotype. This hypothesis is supported by the fact that PRKN mutant brain samples and idiopathic PD samples have both a lower expression of GFAP protein compared to controls, but the decrease seems to be more drastic in the PRKN mutant brain samples. In the LRRK2-G2019S case, we have previously described the role of the genetic background of the patients [40]. A permissive background, due to cumulative genetic variants, certainly enhances LRRK2 mutations-induced cellular abnormalities.

The interaction between neurons and astrocytes has been shown to regulate multiple processes during brain development such as neuronal migration, axonal growth, and synapse formation [55, 56]. For this reason, dysfunctional astrocyte specification is likely to impact neuronal functions. We have previously shown that the use of midbrain organoids carrying the LRRK2-G2019S mutation recapitulated key features of PD-associated dopaminergic degeneration [23]. Changes in the essential cellular functions of astrocytes, due to familial PD mutations, might reduce the ability of astrocytes to correctly support neuronal functions [8]. It has already been shown that astrocyte proliferation is compromised by a loss-of-function mutation in PINK1, resulting in a decreased number of GFAP$^+$ astrocytes from NSCs [57]. Several studies investigated the role of the LRRK2-G2019S mutation in 2D astrocytes generated from iPSC cells [58, 59]. LRRK2-G2019S seems to alter extracellular vesicle biogenesis in astrocytes. These

vesicles could be internalized by dopaminergic neurons, but failed to provide appropriate neurotrophic support[58]. Moreover, in LRRK2-G2019S PD-specific astrocytes a significant decrease of S100β^+ and GFAP$^+$ cells was observed in 2D cultures [59], coherently with the observations reported in this paper in organoids at day 35. In particular, the decreased amount of homeostatic and transcriptional astrocytes in organoids carrying the LRRK2-G2019S mutation would suggest that mutant astrocytes provide limited support to dopaminergic neurons. By focusing on the early time points of astrocyte differentiation, we could observe that apoptosis and mitochondrial morphological abnormalities were detected early on in P-G2019S cultures. Coherently, the pseudo temporal analysis suggested a defect in the differentiation dynamics of astrocytes carrying the LRRK2-G2019S mutation. It is known that subtle changes during brain development might predispose to certain diseases later in life (Marín, 2016; Poduri et al., 2013). Interestingly, the number of astrocytes in the midbrain region is lower compared to other brain regions[60] and this can render the potential defect even more detrimental to neurons. It is tempting to speculate that also in the case of PD, the LRRK2-G2019S mutation affects astrogenesis and renders astrocytes dysfunctional and more prone to senescence. Supporting this point, it has been recently showed that the excitatory amino acid transporter 2 (EAAT2) protein levels are significantly decreased in LRRK2-G2019S human brains, and this is associated with elevated gliosis. As EAAT2 is predominantly expressed in astrocytes this finding points toward a key role of this cell type as a contributor to neurodegeneration on PD[61]. We also observed that, after 70 days of differentiation, P-G2019S organoids had increased expression of GFAP.

Interestingly, *NR2F1* was downregulated in the H-G2019S organoids and also specifically in astrocytes. NR2F, also called Chicken Ovalbumin Upstream Promoter Transcriptional Factors (COUP-TFs), are a family of orphan receptors. The family member NR2F1 plays a key role in development, in particular during neocortical area patterning [62]. It is one of the transcription factors that contribute to regulate the switch of the neural progenitors from neurogenesis to gliogenesis[49]. NR2F1 is then thought to act as a sensor which directs progenitor cells toward an astroglial or neuronal lineage[54]. These processes seem to be mediated via receptor tyrosine kinase signaling and β-catenin-mediated Wnt signaling [63], which we have shown to be affected by LRRK2-G2019S. Interestingly, *NR2F1-2* double knockdown is characterized by sustained neurogenesis in stem cells at the expense of gliogenesis both *in vitro* and *in vivo* in developing mouse brain [49]. This might partly explain how LRRK2-G2019S induces an altered astrocytic differentiation through the observed down-regulation of *NR2F1* and why the pharmacological activation of the pathway determined a partial rescue. Along with *NR2F1*, also the nuclear factor *NFIA* was downregulated in LRRK2-G2019S organoids after 70 days. *NFIA* acts as a molecular switch inducing glia competency [64, 65]. Interestingly, *NFIA* appears in *NR2F1* first level regulatory network (https://ismara.unibas.ch/supp/dataset4_v2/ismara_report/pages/NR2F1.html).

In LRRK2-G2019S organoids we also observed the activation of a senescent phenotype. Senescent cells are not commonly observed even in aged tissue [66, 67]. However, their appearance throughout life represents a key element of aging and the ability to identify and recapitulate it represents a unique opportunity to better understand how it contributes to pathological processes in neurodegenerative diseases such as PD. Senescence was initially described as a loss of replicative capacity, thus excluding post-mitotic cells like neurons. However, more recent studies suggest that this process involves additional changes related to cellular metabolism, epigenetic regulation, and transcriptomic profile [68]. A senescent-like phenotype was observed in Purkinje cells and cortical neurons in response to DNA damage [69]. Interestingly, senescence has been shown to occur also during embryonic development. This would suggest that this process represents a mean to clear unwanted cells and to modulate the tissue microenvironment [70]. In the LRRK2-G2019S organoids, we observed an alteration of SASP-related genes compatible with the profile of senescent cells [51]. *LMNB1* gene expression and protein

17

decreased significantly in 70 day-old LRRK2-G2019S organoids, coherently with what observed in senescent cells [71]. Single markers have been suggested to be inadequate to identify senescent cells, while single cell transcriptomic profiling might be a good alternative [51]. Our study provides a first indication of the possibility of using single-cell analysis for the detection of senescent-associated phenotypes in organoid models. The observed variability in the expression of SASP genes has been hypothesized to result from genomic rearrangement [51] but also from changes in transcriptional activation or repression [72]. Interestingly, TGFβ signaling has been shown to induce senescence *in vitro* [73]. TGFβ release from astrocytes can mediate synapse elimination [74, 75] and has been associated with a synaptic loss in Alzheimer's disease. LRRK2-G2019S activated wnt/β-catenin pathway which has been shown to participate in the regulation of astrocyte fate specification and differentiation [53]. Importantly, the activation of wnt/β-catenin signaling inhibited the specification of astrocytes from progenitor cells through neurogenin 2 (Ngn2) increased expression [53]. Notably, *TGF-β1* and *TGF-β2* were also up-regulated in LRRK2-G2019S cultures after astrocyte induction. TGF-β determined an apoptotic response in several cell types [76]. Many upstream activators have been suggested to trigger TGF-β-mediate apoptosis, with the majority directed toward the mitochondrial pathway through Bcl-2 family members [77, 78]. TGF-β1 is a strong inducer of astrocyte differentiation from neuronal progenitors [79] and stabilization of the blood-brain barrier (reviewed in [80]). The increased expression of mRNA levels of both *TGF-β1* and *TGF-β2* might represent a compensatory mechanism to boost the impaired astrocytic differentiation. Interestingly, *TGF-β*1 was recently found altered in LRRK2-G2019S mature astrocytes [81]. However, a downregulation of the gene was observed instead of an upregulation. This opposite behavior might be due to the different differentiation stage of the astrocytes. In an early stage, TGF-β1 might activate the gliogenic switch while in more mature astrocytes it might be more associated with induced expression of extracellular matrix proteins. Taken together, our data suggest that LRRK2-G2019S mutation impairs astrocytic specification which might trigger, together with dopaminergic degeneration[23], the occurrence of a senescent phenotype in organoids. Further studies are clearly necessary to elucidate the pathway(s) connecting LRRK2-G2019S to senescence but the ability of recapitulating features of aging in this complex 3D patient-specific model opens up the possibility of future *in vitro* screening of compounds able to ablate senescent cells as a novel therapeutic approach against PD. Moreover, the use of molecules to activate NR2F1 levels is a therapeutic strategy worth investigating further.
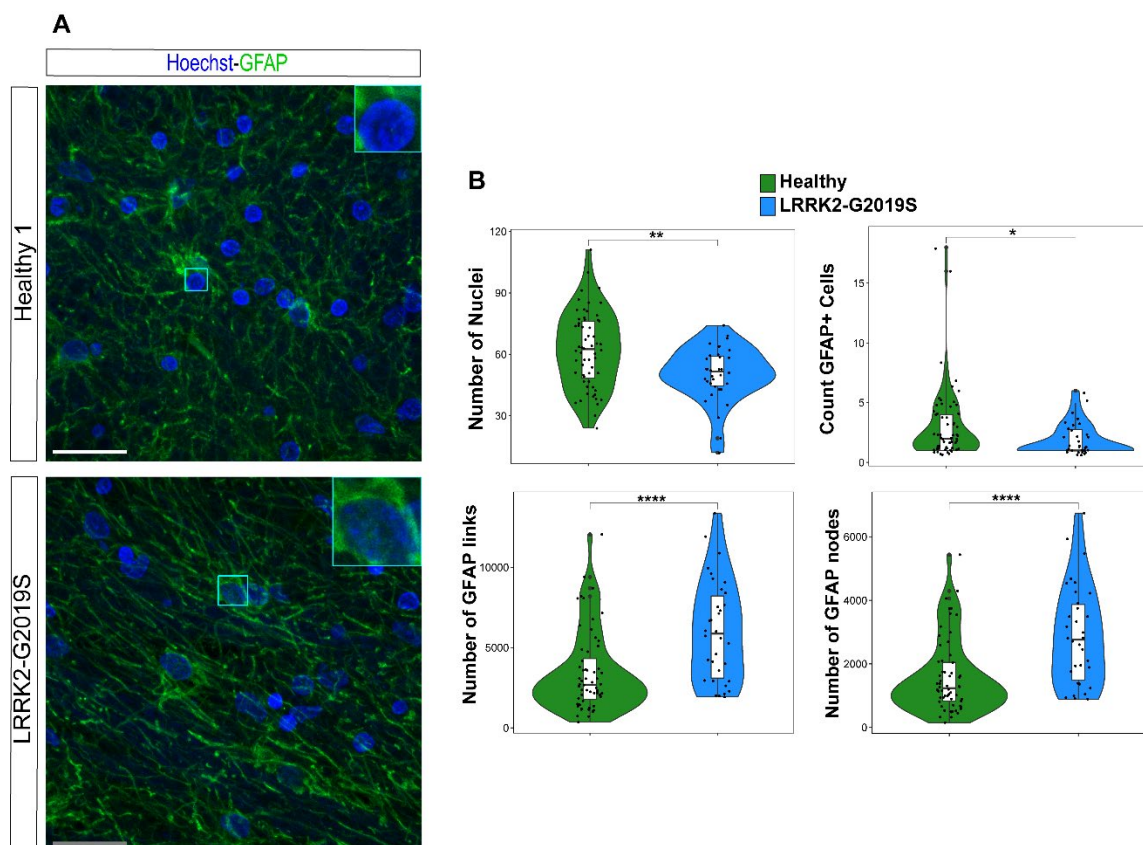
19

Figure 1. Reduced number of astrocytes in a LRRK2-G2019S carrier.

(a) Representative confocal pictures of the midbrain regions showing GFAP expression in a healthy control and a PD patient carrying the LRRK2-G2019S mutation. Hoechst identifies nuclei. **(b)** Violin plots showing the feature extraction performed using a Matlab script that identifies the number of nuclei, the number of GFAP+ cell, the branching of the GFAP+ cells expressed as number of links and nodes (normalized by the number of GFAP+ cells). The green violin plots represent the two healthy controls together. Scale bar 20 μm. Three sections per individual were analyzed, 35 fields per section where automatically acquired using a 63x Yokogawa CV8000 microscope. Each data point in the graphs corresponds to a field. ****P < 0.0001, **P<0.01, *<0.05, Mann-Whitney test in RStudio.
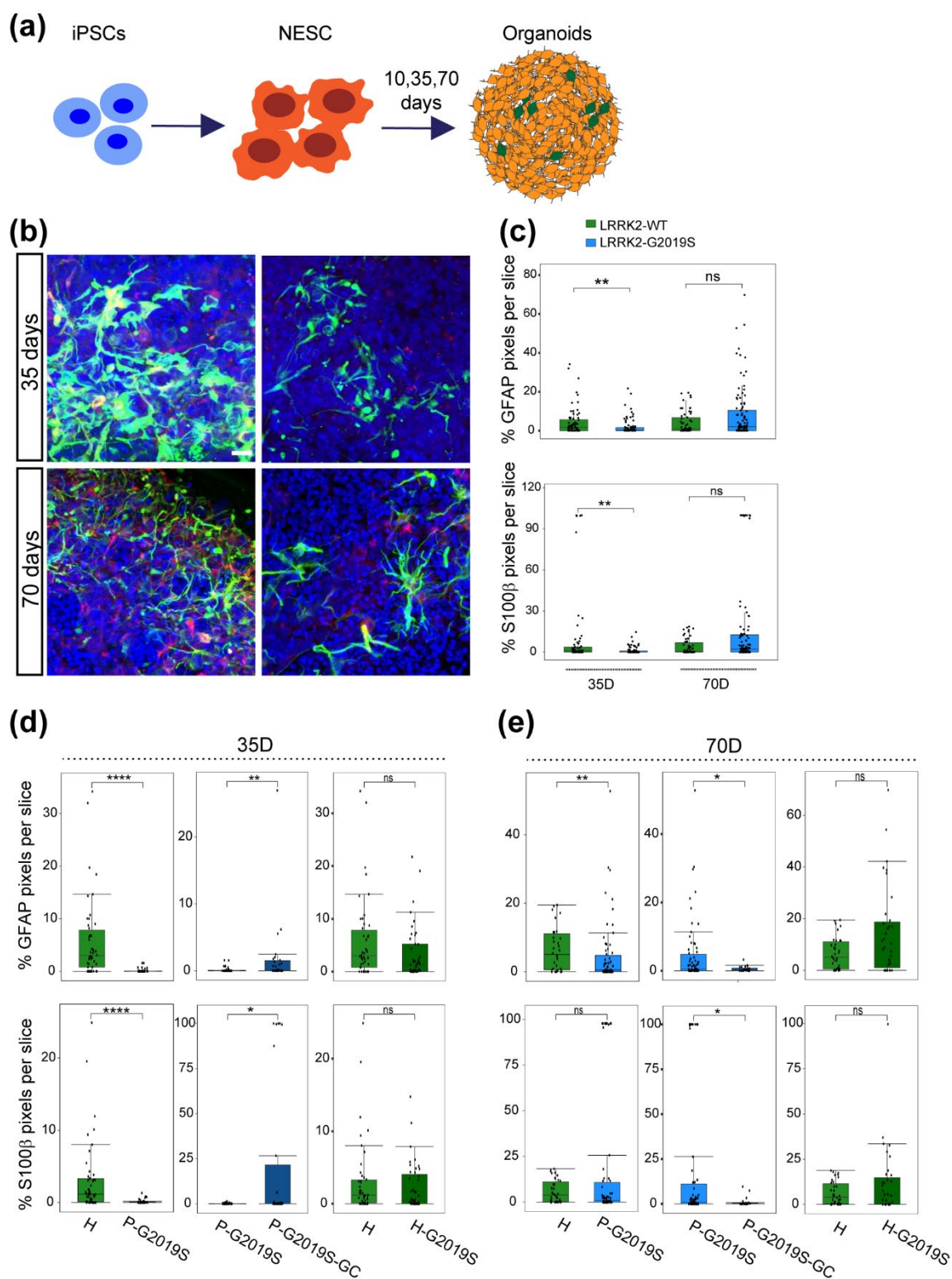
Figure 2. Astrocyte differentiation is impaired in midbrain organoids from PD patients carrying the LRRK2-G2019S mutation.

(a) Cartoon of the 3D experiments. (b) Representative confocal pictures showing S100β and GFAP staining after 35 and 70 days of differentiation (GFAP, green, and S100β, red, Hoechst, blue). (c) Box plots showing the % of GFAP and S100 β positive pixels per organoid slice. **P<0.01, Wilcox test performed in Rstudio. (d) Boxplots showing the % of GFAP and S100 β positive pixels after 35 days

21

in the lines groped according to the genetic background: P, PD-patients carrying the LRRK2-G2019S, H, healthy individuals. The following pairs of isogenic lines were used with the indicated number of organoid slice (n): H2(n=22)/H2-G2019S(n=28), H3(n=21)/H3-G2019S(n=18), PD1(n=19)/PD1-GC(n=4), PD2(n=19)/PD2-GC(n=20). **(e)** Boxplots showing the % of GFAP and S100 β positive pixels after 70 days in the lines groped according to the genetic background: P, PD-patients carrying the LRRK2-G2019S, H, healthy individuals. The following pairs of isogenic lines were used: H2(n=19)/H2-G2019S(n=34), H3(n=13), PD1(n=27)/PD1-GC(n=11), PD2(n=37)/PD2-GC(n=11). *$P<0.05$, **$P<0.01$, ****$P<0.0001$, Wilcox test performed in Rstudio. The image acquisition was performed at 20x. The total number of slices per line at each time point was collected over 3 independent replicates.
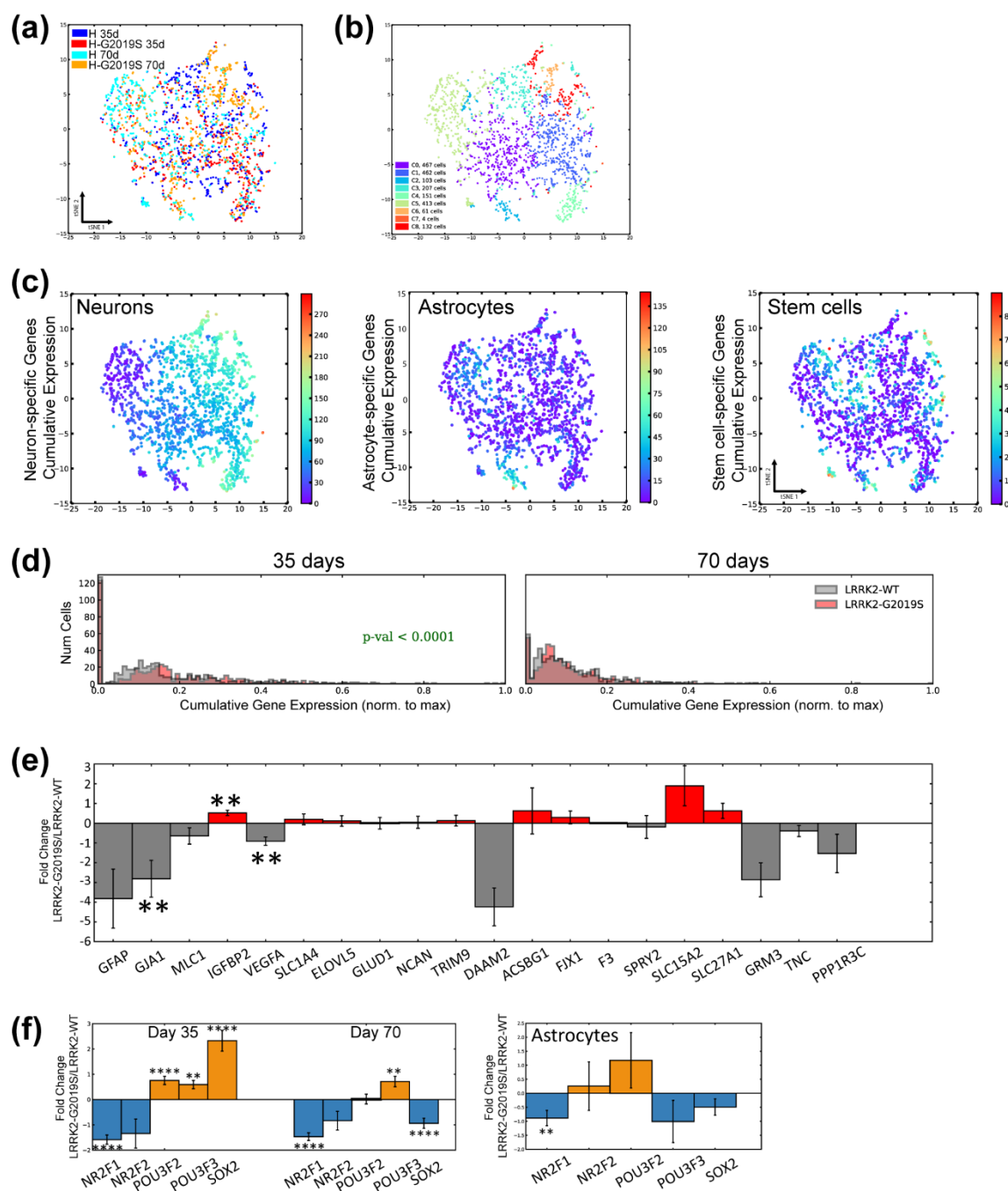
Figure 3. The astrocyte transcriptomic profile is altered in organoids carrying the LRRK2-G2019S mutation

(a) Dimensionality reduction of the scRNA-Seq data (after filtering for high-quality cells) by PCA and subsequent visualization using t-SNE. **(b)** Clustering of the cells performed by the k-means clustering method on the dimensionality reduced (by PCA) data. **(c)** Same data colored by cumulative gene expression score respectively of neuron-, astrocyte-, and stem cell-specific genes. **(d)** Distributions of cells over cumulative gene expression score for the astrocytes-specific list of genes. **(e)** $\log_2$ fold changes in the expression of astrocytes-specific genes, between LRRK2-WT and LRRK2-G2019S, all cell types included, day 70. *P<0.05, **P<0.01. **(f)** $\log_2$ fold changes between LRRK2-WT and LRRK2-G2019S cells, in the expression of the genes belonging to the Core Regulatory Circuit (CRC), considering all cells (left panel) and considering only the cells within each

sample at day 70 which were transcriptionally labelled as astrocytes (right panel). **P<0.01,
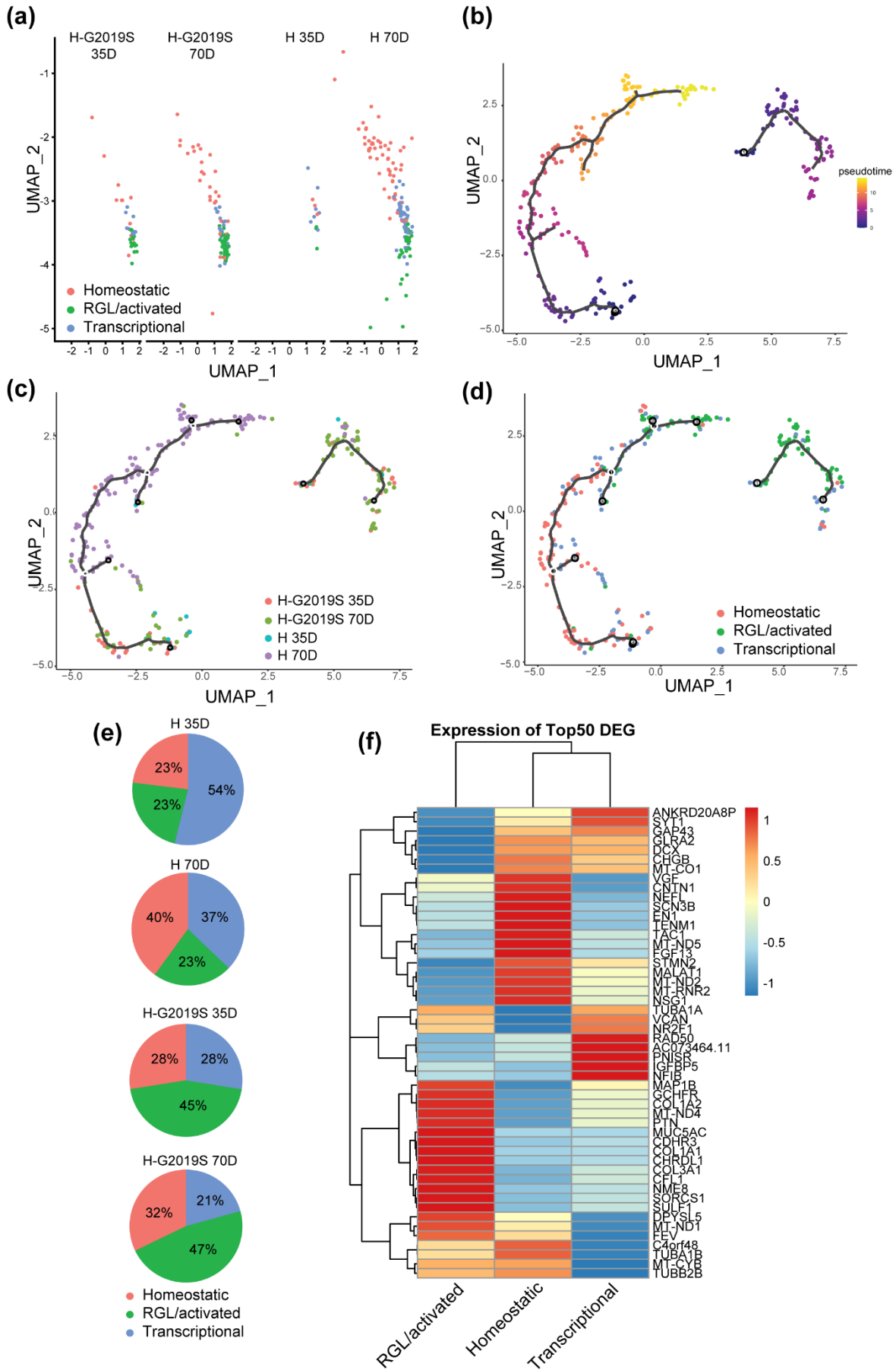***P<0.001, ****P<0.0001.

Figure 4. LRRK2-G2019S organoids have more astrocytes with a reactive transcriptional profile

(a) UMAP plots of the identified astrocytes according to the three sub populations. **(b-d)** Pseudotime trajectory of cells from midbrain organoids colored according to pseudotime **(b)**, astrocytic sub population **(c)** and cell lines at the two time points **(d)**. **(e)** Pie charts indicating the percentage of astrocytes belonging to the three different sub population in the two cell lines at the two time points. **(f)** Heatmap representing the expression of the top 50 DEGs between LRRK2-G2019S and H midbrain organoid astrocytes clustered by astrocyte subtypes.
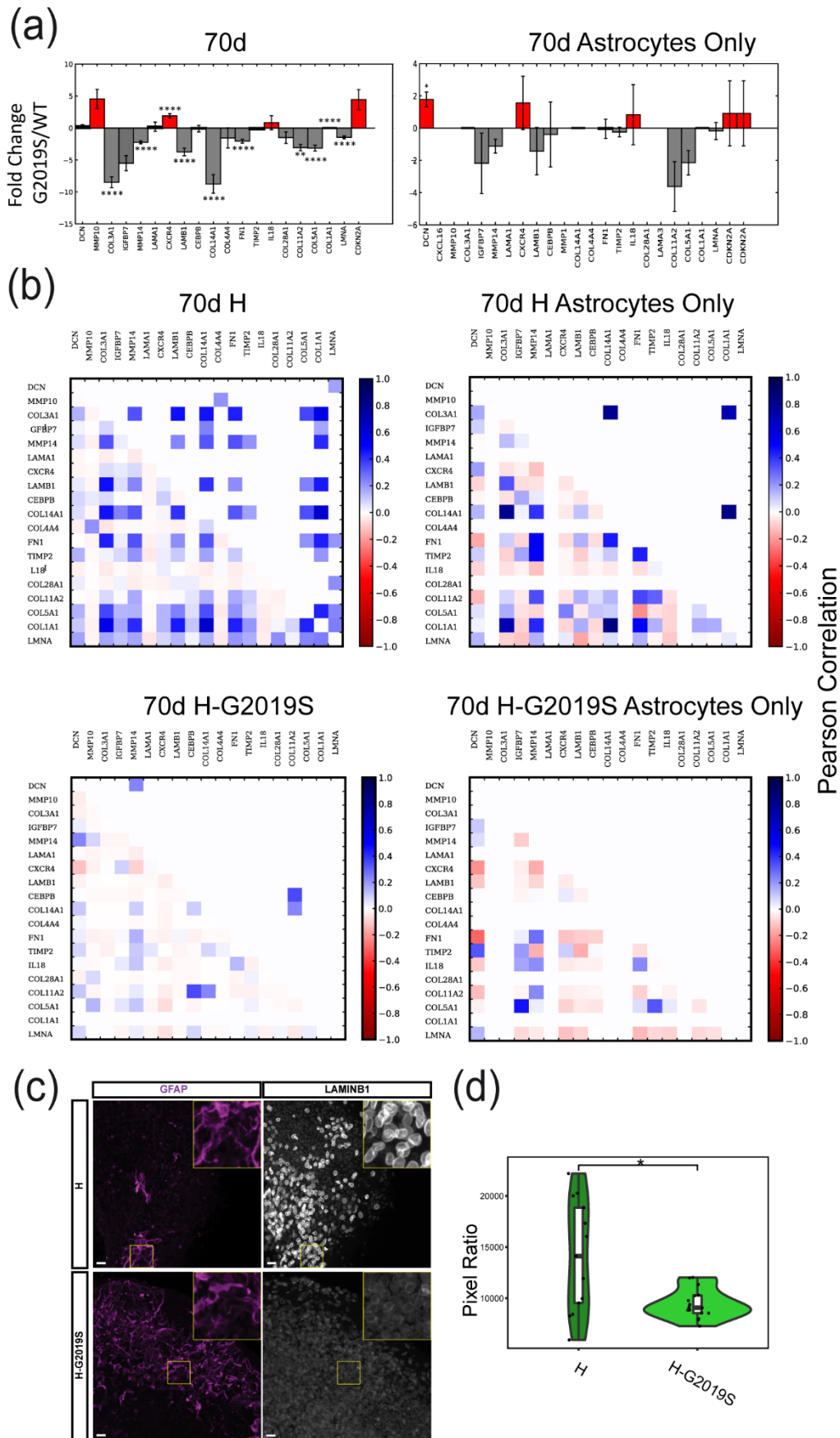
Figure 5. LRRK2-G2019S organoids show a senescent-like phenotype

(a) Gene expression log2 fold changes of senescent-associated genes in H-G2019S compared to H organoids. The right panel is obtained considering only the cells classified as astrocytes **(b)** Heat-maps representing matrices of gene-gene correlation (Pearson correlation coefficient) between senescence-specific genes, computed separately for 70 days and for H and H-G2019S. The matrices on the right correspond to astrocytes only, at day 70. In the upper triangular matrices correlations which were not statistically significant where set to zero, resulting in white squares. The diagonal, by definition having each element equal to 1, is masked with white squares for visual clarity. Genes that are not expressed in a sample are represented as a white line or column. **(c)** Representative confocal pictures and **(d)** violin plots showing the average intensity of Lamin B1 in GFAP⁺ cells. Scale bar 20 μm. All the data in this figure refers to the isogenic pair H2-H2/G2019S.
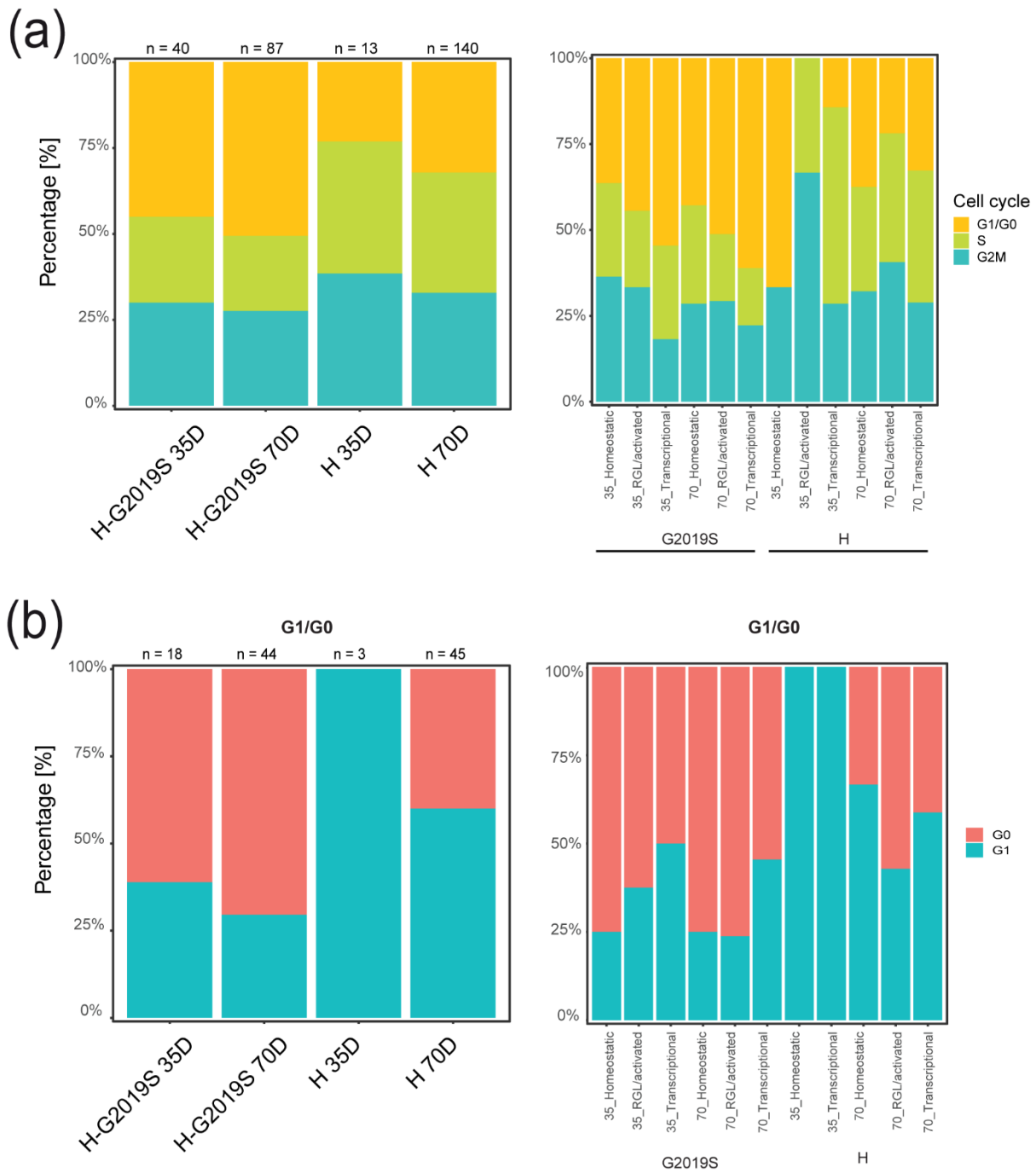
Figure 6. Astrocytes carrying the LRRK2-G2019S mutation are more quiescent

(a) Cell cycle scores represented as percentage of cells (n) per organoid (cell line and time points) and per astrocyte sub population that are found in G1/G0, S and M phase. **(b)** Cell cycle scores are represented as percentage of cells (n) per organoid and per astrocyte sub population that are found in G1 or G0 phase. G1/G0 phase cells are reclassified to either G0 or G1 phase based on G0 marker genes.
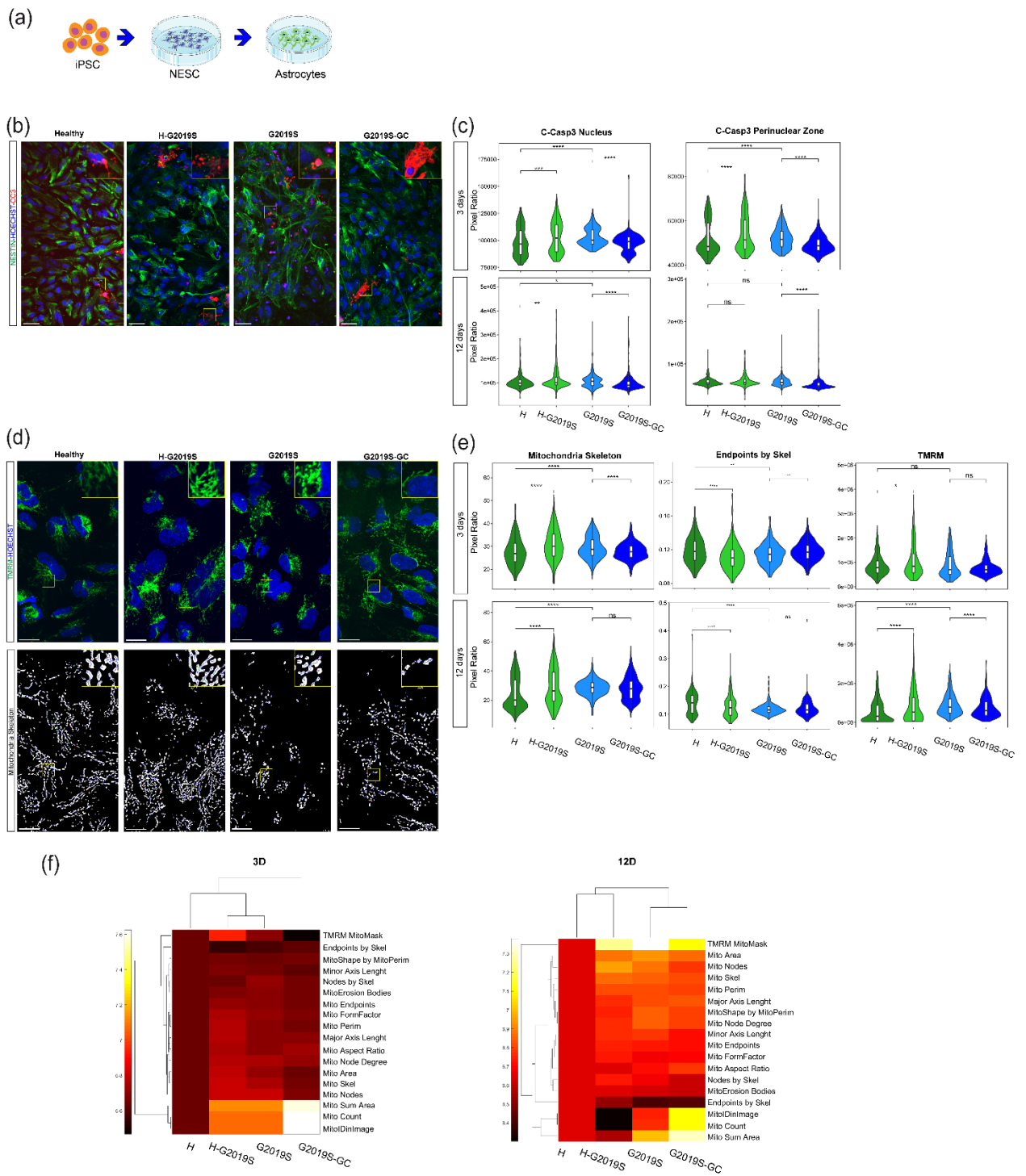
29

Figure 7. 2D astrocytes carrying the LRRK2-G2019S mutation show increased apoptosis and mitochondrial morphological alteration

(a) Cartoon showing the experimental set-up of the 2D study. **(b)** Representative confocal pictures showing nestin and cleaved-caspase 3 (C-Casp3) staining in differentiating astrocytes after 3 days referring to the lines H1/H1-G2019S and PD1/PD1-GC. Scale bar 50 μm. **(c)** Violin plots showing the number of C-Casp3$^+$ staining in the nucleus and perinuclear zone of the differentiating astrocytes after 3 and 12 days. The following pairs of isogenic lines were used H1, H2, PD1, PD2. The total number of fields (f) per line was collected over 3 independent replicates: PD-G2019S(f=), PD-G2019S-GC(f=), H (f=), H-G2019S (f=). ***P<0.001,****P<0.0001, Wilcox test performed in Rstudio. **(d)** Representative confocal pictures showing signal of TMRM and Hoechst and the extracted mitochondrial skeleton in differentiating astrocytes after 3 days referring to the lines H1/H1-G2019S and PD1/PD1-GC. Scale bar 20 μm. **(e)** Violin plots showing the pixel number of the mitochondrial skeleton and TMRM of the differentiating astrocytes after 3 and 12 days. The following pairs of isogenic lines were used H1, H2, PD1, PD2. **(f)** Heatmaps of extracted mitochondrial features after 3 and 12 days of astrocytic differentiation. The image acquisition was performed at 63x (CV8000, Yokogawa). The total number of fields (f) per line was collected over 3 independent replicates: PD-G2019S(f=395), PD-G2019S-GC(f=355), H (f=312), H-G2019S (f=359). *P<0.05, **P<0.01, ***P<0.001,****P<0.0001, Wilcox test performed in Rstudio.
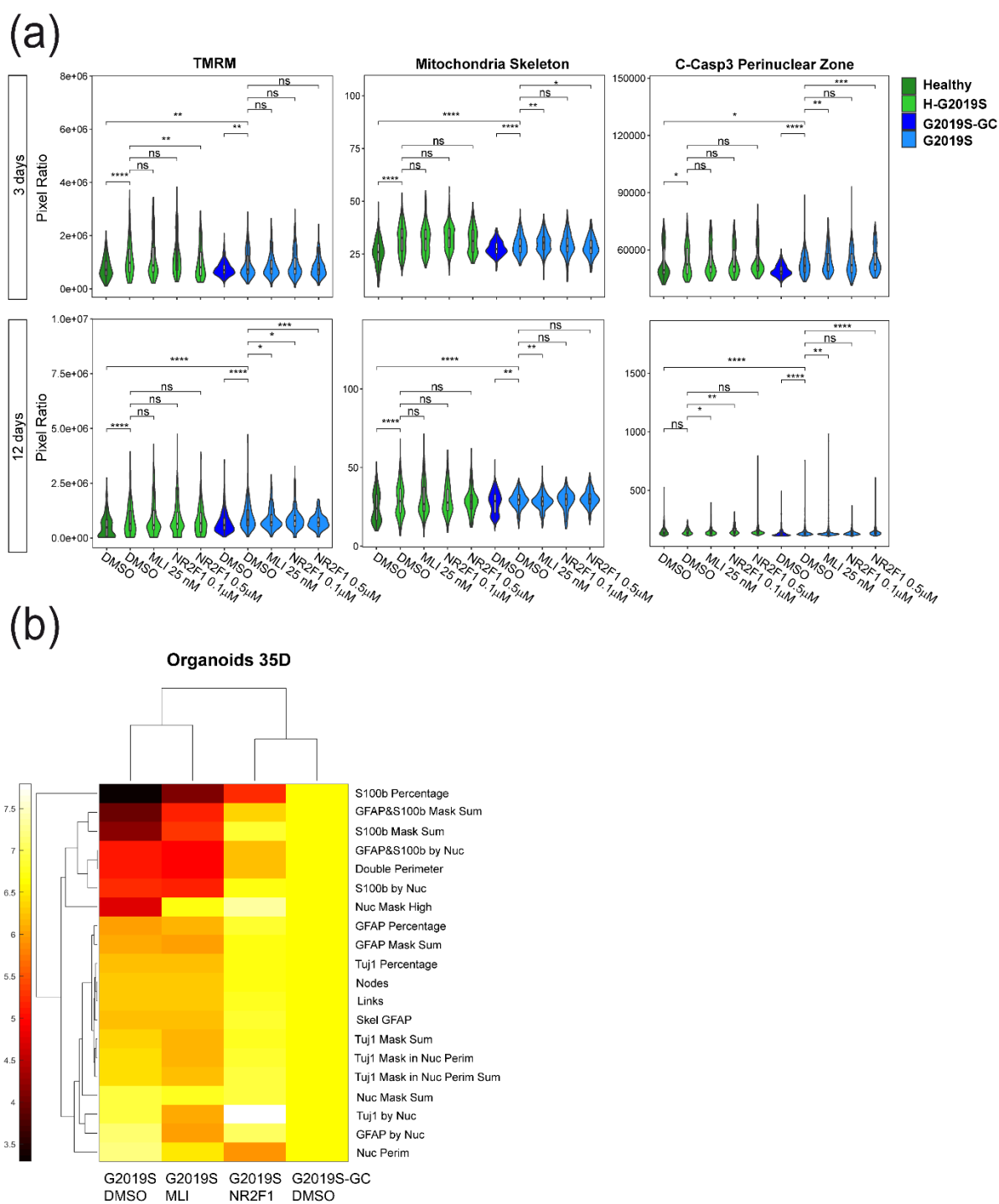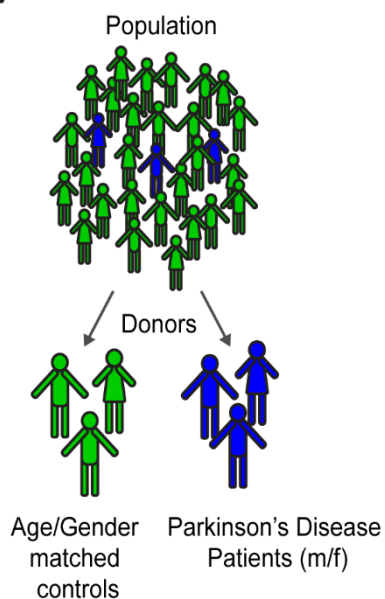
31

Figure 8. Treatment with a NR2F1 activator decreases some of the astrocyte LRRK2-G2019S associated phenotypes

(a) Violin plots showing the number of positive pixels for TMRM, mitochondrial skeleton, and C-Casp3$^+$ staining in the perinuclear zone of the differentiating astrocytes after 3 and 12 days. The following pairs of isogenic lines over 3 independent replicates were used: H1, H2, PD1, PD2. 2D cultures were treated with the LRRK2 inhibitor Mli-2 (25nM) or the NR2F1 activator (0.1 or 0.5 µM). *P<0.05, **P<0.01, ***P<0.001,****P<0.0001, Wilcox test performed in Rstudio. **(b)** Heat map showing the morphometric analysis of 35-day old organoids stained against GFAP, S100β, and Tuj1. The following pair of isogenic lines were used: PD1. Organoids were treated with the LRRK2 inhibitor

Mli-2 (25nM) or the NR2F1 activator (0.1 µM). The image acquisition was performed at 20x (Operetta, PerkinElmer). The total number of slices (n) per line was collected over 3 independent replicates: PD1-DMSO(n=23), PD1-Mli(n=28), PD1-NR2F1(n=28)/PD1-GC-DMSO(n=19).

33

(a)

Population

Donors

Age/Gender matched controls

Parkinson's Disease Patients (m/f)

Healthy Individuals	Lab Identifier	Age of sampling	Age of onset	Sex	References
H1	200	81	-	F	Reinhardt et al., 2013
H1/G2019S	207	81	-	F	Reinhardt et al., 2013
H2	202	55-59	-	M	Qing et al., 2017
H2/G2019S	208	55-59	-	M	Qing et al., 2017
H3	201	-	-	F	GIBCO
H3/G2019S	264	-	-	F	GIBCO

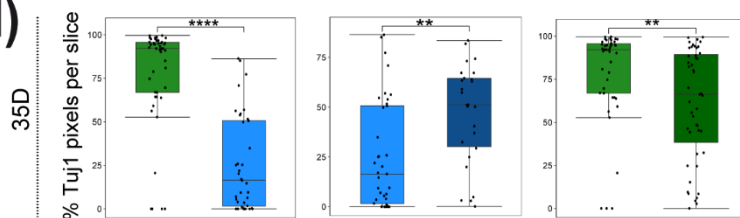| Patients (PD-G2019S)	Lab Identifier	Age of sampling	Age of onset	Sex	References
PD1	209	78	70	F	Reinhardt et al., 2013
PD1/wt	212	78	70	F	Reinhardt et al., 2013
PD2	228	51	40	F	Reinhardt et al., 2013
PD2/wt	229	51	40	F	Reinhardt et al., 2013

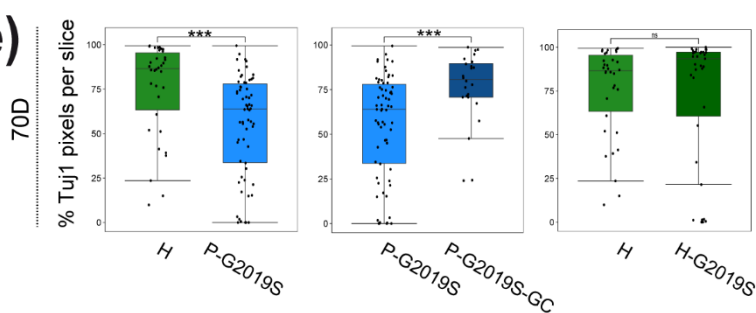**(b)**
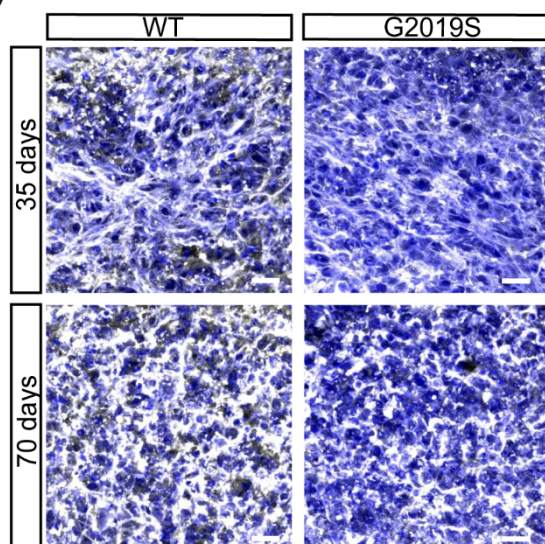
(c)
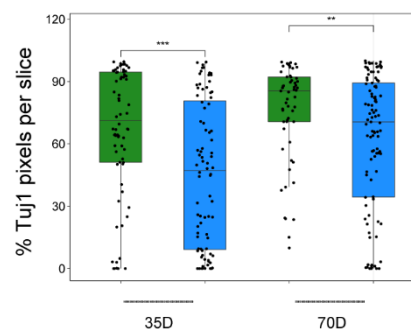
(d)

(e)

Figure S1. Patient-specific organoids carrying the LRRK2-G2019S mutation show reduced neuronal expression

(a) Table showing the lines used in the study. **(b)** Representative confocal pictures showing Tuj1 (white) staining and Hoechst (blue) after 35, and 70 days of differentiation. **(c)** Box plots showing the % of Tuj1 positive pixels per organoid slice. **P<0.01, ***<0.001 Wilcox test performed in Rstudio. **(d)** Boxplots showing the % of Tuj1 positive pixels after 35 days in the lines groped according to the genetic background: P, PD-patients carrying the LRRK2-G2019S, H, healthy individuals. The following pairs of isogenic lines were used with the indicated number of organoid slice (n): H2(n=22)/H2-G2019S(n=28), H3(n=21)/H3-G2019S(n=18), PD1(n=19)/PD1-GC(n=4), PD2(n=19)/PD2-GC(n=20). **(e)** Boxplots showing the % of Tuj1 positive pixels after 70 days in the lines groped according to the genetic background: P, PD-patients carrying the LRRK2-G2019S, H, healthy individuals. The following pairs of isogenic lines were used: H2(n=19)/H2-G2019S(n=34), H3(n=13), PD1(n=27)/PD1-GC(n=11), PD2(n=37)/PD2-GC(n=11). **P<0.01, ***P<0.001,****P<0.0001, Wilcox test performed in Rstudio. The image acquisition was performed at 20x. The total number of slices per line at each time point was collected over 3 independent replicates.

35
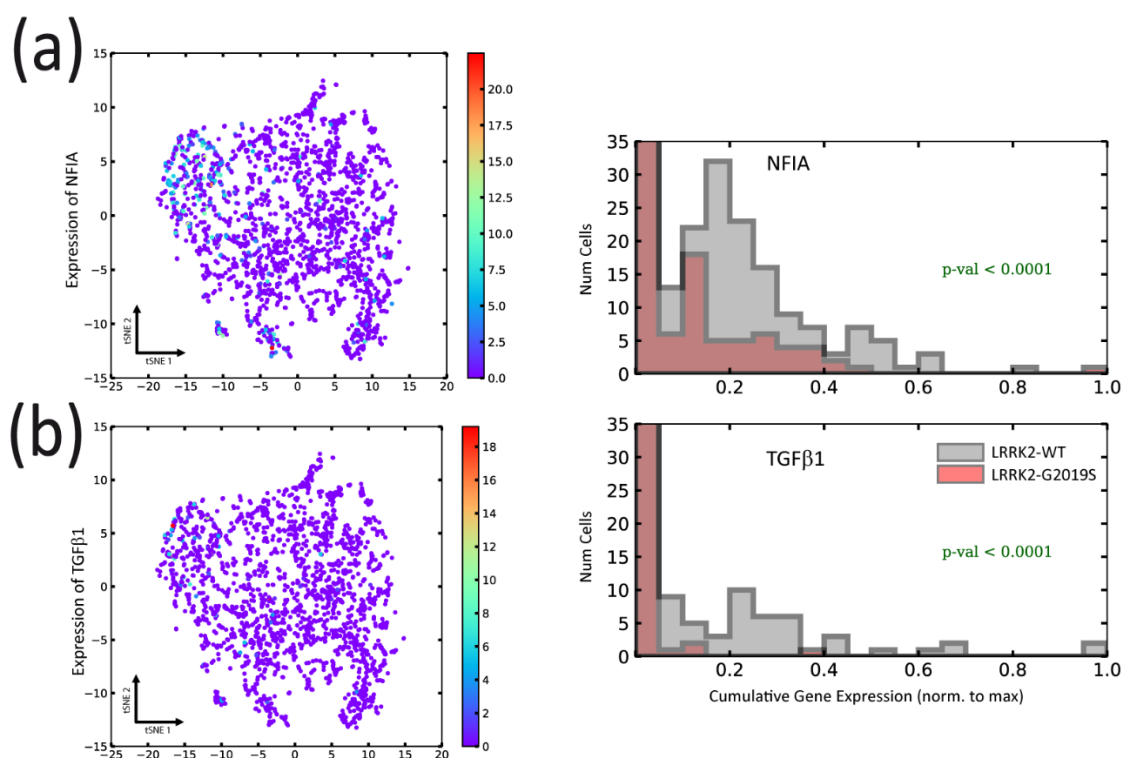
Figure S2. Astrocyte transcriptomic profile in LRRK2-G2019S organoids.

(a, left) Dimensionality reduction of the scRNA-seq data with cells colored according to the expression of the gene NFIA. **(a, right)** Distributions of cells over the gene expression for the gene NFIA at day 70. The vertical scale of this panel is magnified for better visualization, thus cutting part of the column in the histogram which would correspond to cells having 0 gene expression. **(b, left)** Dimensionality reduction of the scRNA-seq with cells colored according to the expression of the gene TGFβ1. **(b, right)** Distributions of cells over the gene expression for the gene TGFBeta1 at day 70 (both NFIA and TGFβ1 genes were almost not expressed at day 30).
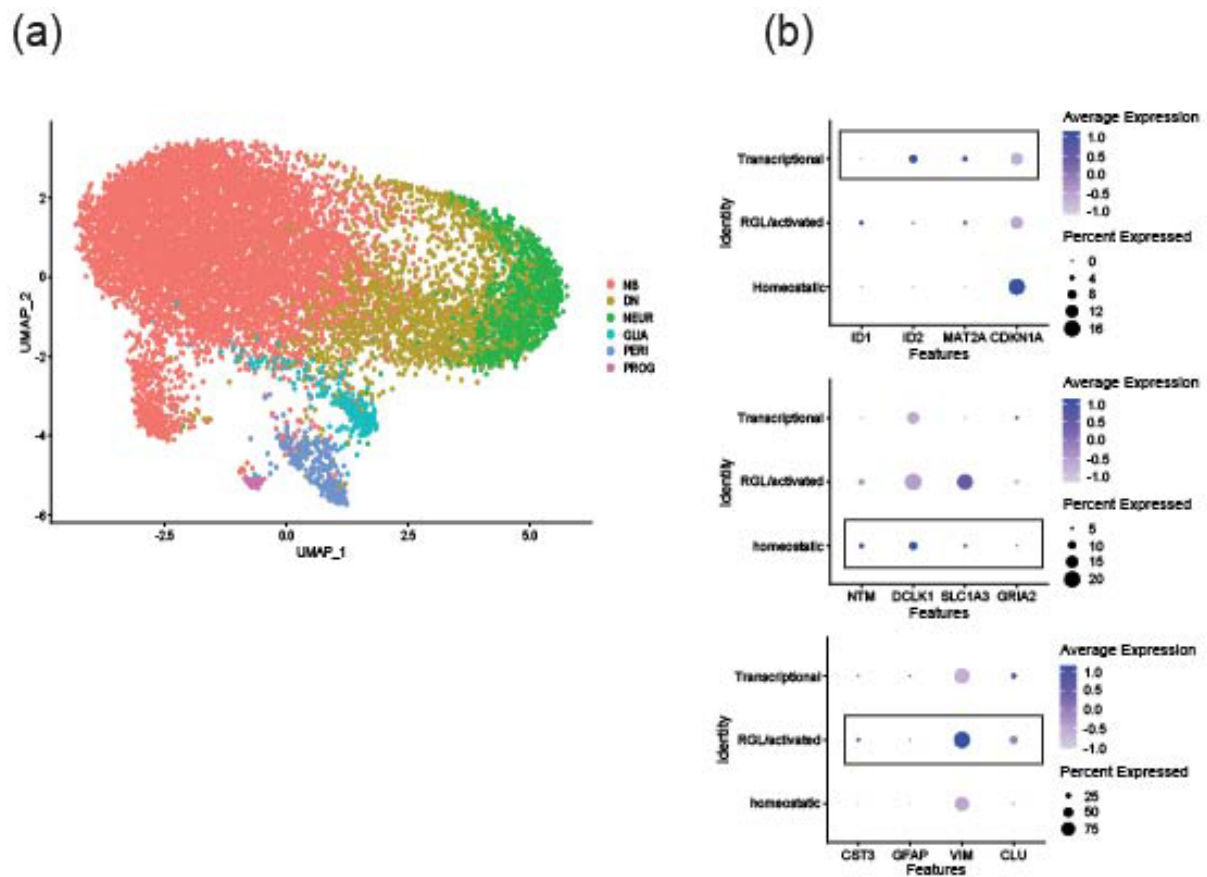
Figure S3. Identification of astrocyte sub populations.

(a) UMAP plot showing the projection of all cells in the scRNA-Seq data used for identifying astrocytes here named Glia (b) Dotplot showing cluster names based on highest average marker expression [35].
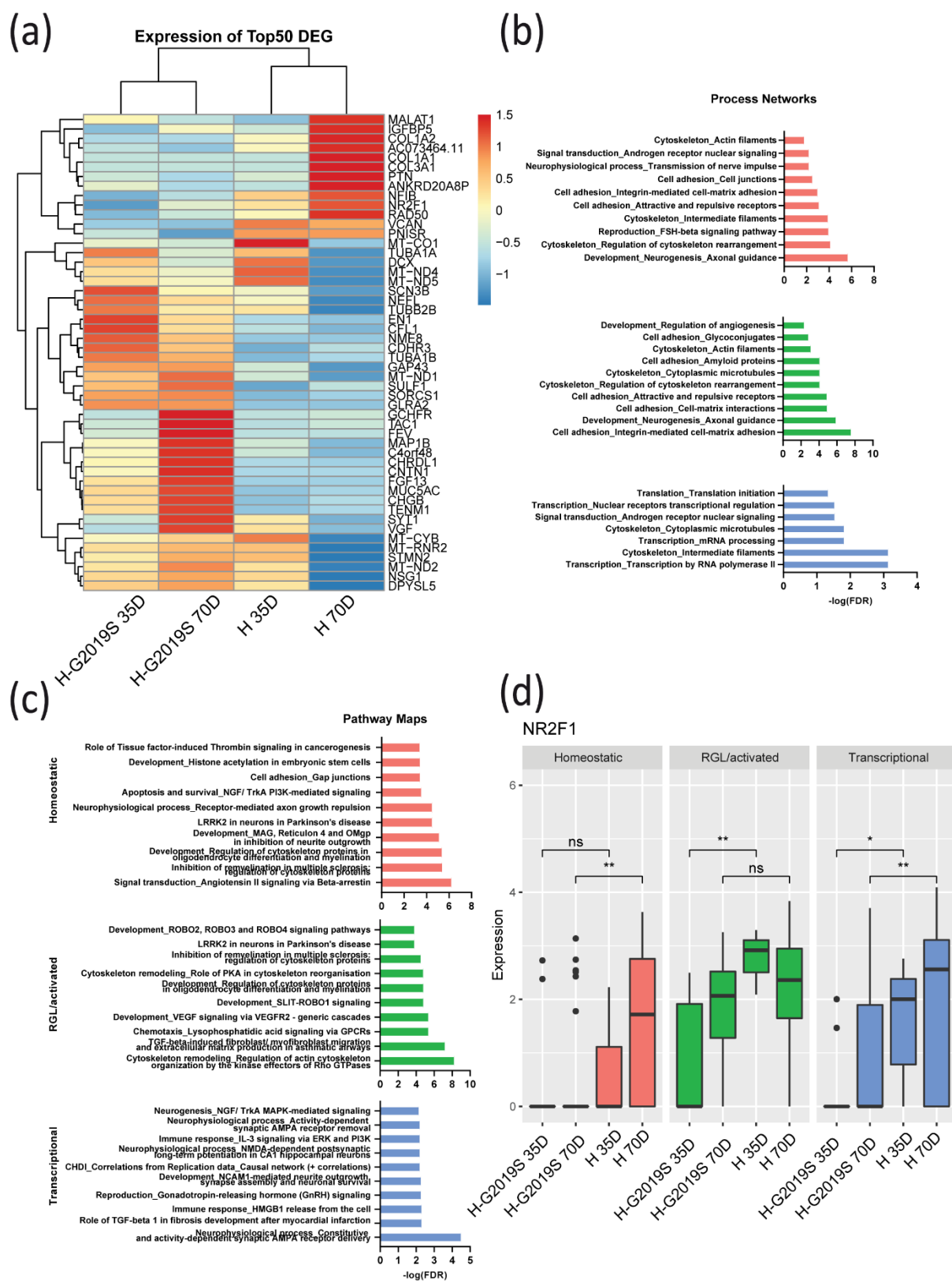
Figure S4. Pathway enrichment analysis shows differential process networks and pathway maps in LRRK2-G2019S astrocytes

(a) Heatmap of top 50 DEG between LRRK2-G2019S and H midbrain organoid in astrocytes, showing the two cell lines at the two time points. **(b-c)** Pathway enrichment analysis of DEGs (p.adj<0.05) of

each sub population showing process networks **(b)** and pathway maps **(c)**. **(d)** Expression of NR2F1 in astrocyte sub population between cell lines and time points. Non-parametric Kruskal Wallis test $p < 0.05$ *, $p<0.01$**.
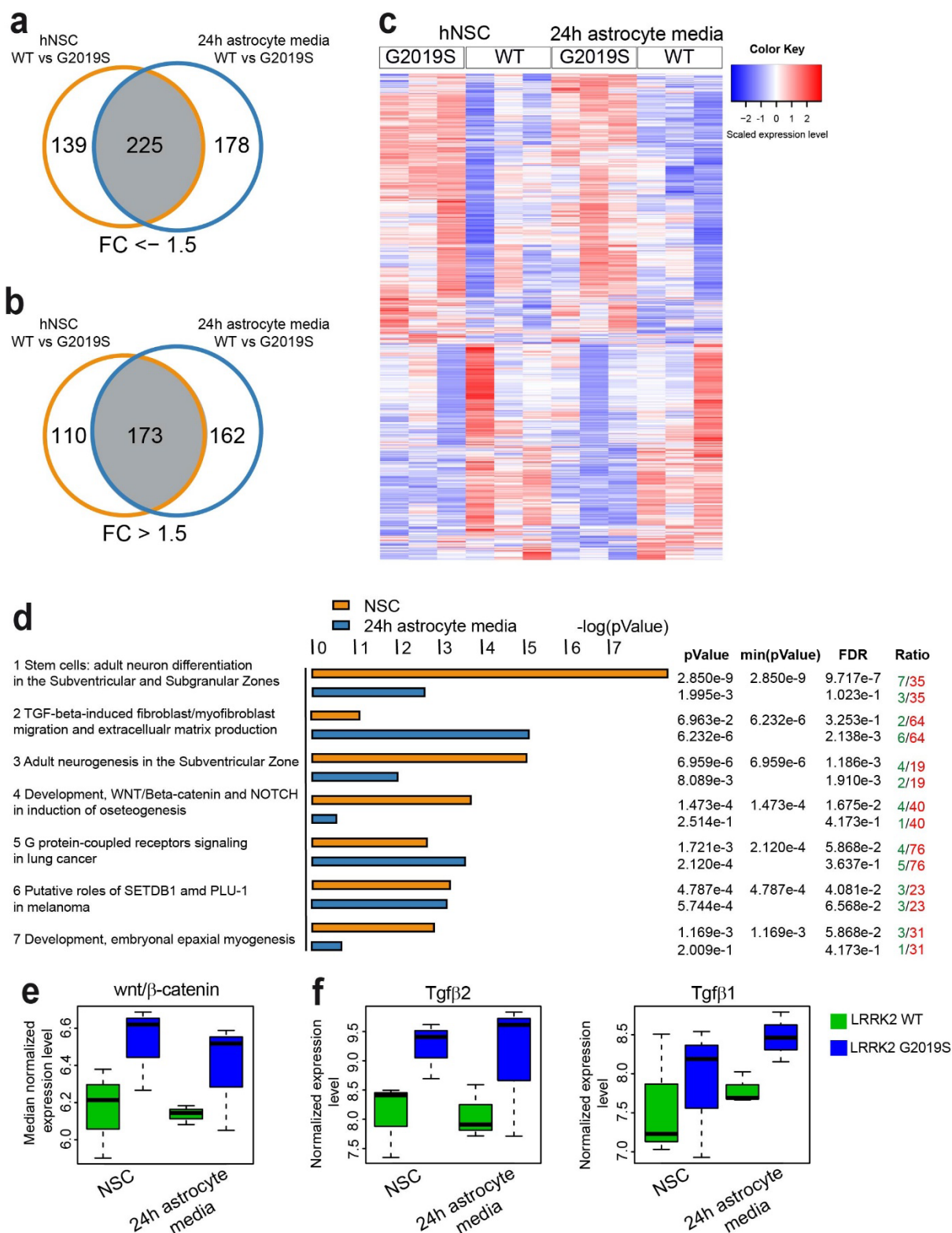
Figure S5. Pathways associated to Wnt/β-catenin and TGF-β signaling are activated upon astrocytic differentiation in 2D cultures carrying the LRRK2-G2019S mutation

(a) Venn diagram showing the overlap of under-expressed genes between LRRK2-WT and LRRK2-G2019S NSCs in maintenance and after 24h of exposure to the astrocyte media. **(b)** Venn diagram showing the overlap of over-expressed genes between LRRK2-WT and LRRK2-G2019S NSCs in maintenance and after 24h of exposure to the astrocyte media. **(c)** Heat map visualization of the genes differentially expressed between LRRK2-WT and LRRK2-G2019S NSCs under maintenance or after 24h exposure to the astrocyte media. For all pairwise comparisons, only genes with an absolute expression fold change above 1.5 were chosen. The color intensities reflect the Z-score standardized gene expression levels. **(b)** and **(c)** The isogenic line PD1/PD1wt was used.

[1] P.G. Haydon, GLIA: listening and talking to the synapse, Nature reviews. Neuroscience 2(3) (2001) 185-93.

[2] U. Hasan, S.K. Singh, The Astrocyte-Neuron Interface: An Overview on Molecular and Cellular Dynamics Controlling Formation and Maintenance of the Tripartite Synapse, Methods in molecular biology 1938 (2019) 3-18.

[3] A. Araque, G. Carmignoto, P.G. Haydon, S.H. Oliet, R. Robitaille, A. Volterra, Gliotransmitters travel in time and space, Neuron 81(4) (2014) 728-39.

[4] N.J. Allen, D.A. Lyons, Glia as architects of central nervous system formation and function, Science 362(6411) (2018) 181-185.

[5] N.J. Allen, Astrocyte regulation of synaptic behavior, Annual review of cell and developmental biology 30 (2014) 439-63.

[6] B.S. Khakh, K.D. McCarthy, Astrocyte calcium signaling: from observations to functions and the challenges therein, Cold Spring Harbor perspectives in biology 7(4) (2015) a020404.

[7] L.F. Lin, D.H. Doherty, J.D. Lile, S. Bektesh, F. Collins, GDNF: a glial cell line-derived neurotrophic factor for midbrain dopaminergic neurons, Science 260(5111) (1993) 1130-2.

[8] H.D.E. Booth, W.D. Hirst, R. Wade-Martins, The Role of Astrocyte Dysfunction in Parkinson's Disease Pathogenesis, Trends in neurosciences 40(6) (2017) 358-370.

[9] J. Miklossy, D.D. Doudet, C. Schwab, S. Yu, E.G. McGeer, P.L. McGeer, Role of ICAM-1 in persisting inflammation in Parkinson disease and MPTP monkeys, Experimental neurology 197(2) (2006) 275-83.

[10] J.B. Koprich, C. Reske-Nielsen, P. Mithal, O. Isacson, Neuroinflammation mediated by IL-1beta increases susceptibility of dopamine neurons to degeneration in an animal model of Parkinson's disease, Journal of neuroinflammation 5 (2008) 8.

[11] I. Lastres-Becker, A. Ulusoy, N.G. Innamorato, G. Sahin, A. Rabano, D. Kirik, A. Cuadrado, alpha-Synuclein expression and Nrf2 deficiency cooperate to aggravate protein aggregation, neuronal death and inflammation in early-stage Parkinson's disease, Human molecular genetics 21(14) (2012) 3173-92.

[12] B. Mirza, H. Hadberg, P. Thomsen, T. Moos, The absence of reactive astrocytosis is indicative of a unique inflammatory process in Parkinson's disease, Neuroscience 95(2) (2000) 425-32.

[13] G.M. Halliday, C.H. Stevens, Glia: initiators and progressors of pathology in Parkinson's disease, Movement disorders : official journal of the Movement Disorder Society 26(1) (2011) 6-17.

[14] J. Trinh, R. Amouri, J.E. Duda, J.F. Morley, M. Read, A. Donald, C. Vilarino-Guell, C. Thompson, C. Szu Tu, E.K. Gustavsson, S. Ben Sassi, E. Hentati, M. Zouari, E. Farhat, F. Nabli, F. Hentati, M.J. Farrer, Comparative study of Parkinson's disease and leucine-rich repeat kinase 2 p.G2019S parkinsonism, Neurobiology of aging 35(5) (2014) 1125-31.

[15] S. Sharma, R. Bandopadhyay, T. Lashley, A.E. Renton, A.E. Kingsbury, R. Kumaran, C. Kallis, C. Vilarino-Guell, S.S. O'Sullivan, A.J. Lees, T. Revesz, N.W. Wood, J.L. Holton, LRRK2 expression in idiopathic and G2019S positive Parkinson's disease subjects: a morphological and quantitative study, Neuropathology and applied neurobiology 37(7) (2011) 777-90.

[16] J. Miklossy, T. Arai, J.P. Guo, A. Klegeris, S. Yu, E.G. McGeer, P.L. McGeer, LRRK2 expression in normal and pathologic human brain and in human cell lines, Journal of neuropathology and experimental neurology 65(10) (2006) 953-63.

[17] N.A. Oberheim, T. Takano, X. Han, W. He, J.H. Lin, F. Wang, Q. Xu, J.D. Wyatt, W. Pilcher, J.G. Ojemann, B.R. Ransom, S.A. Goldman, M. Nedergaard, Uniquely hominid features of adult human astrocytes, The Journal of neuroscience : the official journal of the Society for Neuroscience 29(10) (2009) 3276-87.

[18] N.A. Oberheim, X. Wang, S. Goldman, M. Nedergaard, Astrocytic complexity distinguishes the human brain, Trends in neurosciences 29(10) (2006) 547-53.

[19] Y. Zhang, S.A. Sloan, L.E. Clarke, C. Caneda, C.A. Plaza, P.D. Blumenthal, H. Vogel, G.K. Steinberg, M.S. Edwards, G. Li, J.A. Duncan, 3rd, S.H. Cheshier, L.M. Shuer, E.F. Chang, G.A. Grant, M.G.

Gephart, B.A. Barres, Purification and Characterization of Progenitor and Mature Human Astrocytes Reveals Transcriptional and Functional Differences with Mouse, Neuron 89(1) (2016) 37-53.

[20] G. Tyzack, A. Lakatos, R. Patani, Human Stem Cell-Derived Astrocytes: Specification and Relevance for Neurological Disorders, Current stem cell reports 2 (2016) 236-247.

[21] P. Reinhardt, M. Glatza, K. Hemmer, Y. Tsytsyura, C.S. Thiel, S. Hoing, S. Moritz, J.A. Parga, L. Wagner, J.M. Bruder, G. Wu, B. Schmid, A. Ropke, J. Klingauf, J.C. Schwamborn, T. Gasser, H.R. Scholer, J. Sterneckert, Derivation and expansion using only small molecules of human neural progenitors for neurodegenerative disease modeling, PLoS One 8(3) (2013) e59252.

[22] T. Palm, S. Bolognin, J. Meiser, S. Nickels, C. Trager, R.L. Meilenbrock, J. Brockhaus, M. Schreitmuller, M. Missler, J.C. Schwamborn, Rapid and robust generation of long-term self-renewing human neural stem cells with the ability to generate mature astroglia, Scientific reports 5 (2015) 16321.

[23] L.M. Smits, L. Reinhardt, P. Reinhardt, M. Glatza, A.S. Monzel, N. Stanslowsky, M.D. Rosato-Siri, A. Zanon, P.M. Antony, J. Bellmann, S.M. Nicklas, K. Hemmer, X. Qing, E. Berger, N. Kalmbach, M. Ehrlich, S. Bolognin, A.A. Hicks, F. Wegner, J.L. Sterneckert, J.C. Schwamborn, Modeling Parkinson's disease in midbrain-like organoids, NPJ Parkinson's disease 5 (2019) 5.

[24] K. Yoon, C.C. Chen, A.A. Orr, P.N. Barreto, P. Tamamis, S. Safe, Activation of COUP-TFI by a Novel Diindolylmethane Derivative, Cells 8(3) (2019).

[25] E.Z. Macosko, A. Basu, R. Satija, J. Nemesh, K. Shekhar, M. Goldman, I. Tirosh, A.R. Bialas, N. Kamitaki, E.M. Martersteck, J.J. Trombetta, D.A. Weitz, J.R. Sanes, A.K. Shalek, A. Regev, S.A. McCarroll, Highly Parallel Genome-wide Expression Profiling of Individual Cells Using Nanoliter Droplets, Cell 161(5) (2015) 1202-1214.

[26] J. Walter, S. Bolognin, P.M.A. Antony, S.L. Nickels, S.K. Poovathingal, L. Salamanca, S. Magni, R. Perfeito, F. Hoel, X. Qing, J. Jarazo, J. Arias-Fuenzalida, T. Ignac, A.S. Monzel, L. Gonzalez-Cano, L. Pereira de Almeida, A. Skupin, K.J. Tronstad, J.C. Schwamborn, Neural Stem Cells of Parkinson's Disease Patients Exhibit Aberrant Mitochondrial Morphology and Functionality, Stem cell reports (2019).

[27] L.M. Smits, S. Magni, K. Kinugawa, K. Grzyb, J. Luginbuhl, S. Sabate-Soler, S. Bolognin, J.W. Shin, E. Mori, A. Skupin, J.C. Schwamborn, Single-cell transcriptomics reveals multiple neuronal cell types in human midbrain-specific organoids, Cell Tissue Res 382(3) (2020) 463-476.

[28] L.H. van der Maaten, G. , Visualizing Data using t-SNE, Journal of Machine Learning Research 9 (2008) 2579-2605.

[29] P. Reinhardt, B. Schmid, L.F. Burbulla, D.C. Schondorf, L. Wagner, M. Glatza, S. Hoing, G. Hargus, S.A. Heck, A. Dhingra, G. Wu, S. Muller, K. Brockmann, T. Kluba, M. Maisel, R. Kruger, D. Berg, Y. Tsytsyura, C.S. Thiel, O.E. Psathaki, J. Klingauf, T. Kuhlmann, M. Klewin, H. Muller, T. Gasser, H.R. Scholer, J. Sterneckert, Genetic correction of a LRRK2 mutation in human iPSCs links parkinsonian neurodegeneration to ERK-dependent changes in gene expression, Cell Stem Cell 12(3) (2013) 354-67.

[30] A. Sanchez-Danes, Y. Richaud-Patin, I. Carballo-Carbajal, S. Jimenez-Delgado, C. Caig, S. Mora, C. Di Guglielmo, M. Ezquerra, B. Patel, A. Giralt, J.M. Canals, M. Memo, J. Alberch, J. Lopez-Barneo, M. Vila, A.M. Cuervo, E. Tolosa, A. Consiglio, A. Raya, Disease-specific phenotypes in dopamine neurons from human iPS-based models of genetic and sporadic Parkinson's disease, EMBO Mol Med 4(5) (2012) 380-95.

[31] L. Soreq, U.K.B.E. Consortium, C. North American Brain Expression, J. Rose, E. Soreq, J. Hardy, D. Trabzuni, M.R. Cookson, C. Smith, M. Ryten, R. Patani, J. Ule, Major Shifts in Glial Regional Identity Are a Transcriptional Hallmark of Human Brain Aging, Cell reports 18(2) (2017) 557-570.

[32] M. Ohashi, E. Korsakova, D. Allen, P. Lee, K. Fu, B.S. Vargas, J. Cinkornpumin, C. Salas, J.C. Park, I. Germanguz, J. Langerman, C. Chronis, E. Kuoy, S. Tran, X. Xiao, M. Pellegrini, K. Plath, W.E. Lowry, Loss of MECP2 Leads to Activation of P53 and Neuronal Senescence, Stem cell reports 10(5) (2018) 1453-1463.

[33] A. Zagare, K. Barmpa, S. Smajic, L.M. Smits, K. Grzyb, A. Grunewald, A. Skupin, S.L. Nickels, J.C. Schwamborn, Midbrain organoids mimic early embryonic neurodevelopment and recapitulate LRRK2-p.Gly2019Ser-associated gene expression, Am J Hum Genet 109(2) (2022) 311-327.

[34] T. Stuart, A. Butler, P. Hoffman, C. Hafemeister, E. Papalexi, W.M. Mauck, 3rd, Y. Hao, M. Stoeckius, P. Smibert, R. Satija, Comprehensive Integration of Single-Cell Data, Cell 177(7) (2019) 1888-1902 e21.

[35] C. Wang, M. Xiong, M. Gratuze, X. Bao, Y. Shi, P.S. Andhey, M. Manis, C. Schroeder, Z. Yin, C. Madore, O. Butovsky, M. Artyomov, J.D. Ulrich, D.M. Holtzman, Selective removal of astrocytic APOE4 strongly protects against tau-mediated neurodegeneration and decreases synaptic phagocytosis by microglia, Neuron 109(10) (2021) 1657-1674 e7.

[36] S.A. O'Connor, H.M. Feldman, S. Arora, P. Hoellerbauer, C.M. Toledo, P. Corrin, L. Carter, M. Kufeld, H. Bolouri, R. Basom, J. Delrow, J.L. McFaline-Figueroa, C. Trapnell, S.M. Pollard, A. Patel, P.J. Paddison, C.L. Plaisier, Neural G0: a quiescent-like state found in neuroepithelial-derived cells and glioma, Mol Syst Biol 17(6) (2021) e9522.

[37] M. Kano, M. Takanashi, G. Oyama, A. Yoritaka, T. Hatano, K. Shiba-Fukushima, M. Nagai, K. Nishiyama, K. Hasegawa, T. Inoshita, K.I. Ishikawa, W. Akamatsu, Y. Imai, S. Bolognin, J.C. Schwamborn, N. Hattori, Reduced astrocytic reactivity in human brains and midbrain organoids with PRKN mutations, NPJ Parkinson's disease 6(1) (2020) 33.

[38] J. Tong, L.C. Ang, B. Williams, Y. Furukawa, P. Fitzmaurice, M. Guttman, I. Boileau, O. Hornykiewicz, S.J. Kish, Low levels of astroglial markers in Parkinson's disease: relationship to alpha-synuclein accumulation, Neurobiology of disease 82 (2015) 243-253.

[39] E.M. Hol, M. Pekny, Glial fibrillary acidic protein (GFAP) and the astrocyte intermediate filament system in diseases of the central nervous system, Curr Opin Cell Biol 32 (2015) 121-30.

[40] S. Bolognin, M. Fossepre, X. Qing, J. Jarazo, J. Scancar, E.L. Moreno, S.L. Nickels, K. Wasner, N. Ouzren, J. Walter, A. Grunewald, E. Glaab, L. Salamanca, R.M.T. Fleming, P.M.A. Antony, J.C. Schwamborn, 3D Cultures of Parkinson's Disease-Specific Dopaminergic Neurons for High Content Phenotyping and Drug Testing, Advanced science 6(1) (2019) 1800927.

[41] J.I. Nagy, J.E. Rash, Connexins and gap junctions of astrocytes and oligodendrocytes in the CNS, Brain research. Brain research reviews 32(1) (2000) 29-44.

[42] D.B. Alexander, G.S. Goldberg, Transfer of biologically important molecules between cells through gap junction channels, Current medicinal chemistry 10(19) (2003) 2045-58.

[43] E. Brand-Schieber, P. Werner, D.A. Iacobas, S. Iacobas, M. Beelitz, S.L. Lowery, D.C. Spray, E. Scemes, Connexin43, the major gap junction protein of astrocytes, is down-regulated in inflamed white matter in an animal model of multiple sclerosis, Journal of neuroscience research 80(6) (2005) 798-808.

[44] J.I. Nagy, W.E. Li, A brain slice model for in vitro analyses of astrocytic gap junction and connexin43 regulation: actions of ischemia, glutamate and elevated potassium, The European journal of neuroscience 12(12) (2000) 4567-72.

[45] C. Chapouly, A. Tadesse Argaw, S. Horng, K. Castro, J. Zhang, L. Asp, H. Loo, B.M. Laitman, J.N. Mariani, R. Straus Farber, E. Zaslavsky, G. Nudelman, C.S. Raine, G.R. John, Astrocytic TYMP and VEGFA drive blood-brain barrier opening in inflammatory central nervous system lesions, Brain : a journal of neurology 138(Pt 6) (2015) 1548-67.

[46] A.T. Argaw, Y. Zhang, B.J. Snyder, M.L. Zhao, N. Kopp, S.C. Lee, C.S. Raine, C.F. Brosnan, G.R. John, IL-1beta regulates blood-brain barrier permeability via reactivation of the hypoxia-angiogenesis program, Journal of immunology 177(8) (2006) 5574-84.

[47] J. Walter, S. Bolognin, S.K. Poovathingal, S. Magni, D. Gerard, P.M.A. Antony, S.L. Nickels, L. Salamanca, E. Berger, L.M. Smits, K. Grzyb, R. Perfeito, F. Hoel, X. Qing, J. Ohnmacht, M. Bertacchi, J. Jarazo, T. Ignac, A.S. Monzel, L. Gonzalez-Cano, R. Kruger, T. Sauter, M. Studer, L.P. de Almeida, K.J. Tronstad, L. Sinkkonen, A. Skupin, J.C. Schwamborn, The Parkinson's-disease-associated mutation LRRK2-G2019S alters dopaminergic differentiation dynamics via NR2F1, Cell reports 37(3) (2021) 109864.

[48] D. Hnisz, B.J. Abraham, T.I. Lee, A. Lau, V. Saint-Andre, A.A. Sigova, H.A. Hoke, R.A. Young, Super-enhancers in the control of cell identity and disease, Cell 155(4) (2013) 934-47.

[49] H. Naka, S. Nakamura, T. Shimazaki, H. Okano, Requirement for COUP-TFI and II in the temporal specification of neural stem cells in CNS development, Nature neuroscience 11(9) (2008) 1014-23.

[50] S.J. Chinta, G. Woods, M. Demaria, A. Rane, Y. Zou, A. McQuade, S. Rajagopalan, C. Limbad, D.T. Madden, J. Campisi, J.K. Andersen, Cellular Senescence Is Induced by the Environmental Neurotoxin Paraquat and Contributes to Neuropathology Linked to Parkinson's Disease, Cell reports 22(4) (2018) 930-940.

[51] C.D. Wiley, J.M. Flynn, C. Morrissey, R. Lebofsky, J. Shuga, X. Dong, M.A. Unger, J. Vijg, S. Melov, J. Campisi, Analysis of individual cells identifies cell-to-cell variability following induction of cellular senescence, Aging cell 16(5) (2017) 1043-1050.

[52] F. Hong, R. Breitling, C.W. McEntee, B.S. Wittner, J.L. Nemhauser, J. Chory, RankProd: a bioconductor package for detecting differentially expressed genes in meta-analysis, Bioinformatics 22(22) (2006) 2825-7.

[53] S. Sun, X.J. Zhu, H. Huang, W. Guo, T. Tang, B. Xie, X. Xu, Z. Zhang, Y. Shen, Z.M. Dai, M. Qiu, WNT signaling represses astrogliogenesis via Ngn2-dependent direct suppression of astrocyte gene expression, Glia (2019).

[54] S. Bonzano, I. Crisci, A. Podlesny-Drabiniok, C. Rolando, W. Krezel, M. Studer, S. De Marchis, Neuron-Astroglia Cell Fate Decision in the Adult Mouse Hippocampal Neurogenic Niche Is Cell-Intrinsically Controlled by COUP-TFI In Vivo, Cell reports 24(2) (2018) 329-341.

[55] L.P. Diniz, I.C. Matias, M.N. Garcia, F.C. Gomes, Astrocytic control of neural circuit formation: highlights on TGF-beta signaling, Neurochemistry international 78 (2014) 18-27.

[56] T.C. Spohr, J.W. Choi, S.E. Gardell, D.R. Herr, S.K. Rehen, F.C. Gomes, J. Chun, Lysophosphatidic acid receptor-dependent secondary effects via astrocytes promote neuronal differentiation, The Journal of biological chemistry 283(12) (2008) 7470-9.

[57] I. Choi, D.J. Choi, H. Yang, J.H. Woo, M.Y. Chang, J.Y. Kim, W. Sun, S.M. Park, I. Jou, S.H. Lee, E.H. Joe, PINK1 expression increases during brain development and stem cell differentiation, and affects the development of GFAP-positive astrocytes, Molecular brain 9 (2016) 5.

[58] A. de Rus Jacquet, J.L. Tancredi, A.L. Lemire, M.C. DeSantis, W.P. Li, E.K. O'Shea, The LRRK2 G2019S mutation alters astrocyte-to-neuron communication via extracellular vesicles and induces neuron atrophy in a human iPSC-derived model of Parkinson's disease, Elife 10 (2021).

[59] P. Ramos-Gonzalez, S. Mato, J.C. Chara, A. Verkhratsky, C. Matute, F. Cavaliere, Astrocytic atrophy as a pathological feature of Parkinson's disease with LRRK2 mutation, NPJ Parkinson's disease 7(1) (2021) 31.

[60] C.S. von Bartheld, J. Bahney, S. Herculano-Houzel, The search for true numbers of neurons and glial cells in the human brain: A review of 150 years of cell counting, J Comp Neurol 524(18) (2016) 3865-3895.

[61] L. Iovino, V. Giusti, F. Pischedda, E. Giusto, N. Plotegher, A. Marte, I. Battisti, A. Di Iacovo, A. Marku, G. Piccoli, R. Bandopadhyay, C. Perego, T. Bonifacino, G. Bonanno, C. Roseti, E. Bossi, G. Arrigoni, L. Bubacco, E. Greggio, S. Hilfiker, L. Civiero, Trafficking of the glutamate transporter is impaired in LRRK2-related Parkinson's disease, Acta Neuropathol (2022).

[62] M. Terrigno, M. Bertacchi, L. Pandolfini, M. Baumgart, M. Calvello, A. Cellerino, M. Studer, F. Cremisi, The microRNA miR-21 Is a Mediator of FGF8 Action on Cortical COUP-TFI Translation, Stem cell reports 11(3) (2018) 756-769.

[63] A. Faedo, G.S. Tomassy, Y. Ruan, H. Teichmann, S. Krauss, S.J. Pleasure, S.Y. Tsai, M.J. Tsai, M. Studer, J.L. Rubenstein, COUP-TFI coordinates cortical patterning, neurogenesis, and laminar fate and modulates MAPK/ERK, AKT, and beta-catenin signaling, Cerebral cortex 18(9) (2008) 2117-31.

[64] B. Deneen, R. Ho, A. Lukaszewicz, C.J. Hochstim, R.M. Gronostajski, D.J. Anderson, The transcription factor NFIA controls the onset of gliogenesis in the developing spinal cord, Neuron 52(6) (2006) 953-68.

[65] J. Tchieu, E.L. Calder, S.R. Guttikonda, E.M. Gutzwiller, K.A. Aromolaran, J.A. Steinbeck, P.A. Goldstein, L. Studer, NFIA is a gliogenic switch enabling rapid derivation of functional human astrocytes from pluripotent stem cells, Nature biotechnology 37(3) (2019) 267-275.

[66] D.J. Baker, B.G. Childs, M. Durik, M.E. Wijers, C.J. Sieben, J. Zhong, R.A. Saltness, K.B. Jeganathan, G.C. Verzosa, A. Pezeshki, K. Khazaie, J.D. Miller, J.M. van Deursen, Naturally occurring p16(Ink4a)-positive cells shorten healthy lifespan, Nature 530(7589) (2016) 184-9.

[67] J.A. Kreiling, M. Tamamori-Adachi, A.N. Sexton, J.C. Jeyapalan, U. Munoz-Najar, A.L. Peterson, J. Manivannan, E.S. Rogers, N.A. Pchelintsev, P.D. Adams, J.M. Sedivy, Age-associated increase in heterochromatic marks in murine and primate tissues, Aging cell 10(2) (2011) 292-304.

[68] X. Zhu, Z. Chen, W. Shen, G. Huang, J.M. Sedivy, H. Wang, Z. Ju, Inflammation, epigenetics, and metabolism converge to cell senescence and ageing: the regulation and intervention, Signal Transduct Target Ther 6(1) (2021) 245.

[69] D. Jurk, C. Wang, S. Miwa, M. Maddick, V. Korolchuk, A. Tsolou, E.S. Gonos, C. Thrasivoulou, M.J. Saffrey, K. Cameron, T. von Zglinicki, Postmitotic neurons develop a p21-dependent senescence-like phenotype driven by a DNA damage response, Aging cell 11(6) (2012) 996-1004.

[70] F.C. Tan, E.R. Hutchison, E. Eitan, M.P. Mattson, Are there roles for brain cell senescence in aging and neurodegenerative disorders?, Biogerontology 15(6) (2014) 643-60.

[71] A. Freund, R.M. Laberge, M. Demaria, J. Campisi, Lamin B1 loss is a senescence-associated biomarker, Molecular biology of the cell 23(11) (2012) 2066-75.

[72] R. Bahar, C.H. Hartmann, K.A. Rodriguez, A.D. Denny, R.A. Busuttil, M.E. Dolle, R.B. Calder, G.B. Chisholm, B.H. Pollock, C.A. Klein, J. Vijg, Increased cell-to-cell variation in gene expression in ageing mouse heart, Nature 441(7096) (2006) 1011-4.

[73] J.C. Acosta, A. Banito, T. Wuestefeld, A. Georgilis, P. Janich, J.P. Morton, D. Athineos, T.W. Kang, F. Lasitschka, M. Andrulis, G. Pascual, K.J. Morris, S. Khan, H. Jin, G. Dharmalingam, A.P. Snijders, T. Carroll, D. Capper, C. Pritchard, G.J. Inman, T. Longerich, O.J. Sansom, S.A. Benitah, L. Zender, J. Gil, A complex secretory program orchestrated by the inflammasome controls paracrine senescence, Nature cell biology 15(8) (2013) 978-90.

[74] A.R. Bialas, B. Stevens, TGF-beta signaling regulates neuronal C1q expression and developmental synaptic refinement, Nature neuroscience 16(12) (2013) 1773-82.

[75] A.H. Stephan, D.V. Madison, J.M. Mateos, D.A. Fraser, E.A. Lovelett, L. Coutellier, L. Kim, H.H. Tsai, E.J. Huang, D.H. Rowitch, D.S. Berns, A.J. Tenner, M. Shamloo, B.A. Barres, A dramatic increase of C1q protein in the CNS during normal aging, The Journal of neuroscience : the official journal of the Society for Neuroscience 33(33) (2013) 13460-74.

[76] N. Schuster, K. Krieglstein, Mechanisms of TGF-beta-mediated apoptosis, Cell and tissue research 307(1) (2002) 1-14.

[77] K. Herzer, A. Grosse-Wilde, P.H. Krammer, P.R. Galle, S. Kanzler, Transforming growth factor-beta-mediated tumor necrosis factor-related apoptosis-inducing ligand expression and apoptosis in hepatoma cells requires functional cooperation between Smad proteins and activator protein-1, Molecular cancer research : MCR 6(7) (2008) 1169-77.

[78] S. Ramesh, G.M. Wildey, P.H. Howe, Transforming growth factor beta (TGFbeta)-induced apoptosis: the rise & fall of Bim, Cell cycle 8(1) (2009) 11-7.

[79] J. Stipursky, F.C. Gomes, TGF-beta1/SMAD signaling induces astrocyte fate commitment in vitro: implications for radial glia development, Glia 55(10) (2007) 1023-33.

[80] N.J. Abbott, A.A. Patabendige, D.E. Dolman, S.R. Yusof, D.J. Begley, Structure and function of the blood-brain barrier, Neurobiology of disease 37(1) (2010) 13-25.

[81] H.D.E. Booth, F. Wessely, N. Connor-Robson, F. Rinaldi, J. Vowles, C. Browne, S.G. Evetts, M.T. Hu, S.A. Cowley, C. Webber, R. Wade-Martins, RNA sequencing reveals MMP2 and TGFB1 downregulation in LRRK2 G2019S Parkinson's iPSC-derived astrocytes, Neurobiology of disease 129 (2019) 56-66.

4.3   Manuscript III

Cultivation and characterization of human midbrain organoids in sensor integrated microfluidic chips

Sarah Spitz[1,2], Cristian Zanetti[1], Silvia Bolognin[4], **Mudiwa Nathasia Muwanigwa[4]**, Lisa Smits[4], Emanuel Berger[4], Christian Jordan[3], Michael Harasek[3], Jens C. Schwamborn[4], Peter

Ertl[1,2]*

[1] Institute of Chemical Technologies and Analytics, Vienna University of Technology, Getreidemarkt 9/164, 1060 Vienna, Austria

[2] Institute of Applied Synthetic Chemistry, Vienna University of Technology, Getreidemarkt 9/164, 1060 Vienna, Austria

[3] Institute of Chemical Engineering, Vienna University of Technology, Getreidemarkt 9/164, 1060 Vienna, Austria

[4] Developmental and Cellular Biology, Luxembourg Centre for Systems Biomedicine (LCSB), University of Luxembourg, 7 avenue des Hauts-Fourneaux, 4362 Esch-sur-Alzette, Luxembourg

* Correspondence: peter.ertl@tuwien.ac.at

Preface

As brain organoid technology has rapidly advanced since Lancaster and colleagues' first report showing a protocol for the generation of cerebral organoids (Lancaster *et al.*, 2013), there have simultaneously been efforts to improve some of the inherent limitations of these models. One of these limitations is that many organoid generation protocols lack robust reproducibility. Moreover, limited diffusion of nutrients into the core of organoids as they grow leads to the presence of a necrotic core after long periods of culture which negatively impacts organoid growth (Wang *et al.*, 2017). To address these limitations, microfluidic devices, which are able to recapitulate physiological environments under controlled flow have been developed to improve organoid culture conditions and improve reproducibility (Castiglione *et al.*, 2022). In this study, midbrain organoids were cultured in sensor integrated microfluidic devices, which allowed for long-term organoid maintenance under an interstitial flow regime. Culturing the organoids in the microfluidic devices improved neuronal maturation and long-term cell viability. Thus, this study shows that microfluidic devices improve midbrain organoid culture conditions.

My contribution to this study was performing immunofluorescence stainings of organoid sections to show the robust differentiation of neurons when organoids are cultured under dynamic flow conditions (Fig 3D). I also contributed to reviewing the manuscript.

Cultivation and characterization of human midbrain organoids in sensor integrated microfluidic chips

Sarah Spitz[1,2], Cristian Zanetti[1], Silvia Bolognin[4], Mudiwa Nathasia Muwanigwa[4], Lisa Smits[4], Emanuel Berger[4], Christian Jordan[3], Michael Harasek[3], Jens C. Schwamborn[4], Peter Ertl[1,2*]

[1] Institute of Chemical Technologies and Analytics, Vienna University of Technology, Getreidemarkt 9/164, 1060 Vienna, Austria

[2] Institute of Applied Synthetic Chemistry, Vienna University of Technology, Getreidemarkt 9/164, 1060 Vienna, Austria

[3] Institute of Chemical Engineering, Vienna University of Technology, Getreidemarkt 9/164, 1060 Vienna, Austria

[4] Developmental and Cellular Biology, Luxembourg Centre for Systems Biomedicine (LCSB), University of Luxembourg, 7 avenue des Hauts-Fourneaux, 4362 Esch-sur-Alzette, Luxembourg

* Correspondence: peter.ertl@tuwien.ac.at

1. ABSTRACT

With its ability to emulate microarchitectures and functional characteristics of native organs *in vitro*, induced pluripotent stem cell (iPSC) technology has enabled the generation of a plethora of organotypic constructs, including that of the human midbrain. However, reproducibly engineering and differentiating such human midbrain organoids (hMOs) under a biomimetic environment favorable for brain development still remains challenging. This study sets out to address this problem by combining the potential of iPSC technology with the advantages of microfluidics, namely its precise control over fluid flow combined with sensor integration. Here, we present a novel sensor-integrated platform for the long-term cultivation and non-invasive monitoring of hMOs under an interstitial flow regime. Our results show that dynamic cultivation of iPSC-derived hMOs maintains high cellular viabilities and dopaminergic neuron differentiation over prolonged cultivation periods of up to 50 days.

2. INTRODUCTION

With the emergence of iPSC technology, it has now become possible to emulate complex cytoarchitectures and key characteristics of native tissues *in vitro*, including that of the human brain.[1] In recent years so-called "organoids" have demonstrated their potential as powerful tools for modeling key aspects in organ development, homeostasis as well as pathology.[2–4] Efforts have been made to establish iPSC-derived models of the human midbrain, that recapitulate organotypic characteristics including spatial organization, neuronal activity as well as disease-associated phenotypes.[5,6]

However, the inability of conventional culture techniques, to precisely control and reproduce cellular microenvironments has led to issues with organoid variability, among others, a key limitation of three-dimensional (3D) technology.[7] In addition, common strategies fail to take biophysical cues, such as e.g.

interstitial flow, into account, fundamental aspects in organ development and maturation.[7] Interstitial fluid flow not only plays an important role in the delivery of nutrients and removal of metabolic waste, but it implicates non-synaptic cell-cell communication, ionic homeostasis, cell migration as well as immune function. In addition, interstitial fluid flow is involved in drug delivery, distribution and clearance and thus of considerable importance when considering organoid models in the context of drug screening applications.[8] Overall, the lack of biophysical and other environmental cues restricts the development of physiologic organoids in a more complete and reproducible manner, specifically important when emulating structures of high intrinsic complexity such as those of the human brain.[7]

Microfluidics with its inherent ability to provide precise spatial and temporal control over cellular microenvironments coupled with the capability of non-invasive monitoring (e.g. embedded microsensors), low reagent consumption, and increased throughput provides an ideal tool for tackling said aspects.[8] Organ-on-a-chip approaches were already shown to beneficially impact cerebral organoid differentiation and alter pathological responses in an *in vitro* Alzheimer model under an interstitial flow regime, underlining its potential in neurobiological applications.[13–15] Up to now, however, microfluidic based organoid models focusing on neurobiological aspects are limited and still fail to include non-invasive monitoring strategies, an important tool for addressing the issue of organoid variability. Here, we investigated a novel strategy for differentiating iPSC-derived hMOs in sensor-integrated microfluidic platforms under dynamic conditions by directing interstitial fluid flow via hydrostatic pressure through the growing organoid. Computational fluid dynamic (CFD) simulations were employed to characterize flow characteristics and subsequently ensure low shear stresses as well as interstitial flow regimes within the microfluidic device. Non-invasive oxygen monitoring was established to asses organoid viability and growth, while maturation was confirmed by immunohistochemical analysis.

3. METHODS

Chip Fabrication

Microstructures were fabricated by soft lithography from a CNC milled mold using polydimethylsiloxane (PDMS) (Sylgard® 184 Silicone Elastomer Kit, Down Corning). After polymerization at 80 °C, molded PDMS was bonded to glass substrates using air plasma (Harrick Plasma, High Power, 2 min). As previously described, microfluidic devices equipped with oxygen sensors were generated by the deposition of microparticles into drilled cavities within glass substrates by the use of a pipette. After drying for 2 h at room temperature, the microparticles were immobilized to the glass substrate and the fluidic structures were sealed, employing air plasma.[9] Prior to use microfluidic devices were sterilized employing 70 % ethanol as well as UV plasma.

Finite Volume CFD Simulation

A multipurpose finite volume CFD code (Ansys Fluent 6.3.26, www.ansys.com / OpenFoam www.openfoam.org) was used for solving the flow problem. The geometry consisting of the hydrogel cavity, the two feed channels as well as the two collection units was split into 136.000 hexahedral control volumes. The grid pillars at the gel inflow and outflow boundary have been fully resolved.

For adequate numerical accuracy, second or higher order discretization schemes have been selected for all flow variables (Navier-Stokes equation – momentum conservation, Continuity equation – mass conservation) and for the species equations. All wall boundaries were treated as ideally smooth; no slip boundary conditions (zero flow velocity at the wall) were selected for all surfaces. The outlet was set to pressure outlet at a standard pressure of $p = 1$ atm (101325 Pa). The hydrogel region was approximated as homogeneous and isotropic porous zone (Darcy-Forchheimer equation) with a constant porosity of $\varepsilon = 0.99$ and a viscous resistance of $R = 1.33 \cdot 10^{13}$ 1/m² having been assumed for all directions.[16]

Isothermal flow was assumed, no temperature or energy field was solved. For simplicity, Newtonian fluid behavior was applied for the simulation using a constant dynamic viscosity and constant density (incompressible) for all of the mixture components. As the concentrations of the dissolved species in the fluid are low, the properties of the solvent, water, have been used for the simulation ($\rho = 993$ kg/m³, $\eta = 0.001003$ Pa·s at 37 °C). The diffusion coefficients for the tracer components have been estimated according to literature values (glucose: 0.18 kDa – $4 \cdot 10^{-10}$ m²/s, oxygen: 32 Da – $2 \cdot 10^{-9}$ m²/s, water: 18 Da – $2 \cdot 10^{-9}$ m²/s) assuming a dilute solution.[11] To investigate the cross mixing of the two inlet channel fluids, different water species have been used for both inlets. Simulations were carried out on the cluster server cae.zserv.tuwien.ac.at (operated by the IT department of TU Wien, www.zid.tuwien.ac.at).

As the major flow resistances are inside the hydrogel and in the flow channels, but not in the feed and collection cavities, a simplification was used: To reduce the computational effort, steady state simulations for different selected feed cavity filling levels have been carried out. The simulated filling level was translated into a corresponding relative pressure difference between feed inlet zone and pressure outlet.

Fluorescein Assay

To validate data obtained from the CFD simulation a fluorescein assay was performed. For this purpose, fluorescein (Sigma Aldrich) was added to the medium reservoirs and its propagation within the microfluidic device was monitored using a Live Cell microscope (Pecon). Images were analyzed using ImageJ ($N = 4$).

hMO Generation and On-Chip Cultivation

iPSCs from one healthy individual were used in this study. The maintenance of iPSCs was performed as previously described.[5] From the iPSC line human ventralized neural epithelial stem cells (hvNESC) were generated, which were subsequently used to generate midbrain organoids.[5] For on-chip hMO cultivation, organoids suspended in Matrigel® (Corning®) were transferred into the microfluidic chip on day 0 of maturation phase and cultivated for up to 50 days. Dynamic cultivation was achieved by filling the feed medium reservoirs up to a 3 mm feeding level, while medium at the collector side was kept at 0.6 mm height. Medium was exchanged every 48 h.

On-Chip Oxygen Monitoring

On-chip oxygen monitoring was carried out at a sampling frequency of 1 Hz using a FireStingO$_2$ optical oxygen meter (Pyroscience) connected to optical fibers (length 1 m, outer diameter 2.2 mm, fiber diameter 1 mm). Integrated sensors were calibrated using a CO_2/O_2 oxygen controller (CO2-O2-Controller 2000, Pecon GmbH) equipped with integrated zirconium oxide oxygen sensors. Oxygen measurements were performed once a week (n=4). For this purpose, chips were sealed with PCR foil and transferred into an external incubation chamber setup. Samples were measured for 10 minutes to guarantee proper equilibration. Oxygen demand was subsequently calculated according to the following formula: hMO oxygen demand (ΔP_{O2}) = P_{O2} blank – P_{O2} hMO.

Viability Assay and Morphological Characterization of hMOs

To monitor the viability of hMOs a viability assay employing calcein-AM and ethidium homodimer-1 (Invitrogen, L3224) was performed every week (n=3). Images were analyzed using the ImageJ plugin Color Pixel Counter. Cellular viabilities were determined by dividing the number of green pixels by the total number of red and green pixels, while exposure time and focus plane were kept constant for each analysis. To obtain information on both hMO growth as well as neurite outgrowth, organoid diameter (highest diameter of each organoid) and neurite lengths were assessed manually using ImageJ.

Immunofluorescence

hMOs were fixed with 4 % PFA and washed 3x with phosphate-buffered saline (PBS) for 15 min. They were embedded in 3-4 % low-melting point agarose in PBS. The solid agarose block was sectioned with a vibratome (Leica VT1000s) into 50 μm sections. The sections were blocked on a shaker with 0.5 % Triton X-100, 0.1 % sodium azide, 0.1 % sodium citrate, 2 % bovine serum albumin and 5 % normal goat serum in PBS for 90 min at room temperature. Primary antibodies were diluted in the same solution but with only 0.1 % Triton X-100 and were applied for 48 h at 4 °C. The following first antibodies were used: anti-rabbit Tuj1 (Optim AB Eurogentec, 1:600); anti-rabbit TH (SantaCruz, 1:1000).

After incubation with the primary antibodies, sections were washed 3x with PBS and incubated with the secondary antibodies in 0.05 % Tween-20 in PBS for 2h at RT and washed with 0.05 % Tween-20 in PBS and Milli-Q water before they were mounted in Fluoromount-G mounting medium (Southern Biotech). The organoids were imaged using a confocal microscope (Zeiss).

Statistical Analysis

Data analysis was performed using GraphPad Prism software. A paired *t*-test was performed to determine significant differences between the individual data sets.

2. RESULTS

Hydrostatic pressure driven flow-based microfluidic platform

To allow for the physiologic cultivation of hMOs on chip under an interstitial flow regime, a hydrostatic pressure driven flow-based design was selected (see Figure 1). The PDMS-based microfluidic chip contains three individual chambers, interconnected by two micropillar arrays. While the two outer chambers form the medium channels, the middle chamber is designed to accommodate the differentiating hMO in a three-dimensional matrix such as Matrigel. By adjusting the filling volumes on both sites of the microfluidic chip various hydrostatic pressures can be generated and subsequently direct medium flow of different velocities not only through the hydrogel matrix within the central channel, but also through the embedded organoid. Therefore, nutrient supply is not limited to diffusion, but nutrients are actively transported to the embedded organoid, while simultaneously keeping shear forces at a minimum.
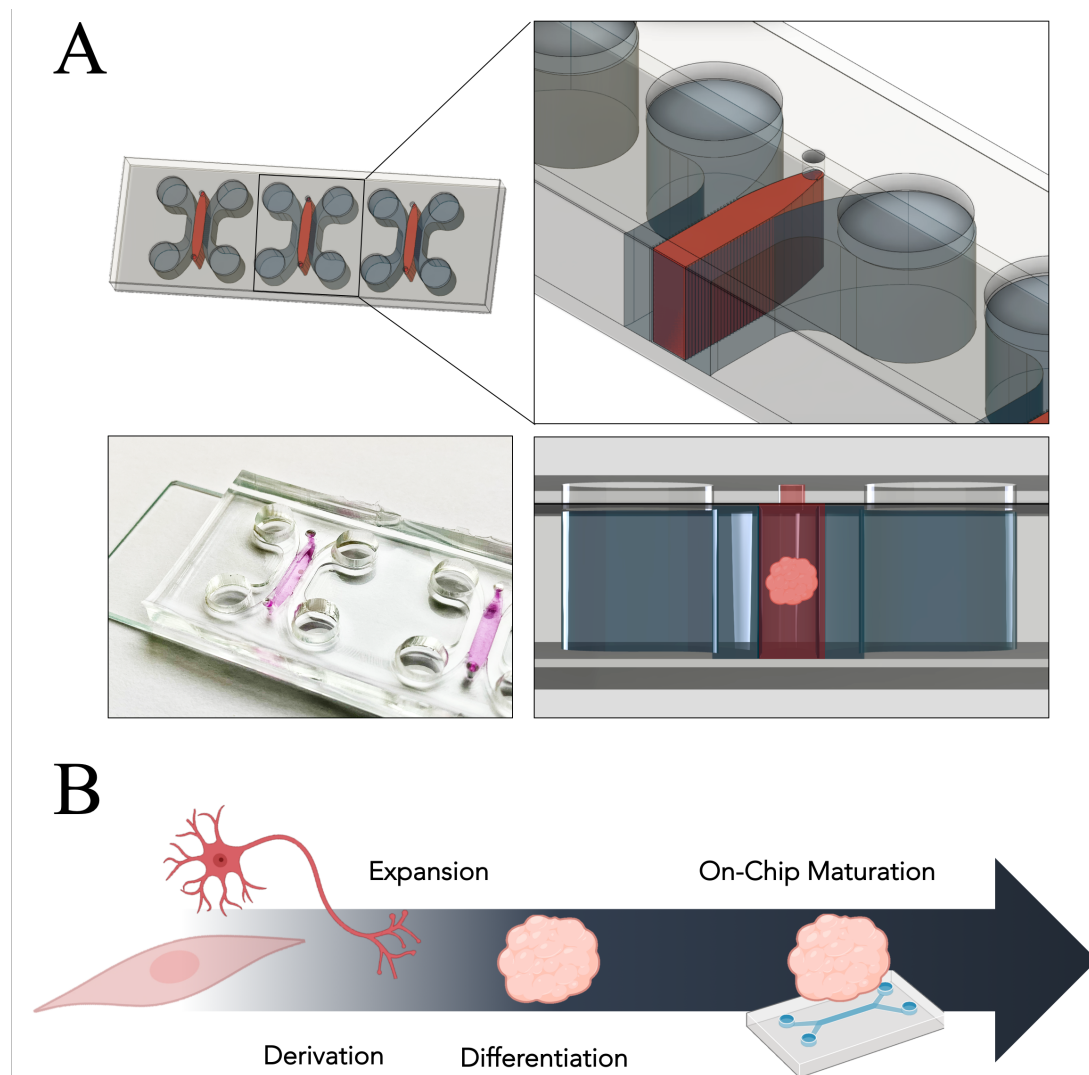

Figure 1: Hydrostatic pressure driven flow design comprising three channels interconnected by two micropillar arrays (A). Workflow of hMO cultivation. (B)

CFD simulation of microfluidic platform reveals interstitial fluid flow

To determine optimal culture conditions and to assess overall flow characteristics within the microfluidic device CFD simulations were performed. The simulations were specifically set out to address platform specific correlations of overall volume flow rates and average velocity magnitudes within the central hydrogel chamber as a function of the relative inlet pressure.
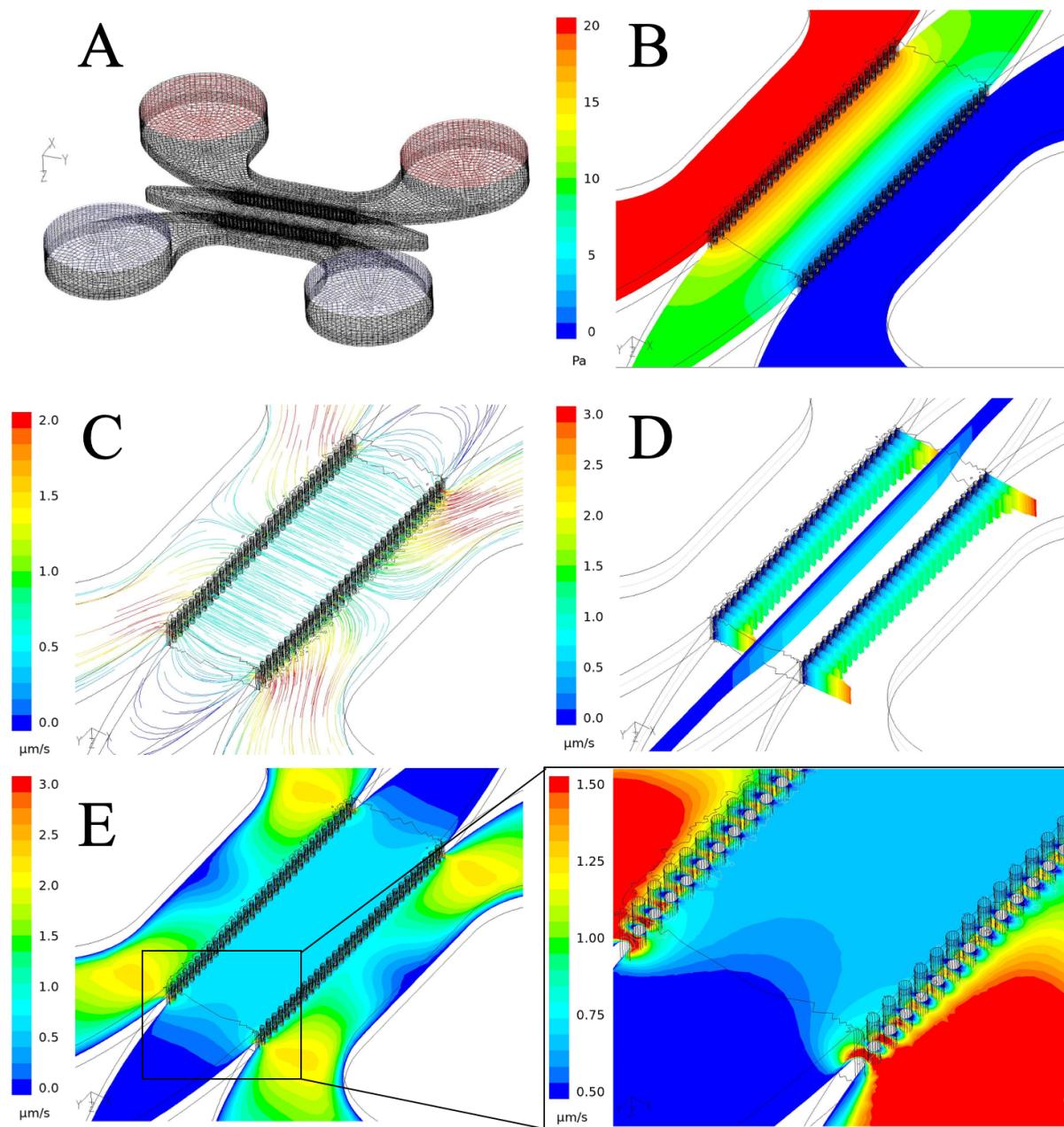
Figure 2: CFD simulation of the hydrostatic pressure driven flow design

Computational mesh of microfluidic device (A). Pressure gradient established within the central hydrogel chamber of the device (B). Streamlines with uniform flow velocities established at a pressure difference equivalent to 1mm level difference (C). Velocity profile in x-projection at the inlet, outlet and within the hydrogel chamber (D). Contour plot of velocity magnitude in symmetry plane of the microfluidic platform (E).

For this purpose, the hydrostatic pressure driven flow-based design was split in hexahedral control volumes, with an example grid depicted in Fig. 2A, indicating the inflow and outflow boundary zones in blue and red, respectively. The flow within the microfluidic device was shown to behave strictly laminar, consequently resulting in a linear relationship between inlet pressure and volume flow rate. Initial assessment further revealed that the pressure drop within the microfluidic device can be mainly attributed to the hydrogel chamber, with negligible pressure loss resulting from the geometry of the device itself (see Figure 2B). As a result thereof, a proportionality function between flow rate and pressure drop was established, allowing for the calculation of flow velocity as a function of matrix permeability. Due to its beneficial properties to support self-organization of brain organoids, the CFD model and subsequent experiments were built upon the hydrogel matrix Matrigel, with a literature matched resistance value of $R = 1.33 \cdot 10^{13}$ 1/m² having been assumed for all directions.[16] The simulated volume flow within the proposed hydrogel matrix of the microfluidic device was shown to behave highly uniformly throughout the most part of the central chamber. Parallelly aligned streamlines retrieved from the simulation at an exemplary level difference of 1 mm (equivalent to approx. 19 Pa pressure difference) confirm the aforementioned uniform velocity profile with an average velocity of 0.7 μm/s within the central part of the hydrogel chamber (see Figure 2C). While the comb structure of the micropillar array creates velocity gradients at the border of the hydrogel, the velocity within the hydrogel chamber, embedding the organoid, remains constant (see Figure 2D). Higher velocities close to the border zone also alter the velocity profiles and thus may induce shear stress on the embedded organoid. Since the occurrence, however, is restricted to both the upper and lower part of the hydrogel chamber flow inflicted shear stress on the organoid situated within the middle of the chamber can be ruled out (see Figure 2E). Overall, due to the uniform distribution of flow velocities within the central region of the hydrogel chamber and thus absence of velocity gradients, shear stresses within the central part of the chamber are kept at a minimum and thus generate optimal culture conditions for hMOs. Based on the established CFD model an initial reservoir pressure difference of 2.4 mm was selected to drive interstitial fluid flow through the hydrogel and thus provide optimal culture conditions for the organoid. By applying said hydrostatic pressure, hMOs were kept under dynamic culture conditions with flow velocities ranging from 1.6 μm/s (the upper limit of interstitial flow) down to 0.1 μm/s (the lower limit of interstitial flow) during the course of cultivation. Finally, to validate CFD simulation data, a fluorescein assay was employed. Fluorescein data were shown to be in good agreement with the calculated fluid regime with an initial measured average velocity of 1.67 ± 0.34 μm/s compared to an CFD estimated initial velocity of 1.6 μm/s.

Midbrain organoids differentiate in microfluidic chips

As an initial assessment of hMO behavior on chip neurite outgrowth, a crucial parameter for the formation of mature neural networks, was determined.[13] After four days of cultivation under an interstitial flow regime hMOs displayed extensive neurite outgrowth, as seen in Figure 3A. While organoids cultivated for 24 h on-chip displayed an average neurite length of 293 ± 78 μm, hMOs cultivated for 96 h already displayed processes extending throughout large sections of the hydrogel chamber with an average neurite length of 1,024.4 ± 193 μm. Consequently, neurites extending from the embedded organoid display an average growth rate of 274.5 ± 26 μm/day, in good agreement with recently published microfluidic neural circuit models.[18] Since midbrain organoid maturation is a time-consuming process with cultivation times ranging up to 100 days, it is of the utmost importance to guarantee prolonged cultivation without impairment of cellular viabilities. To ensure that hMOs remain viable within the proposed microfluidic device, organoids were analyzed using calcein AM/ ethidium homodimer-1 staining (see Figure 3B). Overall, no impairment in organoid viability was detected over the entire cultivation period of 6 weeks with an average viability of 93.8 ± 3.4 % (see Figure 3C). Furthermore, a significant increase in hMO diameter was detected after 42 days on chip ($p < 0.001$). Whereas hMOs displayed an average diameter of 737.4 ± 19.2 μm after one week of cultivation, the diameter increased up to 1,082.6 ± 66.2 μm after 6 weeks of culture within the microfluidic platform, indicative of organoid growth (see Figure 3C). In addition to an endpoint-based cell viability assay luminescent based oxygen sensor spots were integrated into the microfluidic device to ensure proper oxygenation as well as to non-invasively monitor hMO viability and growth (see Figure 3C). While the partial oxygen pressure measured within the blank chips remained constant over the entire cultivation period of 6 weeks with an average of 190.7 ± 16.7 hPa, thus ensuring sensor stability, a three-fold increase in oxygen demand could be detected in chips carrying hMOs. A small increase in oxygen demand was measured during the first three initial weeks of cultivation ranging from 51.6 ± 20.8 hPa up to 69.3 ± 23.8 hPa, followed by a significant increase by week 4 ($p < 0.05$) with an average oxygen demand of 92.5 ± 17.3 hPa which further increased up to 144.4 ± 17.1 hPa by week 6. Overall, the data indicate that hMOs cultivated within microfluidic devices remain viable for prolonged periods of time, while steadily increasing in size under dynamic culture conditions. These results corroborate well with aforementioned endpoint-based viability data. Furthermore, observed increase in oxygen demand may be linked to a metabolic switch from anaerobic glycolysis (exploited by hvNESC) to oxidative phosphorylation (predominant in differentiated neural cells), characteristic for organoid differentiation.[19] Consequently, in a final set of experiments, maturation into midbrain specific organoids was assessed. For this purpose, hMOs dynamically cultivated for 30 days on chip were analyzed using immunohistochemical staining for the neuronal marker TUJ1 as well as for the dopaminergic neuron marker tyrosine hydroxylase (TH). Dynamically cultivated hMOs not only

displayed robust differentiation into TUJ1-positive neurons, as shown in the histological section in Figure 3D (right panel), but in addition stained positive for TH (left panel).
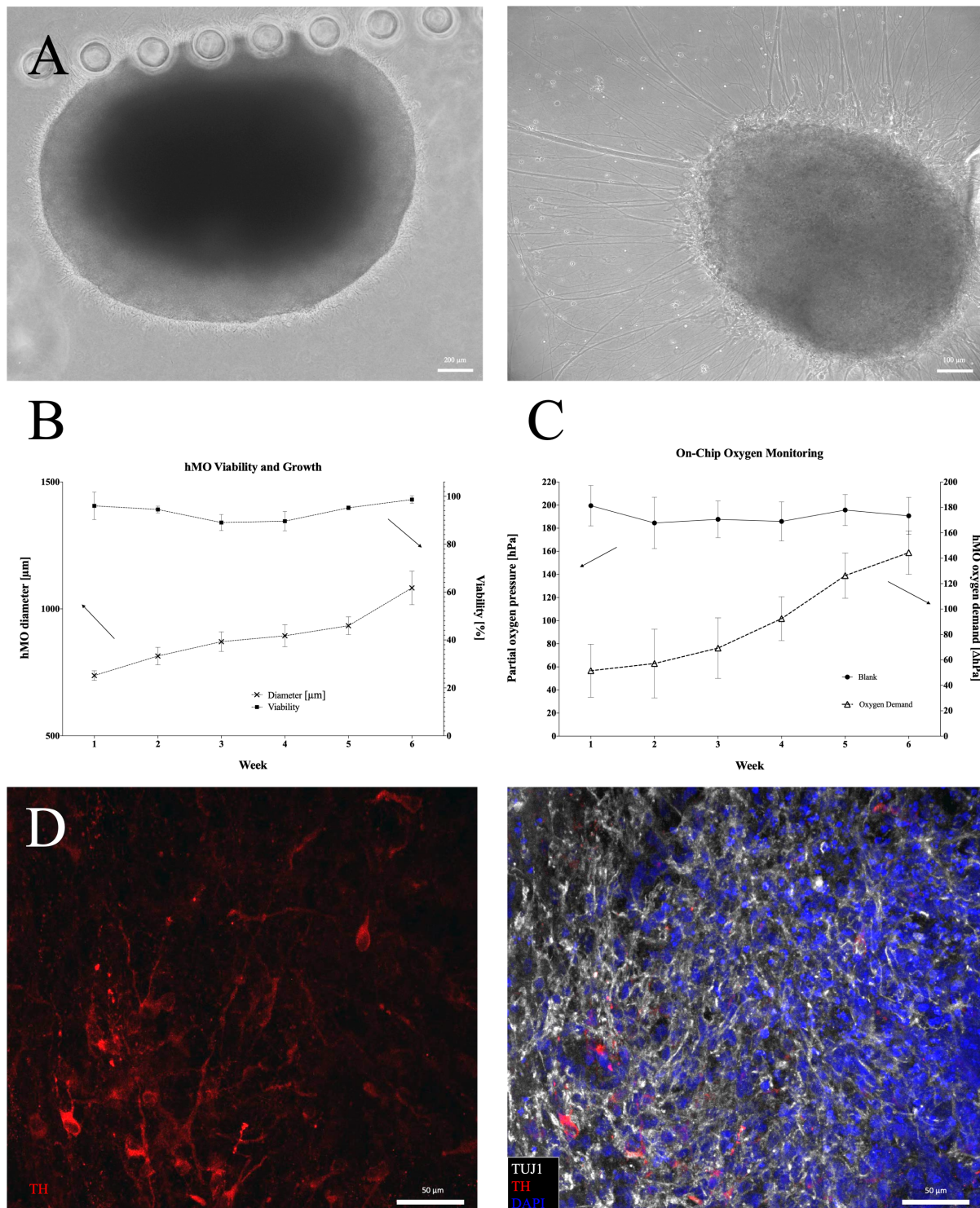
Figure 3: Brightfield images of hMOs after 24 h on chip and after 72 h revealing extensive neurite outgrowth (A). Time resolved graph showing hMO viability and organoid growth over a period of 6 weeks (n=3) (B). Time-resolved oxygen consumption of organoids on chip (n=4) (C). Immunohistochemical staining of hMO after 30 days on chip revealing TH (red) positive dopaminergic neurons as well as the neuronal marker TUJ1 (white) and DAPI stained nuclei (D).

DISCUSSION

In this study, we developed a sensor-integrated microfluidic platform, which addresses not only the 3D cytoarchitecture of the human midbrain but in addition expands the model by the application of interstitial flow, a crucial parameter for nutrient transport, tissue maintenance as well as pathobiology. Overall, we showed that hMOs could be cultivated for prolonged cultivation periods of up to 50 days, without the impairment of cellular viability, essential for long term studies required in the field of 3D technology. These observations could be demonstrated, not only by the use of invasive endpoint assays but in addition were underlined by the integration of luminescent based oxygen sensors.

We have previously shown, that microfluidic culture can be beneficial for neuronal differentiation while simultaneously provide an economically efficient route to personalized drug discovery for Parkinson's disease.[20] However, the microfluidic cultivation of individual neuroepithelial stem cells in a 3D matrix, has resulted in poor cellular viabilities associated with high stress exposure during cell loading, limiting its use within the tested set-up.[6] While our millifluidic approach has shown ameliorated differentiation behavior of hMOs combined with enhanced oxygen supply and a reduction in the necrotic core, the throughput remained limited.[19] By combining hMOs with microfluidic technology we have not only addressed aforementioned limitations such as low viabilities and throughput but further improved aspects such as sensor integration, enabling non-invasive monitoring. Overall, our model integrates well with published midbrain-organoid literature: similar to published conventional culture set-ups, hMOs cultivated for 30 days within the presented microfluidic chip not only stained positive for the neuronal cell marker TUJ1 but also for the dopaminergic neuron marker TH.[5,6,21,22]

In summary, this study has provided a novel *in vitro* model that allows for prolonged organoid cultivation under an interstitial flow regime, favorable neurite outgrowth as well as non-invasive monitoring. The presented model is capable of emulating midbrain associated phenotypes in physiologic microenvironments that meet the need for relevant *in vitro* models and thus may provide a powerful tool in the context of midbrain pathologies such as Parkinson's disease in the near future.

3. AUTHOR CONTRIBUTIONS

S.S. conceived, designed, and conducted experiments and analyzed data; S.B. and E.B. analyzed data and supervised the experiments; L.S. generated the hvNESC and hMOs; MNM performed the immunofluorescence experiments; C.J. and M.H. conducted CFD simulation. C.Z. conducted experiments. P.E. and J.S. supervised the project; S.S., P.E. and J.S. wrote the paper.

4. ACKNOWLEDGEMENTS

5. REFERENCES

1. Takahashi, K. & Yamanaka, S. Induction of Pluripotent Stem Cells from Mouse Embryonic and Adult Fibroblast Cultures by Defined Factors. *Cell* **126**, 663–676 (2006).

2. Sato, T. *et al.* Single Lgr5 stem cells build crypt-villus structures in vitro without a mesenchymal niche. *Nature* **459**, 262–265 (2009).

3. Rossi, G., Manfrin, A. & Lutolf, M. P. Progress and potential in organoid research. *Nat. Rev. Genet.* **19**, 671–687 (2018).

4. Lancaster, M. A. & Knoblich, J. A. Generation of cerebral organoids from human pluripotent stem cells. *Nat. Protoc.* **9**, 2329–2340 (2014).

5. Smits, L. M. *et al.* Modeling Parkinson's disease in midbrain-like organoids. *Npj Park. Dis.* **5**, (2019).

6. Monzel, A. S. *et al.* Derivation of Human Midbrain-Specific Organoids from Neuroepithelial Stem Cells. *Stem Cell Rep.* **8**, 1144–1154 (2017).

7. Park, S. E., Georgescu, A. & Huh, D. Organoids-on-a-chip. *Science* **364**, 960–965 (2019).

8. Abbott, N. J. Evidence for bulk flow of brain interstitial fluid: significance for physiology and pathology. *Neurochem. Int.* **45**, 545–552 (2004).

9. Zirath, H. *et al.* Every Breath You Take: Non-invasive Real-Time Oxygen Biosensing in Two- and Three-Dimensional Microfluidic Cell Models. *Front. Physiol.* **9**, (2018).

10. Rothbauer, M., Zirath, H. & Ertl, P. Recent advances in microfluidic technologies for cell-to-cell interaction studies. *Lab. Chip* **18**, 249–270 (2018).

11. Bachmann, B. *et al.* Engineering of three-dimensional pre-vascular networks within fibrin hydrogel constructs by microfluidic control over reciprocal cell signaling. *Biomicrofluidics* **12**, 042216 (2018).

12. Whitesides, G. M. The origins and the future of microfluidics. *Nature* **442**, 368–373 (2006).

13. Park, J. *et al.* Three-dimensional brain-on-a-chip with an interstitial level of flow and its application as an in vitro model of Alzheimer's disease. *Lab. Chip* **15**, 141–150 (2015).

14. Wang, Y., Wang, L., Zhu, Y. & Qin, J. Human brain organoid-on-a-chip to model prenatal nicotine exposure. *Lab. Chip* **18**, 851–860 (2018).

15. Wang, Y., Wang, L., Guo, Y., Zhu, Y. & Qin, J. Engineering stem cell-derived 3D brain organoids in a perfusable organ-on-a-chip system. *RSC Adv.* **8**, 1677–1685 (2018).

16. Hsu, Y.-H., Moya, M. L., Hughes, C. C. W., George, S. C. & Lee, A. P. A microfluidic platform for generating large-scale nearly identical human microphysiological vascularized tissue arrays. *Lab. Chip* **13**, 2990 (2013).

17. Da Silva, J. S. & Dotti, C. G. Breaking the neuronal sphere: regulation of the actin cytoskeleton in neuritogenesis. *Nat. Rev. Neurosci.* **3**, 694–704 (2002).

18. Bang, S., Na, S., Jang, J. M., Kim, J. & Jeon, N. L. Engineering-Aligned 3D Neural Circuit in Microfluidic Device. *Adv. Healthc. Mater.* **5**, 159–166 (2016).

19. Berger, E. *et al.* Millifluidic culture improves human midbrain organoid vitality and differentiation. *Lab. Chip* **18**, 3172–3183 (2018).

20. Moreno, E. L. *et al.* Differentiation of neuroepithelial stem cells into functional dopaminergic neurons in 3D microfluidic cell culture. *Lab. Chip* **15**, 2419–2428 (2015).

21. Jo, J. *et al.* Midbrain-like Organoids from Human Pluripotent Stem Cells Contain Functional Dopaminergic and Neuromelanin-Producing Neurons. *Cell Stem Cell* **19**, 248–257 (2016).

22. Qian, X., Nguyen, H. N., Jacob, F., Song, H. & Ming, G. Using brain organoids to understand Zika virus-induced microcephaly. *Development* **144**, 952–957 (2017).

5. *Discussion and Future Perspectives*

The increasing global prevalence of PD has emphasized the need for more robust modeling systems that can more accurately recapitulate the disease, allowing for the development of more effective therapeutic interventions. While conventional animal models and 2D cell culture systems have provided many important insights in the mechanisms underlying PD, they are still not able to faithfully reproduce some of the key pathophysiological hallmarks seen in humans (Falkenburger & Schulz, 2006; Potashkin *et al.*, 2011). In the context of PD, hMO have emerged as a powerful tool for disease modeling as they mimic the cellular composition and physiology of the human midbrain.

5.1 Midbrain Organoid Modeling of Genetic Forms of Parkinson's Disease

This thesis, specifically Manuscript I and Manuscript II, highlights the use of patient-specific hMO in modeling two genetic forms of PD, namely *SNCA* triplication and LRRK2-G2019S. While they only constitute around 10-15% of PD cases, the study of genetic forms of PD can help to provide insights on converging mechanisms that may also be observed in idiopathic forms of the disease.

<u>Modeling *SNCA* triplication in hMO</u>

Triplication of the *SNCA* gene is the cause of a rare, early-onset form of PD (Olgiati *et al.*, 2015). Despite the rarity of this aberration, the fact that α-synuclein accumulation and aggregation is observed in most cases of PD, both genetic and idiopathic, means that understanding the *SNCA* triplication may provide valuable insights into the contribution of α-synuclein to disease onset and progression. Manuscript I focuses on the study of patient-specific hMO harboring the *SNCA* triplication. The first aim of this study was to assess whether the hMO could recapitulate the key neuropathological hallmarks of PD, namely the accumulation of pathological α-synuclein aggregates and dopaminergic neuron death. Indeed, the 3xSNCA hMO showed accumulation of intracellular α-synuclein and higher levels of extracellular α-synuclein release. Moreover, the

protein levels of pS129 α-synuclein, which is thought to be the pathological form of the protein, were over two-fold higher in the 3xSNCA hMO across all the analyzed time points, ranging from 15 – 90 days of organoid maturation. Using immunofluorescence stainings, we observed pS129 α-synuclein rich aggregate-like structures in the 3xSNCA hMO as well as structures resembling Lewy neurites. Finally, higher amounts of insoluble α-synuclein were detected using immunoblot, which once again is an indication of increased aggregation in the patient-specific organoids. Taken together, these observations strongly support the development of α-synuclein related pathology in 3xSNCA hMO.

These findings support recent studies that also found α-synuclein pathology in hMO with *SNCA* mutations or induced with α-synuclein overexpression (Jo *et al.*, 2021; Mohamed *et al.*, 2021). An open question is whether the extracellular α-synuclein observed is a result of active release of α-synuclein by cells or the consequence of cell death releasing α-synuclein into the media. Since we did not observe any differences in the dopaminergic neuron levels between the wild type and 3xSNCA hMO at 30 days, but already observe increased extracellular release of α-synuclein, we speculate that this could be an active process. However, further experiments would be required to validate this and there is still debate as to whether α-synuclein is released actively or passively due to cell death (Brás & Outeiro, 2021). Given the important contributions of α-synuclein pathology to PD and other synucleinopathies, hMO present as an ideal tool to further explore the pathogenic mechanisms of α-synuclein.

The progressive loss of SNpc dopaminergic neurons represents the underlying cause of dopamine deficiency in the striatum of PD patients and the onset of motor symptoms. Our 3xSNCA hMO model was able to recapitulate the loss of dopaminergic neurons after 70 days of organoid maturation. We also observed a progressive decline of TH levels over time. The amount of dopamine released by the 3xSNCA hMO was significantly lower than the WT organoids at 70 days, which is probably due of the loss of the dopaminergic neurons but could also be reflective of a loss of functionality. Strikingly, we observed a senescent-like phenotype in the 3xSNCA hMO astrocytes which is further discussed in the next section (5.2). Interestingly, we also observed an increase in the amount of GFAP+ astrocytes in the 3xSNCA hMO, which is consistent with astrogliosis.

While this study showed the recapitulation of PD related phenotypes and provided insights into senescence as a driving mechanism in PD, there are some limitations to be addressed. One of the major limitations of this study is that we did not show the exact mechanisms by which

pathological α-synuclein may induce cellular senescence and thus could only assert an association. To establish a causal link between pathological α-synuclein and senescence, it would be interesting to study whether the removal of pathological α-synuclein in the 3xSNCA hMO model would reduce the presence of senescence associated markers. Recently, it has been shown that antisense oligonucleotides targeting human *SNCA* led to robust clearance of α-synuclein pathology in an α-synuclein pre-formed fibril (PFF) mouse model (Cole *et al.*, 2021). Using antisense oligonucleotides against *SNCA* in hMO presents as a promising strategy in further understanding how pathological α-synuclein may drive disease phenotypes. Conversely, the treatment of wild type organoids with α-synuclein PFFs, which have been suggested to induce α-synuclein pathology *in vivo* and *in vitro*, could also serve as a method to link pathological α-synuclein and senescence. This has already been shown by Vera and colleagues, who found the increased presence of senescence associated markers in α-synuclein PFF-injected mice (Verma *et al.*, 2021).

This study was also not able to directly establish the impact of senescence on the dopaminergic neurons. While the time points at which we start the see the signs of astrocyte senescence (50+ days) precede when we observe dopaminergic decline (70 days), with the current data we can only speculate a causal association. One way this could be addressed could be to treat the organoids with senolytic compounds which selectively kill senescent cells. If ablation of senescent cells would decrease the loss of dopaminergic neurons, this would suggest that senescent cells do indeed have a detrimental impact on dopaminergic neurons in our model. Finally, the lack of isogenic controls was a further limitation of this study. Isogenic control lines would allow us to investigate whether the phenotypes are specifically related to the *SNCA* triplication, or whether the patient genetic background may also play a contributing role.

Nonetheless, despite these limitations, the ability of our hMO to recapitulate PD specific phenotypes will allow us to further explore senescence in PD and other pathogenic mechanisms.

Modeling *LRRK2-G2019S* in hMO

Mutations in *LRRK2* are the most common causes of familial PD, with the LRRK2-G2019s mutation being the most prevalent (Li *et al.*, 2014). hMO harboring the LRRK2-G2019S mutation

have previously been shown to mimic key PD hallmarks such as the increased aggregation of α-synuclein (Kim *et al.*, 2019) and reduced levels of midbrain dopaminergic neurons (Smits *et al.*, 2019).

In Manuscript II, the role of astrocytes in the neurobiology of PD, particularly in the context of the LRRK2-G2019S mutation was studied. Presently, most functional studies investigating the role of astrocytes in PD have been performed in animal models. Mouse astrocytes have been shown to be transcriptionally and functionally distinct from human, limiting the utility of such models in capturing relevant phenotypes (Zhang *et al.*, 2016). To circumvent this, we capitalized on the recapitulation of human astrocyte development in hMO. For this study, we used a panel of LRRK2-G2019S lines along with isogenic control lines as well as healthy derived lines with the LRRk2-G2019S mutation introduced, allowing for the delineation of the specific contribution of the mutation versus the patient background. Our study revealed a novel role of the LRRK2-G2019S mutation in affecting the differentiation dynamics of astrocytes from progenitor cells. LRRK2-G2019S organoids showed a defect in astrocyte differentiation, and this was further confirmed in 2D astrocytes derived from the same patient lines. Moreover, compared to isogenic controls and healthy control lines, the 2D astrocytes carrying the LRRK2-G2019S mutation showed increased apoptosis and alterations in their mitochondrial morphology.

Single cell RNA sequencing revealed that LRRK2-G2019S organoids showed an altered transcriptomic profile. Additionally, LRRK2-G2019S organoids had a higher proportion of astrocytes with a transcriptional profile indicative of reactivity. Similar to the 3xSNCA hMO in Manuscript I, the LRRK2-G2019S organoids show a senescent-like phenotype. In this case, senescence was inferred through scRNA-seq analysis which revealed the expression of SASP related genes compatible with a senescent-like profile. We speculate that the defect in astrocyte specification may contribute to the astrocytes acquiring a senescent-like phenotype. The senescent-like phenotype in the LRRK2-G2019S is further discussed in the following section (5.2). As astrocytes play a critical role in the maintenance of neuronal homeostasis, metabolism and function, the alteration of astrocyte dynamics will have an impact on neurons. Given the vulnerability of dopaminergic neurons, they may be particularly affected by the presence of dysfunctional astrocytes.

This study also identified the downregulation of *NR2F1* as a potential mediator for the observed impaired astrocyte differentiation in LRRK2-G2019S. This supports previous work from

our group, where *NR2F1* was found to be downregulated in LRRK2-G2019S NESC, neurons and hMO (Walter *et al.*, 2021). *NR2F1* has been implicated in regulating the switch between neurogenesis and astrogliogenesis (Bonzano *et al.*, 2018). Treatment with an NR2F1 activator partially rescued the astrocyte phenotypes, thus suggesting that the activation of NR2F1 could be a promising therapeutic approach in the context of LRRK2-G2019S PD.

One of the limitations of this study was that the senescent-like profile was not validated using other methods. While the scRNA-seq data strongly suggests a profile that is reflective of cellular senescence, this would need to be further validated through assessment of established senescence hallmarks. Another limitation of the study is that the NR2F1 activator could only partially rescue the astrocyte phenotypes. This suggests that there are probably other mechanisms mediating the defects observed in the astrocytes. Finally, the assessment of the astrocyte phenotypes in post-mortem PD tissue was only from 1 patient, and thus individual differences across PD patients could not be captured. Regardless of these limitations, this study strongly implicates LRRK2-G2019S in impaired astrocyte specification which may be a trigger for astrosenescence.

Altogether, Manuscript I and II contribute to a growing body of work that has shown the utility of midbrain specific organoids in modeling genetic and idiopathic forms of PD (Chlebanowska *et al.*, 2020; Jarazo *et al.*, 2022; Jo *et al.*, 2021; Kim *et al.*, 2019; Mohamed *et al.*, 2021; Smits *et al.*, 2019). Furthermore, these studies support the presence of senescent cells as a potential mechanism in PD.

5.2 Senescence as a converging mechanism in Parkinson's disease

There is a rapidly growing body of literature that associates cellular senescence with neurodegenerative diseases including PD (Kritsilis *et al.*, 2018; Martínez-Cué & Rueda, 2020). Astrocyte senescence or "astrosenescence" in particular has been a topic of interest as the loss of

function or gain of a neuroinflammatory phenotype due to senescence is thought to have profound implications for neurodegenerative disease and brain aging in general (Cohen & Torres, 2019; Lazic *et al.*, 2022). Manuscript I and Manuscript II of this thesis highlight the potential contribution of astrosenescence as an underlying mechanism contributing to PD pathogenesis. Manuscript I described the association between pathological α-synuclein and the development of a senescent-like phenotype in astrocytes in 3xSNCA hMO. Various senescence associated hallmarks were observed, including the disruption of the nuclear lamina, the increased presence of senescence associated heterochromatin foci and upregulation of genes that mediate cell cycle control. In order to further confirm and validate astrosenescence, it would be ideal to assess the increased activity of senescence associated ß-galactosidase (SA-ß-Gal), which is one of the most prominent biomarkers of senescence. Other validations of senescence could include the absence of the proliferative Ki67 marker, and assessment of other senescence associated heterochromatin foci like histone 3 lysine 9 di- or tri- methylation.

The transcriptomic analysis in Manuscript II also revealed a senescent-like profile in LRRk2-G2019S organoids. *LAMB1* and *LMNA,* which encode lamin B1 and lamin A respectively, were significantly downregulated at 70 days in LRRK2-G2019S organoids compared to LRRK2-WT. This was further validated at the protein level, where the mean intensity of lamin B1 was decreased in GFAP+ astrocytes in LRRK2-G2019S organoids. The differential expression of other senescence associated genes supported a senescent profile in the LRRK2-G2019S organoids. Finally, cell cycle analysis found a higher proportion of astrocytes in the G0/G1 phase, implying that they were in a quiescent non-proliferative state. Taken together, these findings also support an astrosenescent phenotype in LRRK2-G2019S organoids.

Our work supports other studies that have implicated astrosenescence in PD. Post-mortem brain tissue of PD patients display high levels of astrocytes positive for senescence associated markers (Chinta *et al.,* 2018). PD associated neurotoxic compounds like paraquat, rotenone and 2,3,7,8-tetrachlorodibenzo-p-dioxin (TCDD) have also been shown to induce senescence *in vitro* and *in vivo* (Chinta *et al.*, 2018; Simmnacher *et al.*, 2020; Wan *et al.*, 2014). Astrosenescence is mainly thought to play a role in driving neurodegeneration through the promotion of chronic inflammation (Cohen & Torres, 2019). The senescence associated secretory phenotype (SASP) leads to the release of pro-inflammatory mediators, reactive oxygen species and metalloproteinases, which may have a damaging effect on neighboring cells or convert neighboring cells to a senescent-

like state (Kritsilis *et al.*, 2018). Interestingly, there is significant overlap in the SASP of senescent cells and secretions of reactive astrocytes, and this has raised the possibility that previous research of reactive astrocytes may have in fact been examining senescence (Cohen & Torres, 2019). Given the fact that SNpc DA neurons may be significantly vulnerable to insults due to the reasons discussed in section 1.3.3, one could speculate that the SASP released as a consequence of astrosenescence may be particularly detrimental to dopaminergic neurons which are already on the edge of decline. This is supported by the fact that co-culture of senescent astrocytes with healthy neurons leads to neuronal dysfunction, reduction in synaptic maturity and plasticity, and impaired neuronal homeostasis (Bussian *et al.*, 2018; Limbad *et al.*, 2020; Sheeler *et al.*, 2020). Finally, senescence in astrocytes can lead to impaired release of trophic factors that support neuronal survival (Chinta *et al.*, 2015; Pertusa *et al.*, 2007) highlighting another mechanism through which astrosenescence may impact DA neurons. Given the findings of our investigations and these studies, astrosenescence may highlight a converging mechanism across genetic and idiopathic forms of PD.

While nuclear lamina decline was observed in MAP2+ neurons within the 3xSNCA hMO, there was no significant accumulation of senescence associated heterochromatin foci. Therefore, these results did not support the acquisition of a senescent-like phenotype in the neurons. There is still no consensus on whether neuronal cells undergo senescence (Tan *et al.*, 2014). However, there have been multiple studies in the past decade supporting the idea of neuronal senescence. Jurk *et al* were the first to describe senescent-like phenotypes in Purkinje, hippocampal and peripheral neurons in aged C57Bl/6 mice (Jurk *et al.*, 2012). This study showed that accumulation of neurons bearing senescence markers, including oxidative damage, IL-6 production, heterochromatinization and SA-ß-Gal, was initiated by a p21 mediated DNA damage response driven by dysfunctional telomeres and DNA damage. The PD associated environmental toxin TCDD was shown to trigger premature senescence in rat and human neuronal cell lines, showing hallmarks including the expression of SA-ß-Gal, the appearance of pH2AX foci, mitochondrial dysfunction, and upregulation of p16, p21 and pRB (Wan *et al.*, 2014). Long term culture of iPSC derived cortical neurons and cortical organoids develop typical senescence hallmarks which is accompanied by a reduction in Klotho expression (Shaker *et al.*, 2021). Interestingly, deficiencies in Klotho, a transmembrane protein that functions as a co-receptor for FGF receptors, lead to a premature aging phenotype in mouse models (Kuro-o *et al.*, 1997). Several studies have indicated the neuroprotective properties of Klotho in PD mouse models (Baluchnejadmojarad *et al.*, 2017; Leon *et al.*, 2017) and notably, clinical studies have found decreased levels of Klotho in PD patient

cerebrospinal fluid (Sancesario *et al.*, 2021; Zimmermann *et al.*, 2021). Thus, it would be interesting to explore whether Klotho expression is reduced in our patient-specific hMO. Furthermore, the neuroprotective properties of Klotho would be a promising therapeutic intervention to ameliorate the senescent phenotypes we observed. Given the fact that we did observe neuronal nuclear lamina defects in the 3xSNCA hMO, it is possible that other senescent phenotypes could arise if the organoids were cultured for a longer period.

A pertinent question is how senescence would be induced in the context of PD. Given α-synuclein's role in PD pathogenesis, one could speculate that it may play a driving role in promoting cellular senescence. Pathological α-synuclein, which is observed in *SNCA* triplication and LRRK2-G2019S hMO models, has been proposed to be an inducer of senescence in several recent studies (Verma *et al.*, 2021; Yoon *et al.*, 2022). Moreover, α-synuclein has been suggested to be a part of the DNA damage repair machinery, and thus when it is in its pathological form, it may not perform this function adequately, thus promoting the accumulation of double stranded breaks which can be a trigger for senescence (Schaser *et al.*, 2019). Indeed, extracellular α-synuclein is endocytosed by astrocytes, leading to the release of proinflammatory and neuroinhibitory secretions (Di Marco Vieira *et al.*, 2020; H. J. Lee *et al.*, 2010). Interestingly, α-synuclein has also been proposed to be a mediator in the interplay between aging and PD as the impact of its pathogenic effects – for examples mitochondrial, proteasomal and autophagic dysfunction – are observed during the normal aging process (Bobela *et al.*, 2015). As senescence is a hallmark of aging, it is interesting to speculate the relationship between α-synuclein pathology, senescence, and aging, where α-synuclein may drive aging through promoting the accumulation of senescent cells.

The accumulation of senescent cells in PD opens opportunities in therapeutic interventions that can be targeted against this mechanism. Senotherapeutics, which are agents that can specifically target senescent cells, have recently been proposed to be useful in preventing or treating age-associated diseases (Lee *et al.*, 2021; Martínez-Cué & Rueda, 2020). Senotherapies can be categorized into senolytics, which specifically kill senescent cells, or senomorphics, which modulate the phenotype of senescent cells by inhibiting the SASP without directly killing the cells (Lee *et al.*, 2021). Most senolytics work by targeting survival pathways that make senescent cells resistant to apoptosis. One of the most well characterized senolytics is the combination of the compounds Dasatinib and Quercetin (D + Q). Dasatinib is a tyrosine kinase inhibitor, while Quercetin targets B cell lymphoma 2 (BCL2) anti-apoptotic signaling (Dorsey *et al.*, 2000; Lombardo

et al., 2004) and AKT survival signaling (Granado-Serrano *et al.*, 2006). D + Q have been shown to reduce neurofibrillary tangle density, decrease neuronal loss and decrease neuroinflammation in mouse models of AD (Musi *et al.*, 2018; Zhang *et al.*, 2019). There are currently no published studies investigating the use of D + Q in ablating senescent cells in PD models. hMO would be an ideal model for validating the use of D + Q and other senolytic drugs for ameliorating PD related phenotypes. It would be interesting whether these compounds could indeed rescue the observed senescence phenotypes observed in Manuscript I and II.

5.3 Recapitulating phenotypes of age-associated disease in a neurodevelopmental model

An interesting aspect of hMO, and brain organoid models in general, is that they mimic early stages of neurodevelopment more so than the aged brain, the latter of which is the context of adult-onset neurodegenerative diseases like PD. Single cell RNA sequencing shows that gene expression in 35 day old and 70 day old hMO correlates highly to 9 and 10 weeks of embryonic midbrain development (Zagare *et al.*, 2022). Thus, it may be surprising that the organoids are able to recapitulate PD related phenotypes, many of which are only observed in the elderly. However, there are several potential explanations as to why these phenotypes arise in this model. One interesting hypothesis is that PD has a neurodevelopmental component (Schwamborn, 2018) which is supported by numerous studies showing neurodevelopmental defects in PD models (Garcia-Reitboeck *et al.*, 2013; Le Grand *et al.*, 2015; Wulansari *et al.*, 2021). This hypothesis suggests that PD follows a multiple hit hypothesis where a first hit, like a PD related genetic mutation, leads to some developmental defects, which are somehow compensated for over decades. However, these underlying defects render the system vulnerable to additional hits, such as somatic mutations, exposure to environmental toxins, infections, or aging, which arise and accumulate later in life (Schwamborn, 2018).

hMO, and brain organoids in general, likely lack many of the compensatory mechanisms that allow the system to continue to develop, thus some of the PD related pathology can already be observed. The lack of microglia in these models for example may contribute to the acceleration of PD pathology. Microglia, the resident immune cells of the brain, have been shown to clear

extracellular α-synuclein aggregates (Lee *et al.*, 2008), and thus counteract the development of α-synuclein pathology. Given that hMO lack microglia, this may lead to the faster accumulation of α-synuclein pathology, which in turn may drive the other pathological phenotypes observed. It is important to note that although microglia may have a protective role early on in disease progression, continued activation of microglia has been associated with chronic inflammation which can be damaging to neurons and also contributes to driving neurodegeneration (Badanjak *et al.*, 2021). hMO are also an isolated system; in that they are missing cues and input from other brain regions that the midbrain is normally in contact with in the brain. This may have further implications of reducing the compensatory mechanisms that allow the midbrain to develop and function for decades before the dopaminergic decline begins. Another interesting hypothesis that may explain, at least in part, why organoids are able to mimic relevant pathologies is that the media that the organoids are cultured in have very high levels of glucose, considered to be diabetic. Individuals with type II diabetes have an increased risk of developing PD and show faster symptom progression. Interestingly, a recent study showed that diabetic conditions induced senescence in PC12 neuronal cells and primary mouse cortical neurons (Xue *et al.*, 2022). Thus, it is interesting to speculate whether these diabetic conditions may further exacerbate the phenotypes we observed.

5.4 Towards more complex midbrain organoid models

While our organoids are able to robustly model many aspects of human midbrain physiology and function, they still present with several limitations. For example, while hMO contain cellular diversity that closely mimics the cellular composition of the human midbrain, they are still lacking in some key components like vasculature. The lack of vasculature is a significant limitation in brain organoids, as long-term culture of organoids consistently exhibits necrotic cell death at the innermost core due to the inability of nutrients to reach these areas (Qian *et al.*, 2019). In recent years, there have been significant efforts towards improving culture conditions to enable longer cultures of brain organoids with a reduced necrotic core. One of the strategies to achieve this is by combining brain organoid cultures with microfluidic devices to improve culture conditions, physiological relevance, and reproducibility of the organoids. Organoids-on-a-chip (the combination of organoids and microfluidic devices) improve culture conditions by reducing shear stress experienced by cells, enhancing nutrient/waste exchange, improving oxygen supply and

facilitating the implementation of chemical gradients (Castiglione *et al.*, 2022). In Manuscript III, hMO were cultured in sensor integrated microfluidic devices, which allowed for prolonged organoid maintenance under an interstitial flow regime which improved neuronal maturation and long-term cell viability. The microfluidic devices also allowed for the non-invasive monitoring of oxygen consumption through the use of sensors. Thus, we could show that culturing hMO in these devices overall improved organoid development. Further development of microfluidic devices will enable for more complex culture platforms that will be ideal for disease modeling and drug screening.

While hMO contain cellular diversity that closely mimics the specific human midbrain, they are still lacking in key components including vasculature and microglia. The lack of vasculature is a significant limitation in brain organoids, as long-term culture of organoids consistently exhibits apoptotic cell death at the innermost core due to the inability to nutrients to reach these areas (Qian *et al.*, 2019). Furthermore, endothelial cells of the vasculature stimulate the self-renewal of neural stem cells, and thus have an important role in the maintenance of neural stem cell niches and neurodevelopment (Delgado *et al.*, 2014; Ottone *et al.*, 2014; Shen *et al.*, 2004). To address this, several groups have been working on integrating vasculature into brain organoids. Sun *et al* described a protocol for generating vascularized brain organoids by fusing together blood vessel organoids and cerebral organoids (Sun *et al.*, 2022). The resulting fusion organoids showed structures reminiscent of the blood brain barrier, and interestingly, they also found a population of immune competent microglia. In addition, they found an increase in neural progenitors, which is consistent with the role of the vasculature in maintaining the stem cell niche. Another study showed the generation of vascularized cortical organoids by engineering human embryonic stem cells to ectopically express human ETS variant 2 (*ETV2)*, a transcription factor that plays a role in vascular endothelial cell development (Cakir *et al.*, 2019).

hMO lack microglia due to fact that the neuroepithelial stem cells used to derive them are of neuroectodermal lineage whereas microglia are of mesodermal origin. Microglia play a plethora of roles in the brain including immune surveillance, synaptic pruning and organization, phagocytosis of apoptotic neurons during development, phagocytosis of cellular debris, myelin turnover, control of neuronal excitability, brain protection and homeostasis (Bachiller *et al.*, 2018; Tremblay *et al.*, 2011; Wake *et al.*, 2009; Witting *et al.*, 2000). Historically, microglia were seen as a bystander in PD with less than 100 articles recorded on PubMed on microglia in PD as of 2011

(Stefanova, 2022). However, over the last decade the role of microglia in PD pathology has gained much attention. Overactive microglia have been implicated in mediating chronic inflammation in PD which directly contributes to the death of dopaminergic neurons (Qian & Flood, 2008). Microglia appear to be both neuroprotective and neurotoxic in PD, depending on their activation state and the extent of disease progression (Le *et al.*, 2016). Sabate-Soler *et al* recently published the first protocol for the integration of iPSC derived microglia into hMO (Sabate-Soler *et al.*, 2022). Future studies modeling the *SNCA* triplication in microglia containing hMO would allow the better recapitulation of disease phenotypes and allow for the study of relevant neuroinflammatory processes. Indeed, α-synuclein aggregates have been shown to act as chemoattractants which direct microglia towards damaged neurons (Wang *et al.*, 2015) and are able to induce robust microglial activation (Kim *et al.*, 2013; E.-J. Lee *et al.*, 2010; Zhang *et al.*, 2005).

The development of assembloids poses as one of the next steps in the future development of brain organoid models. Assembloids are the fusion and functional integration of multiple organoids, as well as the integration of organoids with missing cell types as described above (Chen *et al.*, 2022). These assembloids would further increase the complexity of the region-specific brain organoids that currently exist and model some of the more complex interactions which occur in the human body. Recent efforts have attempted to reconstruct the nigro-striatal pathway through fusion of human striatal organoids and hMO (Yeap *et al.*, 2023). The establishment of an assembloid system that can combine intestinal and brain organoids to model the gut-brain axis is also a future development that could provide a platform to interrogate the involvement of the gut in PD pathogenesis (Raimondi *et al.*, 2019). Assembloids have the advantage of revealing how interactions between different tissues give rise to new cellular properties, which has significant implications in disease pathogenesis.

PD is an age associated disorder with an average age of onset of 60 years old. A significant limitation of brain organoids is the fact that they are more reflective of a neurodevelopmental model, as discussed in section 5.3. To better mimic the aging brain, experimentally inducing aging in organoids may be a useful strategy. Several efforts in iPSC derived 2D cultures have investigated different strategies to achieve this. One of these strategies was the overexpression of progerin in iPSC derived dopaminergic neurons (Miller *et al.*, 2013). Progerin is a truncated form of lamin A and its expression is the cause of Hutchinson-Gilford Progeria Syndrome, a severe premature aging disease (Gonzalo *et al.*, 2017). iPSC derived dopaminergic neurons overexpressing progerin showed

features consistent with aging such as increased mitochondrial ROS, accumulation of DNA damage, decreased dendrite length and cell death. Overexpression of progerin in iPSC derived dopaminergic neurons with the PD associated PINK1-Q456X and Parkin-V324A mutations also revealed mutation specific phenotypes (Miller *et al.*, 2013). Another strategy to induce aging has been through chemically inducing senescence in stem cell derived neurons. Fathi *et al* screened for chemicals that selectively trigger senescent pathways in primary neonatal fibroblasts and iPSC derived cortical neurons. Chemically induced senescence accelerated the manifestation of disease phenotypes in iPSC derived neurons with the ALS related *TARDBP* mutation (Fathi *et al.*, 2022). Finally, Vera *et al* published a proof-of-concept study that explored manipulating telomere length to model late onset disease in iPSC derived neurons (Vera *et al.*, 2016). The shortening of telomeres is one of the most well characterized mechanisms of aging (Harley *et al.*, 1990) and is a trigger for senescence (Bernadotte *et al.*, 2016). To induce telomere shortening, they treated human embryonic stem cells (hESC) with 2-[(E)-3-naphtalen-2-yl-but-2-enoylamino]-benzoic acid (BIBR1532), a small molecule inhibitor of telomerase activity, and then differentiated the hESC to dopaminergic neurons. Shortening of the telomeres led to the accumulation of DNA damage foci and an increase in mitochondrial ROS in the dopaminergic neurons. Dopaminergic neurons with *PINK1* and *PRKN* treated BIBR1532 displayed shortened telomeres and showed indications of disease specific phenotypes such as the progressive loss of TH over time (Vera *et al.*, 2016). Altogether, these promising strategies could be adapted to be implemented in hMO in order to mimic the aged context in which PD occurs. However, it is still up for debate how physiologically relevant these artificial models of aging are. Nevertheless, these tools could still prove useful in gaining more insights in specific aspects of PD pathogenesis.

To conclude, the work of this thesis has contributed to the rapidly expanding field of 3D *in vitro* modeling of PD. Importantly, it supports the growing body of work that asserts a role of senescence to PD which has significant implications on our understanding of PD pathogenesis and progression. Future work that investigates the underlying mechanisms driving senescence using more complex and physiologically relevant hMO will open opportunities for the development of novel therapeutic interventions for PD.

Bibliography

Abeywardana, T., Lin, Y. H., Rott, R., Engelender, S., & Pratt, M. R. (2013). Site-specific differences in proteasome-dependent degradation of monoubiquitinated α-synuclein. *Chem Biol*, *20*(10), 1207-1213. https://doi.org/10.1016/j.chembiol.2013.09.009

Aguilar, C., Alves da Silva, M., Saraiva, M., Neyazi, M., Olsson, I. A. S., & Bartfeld, S. (2021). Organoids as host models for infection biology – a review of methods. *Experimental & Molecular Medicine*, *53*(10), 1471-1482. https://doi.org/10.1038/s12276-021-00629-4

Ahfeldt, T., Ordureau, A., Bell, C., Sarrafha, L., Sun, C., Piccinotti, S., Grass, T., Parfitt, G. M., Paulo, J. A., Yanagawa, F., Uozumi, T., Kiyota, Y., Harper, J. W., & Rubin, L. L. (2020). Pathogenic Pathways in Early-Onset Autosomal Recessive Parkinson's Disease Discovered Using Isogenic Human Dopaminergic Neurons. *Stem Cell Reports*, *14*(1), 75-90. https://doi.org/10.1016/j.stemcr.2019.12.005

Albanese, A., Valente, E. M., Romito, L. M., Bellacchio, E., Elia, A. E., & Dallapiccola, B. (2005). The PINK1 phenotype can be indistinguishable from idiopathic Parkinson disease. *Neurology*, *64*(11), 1958-1960. https://doi.org/10.1212/01.Wnl.0000163999.72864.Fd

Alessi, D. R., & Sammler, E. (2018). LRRK2 kinase in Parkinson's disease. *Science*, *360*(6384), 36-37. https://doi.org/doi:10.1126/science.aar5683

Alfaro, J. F., Gong, C. X., Monroe, M. E., Aldrich, J. T., Clauss, T. R., Purvine, S. O., Wang, Z., Camp, D. G., 2nd, Shabanowitz, J., Stanley, P., Hart, G. W., Hunt, D. F., Yang, F., & Smith, R. D. (2012). Tandem mass spectrometry identifies many mouse brain O-GlcNAcylated proteins including EGF domain-specific O-GlcNAc transferase targets. *Proc Natl Acad Sci U S A*, *109*(19), 7280-7285. https://doi.org/10.1073/pnas.1200425109

Alves da Costa, C., Paitel, E., Vincent, B., & Checler, F. (2002). α-Synuclein Lowers p53-dependent Apoptotic Response of Neuronal Cells: ABOLISHMENT BY 6-HYDROXYDOPAMINE AND IMPLICATION FOR PARKINSON′S DISEASE*. *Journal of Biological Chemistry*, *277*(52), 50980-50984. https://doi.org/https://doi.org/10.1074/jbc.M207825200

Anderson, J. P., Walker, D. E., Goldstein, J. M., de Laat, R., Banducci, K., Caccavello, R. J., Barbour, R., Huang, J., Kling, K., Lee, M., Diep, L., Keim, P. S., Shen, X., Chataway, T., Schlossmacher, M. G., Seubert, P., Schenk, D., Sinha, S., Gai, W. P., & Chilcote, T. J. (2006). Phosphorylation of Ser-129 is the dominant pathological modification of alpha-synuclein in familial and sporadic Lewy body disease. *J Biol Chem*, *281*(40), 29739-29752. https://doi.org/10.1074/jbc.M600933200

Appel-Cresswell, S., Vilarino-Guell, C., Encarnacion, M., Sherman, H., Yu, I., Shah, B., Weir, D., Thompson, C., Szu-Tu, C., Trinh, J., Aasly, J. O., Rajput, A., Rajput, A. H., Jon Stoessl, A., & Farrer, M. J. (2013). Alpha-synuclein p.H50Q, a novel pathogenic mutation for Parkinson's disease. *Mov Disord*, *28*(6), 811-813. https://doi.org/10.1002/mds.25421

Arenas, E., Denham, M., & Villaescusa, J. C. (2015). How to make a midbrain dopaminergic neuron. *Development*, *142*(11), 1918-1936. https://doi.org/10.1242/dev.097394

Azeredo da Silveira, S., Schneider, B. L., Cifuentes-Diaz, C., Sage, D., Abbas-Terki, T., Iwatsubo, T., Unser, M., & Aebischer, P. (2009). Phosphorylation does not prompt, nor prevent, the formation of alpha-synuclein toxic species in a rat model of Parkinson's disease. *Hum Mol Genet*, *18*(5), 872-887. https://doi.org/10.1093/hmg/ddn417

Baba, M., Nakajo, S., Tu, P. H., Tomita, T., Nakaya, K., Lee, V. M., Trojanowski, J. Q., & Iwatsubo, T. (1998). Aggregation of alpha-synuclein in Lewy bodies of sporadic Parkinson's disease and dementia with Lewy bodies. *Am J Pathol, 152*(4), 879-884.

Bachiller, S., Jiménez-Ferrer, I., Paulus, A., Yang, Y., Swanberg, M., Deierborg, T., & Boza-Serrano, A. (2018). Microglia in Neurological Diseases: A Road Map to Brain-Disease Dependent-Inflammatory Response [Review]. *Frontiers in Cellular Neuroscience, 12*. https://doi.org/10.3389/fncel.2018.00488

Badanjak, K., Fixemer, S., Smajić, S., Skupin, A., & Grünewald, A. (2021). The Contribution of Microglia to Neuroinflammation in Parkinson's Disease. *Int J Mol Sci, 22*(9). https://doi.org/10.3390/ijms22094676

Bagley, J. A., Reumann, D., Bian, S., Lévi-Strauss, J., & Knoblich, J. A. (2017). Fused cerebral organoids model interactions between brain regions. *Nat Methods, 14*(7), 743-751. https://doi.org/10.1038/nmeth.4304

Ball, N., Teo, W. P., Chandra, S., & Chapman, J. (2019). Parkinson's Disease and the Environment. *Front Neurol, 10*, 218. https://doi.org/10.3389/fneur.2019.00218

Baltic, S., Perovic, M., Mladenovic, A., Raicevic, N., Ruzdijic, S., Rakic, L., & Kanazir, S. (2004). α-Synuclein is expressed in different tissues during human fetal development. *Journal of Molecular Neuroscience, 22*(3), 199-203. https://doi.org/10.1385/JMN:22:3:199

Baluchnejadmojarad, T., Eftekhari, S. M., Jamali-Raeufy, N., Haghani, S., Zeinali, H., & Roghani, M. (2017). The anti-aging protein klotho alleviates injury of nigrostriatal dopaminergic pathway in 6-hydroxydopamine rat model of Parkinson's disease: Involvement of PKA/CaMKII/CREB signaling. *Exp Gerontol, 100*, 70-76. https://doi.org/10.1016/j.exger.2017.10.023

Barbour, R., Kling, K., Anderson, J. P., Banducci, K., Cole, T., Diep, L., Fox, M., Goldstein, J. M., Soriano, F., Seubert, P., & Chilcote, T. J. (2008). Red blood cells are the major source of alpha-synuclein in blood. *Neurodegener Dis, 5*(2), 55-59. https://doi.org/10.1159/000112832

Bartels, T., Choi, J. G., & Selkoe, D. J. (2011). α-Synuclein occurs physiologically as a helically folded tetramer that resists aggregation. *Nature, 477*(7362), 107-110. https://doi.org/10.1038/nature10324

Bendor, J. T., Logan, T. P., & Edwards, R. H. (2013). The function of α-synuclein. *Neuron, 79*(6), 1044-1066. https://doi.org/10.1016/j.neuron.2013.09.004

Bernadotte, A., Mikhelson, V. M., & Spivak, I. M. (2016). Markers of cellular senescence. Telomere shortening as a marker of cellular senescence. *Aging (Albany NY), 8*(1), 3-11. https://doi.org/10.18632/aging.100871

Birey, F., Andersen, J., Makinson, C. D., Islam, S., Wei, W., Huber, N., Fan, H. C., Metzler, K. R. C., Panagiotakos, G., Thom, N., O'Rourke, N. A., Steinmetz, L. M., Bernstein, J. A., Hallmayer, J., Huguenard, J. R., & Paşca, S. P. (2017). Assembly of functionally integrated human forebrain spheroids. *Nature, 545*(7652), 54-59. https://doi.org/10.1038/nature22330

Bobela, W., Aebischer, P., & Schneider, B. L. (2015). Alpha-Synuclein as a Mediator in the Interplay between Aging and Parkinson's Disease. *Biomolecules, 5*(4), 2675-2700. https://doi.org/10.3390/biom5042675

Bolam, J. P., & Pissadaki, E. K. (2012). Living on the edge with too many mouths to feed: why dopamine neurons die. *Mov Disord, 27*(12), 1478-1483. https://doi.org/10.1002/mds.25135

Bonzano, S., Crisci, I., Podlesny-Drabiniok, A., Rolando, C., Krezel, W., Studer, M., & De Marchis, S. (2018). Neuron-Astroglia Cell Fate Decision in the Adult Mouse Hippocampal Neurogenic Niche Is Cell-Intrinsically Controlled by COUP-TFI In Vivo. *Cell Rep, 24*(2), 329-341. https://doi.org/10.1016/j.celrep.2018.06.044

Booth, H. D. E., Hirst, W. D., & Wade-Martins, R. (2017). The Role of Astrocyte Dysfunction in Parkinson's Disease Pathogenesis. *Trends Neurosci*, *40*(6), 358-370. https://doi.org/10.1016/j.tins.2017.04.001

Bové, J., & Perier, C. (2012). Neurotoxin-based models of Parkinson's disease. *Neuroscience*, *211*, 51-76. https://doi.org/10.1016/j.neuroscience.2011.10.057

Braak, H., Del Tredici, K., Rüb, U., de Vos, R. A., Jansen Steur, E. N., & Braak, E. (2003). Staging of brain pathology related to sporadic Parkinson's disease. *Neurobiol Aging*, *24*(2), 197-211. https://doi.org/10.1016/s0197-4580(02)00065-9

Brás, I. C., & Outeiro, T. F. (2021). Alpha-Synuclein: Mechanisms of Release and Pathology Progression in Synucleinopathies. *Cells*, *10*(2). https://doi.org/10.3390/cells10020375

Brodacki, B., Staszewski, J., Toczyłowska, B., Kozłowska, E., Drela, N., Chalimoniuk, M., & Stepien, A. (2008). Serum interleukin (IL-2, IL-10, IL-6, IL-4), TNFalpha, and INFgamma concentrations are elevated in patients with atypical and idiopathic parkinsonism. *Neurosci Lett*, *441*(2), 158-162. https://doi.org/10.1016/j.neulet.2008.06.040

Burai, R., Ait-Bouziad, N., Chiki, A., & Lashuel, H. A. (2015). Elucidating the Role of Site-Specific Nitration of α-Synuclein in the Pathogenesis of Parkinson's Disease via Protein Semisynthesis and Mutagenesis. *Journal of the American Chemical Society*, *137*(15), 5041-5052. https://doi.org/10.1021/ja5131726

Burré, J., Sharma, M., Tsetsenis, T., Buchman, V., Etherton, M. R., & Südhof, T. C. (2010). Alpha-Synuclein Promotes SNARE-Complex Assembly in Vivo and in Vitro. *Science*, *329*(5999), 1663-1667. https://doi.org/doi:10.1126/science.1195227

Burré, J., Vivona, S., Diao, J., Sharma, M., Brunger, A. T., & Südhof, T. C. (2013). Properties of native brain α-synuclein. *Nature*, *498*(7453), E4-6; discussion E6-7. https://doi.org/10.1038/nature12125

Burton, E. J., McKeith, I. G., Burn, D. J., Williams, E. D., & O'Brien, J. T. (2004). Cerebral atrophy in Parkinson's disease with and without dementia: a comparison with Alzheimer's disease, dementia with Lewy bodies and controls. *Brain*, *127*(4), 791-800. https://doi.org/10.1093/brain/awh088

Bussian, T. J., Aziz, A., Meyer, C. F., Swenson, B. L., van Deursen, J. M., & Baker, D. J. (2018). Clearance of senescent glial cells prevents tau-dependent pathology and cognitive decline. *Nature*, *562*(7728), 578-582. https://doi.org/10.1038/s41586-018-0543-y

Cakir, B., Xiang, Y., Tanaka, Y., Kural, M. H., Parent, M., Kang, Y.-J., Chapeton, K., Patterson, B., Yuan, Y., He, C.-S., Raredon, M. S. B., Dengelegi, J., Kim, K.-Y., Sun, P., Zhong, M., Lee, S., Patra, P., Hyder, F., Niklason, L. E., . . . Park, I.-H. (2019). Engineering of human brain organoids with a functional vascular-like system. *Nature Methods*, *16*(11), 1169-1175. https://doi.org/10.1038/s41592-019-0586-5

Calne, D., & William Langston, J. (1983). AETIOLOGY OF PARKINSON'S DISEASE. *The Lancet*, *322*(8365), 1457-1459. https://doi.org/https://doi.org/10.1016/S0140-6736(83)90802-4

Camicioli, R., Sabino, J., Gee, M., Bouchard, T., Fisher, N., Hanstock, C., Emery, D., & Martin, W. R. (2011). Ventricular dilatation and brain atrophy in patients with Parkinson's disease with incipient dementia. *Mov Disord*, *26*(8), 1443-1450. https://doi.org/10.1002/mds.23700

Castiglione, H., Vigneron, P. A., Baquerre, C., Yates, F., Rontard, J., & Honegger, T. (2022). Human Brain Organoids-on-Chip: Advances, Challenges, and Perspectives for Preclinical Applications. *Pharmaceutics*, *14*(11). https://doi.org/10.3390/pharmaceutics14112301

Cerri, S., Mus, L., & Blandini, F. (2019). Parkinson's Disease in Women and Men: What's the Difference? *J Parkinsons Dis*, *9*(3), 501-515. https://doi.org/10.3233/jpd-191683

Chambers, S. M., Fasano, C. A., Papapetrou, E. P., Tomishima, M., Sadelain, M., & Studer, L. (2009). Highly efficient neural conversion of human ES and iPS cells by dual inhibition of SMAD signaling. *Nat Biotechnol*, *27*(3), 275-280. https://doi.org/10.1038/nbt.1529

Chan, C. S., Guzman, J. N., Ilijic, E., Mercer, J. N., Rick, C., Tkatch, T., Meredith, G. E., & Surmeier, D. J. (2007). 'Rejuvenation' protects neurons in mouse models of Parkinson's disease. *Nature*, *447*(7148), 1081-1086. https://doi.org/10.1038/nature05865

Chandra, S., Chen, X., Rizo, J., Jahn, R., & Südhof, T. C. (2003). A broken alpha -helix in folded alpha -Synuclein. *J Biol Chem*, *278*(17), 15313-15318. https://doi.org/10.1074/jbc.M213128200

Chandra, S., Gallardo, G., Fernández-Chacón, R., Schlüter, O. M., & Südhof, T. C. (2005). Alpha-synuclein cooperates with CSPalpha in preventing neurodegeneration. *Cell*, *123*(3), 383-396. https://doi.org/10.1016/j.cell.2005.09.028

Chen, X., Saiyin, H., Liu, Y., Wang, Y., Li, X., Ji, R., & Ma, L. (2022). Human striatal organoids derived from pluripotent stem cells recapitulate striatal development and compartments. *PLOS Biology*, *20*(11), e3001868. https://doi.org/10.1371/journal.pbio.3001868

Chinta, S. J., Woods, G., Demaria, M., Rane, A., Zou, Y., McQuade, A., Rajagopalan, S., Limbad, C., Madden, D. T., Campisi, J., & Andersen, J. K. (2018). Cellular Senescence Is Induced by the Environmental Neurotoxin Paraquat and Contributes to Neuropathology Linked to Parkinson's Disease. *Cell Rep*, *22*(4), 930-940. https://doi.org/10.1016/j.celrep.2017.12.092

Chinta, S. J., Woods, G., Rane, A., Demaria, M., Campisi, J., & Andersen, J. K. (2015). Cellular senescence and the aging brain. *Exp Gerontol*, *68*, 3-7. https://doi.org/10.1016/j.exger.2014.09.018

Chlebanowska, P., Tejchman, A., Sułkowski, M., Skrzypek, K., & Majka, M. (2020). Use of 3D Organoids as a Model to Study Idiopathic Form of Parkinson's Disease. *Int J Mol Sci*, *21*(3). https://doi.org/10.3390/ijms21030694

Choi, B. K., Choi, M. G., Kim, J. Y., Yang, Y., Lai, Y., Kweon, D. H., Lee, N. K., & Shin, Y. K. (2013). Large α-synuclein oligomers inhibit neuronal SNARE-mediated vesicle docking. *Proc Natl Acad Sci U S A*, *110*(10), 4087-4092. https://doi.org/10.1073/pnas.1218424110

Choi, D. H., Kim, Y. J., Kim, Y. G., Joh, T. H., Beal, M. F., & Kim, Y. S. (2011). Role of matrix metalloproteinase 3-mediated alpha-synuclein cleavage in dopaminergic cell death. *J Biol Chem*, *286*(16), 14168-14177. https://doi.org/10.1074/jbc.M111.222430

Choi, M. G., Kim, M. J., Kim, D. G., Yu, R., Jang, Y. N., & Oh, W. J. (2018). Sequestration of synaptic proteins by alpha-synuclein aggregates leading to neurotoxicity is inhibited by small peptide. *PLoS One*, *13*(4), e0195339. https://doi.org/10.1371/journal.pone.0195339

Christensen, K. V., Smith, G. P., & Williamson, D. S. (2017). Development of LRRK2 Inhibitors for the Treatment of Parkinson's Disease. *Prog Med Chem*, *56*, 37-80. https://doi.org/10.1016/bs.pmch.2016.11.002

Cilia, R., Tunesi, S., Marotta, G., Cereda, E., Siri, C., Tesei, S., Zecchinelli, A. L., Canesi, M., Mariani, C. B., Meucci, N., Sacilotto, G., Zini, M., Barichella, M., Magnani, C., Duga, S., Asselta, R., Soldà, G., Seresini, A., Seia, M., . . . Goldwurm, S. (2016). Survival and dementia in GBA-associated Parkinson's disease: The mutation matters. *Ann Neurol*, *80*(5), 662-673. https://doi.org/10.1002/ana.24777

Clayton, D. F., & George, J. M. (1998). The synucleins: a family of proteins involved in synaptic function, plasticity, neurodegeneration and disease. *Trends in Neurosciences*, *21*(6), 249-254. https://doi.org/10.1016/S0166-2236(97)01213-7

Clayton, D. F., & George, J. M. (1999). Synucleins in synaptic plasticity and neurodegenerative disorders. *J Neurosci Res*, *58*(1), 120-129.

Cohen, J., & Torres, C. (2019). Astrocyte senescence: Evidence and significance. *Aging Cell*, *18*(3), e12937. https://doi.org/10.1111/acel.12937

Cole, N. B., Murphy, D. D., Grider, T., Rueter, S., Brasaemle, D., & Nussbaum, R. L. (2002). Lipid droplet binding and oligomerization properties of the Parkinson's disease protein alpha-synuclein. *J Biol Chem*, *277*(8), 6344-6352. https://doi.org/10.1074/jbc.M108414200

Cole, T. A., Zhao, H., Collier, T. J., Sandoval, I., Sortwell, C. E., Steece-Collier, K., Daley, B. F., Booms, A., Lipton, J., Welch, M., Berman, M., Jandreski, L., Graham, D., Weihofen, A., Celano, S., Schulz, E., Cole-Strauss, A., Luna, E., Quach, D., . . . Paumier, K. L. (2021). α-Synuclein antisense oligonucleotides as a disease-modifying therapy for Parkinson's disease. *JCI Insight*, *6*(5). https://doi.org/10.1172/jci.insight.135633

Conway, K. A., Harper, J. D., & Lansbury, P. T. (1998). Accelerated in vitro fibril formation by a mutant alpha-synuclein linked to early-onset Parkinson disease. *Nat Med*, *4*(11), 1318-1320. https://doi.org/10.1038/3311

Corsini, N. S., & Knoblich, J. A. (2022). Human organoids: New strategies and methods for analyzing human development and disease. *Cell*, *185*(15), 2756-2769. https://doi.org/10.1016/j.cell.2022.06.051

Cox, D., Carver, J. A., & Ecroyd, H. (2014). Preventing α-synuclein aggregation: The role of the small heat-shock molecular chaperone proteins. *Biochimica et Biophysica Acta (BBA) - Molecular Basis of Disease*, *1842*(9), 1830-1843. https://doi.org/https://doi.org/10.1016/j.bbadis.2014.06.024

Crowther, R. A., Jakes, R., Spillantini, M. G., & Goedert, M. (1998). Synthetic filaments assembled from C-terminally truncated alpha-synuclein. *FEBS Lett*, *436*(3), 309-312. https://doi.org/10.1016/s0014-5793(98)01146-6

D'Amato, R. J., Alexander, G. M., Schwartzman, R. J., Kitt, C. A., Price, D. L., & Snyder, S. H. (1987). Evidence for neuromelanin involvement in MPTP-induced neurotoxicity. *Nature*, *327*(6120), 324-326. https://doi.org/10.1038/327324a0

Dahlmann, B. (2007). Role of proteasomes in disease. *BMC Biochem*, *8 Suppl 1*(Suppl 1), S3. https://doi.org/10.1186/1471-2091-8-s1-s3

Damier, P., Hirsch, E. C., Agid, Y., & Graybiel, A. M. (1999). The substantia nigra of the human brain. II. Patterns of loss of dopamine-containing neurons in Parkinson's disease. *Brain*, *122 (Pt 8)*, 1437-1448. https://doi.org/10.1093/brain/122.8.1437

Danielson, S. R., Held, J. M., Schilling, B., Oo, M., Gibson, B. W., & Andersen, J. K. (2009). Preferentially increased nitration of alpha-synuclein at tyrosine-39 in a cellular oxidative model of Parkinson's disease. *Anal Chem*, *81*(18), 7823-7828. https://doi.org/10.1021/ac901176t

Dauer, W., & Przedborski, S. (2003). Parkinson's Disease: Mechanisms and Models. *Neuron*, *39*(6), 889-909. https://doi.org/10.1016/S0896-6273(03)00568-3

Daugherty, A., & Raz, N. (2013). Age-related differences in iron content of subcortical nuclei observed in vivo: a meta-analysis. *Neuroimage*, *70*, 113-121. https://doi.org/10.1016/j.neuroimage.2012.12.040

Davidi, D., Schechter, M., Elhadi, S. A., Matatov, A., Nathanson, L., & Sharon, R. (2020). α-Synuclein Translocates to the Nucleus to Activate Retinoic-Acid-Dependent Gene Transcription. *iScience*, *23*(3), 100910. https://doi.org/https://doi.org/10.1016/j.isci.2020.100910

Davidson, W. S., Jonas, A., Clayton, D. F., & George, J. M. (1998). Stabilization of alpha-synuclein secondary structure upon binding to synthetic membranes. *J Biol Chem*, *273*(16), 9443-9449. https://doi.org/10.1074/jbc.273.16.9443

Dawson, T. M., Ko, H. S., & Dawson, V. L. (2010). Genetic animal models of Parkinson's disease. *Neuron*, *66*(5), 646-661. https://doi.org/10.1016/j.neuron.2010.04.034

Day, J. O., & Mullin, S. (2021). The Genetics of Parkinson's Disease and Implications for Clinical Practice. *Genes*, *12*(7), 1006. https://www.mdpi.com/2073-4425/12/7/1006

Delenclos, M., Burgess, J. D., Lamprokostopoulou, A., Outeiro, T. F., Vekrellis, K., & McLean, P. J. (2019). Cellular models of alpha-synuclein toxicity and aggregation. *J Neurochem*, *150*(5), 566-576. https://doi.org/10.1111/jnc.14806

Delgado, Ana C., Ferrón, Sacri R., Vicente, D., Porlan, E., Perez-Villalba, A., Trujillo, Carmen M., D'Ocón, P., & Fariñas, I. (2014). Endothelial NT-3 Delivered by Vasculature and CSF Promotes Quiescence of Subependymal Neural Stem Cells through Nitric Oxide Induction. *Neuron*, *83*(3), 572-585. https://doi.org/10.1016/j.neuron.2014.06.015

Dettmer, U., Newman, A. J., Soldner, F., Luth, E. S., Kim, N. C., von Saucken, V. E., Sanderson, J. B., Jaenisch, R., Bartels, T., & Selkoe, D. (2015). Parkinson-causing α-synuclein missense mutations shift native tetramers to monomers as a mechanism for disease initiation. *Nat Commun*, *6*, 7314. https://doi.org/10.1038/ncomms8314

Devi, L., Raghavendran, V., Prabhu, B. M., Avadhani, N. G., & Anandatheerthavarada, H. K. (2008). Mitochondrial import and accumulation of alpha-synuclein impair complex I in human dopaminergic neuronal cultures and Parkinson disease brain. *J Biol Chem*, *283*(14), 9089-9100. https://doi.org/10.1074/jbc.M710012200

Di Maio, R., Barrett, P. J., Hoffman, E. K., Barrett, C. W., Zharikov, A., Borah, A., Hu, X., McCoy, J., Chu, C. T., Burton, E. A., Hastings, T. G., & Greenamyre, J. T. (2016). α-Synuclein binds to TOM20 and inhibits mitochondrial protein import in Parkinson's disease. *Sci Transl Med*, *8*(342), 342ra378. https://doi.org/10.1126/scitranslmed.aaf3634

Di Marco Vieira, B., Radford, R. A. W., Hayashi, J., Eaton, E. D., Greenaway, B., Jambas, M., Petcu, E. B., Chung, R. S., & Pountney, D. L. (2020). Extracellular Alpha-Synuclein Promotes a Neuroinhibitory Secretory Phenotype in Astrocytes. *Life (Basel)*, *10*(9). https://doi.org/10.3390/life10090183

Dickson, D. W. (2012). Parkinson's disease and parkinsonism: neuropathology. *Cold Spring Harb Perspect Med*, *2*(8). https://doi.org/10.1101/cshperspect.a009258

Diederich, N. J., James Surmeier, D., Uchihara, T., Grillner, S., & Goetz, C. G. (2019). Parkinson's disease: Is it a consequence of human brain evolution? *Mov Disord*, *34*(4), 453-459. https://doi.org/10.1002/mds.27628

Doherty, K. M., Silveira-Moriyama, L., Parkkinen, L., Healy, D. G., Farrell, M., Mencacci, N. E., Ahmed, Z., Brett, F. M., Hardy, J., Quinn, N., Counihan, T. J., Lynch, T., Fox, Z. V., Revesz, T., Lees, A. J., & Holton, J. L. (2013). Parkin disease: a clinicopathologic entity? *JAMA Neurol*, *70*(5), 571-579. https://doi.org/10.1001/jamaneurol.2013.172

Dorsey, E. R., & Bloem, B. R. (2018). The Parkinson Pandemic—A Call to Action. *JAMA Neurology*, *75*(1), 9-10. https://doi.org/10.1001/jamaneurol.2017.3299

Dorsey, E. R., Elbaz, A., Nichols, E., Abbasi, N., Abd-Allah, F., Abdelalim, A., Adsuar, J. C., Geleto Ansha, M., Brayne, C., Choi, J. J., Collado-Mateo, D., Dahodwala, N., Phuc Do, H., Edessa, D., Endres, M., Fereshtehnejad, S., Foreman, K. J., Gbetoho Gankpe, F., Gupta, R., . . . Murray, C. J. L. (2018). Global, regional, and national burden of Parkinson's disease, 1990-2016: a systematic analysis for the Global Burden of Disease Study 2016. *Lancet Neurol*, *17*(11), 939-953. https://doi.org/10.1016/s1474-4422(18)30295-3

Dorsey, J. F., Jove, R., Kraker, A. J., & Wu, J. (2000). The pyrido[2,3-d]pyrimidine derivative PD180970 inhibits p210Bcr-Abl tyrosine kinase and induces apoptosis of K562 leukemic cells. *Cancer Res*, *60*(12), 3127-3131.

Double, K. L., Ben-Shachar, D., Youdim, M. B. H., Zecca, L., Riederer, P., & Gerlach, M. (2002). Influence of neuromelanin on oxidative pathways within the human substantia nigra.

Neurotoxicology and teratology, *24*(5), 621-628. https://doi.org/10.1016/s0892-0362(02)00218-0

Du, X.-y., Xie, X.-x., & Liu, R.-t. (2020). The Role of α-Synuclein Oligomers in Parkinson's Disease. *International Journal of Molecular Sciences*, *21*(22), 8645. https://www.mdpi.com/1422-0067/21/22/8645

Dufty, B. M., Warner, L. R., Hou, S. T., Jiang, S. X., Gomez-Isla, T., Leenhouts, K. M., Oxford, J. T., Feany, M. B., Masliah, E., & Rohn, T. T. (2007). Calpain-cleavage of alpha-synuclein: connecting proteolytic processing to disease-linked aggregation. *Am J Pathol*, *170*(5), 1725-1738. https://doi.org/10.2353/ajpath.2007.061232

El-Agnaf, O. M., Jakes, R., Curran, M. D., & Wallace, A. (1998). Effects of the mutations Ala30 to Pro and Ala53 to Thr on the physical and morphological properties of alpha-synuclein protein implicated in Parkinson's disease. *FEBS Lett*, *440*(1-2), 67-70. https://doi.org/10.1016/s0014-5793(98)01419-7

Emamzadeh, F. N. (2016). Alpha-synuclein structure, functions, and interactions. *J Res Med Sci*, *21*, 29. https://doi.org/10.4103/1735-1995.181989

Eura, N., Matsui, T. K., Luginbühl, J., Matsubayashi, M., Nanaura, H., Shiota, T., Kinugawa, K., Iguchi, N., Kiriyama, T., Zheng, C., Kouno, T., Lan, Y. J., Kongpracha, P., Wiriyasermkul, P., Sakaguchi, Y. M., Nagata, R., Komeda, T., Morikawa, N., Kitayoshi, F., . . . Mori, E. (2020). Brainstem Organoids From Human Pluripotent Stem Cells [Original Research]. *Frontiers in Neuroscience*, *14*. https://doi.org/10.3389/fnins.2020.00538

Falkenburger, B. H., & Schulz, J. B. (2006). Limitations of cellular models in Parkinson's disease research. *J Neural Transm Suppl*(70), 261-268. https://doi.org/10.1007/978-3-211-45295-0_40

Fan, T.-S., Liu, S. C.-H., & Wu, R.-M. (2021). Alpha-Synuclein and Cognitive Decline in Parkinson Disease. *Life*, *11*(11), 1239. https://www.mdpi.com/2075-1729/11/11/1239

Fanning, S., Selkoe, D., & Dettmer, U. (2020). Parkinson's disease: proteinopathy or lipidopathy? *NPJ Parkinsons Dis*, *6*, 3. https://doi.org/10.1038/s41531-019-0103-7

Fathi, A., Mathivanan, S., Kong, L., Petersen, A. J., Harder, Cole R. K., Block, J., Miller, J. M., Bhattacharyya, A., Wang, D., & Zhang, S.-C. (2022). Chemically induced senescence in human stem cell-derived neurons promotes phenotypic presentation of neurodegeneration. *Aging Cell*, *21*(1), e13541. https://doi.org/https://doi.org/10.1111/acel.13541

Faucheux, B. A., Martin, M. E., Beaumont, C., Hauw, J. J., Agid, Y., & Hirsch, E. C. (2003). Neuromelanin associated redox-active iron is increased in the substantia nigra of patients with Parkinson's disease. *J Neurochem*, *86*(5), 1142-1148. https://doi.org/10.1046/j.1471-4159.2003.01923.x

Fauvet, B., Mbefo, M. K., Fares, M. B., Desobry, C., Michael, S., Ardah, M. T., Tsika, E., Coune, P., Prudent, M., Lion, N., Eliezer, D., Moore, D. J., Schneider, B., Aebischer, P., El-Agnaf, O. M., Masliah, E., & Lashuel, H. A. (2012). α-Synuclein in central nervous system and from erythrocytes, mammalian cells, and Escherichia coli exists predominantly as disordered monomer. *J Biol Chem*, *287*(19), 15345-15364. https://doi.org/10.1074/jbc.M111.318949

Fearnley, J. M., & Lees, A. J. (1991). Ageing and Parkinson's disease: substantia nigra regional selectivity. *Brain*, *114 (Pt 5)*, 2283-2301. https://doi.org/10.1093/brain/114.5.2283

Fortin, D. L., Nemani, V. M., Voglmaier, S. M., Anthony, M. D., Ryan, T. A., & Edwards, R. H. (2005). Neural activity controls the synaptic accumulation of alpha-synuclein. *J Neurosci*, *25*(47), 10913-10921. https://doi.org/10.1523/jneurosci.2922-05.2005

Fu, Y., Paxinos, G., Watson, C., & Halliday, G. M. (2016). The substantia nigra and ventral tegmental dopaminergic neurons from development to degeneration. *J Chem Neuroanat*, *76*(Pt B), 98-107. https://doi.org/10.1016/j.jchemneu.2016.02.001

Fujioka, S., Ogaki, K., Tacik, P. M., Uitti, R. J., Ross, O. A., & Wszolek, Z. K. (2014). Update on novel familial forms of Parkinson's disease and multiple system atrophy. *Parkinsonism Relat Disord, 20 Suppl 1*(0 1), S29-34. https://doi.org/10.1016/s1353-8020(13)70010-5

Fujiwara, H., Hasegawa, M., Dohmae, N., Kawashima, A., Masliah, E., Goldberg, M. S., Shen, J., Takio, K., & Iwatsubo, T. (2002). alpha-Synuclein is phosphorylated in synucleinopathy lesions. *Nat Cell Biol, 4*(2), 160-164. https://doi.org/10.1038/ncb748

Galet, B., Cheval, H., & Ravassard, P. (2020). Patient-Derived Midbrain Organoids to Explore the Molecular Basis of Parkinson's Disease. *Front Neurol, 11*, 1005. https://doi.org/10.3389/fneur.2020.01005

Galloway, P. G., Mulvihill, P., & Perry, G. (1992). Filaments of Lewy bodies contain insoluble cytoskeletal elements. *Am J Pathol, 140*(4), 809-822.

Garcia-Reitböck, P., Anichtchik, O., Bellucci, A., Iovino, M., Ballini, C., Fineberg, E., Ghetti, B., Della Corte, L., Spano, P., Tofaris, G. K., Goedert, M., & Spillantini, M. G. (2010). SNARE protein redistribution and synaptic failure in a transgenic mouse model of Parkinson's disease. *Brain, 133*(Pt 7), 2032-2044. https://doi.org/10.1093/brain/awq132

Garcia-Reitboeck, P., Anichtchik, O., Dalley, J. W., Ninkina, N., Tofaris, G. K., Buchman, V. L., & Spillantini, M. G. (2013). Endogenous alpha-synuclein influences the number of dopaminergic neurons in mouse substantia nigra. *Exp Neurol, 248*, 541-545. https://doi.org/10.1016/j.expneurol.2013.07.015

Ge, P., Dawson, V. L., & Dawson, T. M. (2020). PINK1 and Parkin mitochondrial quality control: a source of regional vulnerability in Parkinson's disease. *Molecular Neurodegeneration, 15*(1), 20. https://doi.org/10.1186/s13024-020-00367-7

Geertsma, H. M., Suk, T. R., Ricke, K. M., Horsthuis, K., Parmasad, J.-L. A., Fisk, Z. A., Callaghan, S. M., & Rousseaux, M. W. C. (2022). Constitutive nuclear accumulation of endogenous alpha-synuclein in mice causes motor impairment and cortical dysfunction, independent of protein aggregation. *Human Molecular Genetics, 31*(21), 3613-3628. https://doi.org/10.1093/hmg/ddac035

George, J. M. (2002). The synucleins. *Genome Biol, 3*(1), Reviews3002. https://doi.org/10.1186/gb-2001-3-1-reviews3002

George, J. M., Jin, H., Woods, W. S., & Clayton, D. F. (1995). Characterization of a novel protein regulated during the critical period for song learning in the zebra finch. *Neuron, 15*(2), 361-372. https://doi.org/10.1016/0896-6273(95)90040-3

Giasson, B. I., Duda, J. E., Murray, I. V., Chen, Q., Souza, J. M., Hurtig, H. I., Ischiropoulos, H., Trojanowski, J. Q., & Lee, V. M. (2000). Oxidative damage linked to neurodegeneration by selective alpha-synuclein nitration in synucleinopathy lesions. *Science, 290*(5493), 985-989. https://doi.org/10.1126/science.290.5493.985

Giguère, N., Burke Nanni, S., & Trudeau, L. E. (2018). On Cell Loss and Selective Vulnerability of Neuronal Populations in Parkinson's Disease. *Front Neurol, 9*, 455. https://doi.org/10.3389/fneur.2018.00455

Goedert, M. (2015). NEURODEGENERATION. Alzheimer's and Parkinson's diseases: The prion concept in relation to assembled Aβ, tau, and α-synuclein. *Science, 349*(6248), 1255555. https://doi.org/10.1126/science.1255555

Goldberg, M. S., Fleming, S. M., Palacino, J. J., Cepeda, C., Lam, H. A., Bhatnagar, A., Meloni, E. G., Wu, N., Ackerson, L. C., Klapstein, G. J., Gajendiran, M., Roth, B. L., Chesselet, M. F., Maidment, N. T., Levine, M. S., & Shen, J. (2003). Parkin-deficient mice exhibit nigrostriatal deficits but not loss of dopaminergic neurons. *J Biol Chem, 278*(44), 43628-43635. https://doi.org/10.1074/jbc.M308947200

Gómez-Tortosa, E., Newell, K., Irizarry, M. C., Sanders, J. L., & Hyman, B. T. (2000). alpha-Synuclein immunoreactivity in dementia with Lewy bodies: morphological staging and comparison with ubiquitin immunostaining. *Acta Neuropathol, 99*(4), 352-357. https://doi.org/10.1007/s004010051135

Gonzalo, S., Kreienkamp, R., & Askjaer, P. (2017). Hutchinson-Gilford Progeria Syndrome: A premature aging disease caused by LMNA gene mutations. *Ageing Res Rev, 33*, 18-29. https://doi.org/10.1016/j.arr.2016.06.007

Gorbatyuk, O. S., Li, S., Sullivan, L. F., Chen, W., Kondrikova, G., Manfredsson, F. P., Mandel, R. J., & Muzyczka, N. (2008). The phosphorylation state of Ser-129 in human alpha-synuclein determines neurodegeneration in a rat model of Parkinson disease. *Proc Natl Acad Sci U S A, 105*(2), 763-768. https://doi.org/10.1073/pnas.0711053105

Gouider-Khouja, N., Larnaout, A., Amouri, R., Sfar, S., Belal, S., Ben Hamida, C., Ben Hamida, M., Hattori, N., Mizuno, Y., & Hentati, F. (2003). Autosomal recessive parkinsonism linked to parkin gene in a Tunisian family. Clinical, genetic and pathological study. *Parkinsonism Relat Disord, 9*(5), 247-251. https://doi.org/10.1016/s1353-8020(03)00016-6

Granado-Serrano, A. B. n., Martín, M. a. A., Bravo, L., Goya, L., & Ramos, S. (2006). Quercetin Induces Apoptosis via Caspase Activation, Regulation of Bcl-2, and Inhibition of PI-3-Kinase/Akt and ERK Pathways in a Human Hepatoma Cell Line (HepG2). *The Journal of Nutrition, 136*(11), 2715-2721. https://doi.org/10.1093/jn/136.11.2715

Greenbaum, E. A., Graves, C. L., Mishizen-Eberz, A. J., Lupoli, M. A., Lynch, D. R., Englander, S. W., Axelsen, P. H., & Giasson, B. I. (2005). The E46K mutation in alpha-synuclein increases amyloid fibril formation. *J Biol Chem, 280*(9), 7800-7807. https://doi.org/10.1074/jbc.M411638200

Guadagnolo, D., Piane, M., Torrisi, M. R., Pizzuti, A., & Petrucci, S. (2021). Genotype-Phenotype Correlations in Monogenic Parkinson Disease: A Review on Clinical and Molecular Findings. *Front Neurol, 12*, 648588. https://doi.org/10.3389/fneur.2021.648588

Guzman, J. N., Sánchez-Padilla, J., Chan, C. S., & Surmeier, D. J. (2009). Robust pacemaking in substantia nigra dopaminergic neurons. *J Neurosci, 29*(35), 11011-11019. https://doi.org/10.1523/jneurosci.2519-09.2009

Guzman, J. N., Sanchez-Padilla, J., Wokosin, D., Kondapalli, J., Ilijic, E., Schumacker, P. T., & Surmeier, D. J. (2010). Oxidant stress evoked by pacemaking in dopaminergic neurons is attenuated by DJ-1. *Nature, 468*(7324), 696-700. https://doi.org/10.1038/nature09536

Haacke, E. M., Miao, Y., Liu, M., Habib, C. A., Katkuri, Y., Liu, T., Yang, Z., Lang, Z., Hu, J., & Wu, J. (2010). Correlation of putative iron content as represented by changes in R2* and phase with age in deep gray matter of healthy adults. *Journal of Magnetic Resonance Imaging, 32*(3), 561-576. https://doi.org/https://doi.org/10.1002/jmri.22293

Harley, C. B., Futcher, A. B., & Greider, C. W. (1990). Telomeres shorten during ageing of human fibroblasts. *Nature, 345*(6274), 458-460. https://doi.org/10.1038/345458a0

Hart, G. W., Housley, M. P., & Slawson, C. (2007). Cycling of O-linked β-N-acetylglucosamine on nucleocytoplasmic proteins. *Nature, 446*(7139), 1017-1022. https://doi.org/10.1038/nature05815

Hasegawa, M., Fujiwara, H., Nonaka, T., Wakabayashi, K., Takahashi, H., Lee, V. M., Trojanowski, J. Q., Mann, D., & Iwatsubo, T. (2002). Phosphorylated alpha-synuclein is ubiquitinated in alpha-synucleinopathy lesions. *J Biol Chem, 277*(50), 49071-49076. https://doi.org/10.1074/jbc.M208046200

Hawkes, C. H., Del Tredici, K., & Braak, H. (2007). Parkinson's disease: a dual-hit hypothesis. *Neuropathol Appl Neurobiol, 33*(6), 599-614. https://doi.org/10.1111/j.1365-2990.2007.00874.x

Hawkes, C. H., Del Tredici, K., & Braak, H. (2009). Parkinson's disease: the dual hit theory revisited. *Ann N Y Acad Sci*, *1170*, 615-622. https://doi.org/10.1111/j.1749-6632.2009.04365.x

Hayashi, S., Wakabayashi, K., Ishikawa, A., Nagai, H., Saito, M., Maruyama, M., Takahashi, T., Ozawa, T., Tsuji, S., & Takahashi, H. (2000). An autopsy case of autosomal-recessive juvenile parkinsonism with a homozygous exon 4 deletion in the parkin gene. *Mov Disord*, *15*(5), 884-888. https://doi.org/10.1002/1531-8257(200009)15:5<884::aid-mds1019>3.0.co;2-8

Hayflick, L., & Moorhead, P. S. (1961). The serial cultivation of human diploid cell strains. *Experimental Cell Research*, *25*(3), 585-621. https://doi.org/https://doi.org/10.1016/0014-4827(61)90192-6

Hernandez-Segura, A., Nehme, J., & Demaria, M. (2018). Hallmarks of Cellular Senescence. *Trends in Cell Biology*, *28*(6), 436-453. https://doi.org/10.1016/j.tcb.2018.02.001

Hindle, J. V. (2010). Ageing, neurodegeneration and Parkinson's disease. *Age and Ageing*, *39*(2), 156-161. https://doi.org/10.1093/ageing/afp223

Hinkle, K. M., Yue, M., Behrouz, B., Dächsel, J. C., Lincoln, S. J., Bowles, E. E., Beevers, J. E., Dugger, B., Winner, B., Prots, I., Kent, C. B., Nishioka, K., Lin, W.-L., Dickson, D. W., Janus, C. J., Farrer, M. J., & Melrose, H. L. (2012). LRRK2 knockout mice have an intact dopaminergic system but display alterations in exploratory and motor co-ordination behaviors. *Molecular Neurodegeneration*, *7*(1), 25. https://doi.org/10.1186/1750-1326-7-25

Hodara, R., Norris, E. H., Giasson, B. I., Mishizen-Eberz, A. J., Lynch, D. R., Lee, V. M. Y., & Ischiropoulos, H. (2004). Functional Consequences of α-Synuclein Tyrosine Nitration: DIMINISHED BINDING TO LIPID VESICLES AND INCREASED FIBRIL FORMATION*. *Journal of Biological Chemistry*, *279*(46), 47746-47753. https://doi.org/https://doi.org/10.1074/jbc.M408906200

Hoffman-Zacharska, D., Koziorowski, D., Ross, O. A., Milewski, M., Poznanski, J. A., Jurek, M., Wszolek, Z. K., Soto-Ortolaza, A., Awek, J. A. S., Janik, P., Jamrozik, Z., Potulska-Chromik, A., Jasinska-Myga, B., Opala, G., Krygowska-Wajs, A., Czyzewski, K., Dickson, D. W., Bal, J., & Friedman, A. (2013). Novel A18T and pA29S substitutions in α-synuclein may be associated with sporadic Parkinson's disease. *Parkinsonism Relat Disord*, *19*(11), 1057-1060. https://doi.org/10.1016/j.parkreldis.2013.07.011

Hofmann, K. W., Schuh, A. F., Saute, J., Townsend, R., Fricke, D., Leke, R., Souza, D. O., Portela, L. V., Chaves, M. L., & Rieder, C. R. (2009). Interleukin-6 serum levels in patients with Parkinson's disease. *Neurochem Res*, *34*(8), 1401-1404. https://doi.org/10.1007/s11064-009-9921-z

Huang, Z., Xu, Z., Wu, Y., & Zhou, Y. (2011). Determining nuclear localization of alpha-synuclein in mouse brains. *Neuroscience*, *199*, 318-332. https://doi.org/https://doi.org/10.1016/j.neuroscience.2011.10.016

Inglis, K. J., Chereau, D., Brigham, E. F., Chiou, S. S., Schöbel, S., Frigon, N. L., Yu, M., Caccavello, R. J., Nelson, S., Motter, R., Wright, S., Chian, D., Santiago, P., Soriano, F., Ramos, C., Powell, K., Goldstein, J. M., Babcock, M., Yednock, T., . . . Anderson, J. P. (2009). Polo-like kinase 2 (PLK2) phosphorylates alpha-synuclein at serine 129 in central nervous system. *J Biol Chem*, *284*(5), 2598-2602. https://doi.org/10.1074/jbc.C800206200

Ishii, A., Nonaka, T., Taniguchi, S., Saito, T., Arai, T., Mann, D., Iwatsubo, T., Hisanaga, S., Goedert, M., & Hasegawa, M. (2007). Casein kinase 2 is the major enzyme in brain that phosphorylates Ser129 of human alpha-synuclein: Implication for alpha-synucleinopathies. *FEBS Lett*, *581*(24), 4711-4717. https://doi.org/10.1016/j.febslet.2007.08.067

Iwai, A., Masliah, E., Yoshimoto, M., Ge, N., Flanagan, L., de Silva, H. A., Kittel, A., & Saitoh, T. (1995). The precursor protein of non-A beta component of Alzheimer's disease amyloid is

a presynaptic protein of the central nervous system. *Neuron, 14*(2), 467-475. https://doi.org/10.1016/0896-6273(95)90302-x

Iwata, A., Maruyama, M., Akagi, T., Hashikawa, T., Kanazawa, I., Tsuji, S., & Nukina, N. (2003). Alpha-synuclein degradation by serine protease neurosin: implication for pathogenesis of synucleinopathies. *Hum Mol Genet, 12*(20), 2625-2635. https://doi.org/10.1093/hmg/ddg283

Jackson, E. L., & Lu, H. L. (2016). Three-dimensional models for studying development and disease: moving on from organisms to organs-on-a-chip and organoids. *Integrative biology : quantitative biosciences from nano to macro, 8 6*, 672-683.

Jana, S., Sinha, M., Chanda, D., Roy, T., Banerjee, K., Munshi, S., Patro, B. S., & Chakrabarti, S. (2011). Mitochondrial dysfunction mediated by quinone oxidation products of dopamine: Implications in dopamine cytotoxicity and pathogenesis of Parkinson's disease. *Biochim Biophys Acta, 1812*(6), 663-673. https://doi.org/10.1016/j.bbadis.2011.02.013

Jankovic, J. (2008). Parkinson's disease: clinical features and diagnosis. *Journal of Neurology, Neurosurgery & Psychiatry, 79*(4), 368-376. https://doi.org/10.1136/jnnp.2007.131045

Jarazo, J., Barmpa, K., Modamio, J., Saraiva, C., Sabaté-Soler, S., Rosety, I., Griesbeck, A., Skwirblies, F., Zaffaroni, G., Smits, L. M., Su, J., Arias-Fuenzalida, J., Walter, J., Gomez-Giro, G., Monzel, A. S., Qing, X., Vitali, A., Cruciani, G., Boussaad, I., . . . Schwamborn, J. C. (2022). Parkinson's Disease Phenotypes in Patient Neuronal Cultures and Brain Organoids Improved by 2-Hydroxypropyl-β-Cyclodextrin Treatment. *Mov Disord, 37*(1), 80-94. https://doi.org/10.1002/mds.28810

Javier, B., Ines, T. D., Ana, Q. V., & Natalia Lopez-Gonzalez del, R. (2016). Animal Models of Parkinson's Disease. In D. Jolanta & K. Wojciech (Eds.), *Challenges in Parkinson's Disease* (pp. Ch. 10). IntechOpen. https://doi.org/10.5772/63328

Jesús, S., Huertas, I., Bernal-Bernal, I., Bonilla-Toribio, M., Cáceres-Redondo, M. T., Vargas-González, L., Gómez-Llamas, M., Carrillo, F., Calderón, E., Carballo, M., Gómez-Garre, P., & Mir, P. (2016). GBA Variants Influence Motor and Non-Motor Features of Parkinson's Disease. *PLoS One, 11*(12), e0167749. https://doi.org/10.1371/journal.pone.0167749

Jia, F., Fellner, A., & Kumar, K. R. (2022). Monogenic Parkinson's Disease: Genotype, Phenotype, Pathophysiology, and Genetic Testing. *Genes (Basel), 13*(3). https://doi.org/10.3390/genes13030471

Jin, H., Kanthasamy, A., Ghosh, A., Yang, Y., Anantharam, V., & Kanthasamy, A. G. (2011). α-Synuclein negatively regulates protein kinase Cδ expression to suppress apoptosis in dopaminergic neurons by reducing p300 histone acetyltransferase activity. *J Neurosci, 31*(6), 2035-2051. https://doi.org/10.1523/jneurosci.5634-10.2011

Jo, E., McLaurin, J., Yip, C. M., St. George-Hyslop, P., & Fraser, P. E. (2000). α-Synuclein Membrane Interactions and Lipid Specificity *. *Journal of Biological Chemistry, 275*(44), 34328-34334. https://doi.org/10.1074/jbc.M004345200

Jo, J., Xiao, Y., Sun, A. X., Cukuroglu, E., Tran, H. D., Göke, J., Tan, Z. Y., Saw, T. Y., Tan, C. P., Lokman, H., Lee, Y., Kim, D., Ko, H. S., Kim, S. O., Park, J. H., Cho, N. J., Hyde, T. M., Kleinman, J. E., Shin, J. H., . . . Ng, H. H. (2016). Midbrain-like Organoids from Human Pluripotent Stem Cells Contain Functional Dopaminergic and Neuromelanin-Producing Neurons. *Cell Stem Cell, 19*(2), 248-257. https://doi.org/10.1016/j.stem.2016.07.005

Jo, J., Yang, L., Tran, H.-D., Yu, W., Sun, A. X., Chang, Y. Y., Jung, B. C., Lee, S.-J., Saw, T. Y., Xiao, B., Khoo, A. T. T., Yaw, L.-P., Xie, J. J., Lokman, H., Ong, W.-Y., Lim, G. G. Y., Lim, K.-L., Tan, E.-K., Ng, H.-H., & Je, H. S. (2021). Lewy Body–like Inclusions in Human Midbrain Organoids Carrying Glucocerebrosidase and α-Synuclein Mutations. *Annals of Neurology, 90*(3), 490-505. https://doi.org/https://doi.org/10.1002/ana.26166

Johansen, K. K., Torp, S. H., Farrer, M. J., Gustavsson, E. K., & Aasly, J. O. (2018). A Case of Parkinson's Disease with No Lewy Body Pathology due to a Homozygous Exon Deletion in Parkin. *Case Rep Neurol Med*, *2018*, 6838965. https://doi.org/10.1155/2018/6838965

Jordan-Sciutto, K. L., Dorsey, R., Chalovich, E. M., Hammond, R. R., & Achim, C. L. (2003). Expression Patterns of Retinoblastoma Protein in Parkinson Disease. *Journal of Neuropathology & Experimental Neurology*, *62*(1), 68-74. https://doi.org/10.1093/jnen/62.1.68

Jurk, D., Wang, C., Miwa, S., Maddick, M., Korolchuk, V., Tsolou, A., Gonos, E. S., Thrasivoulou, C., Saffrey, M. J., Cameron, K., & von Zglinicki, T. (2012). Postmitotic neurons develop a p21-dependent senescence-like phenotype driven by a DNA damage response. *Aging Cell*, *11*(6), 996-1004. https://doi.org/10.1111/j.1474-9726.2012.00870.x

Kadoshima, T., Sakaguchi, H., Nakano, T., Soen, M., Ando, S., Eiraku, M., & Sasai, Y. (2013). Self-organization of axial polarity, inside-out layer pattern, and species-specific progenitor dynamics in human ES cell–derived neocortex. *Proceedings of the National Academy of Sciences*, *110*(50), 20284-20289. https://doi.org/doi:10.1073/pnas.1315710110

Kalia, L. V., & Lang, A. E. (2015). Parkinson's disease. *The Lancet*, *386*(9996), 896-912. https://doi.org/10.1016/S0140-6736(14)61393-3

Kamath, T., Abdulraouf, A., Burris, S. J., Langlieb, J., Gazestani, V., Nadaf, N. M., Balderrama, K., Vanderburg, C., & Macosko, E. Z. (2022). Single-cell genomic profiling of human dopamine neurons identifies a population that selectively degenerates in Parkinson's disease. *Nature Neuroscience*, *25*(5), 588-595. https://doi.org/10.1038/s41593-022-01061-1

Kestenbaum, M., & Alcalay, R. N. (2017). Clinical Features of LRRK2 Carriers with Parkinson's Disease. *Adv Neurobiol*, *14*, 31-48. https://doi.org/10.1007/978-3-319-49969-7_2

Kiely, A. P., Asi, Y. T., Kara, E., Limousin, P., Ling, H., Lewis, P., Proukakis, C., Quinn, N., Lees, A. J., Hardy, J., Revesz, T., Houlden, H., & Holton, J. L. (2013). α-Synucleinopathy associated with G51D SNCA mutation: a link between Parkinson's disease and multiple system atrophy? *Acta Neuropathol*, *125*(5), 753-769. https://doi.org/10.1007/s00401-013-1096-7

Kim, C., Ho, D. H., Suk, J. E., You, S., Michael, S., Kang, J., Joong Lee, S., Masliah, E., Hwang, D., Lee, H. J., & Lee, S. J. (2013). Neuron-released oligomeric α-synuclein is an endogenous agonist of TLR2 for paracrine activation of microglia. *Nat Commun*, *4*, 1562. https://doi.org/10.1038/ncomms2534

Kim, H., Park, H. J., Choi, H., Chang, Y., Park, H., Shin, J., Kim, J., Lengner, C. J., Lee, Y. K., & Kim, J. (2019). Modeling G2019S-LRRK2 Sporadic Parkinson's Disease in 3D Midbrain Organoids. *Stem Cell Reports*, *12*(3), 518-531. https://doi.org/10.1016/j.stemcr.2019.01.020

Kim, J., Koo, B.-K., & Knoblich, J. A. (2020). Human organoids: model systems for human biology and medicine. *Nature Reviews Molecular Cell Biology*, *21*(10), 571-584. https://doi.org/10.1038/s41580-020-0259-3

Kim, S., Park, J. M., Moon, J., & Choi, H. J. (2014). Alpha-synuclein interferes with cAMP/PKA-dependent upregulation of dopamine β-hydroxylase and is associated with abnormal adaptive responses to immobilization stress. *Exp Neurol*, *252*, 63-74. https://doi.org/10.1016/j.expneurol.2013.11.009

Klivenyi, P., Siwek, D., Gardian, G., Yang, L., Starkov, A., Cleren, C., Ferrante, R. J., Kowall, N. W., Abeliovich, A., & Beal, M. F. (2006). Mice lacking alpha-synuclein are resistant to mitochondrial toxins. *Neurobiol Dis*, *21*(3), 541-548. https://doi.org/10.1016/j.nbd.2005.08.018

Koller, W. C. (1991). Environmental Risk Factors in Parkinson's Disease. In G. Bernardi, M. B. Carpenter, G. Di Chiara, M. Morelli, & P. Stanzione (Eds.), *The Basal Ganglia III* (pp. 717-722). Springer New York. https://doi.org/10.1007/978-1-4684-5871-8_77

Kontopoulos, E., Parvin, J. D., & Feany, M. B. (2006). Alpha-synuclein acts in the nucleus to inhibit histone acetylation and promote neurotoxicity. *Hum Mol Genet*, *15*(20), 3012-3023. https://doi.org/10.1093/hmg/ddl243

Koss, D. J., Erskine, D., Porter, A., Palmoski, P., Menon, H., Todd, O. G. J., Leite, M., Attems, J., & Outeiro, T. F. (2022). Nuclear alpha-synuclein is present in the human brain and is modified in dementia with Lewy bodies. *Acta Neuropathologica Communications*, *10*(1), 98. https://doi.org/10.1186/s40478-022-01403-x

Kritsilis, M., S, V. R., Koutsoudaki, P. N., Evangelou, K., Gorgoulis, V. G., & Papadopoulos, D. (2018). Ageing, Cellular Senescence and Neurodegenerative Disease. *Int J Mol Sci*, *19*(10). https://doi.org/10.3390/ijms19102937

Krüger, R., Kuhn, W., Müller, T., Woitalla, D., Graeber, M., Kösel, S., Przuntek, H., Epplen, J. T., Schöls, L., & Riess, O. (1998). Ala30Pro mutation in the gene encoding alpha-synuclein in Parkinson's disease. *Nat Genet*, *18*(2), 106-108. https://doi.org/10.1038/ng0298-106

Krumova, P., Meulmeester, E., Garrido, M., Tirard, M., Hsiao, H. H., Bossis, G., Urlaub, H., Zweckstetter, M., Kügler, S., Melchior, F., Bähr, M., & Weishaupt, J. H. (2011). Sumoylation inhibits alpha-synuclein aggregation and toxicity. *J Cell Biol*, *194*(1), 49-60. https://doi.org/10.1083/jcb.201010117

Kuro-o, M., Matsumura, Y., Aizawa, H., Kawaguchi, H., Suga, T., Utsugi, T., Ohyama, Y., Kurabayashi, M., Kaname, T., Kume, E., Iwasaki, H., Iida, A., Shiraki-Iida, T., Nishikawa, S., Nagai, R., & Nabeshima, Y. I. (1997). Mutation of the mouse klotho gene leads to a syndrome resembling ageing. *Nature*, *390*(6655), 45-51. https://doi.org/10.1038/36285

Lancaster, M. A., Renner, M., Martin, C.-A., Wenzel, D., Bicknell, L. S., Hurles, M. E., Homfray, T., Penninger, J. M., Jackson, A. P., & Knoblich, J. A. (2013). Cerebral organoids model human brain development and microcephaly. *Nature*, *501*(7467), 373-379. https://doi.org/10.1038/nature12517

Lashuel, H. A., Petre, B. M., Wall, J., Simon, M., Nowak, R. J., Walz, T., & Lansbury, P. T. (2002a). α-Synuclein, Especially the Parkinson's Disease-associated Mutants, Forms Pore-like Annular and Tubular Protofibrils. *Journal of Molecular Biology*, *322*(5), 1089-1102. https://doi.org/https://doi.org/10.1016/S0022-2836(02)00735-0

Lashuel, H. A., Petre, B. M., Wall, J., Simon, M., Nowak, R. J., Walz, T., & Lansbury, P. T., Jr. (2002b). Alpha-synuclein, especially the Parkinson's disease-associated mutants, forms pore-like annular and tubular protofibrils. *J Mol Biol*, *322*(5), 1089-1102. https://doi.org/10.1016/s0022-2836(02)00735-0

Lazic, A., Balint, V., Stanisavljevic Ninkovic, D., Peric, M., & Stevanovic, M. (2022). Reactive and Senescent Astroglial Phenotypes as Hallmarks of Brain Pathologies. *International Journal of Molecular Sciences*, *23*(9), 4995. https://www.mdpi.com/1422-0067/23/9/4995

Le Grand, J. N., Gonzalez-Cano, L., Pavlou, M. A., & Schwamborn, J. C. (2015). Neural stem cells in Parkinson's disease: a role for neurogenesis defects in onset and progression. *Cell Mol Life Sci*, *72*(4), 773-797. https://doi.org/10.1007/s00018-014-1774-1

Le, W., Wu, J., & Tang, Y. (2016). Protective Microglia and Their Regulation in Parkinson's Disease. *Front Mol Neurosci*, *9*, 89. https://doi.org/10.3389/fnmol.2016.00089

Lee, E.-J., Woo, M.-S., Moon, P.-G., Baek, M.-C., Choi, I.-Y., Kim, W.-K., Junn, E., & Kim, H.-S. (2010). α-Synuclein Activates Microglia by Inducing the Expressions of Matrix Metalloproteinases and the Subsequent Activation of Protease-Activated Receptor-1. *The Journal of Immunology*, *185*(1), 615-623. https://doi.org/10.4049/jimmunol.0903480

Lee, H. J., Suk, J. E., Bae, E. J., & Lee, S. J. (2008). Clearance and deposition of extracellular alpha-synuclein aggregates in microglia. *Biochem Biophys Res Commun*, *372*(3), 423-428. https://doi.org/10.1016/j.bbrc.2008.05.045

Lee, H. J., Suk, J. E., Patrick, C., Bae, E. J., Cho, J. H., Rho, S., Hwang, D., Masliah, E., & Lee, S. J. (2010). Direct transfer of alpha-synuclein from neuron to astroglia causes inflammatory responses in synucleinopathies. *J Biol Chem, 285*(12), 9262-9272. https://doi.org/10.1074/jbc.M109.081125

Lee, S., Wang, E. Y., Steinberg, A. B., Walton, C. C., Chinta, S. J., & Andersen, J. K. (2021). A guide to senolytic intervention in neurodegenerative disease. *Mech Ageing Dev, 200*, 111585. https://doi.org/10.1016/j.mad.2021.111585

Lee, Y. H., Cha, J., Chung, S. J., Yoo, H. S., Sohn, Y. H., Ye, B. S., & Lee, P. H. (2019). Beneficial effect of estrogen on nigrostriatal dopaminergic neurons in drug-naïve postmenopausal Parkinson's disease. *Sci Rep, 9*(1), 10531. https://doi.org/10.1038/s41598-019-47026-6

Leon, J., Moreno, A. J., Garay, B. I., Chalkley, R. J., Burlingame, A. L., Wang, D., & Dubal, D. B. (2017). Peripheral Elevation of a Klotho Fragment Enhances Brain Function and Resilience in Young, Aging, and α-Synuclein Transgenic Mice. *Cell Rep, 20*(6), 1360-1371. https://doi.org/10.1016/j.celrep.2017.07.024

Lesage, S., Lunati, A., Houot, M., Romdhan, S. B., Clot, F., Tesson, C., Mangone, G., Toullec, B. L., Courtin, T., Larcher, K., Benmahdjoub, M., Arezki, M., Bouhouche, A., Anheim, M., Roze, E., Viallet, F., Tison, F., Broussolle, E., Emre, M., . . . Brice, A. (2020). Characterization of Recessive Parkinson Disease in a Large Multicenter Study. *Ann Neurol, 88*(4), 843-850. https://doi.org/10.1002/ana.25787

Levine, P. M., Galesic, A., Balana, A. T., Mahul-Mellier, A.-L., Navarro, M. X., De Leon, C. A., Lashuel, H. A., & Pratt, M. R. (2019). α-Synuclein O-GlcNAcylation alters aggregation and toxicity, revealing certain residues as potential inhibitors of Parkinson's disease. *Proceedings of the National Academy of Sciences, 116*(5), 1511-1519. https://doi.org/doi:10.1073/pnas.1808845116

Lewy, F. (1912). *Paralysis agitans. I. Pathologische Anatomie* (Vol. 3). Springer-Verlag.

Li, H., Jiang, H., Zhang, B., & Feng, J. (2018). Modeling Parkinson's Disease Using Patient-specific Induced Pluripotent Stem Cells. *J Parkinsons Dis, 8*(4), 479-493. https://doi.org/10.3233/jpd-181353

Li, J. Q., Tan, L., & Yu, J. T. (2014). The role of the LRRK2 gene in Parkinsonism. *Mol Neurodegener, 9*, 47. https://doi.org/10.1186/1750-1326-9-47

Li, W., & Lee, M. K. (2005). Antiapoptotic property of human alpha-synuclein in neuronal cell lines is associated with the inhibition of caspase-3 but not caspase-9 activity. *J Neurochem, 93*(6), 1542-1550. https://doi.org/10.1111/j.1471-4159.2005.03146.x

Limbad, C., Oron, T. R., Alimirah, F., Davalos, A. R., Tracy, T. E., Gan, L., Desprez, P.-Y., & Campisi, J. (2020). Astrocyte senescence promotes glutamate toxicity in cortical neurons. *PLoS One, 15*(1), e0227887. https://doi.org/10.1371/journal.pone.0227887

Lindquist, N. G., Larsson, B. S., & Lydén-Sokolowski, A. (1988). Autoradiography of [14C]paraquat or [14C]diquat in frogs and mice: accumulation in neuromelanin. *Neurosci Lett, 93*(1), 1-6. https://doi.org/10.1016/0304-3940(88)90002-x

Lindqvist, D., Kaufman, E., Brundin, L., Hall, S., Surova, Y., & Hansson, O. (2012). Non-motor symptoms in patients with Parkinson's disease - correlations with inflammatory cytokines in serum. *PLoS One, 7*(10), e47387. https://doi.org/10.1371/journal.pone.0047387

Liu, C.-W., Giasson, B. I., Lewis, K. A., Lee, V. M., DeMartino, G. N., & Thomas, P. J. (2005). A Precipitating Role for Truncated α-Synuclein and the Proteasome in α-Synuclein Aggregation: IMPLICATIONS FOR PATHOGENESIS OF PARKINSON DISEASE*. *Journal of Biological Chemistry, 280*(24), 22670-22678. https://doi.org/https://doi.org/10.1074/jbc.M501508200

Lodato, M. A., Rodin, R. E., Bohrson, C. L., Coulter, M. E., Barton, A. R., Kwon, M., Sherman, M. A., Vitzthum, C. M., Luquette, L. J., Yandava, C. N., Yang, P., Chittenden, T. W., Hatem, N. E., Ryu, S. C., Woodworth, M. B., Park, P. J., & Walsh, C. A. (2018). Aging and neurodegeneration are associated with increased mutations in single human neurons. *Science, 359*(6375), 555-559. https://doi.org/10.1126/science.aao4426

Lombardo, L. J., Lee, F. Y., Chen, P., Norris, D., Barrish, J. C., Behnia, K., Castaneda, S., Cornelius, L. A., Das, J., Doweyko, A. M., Fairchild, C., Hunt, J. T., Inigo, I., Johnston, K., Kamath, A., Kan, D., Klei, H., Marathe, P., Pang, S., . . . Borzilleri, R. M. (2004). Discovery of N-(2-chloro-6-methyl- phenyl)-2-(6-(4-(2-hydroxyethyl)- piperazin-1-yl)-2-methylpyrimidin-4-ylamino)thiazole-5-carboxamide (BMS-354825), a dual Src/Abl kinase inhibitor with potent antitumor activity in preclinical assays. *J Med Chem, 47*(27), 6658-6661. https://doi.org/10.1021/jm049486a

Lopez-Otin, C., Blasco, M. A., Partridge, L., Serrano, M., & Kroemer, G. (2013). The hallmarks of aging. *Cell, 153*(6), 1194-1217. https://doi.org/10.1016/j.cell.2013.05.039

Lowe, J., McDermott, H., Landon, M., Mayer, R. J., & Wilkinson, K. D. (1990). Ubiquitin carboxyl-terminal hydrolase (PGP 9.5) is selectively present in ubiquitinated inclusion bodies characteristic of human neurodegenerative diseases. *J Pathol, 161*(2), 153-160. https://doi.org/10.1002/path.1711610210

Lücking, C. B., Dürr, A., Bonifati, V., Vaughan, J., De Michele, G., Gasser, T., Harhangi, B. S., Meco, G., Denèfle, P., Wood, N. W., Agid, Y., Nicholl, D., Breteler, M. M. B., Oostra, B. A., De Mari, M., Marconi, R., Filla, A., Bonnet, A.-M., Broussolle, E., . . . Brice, A. (2000). Association between Early-Onset Parkinson's Disease and Mutations in the Parkin Gene. *New England Journal of Medicine, 342*(21), 1560-1567. https://doi.org/10.1056/nejm200005253422103

Lui, J. H., Hansen, D. V., & Kriegstein, A. R. (2011). Development and evolution of the human neocortex. *Cell, 146*(1), 18-36. https://doi.org/10.1016/j.cell.2011.06.030

Mahul-Mellier, A.-L., Burtscher, J., Maharjan, N., Weerens, L., Croisier, M., Kuttler, F., Leleu, M., Knott, G. W., & Lashuel, H. A. (2020). The process of Lewy body formation, rather than simply α-synuclein fibrillization, is one of the major drivers of neurodegeneration. *Proceedings of the National Academy of Sciences, 117*(9), 4971-4982. https://doi.org/doi:10.1073/pnas.1913904117

Manzanza, N. O., Sedlackova, L., & Kalaria, R. N. (2021). Alpha-Synuclein Post-translational Modifications: Implications for Pathogenesis of Lewy Body Disorders. *Front Aging Neurosci, 13*, 690293. https://doi.org/10.3389/fnagi.2021.690293

Maraganore, D. M., de Andrade, M., Elbaz, A., Farrer, M. J., Ioannidis, J. P., Krüger, R., Rocca, W. A., Schneider, N. K., Lesnick, T. G., Lincoln, S. J., Hulihan, M. M., Aasly, J. O., Ashizawa, T., Chartier-Harlin, M. C., Checkoway, H., Ferrarese, C., Hadjigeorgiou, G., Hattori, N., Kawakami, H., . . . Van Broeckhoven, C. (2006). Collaborative analysis of alpha-synuclein gene promoter variability and Parkinson disease. *Jama, 296*(6), 661-670. https://doi.org/10.1001/jama.296.6.661

Maroteaux, L., Campanelli, J., & Scheller, R. (1988). Synuclein: a neuron-specific protein localized to the nucleus and presynaptic nerve terminal. *The Journal of Neuroscience, 8*(8), 2804-2815. https://doi.org/10.1523/jneurosci.08-08-02804.1988

Marotta, N. P., Cherwien, C. A., Abeywardana, T., & Pratt, M. R. (2012). O-GlcNAc modification prevents peptide-dependent acceleration of α-synuclein aggregation. *Chembiochem, 13*(18), 2665-2670. https://doi.org/10.1002/cbic.201200478

Martínez-Cué, C., & Rueda, N. (2020). Cellular Senescence in Neurodegenerative Diseases [Review]. *Frontiers in Cellular Neuroscience, 14*. https://doi.org/10.3389/fncel.2020.00016

Martínez-Zamudio, R. I., Robinson, L., Roux, P. F., & Bischof, O. (2017). SnapShot: Cellular Senescence in Pathophysiology. *Cell*, *170*(5), 1044-1044.e1041. https://doi.org/10.1016/j.cell.2017.08.025

Marton, R. M., & Ioannidis, J. P. A. (2019). A Comprehensive Analysis of Protocols for Deriving Dopaminergic Neurons from Human Pluripotent Stem Cells. *Stem Cells Transl Med*, *8*(4), 366-374. https://doi.org/10.1002/sctm.18-0088

McComish, S. F., MacMahon Copas, A. N., & Caldwell, M. A. (2022). Human Brain-Based Models Provide a Powerful Tool for the Advancement of Parkinson's Disease Research and Therapeutic Development [Review]. *Frontiers in Neuroscience, 16*. https://doi.org/10.3389/fnins.2022.851058

McFarland, N. R., Fan, Z., Xu, K., Schwarzschild, M. A., Feany, M. B., Hyman, B. T., & McLean, P. J. (2009). Alpha-synuclein S129 phosphorylation mutants do not alter nigrostriatal toxicity in a rat model of Parkinson disease. *J Neuropathol Exp Neurol*, *68*(5), 515-524. https://doi.org/10.1097/NEN.0b013e3181a24b53

Mezey, E., Dehejia, A. M., Harta, G., Tresser, N., Suchy, S. F., Nussbaum, R. L., Brownstein, M. J., & Polymeropoulos, M. H. (1998). Alpha synuclein is present in Lewy bodies in sporadic Parkinson's disease. *Mol Psychiatry*, *3*(6), 493-499. https://doi.org/10.1038/sj.mp.4000446

Migliore, L., & Coppedè, F. (2009). Environmental-induced oxidative stress in neurodegenerative disorders and aging. *Mutat Res*, *674*(1-2), 73-84. https://doi.org/10.1016/j.mrgentox.2008.09.013

Miklossy, J., Arai, T., Guo, J. P., Klegeris, A., Yu, S., McGeer, E. G., & McGeer, P. L. (2006). LRRK2 expression in normal and pathologic human brain and in human cell lines. *J Neuropathol Exp Neurol*, *65*(10), 953-963. https://doi.org/10.1097/01.jnen.0000235121.98052.54

Miller, J. D., Ganat, Y. M., Kishinevsky, S., Bowman, R. L., Liu, B., Tu, E. Y., Mandal, P. K., Vera, E., Shim, J. W., Kriks, S., Taldone, T., Fusaki, N., Tomishima, M. J., Krainc, D., Milner, T. A., Rossi, D. J., & Studer, L. (2013). Human iPSC-based modeling of late-onset disease via progerin-induced aging. *Cell Stem Cell*, *13*(6), 691-705. https://doi.org/10.1016/j.stem.2013.11.006

Mishizen-Eberz, A. J., Guttmann, R. P., Giasson, B. I., Day, G. A., 3rd, Hodara, R., Ischiropoulos, H., Lee, V. M., Trojanowski, J. Q., & Lynch, D. R. (2003). Distinct cleavage patterns of normal and pathologic forms of alpha-synuclein by calpain I in vitro. *J Neurochem*, *86*(4), 836-847. https://doi.org/10.1046/j.1471-4159.2003.01878.x

Mogi, M., Harada, M., Kondo, T., Riederer, P., Inagaki, H., Minami, M., & Nagatsu, T. (1994). Interleukin-1 beta, interleukin-6, epidermal growth factor and transforming growth factor-alpha are elevated in the brain from parkinsonian patients. *Neurosci Lett*, *180*(2), 147-150. https://doi.org/10.1016/0304-3940(94)90508-8

Mogi, M., Harada, M., Riederer, P., Narabayashi, H., Fujita, K., & Nagatsu, T. (1994). Tumor necrosis factor-alpha (TNF-alpha) increases both in the brain and in the cerebrospinal fluid from parkinsonian patients. *Neurosci Lett*, *165*(1-2), 208-210. https://doi.org/10.1016/0304-3940(94)90746-3

Mohamed, N. V., Sirois, J., Ramamurthy, J., Mathur, M., Lépine, P., Deneault, E., Maussion, G., Nicouleau, M., Chen, C. X., Abdian, N., Soubannier, V., Cai, E., Nami, H., Thomas, R. A., Wen, D., Tabatabaei, M., Beitel, L. K., Singh Dolt, K., Karamchandani, J., . . . Durcan, T. M. (2021). Midbrain organoids with an SNCA gene triplication model key features of synucleinopathy. *Brain Commun*, *3*(4), fcab223. https://doi.org/10.1093/braincomms/fcab223

Monzel, A. S., Smits, L. M., Hemmer, K., Hachi, S., Moreno, E. L., van Wuellen, T., Jarazo, J., Walter, J., Brüggemann, I., Boussaad, I., Berger, E., Fleming, R. M. T., Bolognin, S., &

Schwamborn, J. C. (2017). Derivation of Human Midbrain-Specific Organoids from Neuroepithelial Stem Cells. *Stem Cell Reports*, *8*(5), 1144-1154. https://doi.org/10.1016/j.stemcr.2017.03.010

Mori, A., Imai, Y., & Hattori, N. (2020). Lipids: Key Players That Modulate α-Synuclein Toxicity and Neurodegeneration in Parkinson's Disease. *International Journal of Molecular Sciences*, *21*(9), 3301. https://www.mdpi.com/1422-0067/21/9/3301

Muguruma, K., Nishiyama, A., Kawakami, H., Hashimoto, K., & Sasai, Y. (2015). Self-organization of polarized cerebellar tissue in 3D culture of human pluripotent stem cells. *Cell Rep*, *10*(4), 537-550. https://doi.org/10.1016/j.celrep.2014.12.051

Muñoz-Espín, D., & Serrano, M. (2014). Cellular senescence: from physiology to pathology. *Nature Reviews Molecular Cell Biology*, *15*(7), 482-496. https://doi.org/10.1038/nrm3823

Muntané, G., Ferrer, I., & Martinez-Vicente, M. (2012). α-synuclein phosphorylation and truncation are normal events in the adult human brain. *Neuroscience*, *200*, 106-119. https://doi.org/10.1016/j.neuroscience.2011.10.042

Musi, N., Valentine, J. M., Sickora, K. R., Baeuerle, E., Thompson, C. S., Shen, Q., & Orr, M. E. (2018). Tau protein aggregation is associated with cellular senescence in the brain. *Aging Cell*, *17*(6), e12840. https://doi.org/10.1111/acel.12840

Nakamura, K., Nemani, V. M., Azarbal, F., Skibinski, G., Levy, J. M., Egami, K., Munishkina, L., Zhang, J., Gardner, B., Wakabayashi, J., Sesaki, H., Cheng, Y., Finkbeiner, S., Nussbaum, R. L., Masliah, E., & Edwards, R. H. (2011). Direct membrane association drives mitochondrial fission by the Parkinson disease-associated protein alpha-synuclein. *J Biol Chem*, *286*(23), 20710-20726. https://doi.org/10.1074/jbc.M110.213538

Nakamura, K., Nemani, V. M., Wallender, E. K., Kaehlcke, K., Ott, M., & Edwards, R. H. (2008). Optical reporters for the conformation of alpha-synuclein reveal a specific interaction with mitochondria. *J Neurosci*, *28*(47), 12305-12317. https://doi.org/10.1523/jneurosci.3088-08.2008

Nayler, S., Agarwal, D., Curion, F., Bowden, R., & Becker, E. B. E. (2021). High-resolution transcriptional landscape of xeno-free human induced pluripotent stem cell-derived cerebellar organoids. *Scientific Reports*, *11*(1), 12959. https://doi.org/10.1038/s41598-021-91846-4

Nemani, V. M., Lu, W., Berge, V., Nakamura, K., Onoa, B., Lee, M. K., Chaudhry, F. A., Nicoll, R. A., & Edwards, R. H. (2010). Increased expression of alpha-synuclein reduces neurotransmitter release by inhibiting synaptic vesicle reclustering after endocytosis. *Neuron*, *65*(1), 66-79. https://doi.org/10.1016/j.neuron.2009.12.023

Nickels, S. L., Modamio, J., Mendes-Pinheiro, B., Monzel, A. S., Betsou, F., & Schwamborn, J. C. (2020). Reproducible generation of human midbrain organoids for in vitro modeling of Parkinson's disease. *Stem Cell Research*, *46*, 101870. https://doi.org/https://doi.org/10.1016/j.scr.2020.101870

Nishioka, K., Ross, O. A., Ishii, K., Kachergus, J. M., Ishiwata, K., Kitagawa, M., Kono, S., Obi, T., Mizoguchi, K., Inoue, Y., Imai, H., Takanashi, M., Mizuno, Y., Farrer, M. J., & Hattori, N. (2009). Expanding the clinical phenotype of SNCA duplication carriers. *Mov Disord*, *24*(12), 1811-1819. https://doi.org/10.1002/mds.22682

Nuscher, B., Kamp, F., Mehnert, T., Odoy, S., Haass, C., Kahle, P. J., & Beyer, K. (2004). Alpha-synuclein has a high affinity for packing defects in a bilayer membrane: a thermodynamics study. *J Biol Chem*, *279*(21), 21966-21975. https://doi.org/10.1074/jbc.M401076200

Oeda, T., Umemura, A., Mori, Y., Tomita, S., Kohsaka, M., Park, K., Inoue, K., Fujimura, H., Hasegawa, H., Sugiyama, H., & Sawada, H. (2015). Impact of glucocerebrosidase mutations

on motor and nonmotor complications in Parkinson's disease. *Neurobiol Aging*, *36*(12), 3306-3313. https://doi.org/10.1016/j.neurobiolaging.2015.08.027

Ogawa, K., Yamada, T., Tsujioka, Y., Taguchi, J., Takahashi, M., Tsuboi, Y., Fujino, Y., Nakajima, M., Yamamoto, T., Akatsu, H., Mitsui, S., & Yamaguchi, N. (2000). Localization of a novel type trypsin-like serine protease, neurosin, in brain tissues of Alzheimer's disease and Parkinson's disease. *Psychiatry and Clinical Neurosciences*, *54*(4), 419-426. https://doi.org/https://doi.org/10.1046/j.1440-1819.2000.00731.x

Okochi, M., Walter, J., Koyama, A., Nakajo, S., Baba, M., Iwatsubo, T., Meijer, L., Kahle, P. J., & Haass, C. (2000). Constitutive phosphorylation of the Parkinson's disease associated alpha-synuclein. *J Biol Chem*, *275*(1), 390-397. https://doi.org/10.1074/jbc.275.1.390

Olgiati, S., Thomas, A., Quadri, M., Breedveld, G. J., Graafland, J., Eussen, H., Douben, H., de Klein, A., Onofrj, M., & Bonifati, V. (2015). Early-onset parkinsonism caused by alpha-synuclein gene triplication: Clinical and genetic findings in a novel family. *Parkinsonism & Related Disorders*, *21*(8), 981-986. https://doi.org/https://doi.org/10.1016/j.parkreldis.2015.06.005

Ottone, C., Krusche, B., Whitby, A., Clements, M., Quadrato, G., Pitulescu, M. E., Adams, R. H., & Parrinello, S. (2014). Direct cell-cell contact with the vascular niche maintains quiescent neural stem cells. *Nat Cell Biol*, *16*(11), 1045-1056. https://doi.org/10.1038/ncb3045

Pajarillo, E., Rizor, A., Lee, J., Aschner, M., & Lee, E. (2019). The role of posttranslational modifications of α-synuclein and LRRK2 in Parkinson's disease: Potential contributions of environmental factors. *Biochimica et Biophysica Acta (BBA) - Molecular Basis of Disease*, *1865*(8), 1992-2000. https://doi.org/https://doi.org/10.1016/j.bbadis.2018.11.017

Pan, Y., Zong, Q., Li, G., Wu, Z., Du, T., Huang, Z., Zhang, Y., & Ma, K. (2022). Nuclear localization of alpha-synuclein affects the cognitive and motor behavior of mice by inducing DNA damage and abnormal cell cycle of hippocampal neurons [Original Research]. *Frontiers in Molecular Neuroscience*, *15*. https://doi.org/10.3389/fnmol.2022.1015881

Parker, W. D., Jr., Parks, J. K., & Swerdlow, R. H. (2008). Complex I deficiency in Parkinson's disease frontal cortex. *Brain Res*, *1189*, 215-218. https://doi.org/10.1016/j.brainres.2007.10.061

Parkinson, J. (2002). An Essay on the Shaking Palsy. *The Journal of Neuropsychiatry and Clinical Neurosciences*, *14*(2), 223-236. https://doi.org/10.1176/jnp.14.2.223

Pasanen, P., Myllykangas, L., Siitonen, M., Raunio, A., Kaakkola, S., Lyytinen, J., Tienari, P. J., Pöyhönen, M., & Paetau, A. (2014). Novel α-synuclein mutation A53E associated with atypical multiple system atrophy and Parkinson's disease-type pathology. *Neurobiol Aging*, *35*(9), 2180.e2181-2185. https://doi.org/10.1016/j.neurobiolaging.2014.03.024

Perez, R. G., Waymire, J. C., Lin, E., Liu, J. J., Guo, F., & Zigmond, M. J. (2002). A role for alpha-synuclein in the regulation of dopamine biosynthesis. *J Neurosci*, *22*(8), 3090-3099. https://doi.org/10.1523/jneurosci.22-08-03090.2002

Periquet, M., Fulga, T., Myllykangas, L., Schlossmacher, M. G., & Feany, M. B. (2007). Aggregated alpha-synuclein mediates dopaminergic neurotoxicity in vivo. *J Neurosci*, *27*(12), 3338-3346. https://doi.org/10.1523/jneurosci.0285-07.2007

Pertusa, M., García-Matas, S., Rodríguez-Farré, E., Sanfeliu, C., & Cristòfol, R. (2007). Astrocytes aged in vitro show a decreased neuroprotective capacity. *J Neurochem*, *101*(3), 794-805. https://doi.org/10.1111/j.1471-4159.2006.04369.x

Pinho, R., Paiva, I., Jercic, K. G., Fonseca-Ornelas, L., Gerhardt, E., Fahlbusch, C., Garcia-Esparcia, P., Kerimoglu, C., Pavlou, M. A. S., Villar-Piqué, A., Szego, É., Lopes da Fonseca, T., Odoardi, F., Soeroes, S., Rego, A. C., Fischle, W., Schwamborn, J. C., Meyer, T., Kügler, S., . . . Outeiro, T. F. (2019). Nuclear localization and phosphorylation modulate pathological

effects of alpha-synuclein. *Hum Mol Genet*, *28*(1), 31-50. https://doi.org/10.1093/hmg/ddy326

Pinho, R., Paiva, I., Jerčić, K. G., Fonseca-Ornelas, L., Gerhardt, E., Fahlbusch, C., Garcia-Esparcia, P., Kerimoglu, C., Pavlou, M. A. S., Villar-Piqué, A., Szegő, É., Lopes da Fonseca, T., Odoardi, F., Soeroes, S., Rego, A. C., Fischle, W., Schwamborn, J. C., Meyer, T., Kügler, S., . . . Outeiro, T. F. (2018). Nuclear localization and phosphorylation modulate pathological effects of alpha-synuclein. *Human Molecular Genetics*, *28*(1), 31-50. https://doi.org/10.1093/hmg/ddy326

Polymeropoulos, M. H., Lavedan, C., Leroy, E., Ide, S. E., Dehejia, A., Dutra, A., Pike, B., Root, H., Rubenstein, J., Boyer, R., Stenroos, E. S., Chandrasekharappa, S., Athanassiadou, A., Papapetropoulos, T., Johnson, W. G., Lazzarini, A. M., Duvoisin, R. C., Di Iorio, G., Golbe, L. I., & Nussbaum, R. L. (1997). Mutation in the alpha-synuclein gene identified in families with Parkinson's disease. *Science*, *276*(5321), 2045-2047. https://doi.org/10.1126/science.276.5321.2045

Potashkin, J. A., Blume, S. R., & Runkle, N. K. (2011). Limitations of Animal Models of Parkinson's Disease. *Parkinson's Disease*, *2011*, 658083. https://doi.org/10.4061/2011/658083

Pozo Devoto, V. M., Dimopoulos, N., Alloatti, M., Pardi, M. B., Saez, T. M., Otero, M. G., Cromberg, L. E., Marín-Burgin, A., Scassa, M. E., Stokin, G. B., Schinder, A. F., Sevlever, G., & Falzone, T. L. (2017). αSynuclein control of mitochondrial homeostasis in human-derived neurons is disrupted by mutations associated with Parkinson's disease. *Sci Rep*, *7*(1), 5042. https://doi.org/10.1038/s41598-017-05334-9

Priyadarshi, A., Khuder, S. A., Schaub, E. A., & Priyadarshi, S. S. (2001). Environmental risk factors and Parkinson's disease: a metaanalysis. *Environ Res*, *86*(2), 122-127. https://doi.org/10.1006/enrs.2001.4264

Pronin, A. N., Morris, A. J., Surguchov, A., & Benovic, J. L. (2000). Synucleins are a novel class of substrates for G protein-coupled receptor kinases. *J Biol Chem*, *275*(34), 26515-26522. https://doi.org/10.1074/jbc.M003542200

Qian, L., & Flood, P. M. (2008). Microglial cells and Parkinson's disease. *Immunologic Research*, *41*(3), 155. https://doi.org/10.1007/s12026-008-8018-0

Qian, X., Nguyen, H. N., Song, M. M., Hadiono, C., Ogden, S. C., Hammack, C., Yao, B., Hamersky, G. R., Jacob, F., Zhong, C., Yoon, K. J., Jeang, W., Lin, L., Li, Y., Thakor, J., Berg, D. A., Zhang, C., Kang, E., Chickering, M., . . . Ming, G. L. (2016). Brain-Region-Specific Organoids Using Mini-bioreactors for Modeling ZIKV Exposure. *Cell*, *165*(5), 1238-1254. https://doi.org/10.1016/j.cell.2016.04.032

Qian, X., Song, H., & Ming, G.-l. (2019). Brain organoids: advances, applications and challenges. *Development*, *146*(8). https://doi.org/10.1242/dev.166074

Raimondi, M. T., Albani, D., & Giordano, C. (2019). An Organ-On-A-Chip Engineered Platform to Study the Microbiota-Gut-Brain Axis in Neurodegeneration. *Trends Mol Med*, *25*(9), 737-740. https://doi.org/10.1016/j.molmed.2019.07.006

Riboldi, G. M., & Di Fonzo, A. B. (2019). GBA, Gaucher Disease, and Parkinson's Disease: From Genetic to Clinic to New Therapeutic Approaches. *Cells*, *8*(4). https://doi.org/10.3390/cells8040364

Rott, R., Szargel, R., Haskin, J., Bandopadhyay, R., Lees, A. J., Shani, V., & Engelender, S. (2011). α-Synuclein fate is determined by USP9X-regulated monoubiquitination. *Proceedings of the National Academy of Sciences*, *108*(46), 18666-18671. https://doi.org/doi:10.1073/pnas.1105725108

Rott, R., Szargel, R., Shani, V., Hamza, H., Savyon, M., Abd Elghani, F., Bandopadhyay, R., & Engelender, S. (2017). SUMOylation and ubiquitination reciprocally regulate α-synuclein

degradation and pathological aggregation. *Proceedings of the National Academy of Sciences, 114*(50), 13176-13181. https://doi.org/doi:10.1073/pnas.1704351114

Rui, Q., Ni, H., Li, D., Gao, R., & Chen, G. (2018). The Role of LRRK2 in Neurodegeneration of Parkinson Disease. *Curr Neuropharmacol, 16*(9), 1348-1357. https://doi.org/10.2174/1570159x16666180222165418

Sabate-Soler, S., Nickels, S. L., Saraiva, C., Berger, E., Dubonyte, U., Barmpa, K., Lan, Y. J., Kouno, T., Jarazo, J., Robertson, G., Sharif, J., Koseki, H., Thome, C., Shin, J. W., Cowley, S. A., & Schwamborn, J. C. (2022). Microglia integration into human midbrain organoids leads to increased neuronal maturation and functionality. *Glia, 70*(7), 1267-1288. https://doi.org/https://doi.org/10.1002/glia.24167

Sakamoto, M., Arawaka, S., Hara, S., Sato, H., Cui, C., Machiya, Y., Koyama, S., Wada, M., Kawanami, T., Kurita, K., & Kato, T. (2009). Contribution of endogenous G-protein-coupled receptor kinases to Ser129 phosphorylation of alpha-synuclein in HEK293 cells. *Biochem Biophys Res Commun, 384*(3), 378-382. https://doi.org/10.1016/j.bbrc.2009.04.130

Sancesario, G. M., Di Lazzaro, G., Grillo, P., Biticchi, B., Giannella, E., Alwardat, M., Pieri, M., Bernardini, S., Mercuri, N. B., Pisani, A., & Schirinzi, T. (2021). Biofluids profile of α-Klotho in patients with Parkinson's disease. *Parkinsonism Relat Disord, 90*, 62-64. https://doi.org/10.1016/j.parkreldis.2021.08.004

Sanchez, G., Varaschin, R. K., Büeler, H., Marcogliese, P. C., Park, D. S., & Trudeau, L.-E. (2014). Unaltered Striatal Dopamine Release Levels in Young Parkin Knockout, Pink1 Knockout, DJ-1 Knockout and LRRK2 R1441G Transgenic Mice. *PLoS One, 9*(4), e94826. https://doi.org/10.1371/journal.pone.0094826

Scalzo, P., Kümmer, A., Cardoso, F., & Teixeira, A. L. (2010). Serum levels of interleukin-6 are elevated in patients with Parkinson's disease and correlate with physical performance. *Neurosci Lett, 468*(1), 56-58. https://doi.org/10.1016/j.neulet.2009.10.062

Schapira, A. H. (2015). Glucocerebrosidase and Parkinson disease: Recent advances. *Mol Cell Neurosci, 66*(Pt A), 37-42. https://doi.org/10.1016/j.mcn.2015.03.013

Schapira, A. H., Cooper, J. M., Dexter, D., Clark, J. B., Jenner, P., & Marsden, C. D. (1990). Mitochondrial complex I deficiency in Parkinson's disease. *J Neurochem, 54*(3), 823-827. https://doi.org/10.1111/j.1471-4159.1990.tb02325.x

Schaser, A. J., Osterberg, V. R., Dent, S. E., Stackhouse, T. L., Wakeham, C. M., Boutros, S. W., Weston, L. J., Owen, N., Weissman, T. A., Luna, E., Raber, J., Luk, K. C., McCullough, A. K., Woltjer, R. L., & Unni, V. K. (2019). Alpha-synuclein is a DNA binding protein that modulates DNA repair with implications for Lewy body disorders. *Scientific Reports, 9*(1), 10919. https://doi.org/10.1038/s41598-019-47227-z

Schwamborn, J. C. (2018). Is Parkinson's Disease a Neurodevelopmental Disorder and Will Brain Organoids Help Us to Understand It? *Stem Cells Dev, 27*(14), 968-975. https://doi.org/10.1089/scd.2017.0289

Segura-Aguilar, J., Paris, I., Muñoz, P., Ferrari, E., Zecca, L., & Zucca, F. A. (2014). Protective and toxic roles of dopamine in Parkinson's disease. *Journal of Neurochemistry, 129*(6), 898-915. https://doi.org/https://doi.org/10.1111/jnc.12686

Sevlever, D., Jiang, P., & Yen, S. H. (2008). Cathepsin D is the main lysosomal enzyme involved in the degradation of alpha-synuclein and generation of its carboxy-terminally truncated species. *Biochemistry, 47*(36), 9678-9687. https://doi.org/10.1021/bi800699v

Shaker, M. R., Aguado, J., Chaggar, H. K., & Wolvetang, E. J. (2021). Klotho inhibits neuronal senescence in human brain organoids. *npj Aging and Mechanisms of Disease, 7*(1), 18. https://doi.org/10.1038/s41514-021-00070-x

Shamoto-Nagai, M., Maruyama, W., Akao, Y., Osawa, T., Tribl, F., Gerlach, M., Zucca, F. A., Zecca, L., Riederer, P., & Naoi, M. (2004). Neuromelanin inhibits enzymatic activity of 26S proteasome in human dopaminergic SH-SY5Y cells. *J Neural Transm (Vienna)*, *111*(10-11), 1253-1265. https://doi.org/10.1007/s00702-004-0211-2

Sheeler, C., Rosa, J. G., Ferro, A., McAdams, B., Borgenheimer, E., & Cvetanovic, M. (2020). Glia in Neurodegeneration: The Housekeeper, the Defender and the Perpetrator. *Int J Mol Sci*, *21*(23). https://doi.org/10.3390/ijms21239188

Shen, Q., Goderie, S. K., Jin, L., Karanth, N., Sun, Y., Abramova, N., Vincent, P., Pumiglia, K., & Temple, S. (2004). Endothelial cells stimulate self-renewal and expand neurogenesis of neural stem cells. *Science*, *304*(5675), 1338-1340. https://doi.org/10.1126/science.1095505

Sherer, T. B., Betarbet, R., Testa, C. M., Seo, B. B., Richardson, J. R., Kim, J. H., Miller, G. W., Yagi, T., Matsuno-Yagi, A., & Greenamyre, J. T. (2003). Mechanism of toxicity in rotenone models of Parkinson's disease. *J Neurosci*, *23*(34), 10756-10764. https://doi.org/10.1523/jneurosci.23-34-10756.2003

Siddiqui, A., Chinta, S. J., Mallajosyula, J. K., Rajagopolan, S., Hanson, I., Rane, A., Melov, S., & Andersen, J. K. (2012). Selective binding of nuclear alpha-synuclein to the PGC1alpha promoter under conditions of oxidative stress may contribute to losses in mitochondrial function: implications for Parkinson's disease. *Free Radic Biol Med*, *53*(4), 993-1003. https://doi.org/10.1016/j.freeradbiomed.2012.05.024

Sidhu, A., Wersinger, C., & Vernier, P. (2004). α-Synuclein regulation of the dopaminergic transporter: a possible role in the pathogenesis of Parkinson's disease. *FEBS Letters*, *565*(1-3), 1-5. https://doi.org/https://doi.org/10.1016/j.febslet.2004.03.063

Sidransky, E., Nalls, M. A., Aasly, J. O., Aharon-Peretz, J., Annesi, G., Barbosa, E. R., Bar-Shira, A., Berg, D., Bras, J., Brice, A., Chen, C. M., Clark, L. N., Condroyer, C., De Marco, E. V., Dürr, A., Eblan, M. J., Fahn, S., Farrer, M. J., Fung, H. C., . . . Ziegler, S. G. (2009). Multicenter analysis of glucocerebrosidase mutations in Parkinson's disease. *N Engl J Med*, *361*(17), 1651-1661. https://doi.org/10.1056/NEJMoa0901281

Simmnacher, K., Krach, F., Schneider, Y., Alecu, J. E., Mautner, L., Klein, P., Roybon, L., Prots, I., Xiang, W., & Winner, B. (2020). Unique signatures of stress-induced senescent human astrocytes. *Experimental Neurology*, *334*, 113466. https://doi.org/https://doi.org/10.1016/j.expneurol.2020.113466

Singleton, A. B., Farrer, M., Johnson, J., Singleton, A., Hague, S., Kachergus, J., Hulihan, M., Peuralinna, T., Dutra, A., Nussbaum, R., Lincoln, S., Crawley, A., Hanson, M., Maraganore, D., Adler, C., Cookson, M. R., Muenter, M., Baptista, M., Miller, D., . . . Gwinn-Hardy, K. (2003). alpha-Synuclein locus triplication causes Parkinson's disease. *Science*, *302*(5646), 841. https://doi.org/10.1126/science.1090278

Sison, S. L., Vermilyea, S. C., Emborg, M. E., & Ebert, A. D. (2018). Using Patient-Derived Induced Pluripotent Stem Cells to Identify Parkinson's Disease-Relevant Phenotypes. *Curr Neurol Neurosci Rep*, *18*(12), 84. https://doi.org/10.1007/s11910-018-0893-8

Skrahina, V., Gaber, H., Vollstedt, E. J., Förster, T. M., Usnich, T., Curado, F., Brüggemann, N., Paul, J., Bogdanovic, X., Zülbahar, S., Olmedillas, M., Skobalj, S., Ameziane, N., Bauer, P., Csoti, I., Koleva-Alazeh, N., Grittner, U., Westenberger, A., Kasten, M., . . . Rolfs, A. (2021). The Rostock International Parkinson's Disease (ROPAD) Study: Protocol and Initial Findings. *Mov Disord*, *36*(4), 1005-1010. https://doi.org/10.1002/mds.28416

Smith, L., Mullin, S., & Schapira, A. H. V. (2017). Insights into the structural biology of Gaucher disease. *Experimental Neurology*, *298*, 180-190. https://doi.org/https://doi.org/10.1016/j.expneurol.2017.09.010

Smits, L. M., Magni, S., Kinugawa, K., Grzyb, K., Luginbühl, J., Sabate-Soler, S., Bolognin, S., Shin, J. W., Mori, E., Skupin, A., & Schwamborn, J. C. (2020). Single-cell transcriptomics reveals multiple neuronal cell types in human midbrain-specific organoids. *Cell Tissue Res*, *382*(3), 463-476. https://doi.org/10.1007/s00441-020-03249-y

Smits, L. M., Reinhardt, L., Reinhardt, P., Glatza, M., Monzel, A. S., Stanslowsky, N., Rosato-Siri, M. D., Zanon, A., Antony, P. M., Bellmann, J., Nicklas, S. M., Hemmer, K., Qing, X., Berger, E., Kalmbach, N., Ehrlich, M., Bolognin, S., Hicks, A. A., Wegner, F., . . . Schwamborn, J. C. (2019). Modeling Parkinson's disease in midbrain-like organoids. *npj Parkinson's Disease*, *5*(1), 5. https://doi.org/10.1038/s41531-019-0078-4

Spillantini, M. G., Schmidt, M. L., Lee, V. M. Y., Trojanowski, J. Q., Jakes, R., & Goedert, M. (1997). α-Synuclein in Lewy bodies. *Nature*, *388*(6645), 839-840. https://doi.org/10.1038/42166

Stefanova, N. (2022). Microglia in Parkinson's Disease. *Journal of Parkinson's Disease*, *12*, S105-S112. https://doi.org/10.3233/JPD-223237

Sulzer, D., & Surmeier, D. J. (2013). Neuronal vulnerability, pathogenesis, and Parkinson's disease. *Mov Disord*, *28*(1), 41-50. https://doi.org/10.1002/mds.25095

Sun, X.-Y., Ju, X.-C., Li, Y., Zeng, P.-M., Wu, J., Zhou, Y.-Y., Shen, L.-B., Dong, J., Chen, Y.-J., & Luo, Z.-G. (2022). Generation of vascularized brain organoids to study neurovascular interactions. *eLife*, *11*, e76707. https://doi.org/10.7554/eLife.76707

Sung, J. Y., Park, S. M., Lee, C. H., Um, J. W., Lee, H. J., Kim, J., Oh, Y. J., Lee, S. T., Paik, S. R., & Chung, K. C. (2005). Proteolytic cleavage of extracellular secreted {alpha}-synuclein via matrix metalloproteinases. *J Biol Chem*, *280*(26), 25216-25224. https://doi.org/10.1074/jbc.M503341200

Surmeier, D. J., Obeso, J. A., & Halliday, G. M. (2017). Selective neuronal vulnerability in Parkinson disease. *Nat Rev Neurosci*, *18*(2), 101-113. https://doi.org/10.1038/nrn.2016.178

Takahashi, K., & Yamanaka, S. (2006). Induction of pluripotent stem cells from mouse embryonic and adult fibroblast cultures by defined factors. *Cell*, *126*(4), 663-676. https://doi.org/10.1016/j.cell.2006.07.024

Takahashi, M., Kanuka, H., Fujiwara, H., Koyama, A., Hasegawa, M., Miura, M., & Iwatsubo, T. (2003). Phosphorylation of alpha-synuclein characteristic of synucleinopathy lesions is recapitulated in alpha-synuclein transgenic Drosophila. *Neurosci Lett*, *336*(3), 155-158. https://doi.org/10.1016/s0304-3940(02)01258-2

Tan, F. C., Hutchison, E. R., Eitan, E., & Mattson, M. P. (2014). Are there roles for brain cell senescence in aging and neurodegenerative disorders? *Biogerontology*, *15*(6), 643-660. https://doi.org/10.1007/s10522-014-9532-1

Tenreiro, S., Reimão-Pinto, M. M., Antas, P., Rino, J., Wawrzycka, D., Macedo, D., Rosado-Ramos, R., Amen, T., Waiss, M., Magalhães, F., Gomes, A., Santos, C. N., Kaganovich, D., & Outeiro, T. F. (2014). Phosphorylation Modulates Clearance of Alpha-Synuclein Inclusions in a Yeast Model of Parkinson's Disease. *PLOS Genetics*, *10*(5), e1004302. https://doi.org/10.1371/journal.pgen.1004302

Terada, M., Suzuki, G., Nonaka, T., Kametani, F., Tamaoka, A., & Hasegawa, M. (2018). The effect of truncation on prion-like properties of α-synuclein. *J Biol Chem*, *293*(36), 13910-13920. https://doi.org/10.1074/jbc.RA118.001862

Therese, B., & Sebastian, H. (2013). Molecular Mechanisms of Cellular Senescence. In W. Zhiwei & I. Hiroyuki (Eds.), *Senescence and Senescence-Related Disorders* (pp. Ch. 2). IntechOpen. https://doi.org/10.5772/54120

Thiruchelvam, M. J., Powers, J. M., Cory-Slechta, D. A., & Richfield, E. K. (2004). Risk factors for dopaminergic neuron loss in human alpha-synuclein transgenic mice. *Eur J Neurosci*, *19*(4), 845-854. https://doi.org/10.1111/j.0953-816x.2004.03139.x

Tieng, V., Stoppini, L., Villy, S., Fathi, M., Dubois-Dauphin, M., & Krause, K. H. (2014). Engineering of midbrain organoids containing long-lived dopaminergic neurons. *Stem Cells Dev, 23*(13), 1535-1547. https://doi.org/10.1089/scd.2013.0442

Tofaris, G. K., Garcia Reitböck, P., Humby, T., Lambourne, S. L., O'Connell, M., Ghetti, B., Gossage, H., Emson, P. C., Wilkinson, L. S., Goedert, M., & Spillantini, M. G. (2006). Pathological changes in dopaminergic nerve cells of the substantia nigra and olfactory bulb in mice transgenic for truncated human alpha-synuclein(1-120): implications for Lewy body disorders. *J Neurosci, 26*(15), 3942-3950. https://doi.org/10.1523/jneurosci.4965-05.2006

Tofaris, G. K., Kim, H. T., Hourez, R., Jung, J.-W., Kim, K. P., & Goldberg, A. L. (2011). Ubiquitin ligase Nedd4 promotes α-synuclein degradation by the endosomal–lysosomal pathway. *Proceedings of the National Academy of Sciences, 108*(41), 17004-17009. https://doi.org/doi:10.1073/pnas.1109356108

Tofaris, G. K., Layfield, R., & Spillantini, M. G. (2001). alpha-synuclein metabolism and aggregation is linked to ubiquitin-independent degradation by the proteasome. *FEBS Lett, 509*(1), 22-26. https://doi.org/10.1016/s0014-5793(01)03115-5

Tofaris, G. K., Razzaq, A., Ghetti, B., Lilley, K. S., & Spillantini, M. G. (2003). Ubiquitination of alpha-synuclein in Lewy bodies is a pathological event not associated with impairment of proteasome function. *J Biol Chem, 278*(45), 44405-44411. https://doi.org/10.1074/jbc.M308041200

Tremblay, M.-È., Stevens, B., Sierra, A., Wake, H., Bessis, A., & Nimmerjahn, A. (2011). The Role of Microglia in the Healthy Brain. *The Journal of Neuroscience, 31*(45), 16064-16069. https://doi.org/10.1523/jneurosci.4158-11.2011

Trétiakoff, C. (1919). *Contribution a l'etude de l'Anatomie pathologique du Locus Niger de Soemmering avec quelques deduction relatives a la pathogenie des troubles du tonus musculaire et de la maladie de Parkinson* University of Paris]. Paris.

Twelves, D., Perkins, K. S. M., & Counsell, C. (2003). Systematic review of incidence studies of Parkinson's disease. *Movement Disorders, 18*(1), 19-31. https://doi.org/https://doi.org/10.1002/mds.10305

Ueda, K., Fukushima, H., Masliah, E., Xia, Y., Iwai, A., Yoshimoto, M., Otero, D. A., Kondo, J., Ihara, Y., & Saitoh, T. (1993). Molecular cloning of cDNA encoding an unrecognized component of amyloid in Alzheimer disease. *Proc Natl Acad Sci U S A, 90*(23), 11282-11286. https://doi.org/10.1073/pnas.90.23.11282

Uversky, V. N. (2007). Neuropathology, biochemistry, and biophysics of alpha-synuclein aggregation. *J Neurochem, 103*(1), 17-37. https://doi.org/10.1111/j.1471-4159.2007.04764.x

van der Wateren, I. M., Knowles, T. P. J., Buell, A. K., Dobson, C. M., & Galvagnion, C. (2018). C-terminal truncation of α-synuclein promotes amyloid fibril amplification at physiological pH [10.1039/C8SC01109E]. *Chemical Science, 9*(25), 5506-5516. https://doi.org/10.1039/C8SC01109E

Váradi, C. (2020). Clinical Features of Parkinson's Disease: The Evolution of Critical Symptoms. *Biology (Basel), 9*(5). https://doi.org/10.3390/biology9050103

Vasquez, V., Mitra, J., Hegde, P. M., Pandey, A., Sengupta, S., Mitra, S., Rao, K. S., & Hegde, M. L. (2017). Chromatin-Bound Oxidized α-Synuclein Causes Strand Breaks in Neuronal Genomes in in vitro Models of Parkinson's Disease. *J Alzheimers Dis, 60*(s1), S133-s150. https://doi.org/10.3233/jad-170342

Vera, E., Bosco, N., & Studer, L. (2016). Generating Late-Onset Human iPSC-Based Disease Models by Inducing Neuronal Age-Related Phenotypes through Telomerase Manipulation. *Cell Rep, 17*(4), 1184-1192. https://doi.org/10.1016/j.celrep.2016.09.062

Verma, D. K., Seo, B. A., Ghosh, A., Ma, S. X., Hernandez-Quijada, K., Andersen, J. K., Ko, H. S., & Kim, Y. H. (2021). Alpha-Synuclein Preformed Fibrils Induce Cellular Senescence in Parkinson's Disease Models. *Cells*, *10*(7). https://doi.org/10.3390/cells10071694

Viceconte, N., Burguillos, M. A., Herrera, A. J., De Pablos, R. M., Joseph, B., & Venero, J. L. (2015). Neuromelanin activates proinflammatory microglia through a caspase-8-dependent mechanism. *Journal of Neuroinflammation*, *12*(1), 5. https://doi.org/10.1186/s12974-014-0228-x

Visanji, N. P., Brooks, P. L., Hazrati, L.-N., & Lang, A. E. (2013). The prion hypothesis in Parkinson's disease: Braak to the future. *Acta Neuropathologica Communications*, *1*(1), 2. https://doi.org/10.1186/2051-5960-1-2

Volpicelli-Daley, L. A., Luk, K. C., Patel, T. P., Tanik, S. A., Riddle, D. M., Stieber, A., Meaney, D. F., Trojanowski, J. Q., & Lee, V. M. (2011). Exogenous α-synuclein fibrils induce Lewy body pathology leading to synaptic dysfunction and neuron death. *Neuron*, *72*(1), 57-71. https://doi.org/10.1016/j.neuron.2011.08.033

Wakamatsu, M., Ishii, A., Iwata, S., Sakagami, J., Ukai, Y., Ono, M., Kanbe, D., Muramatsu, S., Kobayashi, K., Iwatsubo, T., & Yoshimoto, M. (2008). Selective loss of nigral dopamine neurons induced by overexpression of truncated human alpha-synuclein in mice. *Neurobiol Aging*, *29*(4), 574-585. https://doi.org/10.1016/j.neurobiolaging.2006.11.017

Wake, H., Moorhouse, A. J., Jinno, S., Kohsaka, S., & Nabekura, J. (2009). Resting microglia directly monitor the functional state of synapses in vivo and determine the fate of ischemic terminals. *J Neurosci*, *29*(13), 3974-3980. https://doi.org/10.1523/jneurosci.4363-08.2009

Walter, J., Bolognin, S., Poovathingal, S. K., Magni, S., Gérard, D., Antony, P. M. A., Nickels, S. L., Salamanca, L., Berger, E., Smits, L. M., Grzyb, K., Perfeito, R., Hoel, F., Qing, X., Ohnmacht, J., Bertacchi, M., Jarazo, J., Ignac, T., Monzel, A. S., . . . Schwamborn, J. C. (2021). The Parkinson’s-disease-associated mutation LRRK2-G2019S alters dopaminergic differentiation dynamics via NR2F1. *Cell Reports*, *37*(3). https://doi.org/10.1016/j.celrep.2021.109864

Wan, C., Liu, J., Nie, X., Zhao, J., Zhou, S., Duan, Z., Tang, C., Liang, L., & Xu, G. (2014). 2, 3, 7, 8-Tetrachlorodibenzo-P-dioxin (TCDD) induces premature senescence in human and rodent neuronal cells via ROS-dependent mechanisms. *PLoS One*, *9*(2), e89811. https://doi.org/10.1371/journal.pone.0089811

Wang, C., Yang, T., Liang, M., Xie, J., & Song, N. (2021). Astrocyte dysfunction in Parkinson's disease: from the perspectives of transmitted α-synuclein and genetic modulation. *Translational Neurodegeneration*, *10*(1), 39. https://doi.org/10.1186/s40035-021-00265-y

Wang, S., Chu, C. H., Stewart, T., Ginghina, C., Wang, Y., Nie, H., Guo, M., Wilson, B., Hong, J. S., & Zhang, J. (2015). α-Synuclein, a chemoattractant, directs microglial migration via H_2O_2-dependent Lyn phosphorylation. *Proc Natl Acad Sci U S A*, *112*(15), E1926-1935. https://doi.org/10.1073/pnas.1417883112

Wang, W., Perovic, I., Chittuluru, J., Kaganovich, A., Nguyen, L. T. T., Liao, J., Auclair, J. R., Johnson, D., Landeru, A., Simorellis, A. K., Ju, S., Cookson, M. R., Asturias, F. J., Agar, J. N., Webb, B. N., Kang, C., Ringe, D., Petsko, G. A., Pochapsky, T. C., & Hoang, Q. Q. (2011). A soluble α-synuclein construct forms a dynamic tetramer. *Proceedings of the National Academy of Sciences*, *108*(43), 17797-17802. https://doi.org/doi:10.1073/pnas.1113260108

Wang, Z., Udeshi, N. D., O'Malley, M., Shabanowitz, J., Hunt, D. F., & Hart, G. W. (2010). Enrichment and site mapping of O-linked N-acetylglucosamine by a combination of chemical/enzymatic tagging, photochemical cleavage, and electron transfer dissociation

mass spectrometry. *Mol Cell Proteomics*, *9*(1), 153-160. https://doi.org/10.1074/mcp.M900268-MCP200

Wang, Z., Wang, S. N., Xu, T. Y., Miao, Z. W., Su, D. F., & Miao, C. Y. (2017). Organoid technology for brain and therapeutics research. *CNS Neurosci Ther*, *23*(10), 771-778. https://doi.org/10.1111/cns.12754

Weinreb, P. H., Zhen, W., Poon, A. W., Conway, K. A., & Lansbury, P. T., Jr. (1996). NACP, a protein implicated in Alzheimer's disease and learning, is natively unfolded. *Biochemistry*, *35*(43), 13709-13715. https://doi.org/10.1021/bi961799n

Witting, A., Müller, P., Herrmann, A., Kettenmann, H., & Nolte, C. (2000). Phagocytic clearance of apoptotic neurons by Microglia/Brain macrophages in vitro: involvement of lectin-, integrin-, and phosphatidylserine-mediated recognition. *J Neurochem*, *75*(3), 1060-1070. https://doi.org/10.1046/j.1471-4159.2000.0751060.x

Wulansari, N., Darsono, W. H. W., Woo, H. J., Chang, M. Y., Kim, J., Bae, E. J., Sun, W., Lee, J. H., Cho, I. J., Shin, H., Lee, S. J., & Lee, S. H. (2021). Neurodevelopmental defects and neurodegenerative phenotypes in human brain organoids carrying Parkinson's disease-linked DNAJC6 mutations. *Sci Adv*, *7*(8). https://doi.org/10.1126/sciadv.abb1540

Xiang, Y., Tanaka, Y., Cakir, B., Patterson, B., Kim, K. Y., Sun, P., Kang, Y. J., Zhong, M., Liu, X., Patra, P., Lee, S. H., Weissman, S. M., & Park, I. H. (2019). hESC-Derived Thalamic Organoids Form Reciprocal Projections When Fused with Cortical Organoids. *Cell Stem Cell*, *24*(3), 487-497.e487. https://doi.org/10.1016/j.stem.2018.12.015

Xu, L., Bhattacharya, S., & Thompson, D. (2019). On the ubiquity of helical α-synuclein tetramers [10.1039/C9CP02464F]. *Physical Chemistry Chemical Physics*, *21*(22), 12036-12043. https://doi.org/10.1039/C9CP02464F

Xu, Y., Deng, Y., & Qing, H. (2015). The phosphorylation of α-synuclein: development and implication for the mechanism and therapy of the Parkinson's disease. *J Neurochem*, *135*(1), 4-18. https://doi.org/10.1111/jnc.13234

Xue, W.-J., He, C.-F., Zhou, R.-Y., Xu, X.-D., Xiang, L.-X., Wang, J.-T., Wang, X.-R., Zhou, H.-G., & Guo, J.-C. (2022). High glucose and palmitic acid induces neuronal senescence by NRSF/REST elevation and the subsequent mTOR-related autophagy suppression. *Molecular Brain*, *15*(1), 61. https://doi.org/10.1186/s13041-022-00947-2

Yamin, G., Uversky, V. N., & Fink, A. L. (2003). Nitration inhibits fibrillation of human alpha-synuclein in vitro by formation of soluble oligomers. *FEBS Lett*, *542*(1-3), 147-152. https://doi.org/10.1016/s0014-5793(03)00367-3

Yeap, Y. J., Teddy, T. J. W., Lee, M. J., Goh, M., & Lim, K. L. (2023). From 2D to 3D: Development of Monolayer Dopaminergic Neuronal and Midbrain Organoid Cultures for Parkinson’s Disease Modeling and Regenerative Therapy. *International Journal of Molecular Sciences*, *24*(3), 2523. https://www.mdpi.com/1422-0067/24/3/2523

Yonetani, M., Nonaka, T., Masuda, M., Inukai, Y., Oikawa, T., Hisanaga, S., & Hasegawa, M. (2009). Conversion of wild-type alpha-synuclein into mutant-type fibrils and its propagation in the presence of A30P mutant. *J Biol Chem*, *284*(12), 7940-7950. https://doi.org/10.1074/jbc.M807482200

Yoon, S. J., Elahi, L. S., Paşca, A. M., Marton, R. M., Gordon, A., Revah, O., Miura, Y., Walczak, E. M., Holdgate, G. M., Fan, H. C., Huguenard, J. R., Geschwind, D. H., & Paşca, S. P. (2019). Reliability of human cortical organoid generation. *Nat Methods*, *16*(1), 75-78. https://doi.org/10.1038/s41592-018-0255-0

Yoon, Y.-S., You, J. S., Kim, T.-K., Ahn, W. J., Kim, M. J., Son, K. H., Ricarte, D., Ortiz, D., Lee, S.-J., & Lee, H.-J. (2022). Senescence and impaired DNA damage responses in alpha-

synucleinopathy models. *Experimental & Molecular Medicine, 54*(2), 115-128. https://doi.org/10.1038/s12276-022-00727-x

Zagare, Barmpa, K., Smajic, S., Smits, L. M., Grzyb, K., Grünewald, A., Skupin, A., Nickels, S. L., & Schwamborn, J. C. (2022). Midbrain organoids mimic early embryonic neurodevelopment and recapitulate LRRK2-p.Gly2019Ser-associated gene expression. *The American Journal of Human Genetics, 109*(2), 311-327. https://doi.org/https://doi.org/10.1016/j.ajhg.2021.12.009

Zarranz, J. J., Alegre, J., Gómez-Esteban, J. C., Lezcano, E., Ros, R., Ampuero, I., Vidal, L., Hoenicka, J., Rodriguez, O., Atarés, B., Llorens, V., Gomez Tortosa, E., del Ser, T., Muñoz, D. G., & de Yebenes, J. G. (2004). The new mutation, E46K, of alpha-synuclein causes Parkinson and Lewy body dementia. *Ann Neurol, 55*(2), 164-173. https://doi.org/10.1002/ana.10795

Zecca, L., Bellei, C., Costi, P., Albertini, A., Monzani, E., Casella, L., Gallorini, M., Bergamaschi, L., Moscatelli, A., Turro, N. J., Eisner, M., Crippa, P. R., Ito, S., Wakamatsu, K., Bush, W. D., Ward, W. C., Simon, J. D., & Zucca, F. A. (2008). New melanic pigments in the human brain that accumulate in aging and block environmental toxic metals. *Proc Natl Acad Sci U S A, 105*(45), 17567-17572. https://doi.org/10.1073/pnas.0808768105

Zecca, L., Fariello, R., Riederer, P., Sulzer, D., Gatti, A., & Tampellini, D. (2002). The absolute concentration of nigral neuromelanin, assayed by a new sensitive method, increases throughout the life and is dramatically decreased in Parkinson's disease. *FEBS Lett, 510*(3), 216-220. https://doi.org/10.1016/s0014-5793(01)03269-0

Zecca, L., Pietra, R., Goj, C., Mecacci, C., Radice, D., & Sabbioni, E. (1994). Iron and other metals in neuromelanin, substantia nigra, and putamen of human brain. *J Neurochem, 62*(3), 1097-1101. https://doi.org/10.1046/j.1471-4159.1994.62031097.x

Zecca, L., Tampellini, D., Gerlach, M., Riederer, P., Fariello, R. G., & Sulzer, D. (2001). Substantia nigra neuromelanin: structure, synthesis, and molecular behaviour. *Mol Pathol, 54*(6), 414-418.

Zhang, J., Lei, H., Chen, Y., Ma, Y. T., Jiang, F., Tan, J., Zhang, Y., & Li, J. D. (2017). Enzymatic O-GlcNAcylation of α-synuclein reduces aggregation and increases SDS-resistant soluble oligomers. *Neurosci Lett, 655*, 90-94. https://doi.org/10.1016/j.neulet.2017.06.034

Zhang, P., Kishimoto, Y., Grammatikakis, I., Gottimukkala, K., Cutler, R. G., Zhang, S., Abdelmohsen, K., Bohr, V. A., Misra Sen, J., Gorospe, M., & Mattson, M. P. (2019). Senolytic therapy alleviates Aβ-associated oligodendrocyte progenitor cell senescence and cognitive deficits in an Alzheimer's disease model. *Nat Neurosci, 22*(5), 719-728. https://doi.org/10.1038/s41593-019-0372-9

Zhang, W., Phillips, K., Wielgus, A. R., Liu, J., Albertini, A., Zucca, F. A., Faust, R., Qian, S. Y., Miller, D. S., Chignell, C. F., Wilson, B., Jackson-Lewis, V., Przedborski, S., Joset, D., Loike, J., Hong, J. S., Sulzer, D., & Zecca, L. (2011). Neuromelanin activates microglia and induces degeneration of dopaminergic neurons: implications for progression of Parkinson's disease. *Neurotox Res, 19*(1), 63-72. https://doi.org/10.1007/s12640-009-9140-z

Zhang, W., Wang, T., Pei, Z., Miller, D. S., Wu, X., Block, M. L., Wilson, B., Zhang, W., Zhou, Y., Hong, J. S., & Zhang, J. (2005). Aggregated alpha-synuclein activates microglia: a process leading to disease progression in Parkinson's disease. *Faseb j, 19*(6), 533-542. https://doi.org/10.1096/fj.04-2751com

Zhang, Y., Sloan, S. A., Clarke, L. E., Caneda, C., Plaza, C. A., Blumenthal, P. D., Vogel, H., Steinberg, G. K., Edwards, M. S., Li, G., Duncan, J. A., 3rd, Cheshier, S. H., Shuer, L. M., Chang, E. F., Grant, G. A., Gephart, M. G., & Barres, B. A. (2016). Purification and Characterization of Progenitor and Mature Human Astrocytes Reveals Transcriptional and

Functional Differences with Mouse. *Neuron, 89*(1), 37-53. https://doi.org/10.1016/j.neuron.2015.11.013

Zhao, Z. (2019). Iron and oxidizing species in oxidative stress and Alzheimer's disease. *Aging Med (Milton), 2*(2), 82-87. https://doi.org/10.1002/agm2.12074

Zhou, M., Xu, S., Mi, J., Uéda, K., & Chan, P. (2013). Nuclear translocation of alpha-synuclein increases susceptibility of MES23.5 cells to oxidative stress. *Brain Research, 1500*, 19-27. https://doi.org/https://doi.org/10.1016/j.brainres.2013.01.024

Zimmermann, M., Köhler, L., Kovarova, M., Lerche, S., Schulte, C., Wurster, I., Machetanz, G., Deuschle, C., Hauser, A.-K., Gasser, T., Berg, D., Schleicher, E., Maetzler, W., & Brockmann, K. (2021). The longevity gene Klotho and its cerebrospinal fluid protein profiles as a modifier for Parkinson´s disease. *European journal of neurology, 28*(5), 1557-1565. https://doi.org/10.1111/ene.14733